CHEMISTRY HALL LIBRARY

Mutual Solubilities of Some Hydrocarbon Oils and Liquid Ammonia. I. Solubility Data

By Kiyoharu ISHIDA

(Received September 13, 1957)

Liquid ammonia has good solvency and selectivity for the extraction of aromatic hydrocarbons[1,2], olefinic hydrocarbons[1,2] or phenols[3] from hydrocarbon mixtures, and there is a possibility of the use of liquid ammonia as a solvent for the separation of hydrocarbons. It is desirable to have at hand accurate liquid-equilibrium data in order that the relative value of various solvents can be compared. However, relatively few ternary systems containing liquid ammonia have been investigated. Moreover, even for the binary systems, only a few solubility data of hydrocarbon oils and liquid ammonia have been reported[3,4-6]. When data on the mutual solubilities are available, it is possible to predict the equilibrium relations for the ternary system from the mutual solubilities between solvent and each of two components[7].

The paucity of information about the liquid equilibrium data for hydrocarbons and liquid ammonia prompted the author to obtain the knowledge of quantitative solubility relations. This paper includes solubility data for the representative compounds of olefins and saturated hydrocarbons at around room temperature, and those for aromatics at the temperatures near the critical solution temperature. As representative compounds of hydrocarbons, those in the C_7 to C_9 range for aromatics and in the C_6 to C_8 range for olefins and saturated hydrocarbons were mainly selected.

Experimental Procedure and Materials

Solubilities were determined by the same method as described in the previous paper[8,9]. Cloud points could be determined to within ± 0.05°C or better by using the thermometer which was graduated in tenths of a degree and corrected by the P. T. R. thermometer. Mutual solubilities at the temperatures far from the critical solution temperature were obtained by determining the composition of the two liquid phases in equilibrium at a given temperature (± 0.05°C). About five grams (± 0.0005 g) of each of the separate phases were used for the analysis at each time, and the concentration of ammonia was determined by titrating with 0.5 N sodium hydroxide solution the excess of sulfuric acid which absorbed all ammonia in the liquid phase. The determination was repeated several times for each phase at a given temperature, and averaged. The average error was less than 0.1% with a maximum error of 0.4%.

Except for some of the materials, which were commercially available products purified by the ordinary methods, many hydrocarbons used for the determination were synthesized and carefully purified. In Table 1, their physical constants are listed together with the values in the literature[10].

n-Hexane and *n*-octane were synthesized from corresponding alkyl bromides according to Wurtz's method. Propylbenzene was prepared from bromobenzene and propyl bromide by Fittig reaction. *iso*-Propylbenzene was synthesized according to H. Meyer et al[11]. *o*-Xylene was prepared by the condensation of *o*-bromotoluene, which was synthesized by means of Sandmeyer reaction from acet-*o*-toluide of melting point 110°C as a starting material and methyl iodide using metallic sodium and purified by careful distillation. *m*-Xylene was obtained by decomposing *m*-xylene sulfonate of melting point 60°C which was prepared and purified from a commercial product by removing the *p*-isomer according to Clark et al.[15] after the sulfonation and the decomposition were repeated. *p*-Xylene was prepared by reducing *p*-chloromethyltoluene obtained by chloro-

1) K. Ishida, This Bulletin, **30**, 612 (1957).
2) M. R. Fenske, R. H. McCormick, H. Lawroski and R. G. Geier, *A. I. Ch. E. Journal*, **1**, 335 (1955).
3) K. Ishida, *Science Repts. Research Inst. Tohoku Univ.*, Ser. A, **5**, 377 (1953).
4) C. A. Kraus and E. H. Zeitfuchs, *J. Am. Chem. Soc.*, **44**, 1249 (1922).
5) A. W. Francis, *Ind. Eng. Chem.*, **36**, 764 (1944).
6) Idem. ibid., **36**, 1096 (1944).
7) K. Ishida, *J. Chem. Soc. Japan, Ind. Chem. Sec.* (*Kogyo Kagaku Zassi*), **58**, 637 (1955); E. N. Pennington and S. J. Marwil, *Ind. Eng. Chem.*, **45**, 1371 (1953); R. E. Treybal, "Liquid Extraction", Chap. 3, McGraw-Hill Book Company, Inc., New York 1951.
8) K. Ishida, *J. Chem. Soc. Japan, Ind. Chem. Sec.* (*Kogyo Kagaku Zassi*), **56**, 469 (1953).
9) K. Ishida, This Bulletin, **29**, 956 (1956).
10) S. W. Ferris, "Handbook of Hydrocarbons," Academic Press Inc. Pub., New York, 1955.
11) K. Ishida, *J. Chem. Soc. Japan, Ind. Chem. Sec.* (*Kogyo Kagaku Zassi*), **57**, 479 (1954).
12) Idem., ibid., **60**, 864 (1957).
13) H. Mayer and K. Bernhauer, *Monatsh. Chem.*, **53/54**, 721 (1929).
14) Org. Syntheses, Vol. II, (1922), p. 41.
15) H. T. Clark and E. R. Taylor, *J. Am. Chem. Soc.*, **45**, 830 (1923).

TABLE I
PHYSICAL PROPERTIES OF HYDROCARBONS USED FOR THE DETERMINATIONS

Name	b. p., °C		d_4^{20}		n_D^{20}		Remarks
	Obs.	Lit.[10]	Obs.	Lit.[10]	Obs.	Lit.[10]	
n-Hexane	68.7	68.740	0.6594	0.65937	1.3749	1.37486	a
n-Heptane	98.3	98.427	0.6838	0.68376	1.3878	1.38764	b[8,9]
n-Octane	125.4	125.665	0.7026	0.70252	1.3976	1.39743	a
2,2,4-Trimethylpentane	99.2	99.238	0.6919	0.69192	1.3916	1.39145	b
n-Cetane	286.6	286.793	0.7749	0.77344	1.4350	1.43453	c, m. p. 17.2 Lit. 18.165
Cyclohexane	80.5-81.0	80.738	0.7788	0.77855	1.4263	1.42623	d[11], m. p. 6.32 Lit. 6.554
Methylcyclohexane	100.9	100.934	0.7686	0.76939	1.4231	1.42312	c
Decalin *cis*	189-190	195.69	0.8859	0.8965	1.4750	1.4810	c[12]
Decalin *trans*		187.25		0.8699		1.4695	
Cyclohexene	82.8	82.979	0.8096	0.81096	1.4465	1.44654	c, Br. No. 194.6 Theor. 194.58
1-Octene	122.6	121.280	0.7161	0.71492	1.4086	1.40870	a[11], Br. No. 142.2 Theor. 142.7
Styrene	48/24.1	145.2	0.9059	0.90600	1.5468	1.54682	c[1], Br. No. 151.2 Theor. 153.5
Toluene	110.5	110.625	0.8660	0.86694	1.4961	1.49693	c[8,9]
Ethylbenzene	136.0	136.186	0.8670	0.86702	1.4959	1.49588	a[1]
o-Xylene	144.2	144.414	0.8805	0.88020	1.5045	1.50545	a, m. p. −25.3 Lit. −25.182
m-Xylene	139.1	139.103	0.8636	0.86417	1.4971	1.49722	d, m. p. −47.9 Lit. −47.872
p-Xylene	138.4	138.351	0.8605	0.86105	1.4957	1.49582	a, m. p. 13.2 Lit. 13.263
Propylbenzene	159.2	159.217	0.8619	0.86204	1.4920	1.49202	a
iso-Propylbenzene	152.4	152.392	0.8618	0.86179	1.4912	1.49145	a[13]
Mesitylene	164.7	164.715	0.8647	0.86518	1.4993	1.49937	a[14]
1-Methylnaphthalene	244.4	244.642	1.0200	1.02015	1.6174	1.6174	a
Tetralin	207	207.57	0.9702	0.9702	1.5414	1.54135	d[12]

a) This material was synthesized.
b) This material is the reference fuel for Octane Number determination.
c) Commercially available product was purified according to the ordinary method.
d) Commercially available product was purified according to the description in the literature.

methylation of toluene, and purified by the conversion in to the sulfonate which melted at 86°C after three recrystallizations from water.

Mesitylene was synthesized by sulfuric acid condensation of acetone[14]. 1-Methylnaphthalene was synthesized by the reduction of 1-chloromethylnaphthalene which was obtained by the chloromethylation of naphthalene, and purified by applying chromatographic cleavage of the picrate whose melting point was 141—141.5°C. Methods of purifying for the other materials have been described in the previous paper[8,11,12].

Results

Mutual solubility data of liquid ammonia and paraffins, naphthenes and olefins are given in Table II.

Values for *n*-heptane[9], cyclohexane[1], decalin[12] and purified commercial hexane which is used for the extraction of vegetable oils[1,11] are also given in Table II for convenience of comparison.

As will be clear from Table II, it is observed for liquid ammonia-saturated hydrocarbons systems that within the experimental range, naphthenic hydrocarbons are more soluble in liquid ammonia at a given temperature than paraffins which have the same number of carbon atoms, whereas the quantities of ammonia dissolved in hydrocarbon rich phase are greater in paraffins; it is also observed that solubilities decrease as the molecular weight increases. For binary systems of aliphatic hydrocarbons and liquid ammonia, it is observed that logarithms of solubilities of paraffins in each phase are almost proportional to those of vapor pressures of these hydrocarbons at a given temperature, and that their solubilities are small compared with those of olefins.

The experimental data for aromatic

TABLE II

MUTUAL SOLUBILITY DATA FOR PARAFFINS, NAPHTHENES AND OLEFINS WITH LIQUID AMMONIA, Wt. % OF NH_3

Material	Phase	Temperature, °C					
		30	20	10	0	−7.5	−15
Purified Hexane Used for Vegetable Oil Extraction	Upper		94.4				
	Lower		6.1				
n-Hexane	Upper		94.9_4		97.4_1		
	Lower		5.7_8		3.0_2		
n-Heptane	Upper		96.9_2		98.1_6	98.4_9	98.8_0
	Lower		4.8_5		2.7_3	2.2_3	1.7_1
n-Octane	Upper		97.7_5		98.5_6		
	Lower		4.1_3		2.2_9		
2,2,4-Trimethylpentane	Upper		96.8_9		98.5_1		
	Lower		5.0_8		2.7_3		
n-Cetane	Upper	98.5_7	99.4_4				
	Lower	3.0_8	2.4_3				
Cyclohexane	Upper		94.2_2		96.7_8		
	Lower		3.9_9		2.1_2		
Methylcyclohexane	Upper		94.7_2		97.8_3		
	Lower		4.1_5		2.2_0		
Decalin	Upper		97.8_4		98.3_5		
	Lower		2.2_8		1.4_0		
1-Octene	Upper		93.6_9		96.8_3		
	Lower		7.8_8		4.0_9		
Cyclohexene	Upper	72.6_4	82.1_9	88.0_0	91.6_1		
	Lower	15.2_2	9.3_9	6.3_7	4.5_5		

TABLE III

SOLUBILITY OF AROMATICS IN LIQUID AMMONIA, Wt. % of NH_3

Material	Temperature, °C								
	30	25	20	15	10	5	0	−5	−15.5
Ethylbenzene		miscible			57.0_1	71.4_7	78.1_1	82.2_5	87.0_2
o-Xylene		miscible			61.8_3	72.6_3	78.8_2	82.9_6	
m-Xylene		miscible			69.5_0	76.7_2	81.0_2	84.2_0	
p-Xylene		miscible			64.9_2	74.4_7	79.9_4	83.7_5	
Propylbenzene	miscible		68.5_0	77.3_5	82.8_2	86.4_6	88.8_9		
iso-Propylbenzene	miscible		C.S.T.	70.8_2	78.9_2	83.3_1	86.7_2		
Mesitylene	67.6_7	76.2_0	81.0_9	84.8_5	87.5_7	89.9_2	91.4_4		
1-Methylnaphthalene		64.3_7	71.7_5	77.1_6	81.1_2	83.9_4	85.9_4		
Tetralin			86.3_9				93.7_2		

Temperature, °C (±0.1°)	−10	−15	−20	−25	−30
Material					
Toluene	64.4_4	73.1_8	78.5_9		
Styrene			68.7_6	76.3_4	79.8_8

hydrocarbons are given in Tables III and IV. *p*-Xylene is present as crystals at the experimental temperatures, but the mixture with liquid ammonia was liquid over the experimental temperature range above 5°C. *p*-Xylene-rich layer stayed in a supercooled liquid state at the temperatures of 0° and −5°C, and it was difficult to cause it to crystallize by mere agitation. Occasionally, *p*-xylene-rich layer was caused to crystallize by the stimulation such as the release of a portion of the solution from the bottle containing the system, which closed the reducing valve and made it impossible to continue the experiment. The data for *p*-xylene at the temperatures of 0° and −5°C given in Table IV are values in a supercooled condition. In Tables III and IV, the data for tetralin[12] and toluene[9] are also adopted for comparison from the previous paper.

In Table V are given the results of the determinations of compositions and cloud points for the binary systems of aromatics and liquid ammonia at temperatures near the critical solution temperature. The critical solution temperatures and their compositions estimated graphically from

TABLE IV

SOLUBILITY OF LIQUID AMMONIA IN AROMATIC HYDROCARBONS, WT. % OF NH_3

Material	Temperature, °C								
	30	25	20	15	10	5	0	−5	−15.5
Ethylbenzene		miscible			30.7_6	18.9_0	14.1_3	11.3_1	8.0_0
o-Xylene		miscible			24.3_2	16.9_5	13.0_7	10.8_3	
m-Xylene		miscible			20.2_5	15.0_3	11.8_7	9.6_7	
p-Xylene		miscible			22.1_3	16.1_2	12.7_9	10.3_3	
Propylbenzene	miscible		22.5_4	16.5_5	13.1_7	10.8_9	9.1_5		
iso-Propylbenzene	miscible		C.S.T.	20.5_7	15.2_6	12.2_3	10.0_1		
Mesitylene	21.0_4	15.5_2	12.5_7	10.3_6	8.6_2	7.2_6	6.2_9		
1-Methylnaphthalene		22.2_4	17.3_6	14.3_9	12.1_9	10.4_3	9.1_2		
Tetralin			8.0_9				4.7_1		

Temperature, °C (±0.1°)	−10	−15	−20	−25	−30
Material					
Toluene	20.2_2	15.3_4	12.4_1		
Styrene			20.7_5	14.6_6	11.9_5

TABLE V

CLOUD POINTS AND THEIR COMPOSITION FOR AROMATICS WITH LIQUID AMMONIA

Cloud Pt., °C	NH_3 Wt. %	Cloud Pt., °C	NH_3 Wt. %	Cloud Pt., °C	NH_3 Wt. %
Styrene		*o*-Xylene		*p*-Xylene	
−16.8	27.6_5	11.5	34.3_8	12.3	29.9_3
−16.3	30.2_5	11.9	41.9_7	12.8	42.9_0
−15.85	32.1_1	11.9	45.3_4	12.6	48.0_9
−15.7	34.7_1	11.8	47.9_3	12.6	48.2_2
−15.5	40.3_8	11.5	54.5_5	12.5	52.0_0
−15.5	42.4_4	11.3	56.6_8	11.7	58.0_3
−15.5	43.9_1	11.2	57.0_6	11.6	58.9_9
−15.8	50.2_2	11.1	57.6_2	10.2	64.0_9
−17.8	62.5_3	10.6	60.2_6	12.8*	40.5**
−15.5*	43.9**	11.9*	43.3**		
Ethylbenzene		*m*-Xylene		Propylbenzene	
9.0	26.2_1	14.1	31.6_3	21.3	24.9_3
10.2	32.1_1	14.6	42.1_0	23.6	36.0_4
10.5	36.0_7	14.4	46.5_1	23.9	40.2_3
10.6	37.2_2	13.9	54.0_9	23.9	41.8_7
10.7	44.2_4	13.8	54.9_4	23.0_5	56.7_4
10.4	51.7_7	13.5	56.7_5	22.6	58.8_5
10.1	55.4_4	11.6	65.0_7	22.4_5	59.5_9
0.0	62.2_0	14.6*	41.5**	23.9*	44.7**
10.7*	43.4**				
iso-Propylbenzene		Mesitylene		1-Methylnaphthalene	
18.0	25.2_7	32.6	26.8_2	26.0	23.7_3
19.0_5	28.5_0	33.8	36.5_1	27.4	27.4_1
19.8	34.2_3	33.9	39.6_2	27.4_5	27.4_8
20.0	42.5_7	33.9	41.8_3	28.6	36.1_7
19.9	48.5_3	33.9	45.0_2	28.8	42.3_4
19.7	52.7_4	33.9	45.4_7	28.8	44.4_7
19.6	54.3_4	33.8_5	48.7_2	28.7_5	47.6_7
19.3	56.7_8	33.7	52.7_3	28.7	48.8_3
18.0	63.7_3	33.6	53.0_7	28.5	50.9_3
20.0*	71.7**	33.5_2	53.6_1	28.2	53.5_2
		32.9	59.5_6	27.0	59.2_6
		32.4_5	61.1_8	28.8*	42.6**
		33.9*	42.9**		

* Critical solution Temperature.
** Critical Composition.

the data given in Tables III, IV and V are also given in Table V.

The critical solution temperatures for toluene[9] and *iso*-propylbenzene with liquid ammonia in the present investigation, −7.4° and 20.0°C, are lower than those given in the literature[6], −5° and 25°C, respectively. But, the value for *m*-xylene, 14.6°C, agrees with that obtained by Kraus, et al.[1], 14.7°C, which is believed to be accurate. The critical composition for this system is 81.5 mole per cent. of ammonia and compared with the Kraus' value of 81.4 mole per cent. ammonia. The critical solution temperature for 1-methylnaphthalene with liquid ammonia is 28.8°C by the present determination, compared with the Francis' value of 28°C[6].

In the case of all these systems, it will be clear from Tables II, III and IV that solubilities in both phases are smaller at lower temperatures exhibiting positive deviations from Raoult's law, and roughly symmetrical on the basis of weight fraction. However, as the molecular weight of ammonia is considerably small compared with that of any other component, the solubility curves lean to the ammonia side on the basis of mole fraction expressing unsymmetrical form, as shown in Fig. 1. The mole fractions of ammonia in hydrocarbon-rich phase are greater than those of oils in liquid ammonia rich phase. Solubilities of these hydrocarbons in liquid ammonia are less than 10 mole per cent., except for the cases in the neighborhood of the critical solution temperature, and the solubility change in ammonia-rich phase due to temperature variation is small compared with that in the hydrocarbon-rich phase.

In Fig. 1, in addition to the mutual solubilities of aromatic hydrocarbons and liquid ammonia, the concentrations of ammonia in hydrocarbon-rich phase for other representative hydrocarbons are shown on the basis of mole fraction. The values of Kraus, et al. for *m*-xylene are also given for comparison. Solubility curves for paraffins, naphthenes and olefins in liquid ammonia-rich phase are omitted in the figure except for *n*-heptane, because they are so nearly of the same order that the curves for them can not be expressed clearly without overlapping.

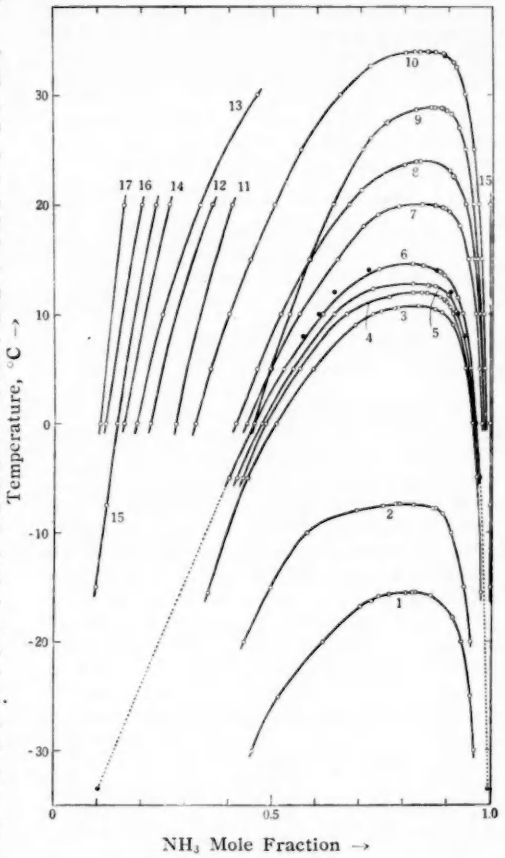

Fig. 1. Solubility curves for some hydrocarbons and liquid ammonia.

1. Styrene
2. Toluene
3. Ethylbenzene
4. *o*-Xylene
5. *p*-Xylene
6. *m*-Xylene (• Kraus value)
7. *iso*-Propylbenzene
8. Propylbenzene
9. 1-Methylnaphthalene
10. Mesitylene
11. Tetralin
12. 1-Octene
13. Cyclohexene
14. 2, 2, 4-Trimethylpentane
15. *n*-Heptane
16. Methylcyclohexane
17. Decalin

Summary

In order to obtain the quantitative knowledge on the solubility relations for liquid ammonia systems, mutual solubilities of aromatic hydrocarbons and liquid ammonia were determined at the several temperatures near the critical

solution temperature, and data for other hydrocarbons were mainly obtained at 20° and 0°C. These results were presented in tables and a figure.

The Chemical Research Institute of Non-Aqueous Solutions Tohoku University Katabira-cho, Sendai

Mutual Solubilities of Some Hydrocarbon Oils and Liquid Ammonia. II. Application of the Solubility Parameter Theory

By Kiyoharu ISHIDA

(Received September 13, 1957)

The simple expression according to solubility parameter theory which has been developed by Hildebrand[1,2] and Scatchard[3] about nonpolar components, or its variant with the Flory-Huggins configurational term, has proved useful in interpreting qualitatively and often semi-quantitatively a wide variety of nonelectrolyte solutions including those of high polymers, especially when solubility phenomena are involved and when components are nonpolar. Liquid ammonia has not only a rather high dielectric constant and a dipole moment, but also hydrogen bonding capacity, although weaker than that of water or hydrogen fluoride. However, it has been observed that this theory interprets satisfactorily the solubility relationships even for the case including polar components such as water and aniline; for the systems of hydrocarbons and aniline, hydrocarbons and water, etc., values for solubility parameter of polar component, obtained from the solubility using the expression according to solubility parameter theory, are almost identical with values calculated from the vaporization energy[2]. It is interesting to study what relations are obtained for liquid ammonia systems. And also, some knowledge of the special interaction induced by polarity might be given from the differences between the theory and the experiment, which are obtained by applying the solubility data for liquid ammonia and hydrocarbon oils to the solubility parameter theory.

1) J. H. Hildebrand, *J. Am. Chem. Soc.*, **38**, 1452 (1916); **41**, 1067 (1919); **42**, 2180 (1920); **51**, 66 (1929); **57**, 866 (1935). J. H. Hildebrand and S. E. Wood, *J. Chem. Phys.*, **1**, 817 (1933).

2) J. H. Hildebrand and R. L. Scott, "The Solubility of Nonelectrolytes", 3rd. Ed., Reinhold Pub. Corp., New York, 1950.

3) G. Scatchard, *Chem. Revs.*, **8**, 321 (1931); *Trans. Faraday Soc.*, **33**, 160 (1937).

Expressions according to the Solubility Parameter Theory

Solubility parameter theory, which is derived under the assumption that in a mixture of two nonpolar molecules having spherical symmetry, the partial molal free energy of a component is the sum of a term from the entropy of mixing which is assumed to be ideal, and one from the heat of mixing which is derived from the London theory of dispersion forces neglecting the difference between arithmetic and geometric means, may be expressed in its simplest form as follows:

$$\boldsymbol{RT} \ln \gamma_1 = V_1 \varphi_2^2 (\delta_1 - \delta_2)^2 \qquad (1a)$$

$$\boldsymbol{RT} \ln \gamma_2 = V_2 \varphi_1^2 (\delta_1 - \delta_2)^2 \qquad (1b)$$

where γ_1 and γ_2 are the respective activity coefficients, V_1 and V_2 are the molal volumes of the pure components, φ_1 and φ_2 are the volume fractions, and δ_1 and δ_2 are solubility parameters defined as

$$\delta = (\Delta E^v / V)^{1/2} \qquad (2)$$

where ΔE^v is the energy of vaporization of the pure component and V its molal volume, all at the temperature T. $\Delta E^v / V$ is of course the "internal pressure" or "cohesive energy density". Equations (1a) and (1b) are exactly equivalent to equations of the form given by van Laar,[4] equations (3a, b) and (12).

Further complications are introduced if the effect of volume change on mixing or difference in molecular size is taken into consideration. Solutions which exhibit positive deviations from Raoult's law are formed from their constituents with an absorption of heat and volume expansion, although effect on volume change is fairly small. Effect of differences in molecular

4) J. J. van Laar, *Z. physik. Chem.*, **72**, 723 (1910).

size upon the entropy of mixing can not be disregarded when molecular volumes are considerably different, and exhibit negative deviations from the ideal entropy ($-R\ln x$). However, it has recently been confident[5] that since expansion of volume on mixing increases both the entropy and the enthalpy, free energy or isothermal solubility may be treated without serious error by the equations (1a, b) in which the entropy of mixing is assumed to be ideal and volume changes on mixing are neglected, despite the fact that both the actual entropy and the enthalpy are far from ideal.

When the volumes V_1 and V_2 in equations (1a, b) are replaced by empirical parameters q_1 and q_2 which may be related to the "effective volumes" of molecules of different shapes, and the term of intermolecular energy on mixing is represented by the more generalized form of D included also the contributions due to polarity instead of $\left\{\left(\frac{\Delta E_1^v}{q_1}\right)^{1/2}-\left(\frac{\Delta E_2^v}{q_2}\right)^{1/2}\right\}^2$, extensive empirical use of the van Laar equation may be possible even in the case of containing polar components, as well as nonpolar components. Then, equations (1a, b) may lead to

$$\log\gamma_1=A_{12}\Big/\left(1+\frac{x_1A_{12}}{x_2A_{21}}\right)^2 \qquad (3a)$$

$$\log\gamma_2=A_{21}\Big/\left(1+\frac{x_2A_{21}}{x_1A_{12}}\right)^2 \qquad (3b)$$

and

$$A_{12}=q_1D/2.303RT \qquad (4a)$$

$$A_{21}=q_2D/2.303RT \qquad (4b)$$

where x_1 and x_2 are the respective mole fractions, and A_{12} and A_{21} the van Laar constants.

Critical solution temperature, T_c, and the critical composition, x', are obtained by applying the following conditions to both components:

$$\partial a/\partial x=0, \qquad \partial^2 a/\partial x^2=0$$

where a is the activity.

When activity coefficients are expressed by Eqs. (1a, b), the followings are obtained:

$$RT_c=\frac{2x_1'x_2'V_1^2V_2^2}{(x_1'V_1+x_2'V_2)^3}(\delta_1-\delta_2)^2 \qquad (5)$$

and at T_c,

$$x_1'=1-x_2'=\frac{(V_1^2+V_2^2-V_1V_2)^{1/2}-V_1}{V_2-V_1} \qquad (6)$$

If the molal volumes of two components are noticeably unequal and the Flory-Huggins equation[6] is applicable to the athermal mixing of liquids, and the relation of activity follows to equations of the form (7),

$$\ln\gamma_1=\ln V_1-\ln(x_1V_1+x_2V_2)+\varphi_2\left(1-\frac{V_1}{V_2}\right)+V_1\varphi_2^2D/RT \qquad (7)$$

then, T_c and x' may be obtained from the equations (8) and (9), respectively:

$$RT_c=\frac{2\varphi_1\varphi_2V_1V_2}{V_1\varphi_1+V_2\varphi_2}D \qquad (8)$$

and at T_c,

$$\varphi_1=\frac{V_2-(V_1V_2)^{1/2}}{V_2-V_1}, \quad x_1'=\frac{V_2^{3/2}}{V_1^{3/2}+V_2^{3/2}} \qquad (9)$$

TABLE I

COMPARISON OF D CALCULATED FROM CRITICAL DATA WITH $(\delta_1-\delta_2)^2$.
Suffix 1 and 2 represent hydrocarbon and liquid ammonia, respectively

Component, 1	T_c, °K	Eq. (10) δ_1	Eq. (10) δ_2	$(\delta_1-\delta_2)^2$	D, Eq. (5) using obs. value for x_1'	D, Eq. (5) using calcd. value by Eq. (6) for x_1'	obs. x_1'	Eq. (6) x_1'
Toluene	265.8	9.36	13.40	16.32	16.23	15.14	0.200	0.134
Styrene	257.7	9.65	13.68	16.24	14.50	13.79	0.173	0.122
Ethylbenzene	283.9	8.93	12.70	14.21	14.92	14.07	0.173	0.119
o-Xylene	285.1	9.12	12.66	12.53	15.04	14.13	0.174	0.120
m-Xylene	287.8	8.94	12.56	13.10	15.29	14.07	0.184	0.118
p-Xylene	286.0	8.91	12.63	13.84	15.43	13.97	0.191	0.117$_5$
Propylbenzene	297.1	8.64	12.16	12.39	13.49	12.83	0.149	0.105
iso-Propylbenzene	293.2	8.62	12.34	13.84	13.86	12.72	0.165	0.104
Mesitylene	307.1	8.66	11.73	9.43	14.02	13.17	0.159	0.107
1-Methylnaphthalene	302.0	10.0*	11.96	3.84	13.38	13.00	0.139	0.106

* Calculated by the equation[10], $\Delta H^v_{298}=-2950+23.7\,Tb+0.020\,Tb^2$.

5) L. W. Reeves and J. H. Hildebrand, *J. Phys. Chem.*, **60**, 949 (1956).

6) M. L. Huggins, *J. Chem. Phys.*, **9**, 449 (1941); P. J. Flory, ibid., **9**, 660 (1941); **10**, 51 (1942).

TABLE II

COMPARISON OF ACTIVITY COEFFICIENTS AT INFINITE DILUTION

Suffiix 1 and 2 represent hydrocarbon and liquid ammonia, respectively

Component, 1	Temp. °C	V_1 ml./mole	δ_1 (cal./ml.)$^{1/2}$	$\frac{V_1(\delta_1-\delta_2)^2}{2.303RT}$	A_{12}	$\frac{V_2(\delta_1-\delta_2)^2}{2.303RT}$	A_{21}	$\frac{A_{12}}{A_{21}}\frac{V_1}{V_2}$
n-Hexane	20	130.6	7.42	2.36	1.991	0.50	0.782	0.544
	0	127.2	7.61	3.10	2.282	0.65	0.986	0.485
n-Heptane	20	146.5	7.54	2.52	2.244	0.48	0.773	0.553
	0	142.9	7.76	3·30	2.481	0.62	0.959	0.483
n-Octane	20	162.8	7.59	2.74	2.424	0.47	0.773	0.538
	0	159.2	7.90	3.48	2.638	0.58	0.969	0.456
n-Cetane	20	292.3	7.64[a]	4.81	3.276	0.46	0.691	0.452
2, 2, 4-Trimethyl-pentane	20	165.1	6.92	3.62	2.280	0.61	0.713	0.540
	0	161.5[b]	7.17	4.59	2.616	0.76	0.907	0.476
Cyclohexane	20	108.0	8.34	1.29	1.944	0.33	0.919	0.546
	0	105.5[f]	8.89	1.52	2.193	0.38	1.127	0.492
Methylcyclohexane	20	127.6	7.90	1.88	2.031	0.41	0.848	0.524
	0	124.7[b]	8.15	2.47	2.422	0.53	1.047	0.495
1-Octene	20	157.0	7.49[c]	2.75	1.968	0.49	0.605	0.579
	0	153.7[d]	7.79[c]	3.51	2.280	0.61	0.791	0.500
Cyclohexene	20	101.3	8.50[e]	1.11	1.492	0.31	0.710	0.579
	0	98.8[b]	8.84[e]	1.45	1.787	0.39	0.898	0.537
Ethylbenzene	0	119.1	9.01	1.62	1.478	0.36	0.529	0.625
o-Xylene	0	118.2	9.24	1.43	1.491	0.32	0.547	0.615
m-Xylene	0	120.3	9.09	1.57	1.532	0.35	0.565	0.601
p-Xylene[f]	0	120.7	9.04	1.62	1.511	0.36	0.549	0.608
Propylbenzene	20	139.4	8.68	1.39	1.376	0.28	0.413	0.666
	0	136.9	8.82[a]	2.03	1.767	0.40	0.566	0.609
iso-Propylbenzene	0	136.7[b]	8.75	2.10	1.697	0.41	0.550	0.602
Mesitylene	20	138.9	8.85	1.26	1.561	0.25	0.511	0.613
	0	136.5[g]	9.09[a]	1.78	1.888	0.35	0.664	0.555
1-Methylnaphtha-lene	20	139.4	10.05[c]	0.54	1.449	0.11	0.417	0.695
	0	137.6[g]	10.30[c]	0.88	1.725	0.17	0.528	0.633
Decalin	20	156.0[g]	7.85[h]	2.34	2.540	0.42	0.909	0.500
	0	153.4[h]	8.08[a,h]	3.13	2.670	0.54	1.079	0.430
Tetralin	20	136.1	9.50[i]	0.82	1.726	0.17	0.583	0.606
	0	133.8[i]	9.73[a]	1.24	2.053	0.25	0.711	0.576

Liquid ammonia, at 20°C, $V_2=27.90$, $\delta_2=12.34$; at 0°C, $V_2=26.67$, $\delta_2=13.13$

a) ΔH^v was estimated by extrapolation.
b) Calculated from Geist and Cannon's data[12].
c) Calculated from the equation[13], $\delta=4.1(\gamma/V^{1/3})^{0.43}$. Surface tension for 1-methylnaphthalene was estimated from parachor[19] neglecting vapor density.
d) Estimated from surface tension[14] and density at 20°C assuming that the dependency of parachor upon temperature and vapor density are negligible.
e) ΔH was estimated from vapor pressure-temperature relations according to Lister[15].
f) Values in the supercooled condition.
g) Observed value.
h) Calculated value as a mixture of 60% *cis* form and 40% *trans* form. Seyer's data[16] for density were used in calculation.
i) Estimated by extrapolation from the data in reference[17].

In equations (6) and (9) the composition at the critical solution temperature is expressed in terms of molal volumes only.

Comparison of Solubility Data with Theory

The values for the term of intermolecular energy on mixing, D, calculated from Eq. (5) using the data on the critical point for some aromatic hydrocarbons with liquid ammonia reported in Part I are shown in Table I, compared with the values obtained from heat of vaporization at each of critical solution temperature. The values of critical compositions calculated from Eq. (6) are also given in Table I, and compared with the values which are obtained graphically from the solubility data in the neighborhood of the critical solution temperature. The solubility parameter of hydrocarbons, δ_1, and

TABLE III

COMPARISON OF VAN LAAR CONSTANTS FROM MUTUAL SOLUBILITIES WITH THOSE FROM EQUATION (12)

Suffix 1 and 2 represent hydrocarbon and liquid ammonia, respectively

	Temp. °C	P[19]	ΔE^v kcal./mole	A_{12}		A_{21}	
				Eq.	obs.	Eq.	obs.
n-Heptane	20	311.3	8.34	0.325	2.244	0.110	0.773
2,2,4-Trimethylpentane	20	343.7	7.92	0.542	2.280	0.171	0.713
Methylcyclohexane	20	281.6	7.95	0.279	2.031	0.101	0.848
1-Octene	20	339.6[a]	8.80[b]	0.349	1.968	0.111	0.605
Cyclohexene	20	230	7.32[c]	0.188	1.492	0.078	0.710
m-Xylene	0	284.2	9.94	0.151	1.532	0.054	0.565
Propylbenzene	0	323.1	10.66	0.182	1.767	0.060	0.566
Decalin	20	369.4	9.60	0.321	2.540	0.097	0.909
Tetralin	20	335.9	12.29	0.013	1.726	0.0042	0.583
1-Methylnaphthalene	20	353.8	14.08[b]	0.002	1.449	0.0006	0.417
Liquid ammonia	20	61.1[d]	4.25				
	0	60.8[d]	4.60				

a) Estimated from surface tension[14] and liquid density neglecting vapor density.
b) Cf. Table II, c. Estimated from δ.
c) Cf. Table II, e.
d) Calculated value. Values according to King[20] were used for surface tension and densities for liquid and vapor were taken from "International Critical Tables", Vol. III, p. 235.

of liquid ammonia, δ_2, were estimated from the equation[2]

$$\delta=\left(\frac{\Delta H^v-RT}{V}\right)^{1/2} \tag{10}$$

where ΔH^v is the heat of vaporization at temperature T. Heats of vaporization for hydrocarbons at T_c were evaluated from the slopes of the vapor pressure—temperature curves[7]. Heat of vaporization for liquid ammonia[8] and most of densities[9] used in calculating molal volumes were taken from tabulations. The critical compositions derived from the equation (6) agree with the experimental values qualitatively, but not quantitatively. However, except for two systems of mesitylene-liquid ammonia and 1-methylnaphthalene-liquid ammonia, the values for D or solubility parameter of ammonia, δ_2, calculated from Eq. (5) are, surprisingly enough, practically identical with that obtained from the heat of vaporization and the molal volume at the critical solution temperature, as in the cases of hydrocarbon-aniline system and hydrocarbon-water system. But, this agreement should be regarded as sheer good luck, owing to a compensation of disturbing factors.

As the solubility parameter of ammonia obtained from the data for the critical point is almost identical with the value calculated from the heat of vaporization as stated above, it seems that this agreement is held at other temperatures. Namely, the following equation may be written approximately;

$$D=(\delta_1-\delta_2)^2 \tag{11}$$

In Table II, logarithms of activity coefficients at infinite dilution at the temperatures 0° and 20°C which are calculated according to equations (1a, b) or (4a, b) assumed $q=V$ and (11) are given, compared with the experimental values for the van Laar constants which are obtained from the mutual solubility data in Part I according to the equations derived by Carlson and Colburn[11]. A_{12} and A_{21} are logarithums of activity coefficients at infinite dilution of hydrocarbons in liquid ammonia-rich layer and of liquid ammonia in hydrocarbon-rich layer, respectively.

Although the experimental error and uncertainty of the numerical values for

7) D. R. Stull, *Ind. Eng. Chem.*, **39**, 517 (1947).
8) "International Critical Tables", McGraw-Hill Book Company Inc., New York, 1928, Vol. V, p. 138.
9) Ibid., Vol. III, p. 27.
10) Cf. ref. 2, p. 427.
11) H. C. Carlson and A. P. Colburn, *Ind. Eng. Chem.*, **34**, 581 (1942).
12) J. M. Geist and M. R. Cannon, *Ind. Eng. Chem. Anal. Ed.*, **18**, 611 (1946).
13) Cf. ref. 2, p. 431.
14) J. J. Jasper and E. R. Kerr, *J. Am. Chem. Soc.*, **76**, 2659 (1954).
15) M. W. Lister, ibid., **63**, 143 (1941).
16) W. F. Seyer and C. H. Davenport, ibid., **63**, 2425 (1941).
17) S. Doldi, *Ann. chim. applicata*, **28**, 454 (1938); *Chem. Abst.*, **33**, 5250[5] (1939).

TABLE IV

COMPARISON OF D AND CRITICAL COMPOSITION ASSUMING DIMERIZATION OF AMMONIA WITH THOSE NOT ASSUMING DIMERIZATION

Suffix 1 and 2 represent hydrocarbon and liquid ammonia, respectively

Component, 1		Assuming $V_1=q_1$, $V_2=q_2$			Assuming $V_1=q_1$, $2V_2=q_2$				
		D	x_1'		D		x_1'		
	$(\delta_1-\delta_2)^2$	Eq. (8)	obs.	Eq. (9)	Eq. (8)	Eq. (5)	obs.	Eq. (9)	Eq. (6)
Toluene	16.32	22.75	0.200	0.114	14.79	13.22	0.334	0.266	0.272
Styrene	16.24	21.74	0.173	0.101	13.99	12.19	0.295	0.241	0.249
Ethylbenzene	14.21	22.50	0.173	0.097	14.46	12.47	0.295	0.234	0.243
o-Xylene	12.53	22.61	0.174	0.099	14.54	12.57	0.296	0.237	0.245
m-Xylene	13.10	22.57	0.184	0.097	14.50	12.49	0.312	0.232	0.241
p-Xylene	13.84	22.48	0.191	0.096	14.43	12.41	0.320	0.231	0.240
Propylbenzene	12.39	21.97	0.149	0.083	13.98	11.53	0.260	0.203	0.215
iso-Propylbenzene	13.84	21.86	0.165	0.082	13.91	11.44	0.284	0.202	0.214
Mesitylene	9.43	22.28	0.159	0.085	14.20	11.81	0.274	0.208	0.220
1-Methylnaphthalene	3.84	22.13	0.139	0.084	14.10	11.67	0.244	0.206	0.217

TABLE V

COMPARISON OF VAN LAAR CONSTANTS ASSUMING DIMERIZATION OF AMMONIA WITH THOSE NOT ASSUMING DIMERIZATION

Component, 1	Temp. °C	Assuming NH_3				Assuming $(NH_3)_2$					
		A_{12}		A_{21}		A_{12}			A_{21}		
		Eq. (7)	obs.	Eq. (7)	obs.	obs.	Eq. (7)	Eq. (1)	obs.	Eq. (7)	Eq. (1)
n-Heptane	20	1.39	2.244	0.11	0.773	2.003	2.23	2.52	1.020	0.81	0.96
2, 2, 4-Trimethylpentane	20	2.26	2.280	0.20	0.713	2.045	3.24	3.62	0.956	1.04	1.22
Methylcyclohexane	20	0.98	2.031	0.09	0.848	1.787	1.68	1.88	1.099	0.71	0.82
1-Octene	20	1.28	1.968	0.09_6	0.605	1.975	2.42	2.75	0.941	0.81	0.98
Cyclohexene	20	0.53	1.492	0.06	0.710	1.282	1.02	1.11	0.943	0.55	0.61
m-Xylene	0	0.70	1.532	0.03	0.565	1.343	1.38	1.57	0.789	0.58	0.70
Propylbenzene	0	0.95	1.767	0.03_6	0.566	1.569	1.76	2.03	0.793	0.65	0.79
Decalin	20	0.30	2.540	−0.11	0.909	2.280	1.22	1.55	1.166	0.39	0.55
Tetralin	20	−0.18	1.726	−0.18	0.583	1.526	0.58	0.82	0.811	0.20	0.34
1-Methylnaphthalene	20	−0.49	1.449	−0.24	0.417	1.295	0.29	0.54	0.623	0.08	0.22

solubility parameters used in the calculation should be taken into account, values of A_{12} according to equations (1a, b), $V_1(\delta_1-\delta_2)^2/2.303RT$, are generally similar to those calculated from the mutual solubility data but A_{21}'s are smaller. It may be shown from this result that the effective volumes, $q's$, are not exactly identical with molal volumes and they are related not only to molecular volumes, but also to their shapes and surfaces.

The semi-empirical expression proposed by Erdos[18] for calculating the constants of van Laar equations from the properties of pure components, which may be considered as a modification replaced the molal volumes in equations (1a, b) by the surface areas in terms of parachors, may be written as follows:

$$A_{12}=\frac{P_1^{2/3}}{2.303RT}\left\{\left(\frac{\Delta E_1}{P_1^{2/3}}\right)^{1/2}-\left(\frac{\Delta E_2}{P_2^{2/3}}\right)^{1/2}\right\}^2 \qquad (12)$$

where P_1 and P_2 are the parachors of the pure components 1 and 2.

The values for some representative compounds calculated from equation (12) are shown in Table III, compared with the experimental values. The ratios of effective volumes, A_{12}/A_{21}, almost agree with the experimental values, but values for each van Laar constant calculated according to equation (12) are considerably smaller than the experimental values, and the disagreement between these values is greater when compared with that obtained

18) E. Erdös, *Chem. Listy*, **50**, 503 (1956); *Chem. Abst.* **50**, 11752g (1956).

by equations (1a, b), or equations (4a, b) assuming $q=V$ and equation (11). It may be considered from the results shown in Table III that the effective volumes related to the difference in molecular shape or effective surface can not be expressed with only the surface areas in terms of parachors.

As the molal volumes of ammonia and hydrocarbons are considerably different, it may be impossible to expect the entropy of mixing to be ideal. The critical compositions for aromatic hydrocarbons with liquid ammonia obtained by equation (9) which is derived under the assumption that the entropy of mixing is expressed by the Flory-Huggins equation, are shown in the left half column of Table IV. Values for D which are calculated by equation (8) using the calculated values for critical compositions by equation (9) are also shown in Table IV. Calculated values for D by equation (8) are considerably greater and for compositions by equation (9) are smaller, and the disagreement is larger than the result shown in Table I, the reason being that the Flory-Huggins equation may be almost an over-correction for the size effect[5].

Ratio of van Laar constants, A_{12}/A_{21}, namely, the ratio of effective volumes corresponds to molal volume ratio in equations (1a, b), V_1/V_2. The ratios of effective volumes to those of molal volumes are given in the last column in Table II. For every case of the long chain molecule such as *n*-paraffin, the plain molecule of aromatic hydrocarbon and the semi-spherical one of *iso*-octane, values for V_1/V_2 are larger than A_{12}/A_{21}, and the ratios of the latter to the former are about 0.5 in all systems of hydrocarbon oils and liquid ammonia which have been studied. Morever, this ratio at lower temperature for a binary mixture is less than that at higher temperature; namely, it shows that effective volume for liquid ammonia derived from the solubility data is larger at lower temperature. Ratios for styrene and toluene at low temperatures, which are given in Table II, show also the same result. It will be seen from these results that though the different shape and surface of molecule may be related to the effective volume, they are not large factors for these ammonia systems, and that when V_2 is roughly doubled the ratios of molal volumes are almost similar to those of effective volumes. The change for molal volume of liquid ammonia, V_2, results in the change of mole fraction and so van Laar constants. But it may be clear that unless V_2 becomes larger, theoretical values are too far apart from the experimental.

In the case of water having strong hydrogen bonding capacity, the presence of the association states of 2, 4, and 8 molecules has been considered in addition to H_2O[21]. Also in the case of ammonia, the dimerization of ammonia has been known even in the gaseous state[22], and the molecular weight of liquid ammonia has been found to be 24.5 from the surface tension determination[20]. It is probable that a different kind of association may occur in various rates in liquid ammonia and its solution. If ammonia is assumed to form double molecules in liquid state on the average, for the sake of simplicity, the apparent mole fraction will be different from that for single molecule, but the value for solubility parameter calculated by equation (10) would be scarecely different from δ_2 used in the preceding calculations, since the dimerization of ammonia in vapor phase is almost negligible[22] and the heat of vaporization per gram is identical for both NH_3 and $(NH_3)_2$.

Values for D and for the critical composition, x', by equations (8) and (9) or (5) and (6) assuming the dimerization of ammonia are given in the right half column of Table IV, where the agreement with the experimental values is improved compared with those of the left half column calculated for the case of not assuming the association. Table V shows the comparison of the observed van Laar constants for representative compounds with values calculated from equation (7) assuming no association of ammonia and with values obtained by equations (7) and (1a, b); in both cases ammonia is assumed to form double molecules in liquid.

The result obtained by assuming the dimerization of ammonia may exhibit a far closer agreement than that the dimerization is not assumed, in view of all the approximations involved.

Summary

The result of the comparison of experimental data for the critical compositions

19) O. R. Quayle, *Chem. Revs.*, **53**, 439 (1953).
20) H. H. King, J. L. Hall and G. C. Ware, *J. Am. Chem. Soc.*, **52**, 5128 (1930).
21) A. Eucken, *Nachr. Akad. Wiss. Göttingen, Math.-physik. Klasse*, 38 (1946); *Chem. Abst.*, **43**, 7283d (1949); *Z. Elektrochem.*, **52**, 255 (1948); **53**, 102 (1949).
22) J. D. Lambert and E. D. T. Strong, *Proc. Roy. Soc.*, A, **200**, 565 (1960).

and the logarithms of activity coefficients at infinite dilution for binary systems of some hydrocarbon oils and liquid ammonia with those expected from the solubility parameter theory, is that the solubility relations may be more satisfactorily interpreted by the theory by assuming that ammonia is associated nearly to dimerized form in the liquid state.

The author is greatly indebted to Professor T. Toriumi for his interest and encouragement during this investigation.

The Chemical Research Institute of Non-Aqueous Solutions, Tohoku University, Katabira-cho, Sendai

The Infrared Spectra of Ethoxy- and Methylethoxy-polysiloxanes

By Rokuro ŌKAWARA

(Received August 26, 1957)

In this report, the studies of infrared spectra of three types of methylethoxypolysiloxanes represented by A, B and C, and linear and cyclic ethoxypolysiloxanes D and E will be described, of which the spectra of A_1[1], B_1[1] and D_1[2] have already been reported briefly.

A_n $C_2H_5O((CH_3)_2SiO)_nC_2H_5$ $n=1,2,3,4$
B_n $C_2H_5O((CH_3)Si(OC_2H_5)O)_nC_2H_5$ $n=1,2,3,4,5$
C_n $((CH_3)Si(OC_2H_5)O)_n$ $n=3,4$
D_n $C_2H_5O(Si(OC_2H_5)_2O)_nC_2H_5$ $n=1,2,3$
E_n $(Si(OC_2H_5)_2O)_n$ $n=4,5$

One of the objects of this study is to find characteristic absorption bands associated with the group $(Si)OC_2H_5$*. The spectra of methylpolysiloxanes F and G, which were discussed by Wright[3] and Richards[1], are used to explain the spectra obtained in this study.

F $CH_3((CH_3)_2SiO)_nSi(CH_3)_3$
G $((CH_3)_2SiO)_n$

Experimental

Materials.—The preparation and the properties of the members of B, C and E used in this experiment have already been reported[4,5]. Authentic samples were used for the measurement of the spectra of A and D.

Measurements.—Spectra were obtained with a Hilger H-800 infrared spectrophotometer with a rock salt prism. Samples were used both as pure liquid and as solutions, 2—5% in carbon disulfide for 700 to 1500 cm^{-1}, and 5—10% in carbon tetrachloride for 1250 to 3500 cm^{-1}. No appreciable difference was observed between the two cases. The cells were 0.03 mm. thick for the solution and less than 0.01 mm. for pure liquid. In order to compare relative intensity, the absorption of the compounds belonging to the same series was recorded on the same chart, keeping the conditions as much alike as possible.

TABLE I
INFRARED SPECTRA OF METHYLETHOXYPOLYSILOXANES: POSITIONS OF BANDS (in cm^{-1})

A_n					B_n						C_n	
$n=1$*	$n=1$	$n=2$	$n=3$	$n=4$	$n=1$*	$n=1$	$n=2$	$n=3$	$n=4$	$n=5$	$n=3$	$n=4$
798	785	797	798	803	732		759	760	760	762	755	761
841	835	841	838	844	780	775	779	785	784		791	
846					806		794	799		791	809	801
953	949	955	953	952	820	818						
		1059	1043	1034	831	824	820	821	820	827	843	
1078	1075	1080	1080	1078	960	956	959	958	960	959	960	957
1105	1102	1111	1109	1111			1060	1056	1060	1056	1023	1068
1166	1160	1162	1156	1162	1078	1074	1073	1071	1071	1070	1078	1087
1260	1254	1256	1256	1256	1100	1098	1099	1096	1096	1096		
					1120		1116	1114	1117	1114	1111	1117
					1166	1164	1163	1162	1162	1158	1160	1159
					1266	1259	1260	1260	1259	1262	1260	1262

* R. E. Richards and H. W. Thompson, *loc. cit.*[1]

1) R. E. Richards and H. W. Thompson, *J. Chem. Soc.*, **1949**, 124.
2) I. Šimon and H. O. McMahon, *J. Chem. Phys.*, **20**, 905 (1952).
3) N. Wright and M. J. Hunter, *J. Am. Chem. Soc.*, **69**, 803 (1947).

* $(Si)OC_2H_5$ indicates an ethoxy group attached to silicon atom.
4) R. Ōkawara, S. Hotta and T. Shimura, This Bulletin, **28**, 541 (1955).
5) R. Ōkawara, G. Minami and Z. Oku, ibid., **31**, (1958).

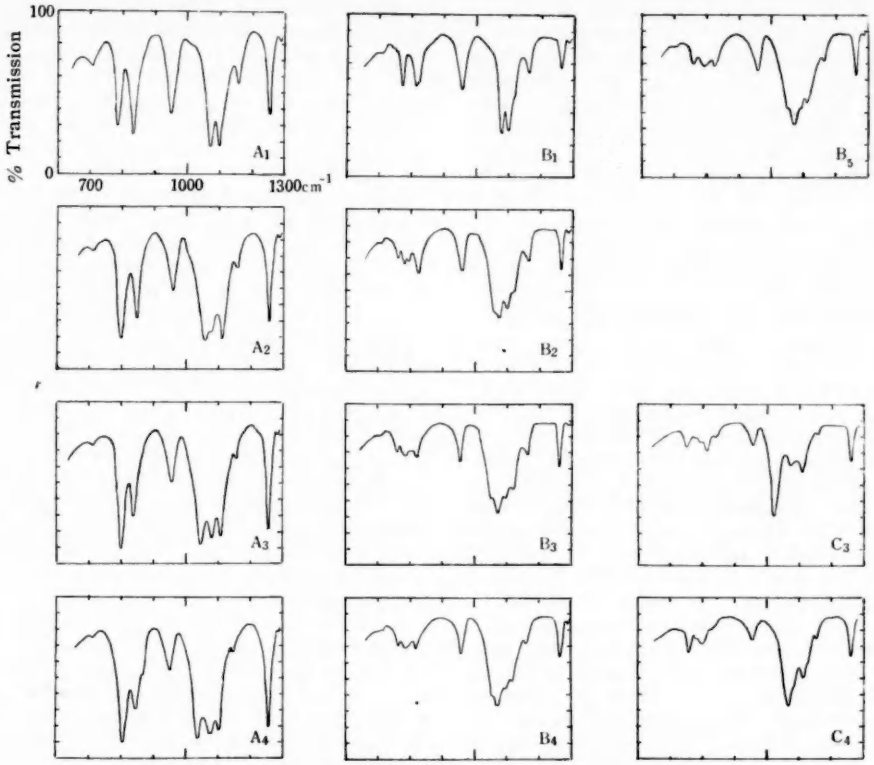

Fig. 1. Infrared spectra of methylethoxypolysiloxanes.

A_n: $C_2H_5O((CH_3)_2SiO)_nC_2H_5$, 5% in CS_2
B_n: $C_2H_5O((CH_3)Si(OC_2H_5)O)_nC_2H_5$, 3% in CS_2
C_n: $((CH_3)Si(OC_2H_5)O)_n$, 2% in CS_2

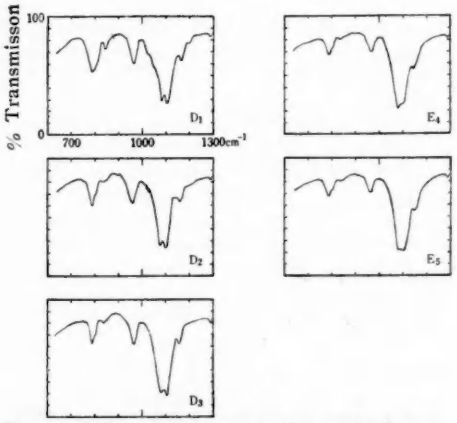

Fig. 2. Infrared spectra of ethoxypolysiloxanes.
D_n: $C_2H_5O(Si(OC_2H_5)_2O)_nC_2H_5$, 2% in CS_2
E_n: $(Si(OC_2H_5)_2O)_n$, 2% in CS_2

TABLE II
INFRARED SPECTRA OF ETHOXYPOLYSILOXANES: POSITIONS OF BANDS (in cm^{-1})

D_n			E_n	
$n=1$	$n=2$	$n=3$	$n=4$	$n=5$
790	790	788	791	790
846	847	848		
962	966	968	968	968
1081	1079	1080	1078	1079
1104	1102	1102	1101	1099
1163	1162	1160	1163	1163

The spectra of A, B and C, and those of D and E are shown in Fig. 1 and Fig. 2, respectively. The positions of the bands up to 1300 cm^{-1} are given in Table I and II.

Discussion of the Results

In the region 750—1000 cm^{-1}, there are some strong bands. Among them the one

near 930 cm^{-1} has an approximately constant wave number and no neighboring absorption band in any of the compounds investigated. Since this band does not appear in F and G, it seems certain that the band is associated with the grouping $(Si)OC_3H_5$. This presumption is further supported by comparing the relative intensity of the band of each member belonging to the same series. For example in A and B, the intensity of this band decreases as n increases. A similar band appears at 960 cm^{-1} in the compounds having $(Si)CH_2CH_3$ grouping[6]; accordingly it is probably possible to attribute those to the vibration in ethyl group, probably to that of the stretching of C—C bond.

In A, there are two common bands near 800 cm^{-1} and 840 cm^{-1}. The intensity of the former becomes stronger and that of the latter becomes weaker, as n increases. It may be concluded that the former corresponds to 800 cm^{-1} band characteristic of $(CH_3)_2SiO$[1,3] unit in F and G, and the latter is connected with the OC_2H_5 group in $(CH_3)_2Si(OC_2H_5)O_{1/2}$ unit. In B and C, there are overlap bands near 800 cm^{-1}, and their shape is so complex that they may be considered to consist of many bands. In D and E, a band is observed near 790 cm^{-1}, which may be thought to be a characteristic band of ethoxypolysiloxanes.

The absorption bands in 1000—1200 cm^{-1} are probably associated with Si—O—Si and Si—O—C linkages. Since the absorption band, though not very strong in intensity, appeared at constant wave number of 1160 cm^{-1} in all the compounds, and the intensity decreases clearly with increasing polymer size in A, it seems certain that this band is associated with $(Si)OC_2H_5$ grouping. Though quite tentative, this band would be connected with the stretching vibration of C—O bond, because this band is not found in the spectra of the compounds containing $(Si)CH_2CH_3$ group[6]. In A and B, common strong bands occur at 1080 cm^{-1} and 1110 cm^{-1} which may be connected with the Si—O—C linkage and are attributed probably to the stretching of Si—O bond. In A_n except A_1, another band of comparative intensity is observed near 1050 cm^{-1}, which decreases in wave number as n increases. Since Wright and Hunter have assigned 1050 cm^{-1} band in F and G to the stretching mode of Si—O vibration and have pointed out their shift to a smaller wave number with increasing polymer size, it seems possible to connect this band with Si—O stretching mode of Si—O—Si linkage. B_1 has only two bands at 1070 and 1098 cm^{-1} in this region, while in the higher members of this series another two bands are observed, of which the one found at 1030—1053 cm^{-1} would correspond to the band at 1050 cm^{-1} in A. It has been known[7] that stable cyclotrisiloxanes of the type $(RR'SiO)_3$ (R, R'= alkyl or aryl group) have their Si—O(—Si) stretching band in the region 1000—1020 cm^{-1}. As already reported[5], this band appears also in the spectra of unstable C_3 as well as $(C_2H_5Si(OC_2H_5)O)_3$ at 1023 cm^{-1}. With samples of the former reserved in a glass ampule, this band decreased in intensity after 500 days, while the refractive index and the viscosity increased. As in the case of unstable $((C_2H_5)HSiO)_3$[8], this band will be associated with the stretching vibration of Si—O bond of cyclotrisiloxane ring, and the 1068 cm^{-1} band of C_4 will be attributed to the same vibration of cyclotetrasiloxane ring.

A fairly successful explanation of the spectra of this region from the similarity of the structure to dimethylpolysiloxanes may be made only in the case of A, and it becomes difficult in the case of D and E. All the members of series D and E appear to have only two bands. It is likely that the bands associated with Si—O—Si and Si—O—C linkages cover each other.

To a sharp intense band near 1265 cm^{-1}, some different assignments[9] have been

TABLE III

INFRARED SPECTRA OF POLYSILOXANES IN 1300—1500 cm^{-1} REGION:

POSITIONS OF BANDS (in cm^{-1})

A, B, C	D, E	F*	G**
1295	1295	—	1300
1365	1365	—	—
1390	1390	—	—
1410	—	1410	1405
			1417
1440	1442	1442	1446
1485	1483	—	—

* N. Wright and M. J. Hunter, *loc. cit.*[3]

** R. E. Richards and H. W. Thompson, *loc. cit.*[1]

6) M. Sakiyama, *J. Chem. Soc. Japan, Ind. Chem. Sec.* (*Kogyo Kagaku Zassi*), **60**, 1385 (1957).

7) C. W. Young, P. C. Servais, C. C. Currie and M. J. Hunter, *J. Am. Chem. Soc.*, **70**, 3758 (1948).

8) R. Ōkawara, U. Takahashi and M. Sakiyama, This Bulletin, **30**, 608 (1957).

9) C. W. Young, J. S. Koheler and D. S. McKinney, *J. Am. Chem. Soc.*, **69**, 1410 (1947); D. H. Rank, B. D. Saksena and E. R. Shull, *Discuss. Farad. Soc.*, **9**, 187 (1950).

made. In this study, it has become clear that this band is related to the $(Si)CH_3$ group since this band is observed in A, B and C.

In 1300—1500 cm^{-1} region, six weak bands are observed. For comparison the absorption bands in this region are presented in Table III together with those of F and G.

From Table III, 1295, 1365, 1390, 1440 and 1485 cm^{-1} bands are supposed to be associated with $(Si)OC_2H_5$ group.

Summary

1) The infrared spectra of the lower members of ethoxy-, and methylethoxypolysiloxanes measured in the rock salt region are discussed.

2) Up to 1200 cm^{-1}, the common bands near 960 and 1160 cm^{-1} are certainly to be connected with the grouping $(Si)OC_2H_5$.

3) Moreover, characteristic bands of $(Si)OC_2H_5$ group appear near 840 cm^{-1} in ethoxy end-blocked dimethylpolysiloxanes and near 790 cm^{-1} in ethoxypolysiloxanes.

The author wishes to express his hearty thanks to Mr. M. Sakiyama and Dr. T. Matsuura for their helpful discussion.

Department of Applied Chemistry
Faculty of Engineering
Osaka University
Miyakojima-ku, Osaka

Studies on the Effect of Substituents on the Spectra of Quinoline Derivatives

By Tadashi SATO and Masaki OHTA

(Received September 3, 1957)

For interpreting the effect of substituents on the spectra of triphenylmethyl ions and other dyes, Lewis et al.[1] took account of the orientation of the molecule in the electric field and designated the absorption bands as *x*-bands or *y*-bands on the assumption that they were associated with electric moments directed along mutually perpendicular axes in the main plane of the molecule. Later, this assumption was extended to the other types of molecules and treated theoretically by some physical chemists.

In 1949, Klevens and Platt[2], using the free electron model, classified the spectra of cata-condensed hydrocarbons and gave them a systematic nomenclature: with naphthalene, they designated its absorption bands as Lb-, La- and Bb-bands in the order of decreasing wave length. The polarization diagrams were represented in Fig. 1. They stated that the Lb-band showed a red shift with increasing chain length and was therefore longitudinally polarized along an axis of molecular

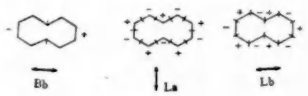

Fig. 1.

length, and that the La-band exhibited a bathochromic shift as molecular width increased. This band was, therefore, transversely polarized. A similar phenomenon was observed by Jones[3] with anthracene derivatives.

Ewing et al.[4], without referring to the above discussion, reported on the spectra of naphthols, naphthylamines, hydroxy- and aminoquinolines. These spectra showed the properties corresponding to the above discussion: in molecules of β-type, the Lb-bands were bathochromically shifted and the intensities increased, indicating the existence of three clearly distinguishable bands, whereas in α-type, the La-bands were so much bathochromically shifted that the weak Lb-bands were almost covered.

1) G. N. Lewis and M. Calvin, *Chem. Rev.*, **25**, 273 (1939); G. N. Lewis and J. Bigeleisen, *J. Am. Chem. Soc.*, **65**, 520, 2120, 2107 (1943).
2) H. B. Klevens and J. R. Platt, *J. Chem. Phys.*, **17**, 486 (1949).
3) R. N. Jones, *Chem. Rev.*, **41**, 353 (1947).
4) G. W. Ewing and E. A. Steck, *J. Am. Chem. Soc.*, **68**, 2181 (1945); **70**, 3397 (1948).

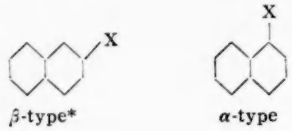

β-type* α-type

Knight et al.[5] classified the spectra of bromoquinolines along this consideration and observed the same regularity as described above. All studies so far reported have dealt with the simple monosubstituted molecules. In our synthetic study of furoquinoline alkaloid, it was necessary to determine where the nitro group would enter when methoxy-dihydrofuroquinoline derivative II was subjected to nitration. With the intention of predicting its position spectroscopically, we investigated whether the regularity existing between the displacement of bands and the position of the substituents could be observed in these rather complicated molecules.

The spectra of four compounds (I—IV) are compared in Fig. 2.** As can be noted from the comparison of the spectrum of IV

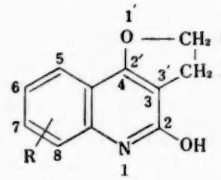

I R=H
II R=8-OCH_3
III R=7-OCH_3
IV R=6-OCH_3

with that of I, introduction of the methoxyl group in 6-position displaces the Lb-band to the red, while the La-band remains almost unchanged. In the other two cases (II and III), λ_{max} is hardly affected at all, while the intensities are much affected; as for 7-isomer, the Lb-band increases with the depression of the La-band, and with 8-isomer, the circumstance is the reverse. As noted from these data, there are two modes of exerting the effect, namely on the wave length

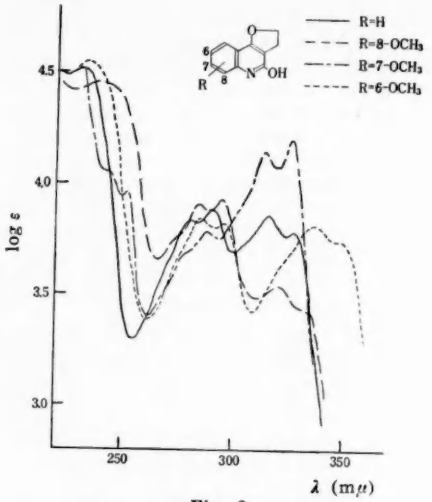

Fig. 2

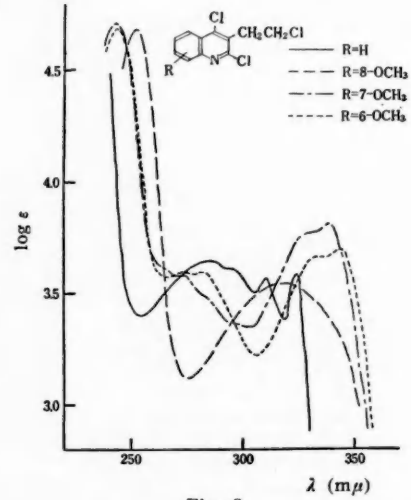

Fig. 3

in one case, and on the intensity in the other. Though we can not find a satisfactory explanation to this difference, a generalization can be observed that the substitution which increases the molecular length (6- and 7-position) acts so as to displace the Lb-band bathochromically or to increase the intensity, while substitution perpendicular to this direction exerts the same influence on La-band.

In Fig. 3, the spectra of another series of molecules (V—VIII) are shown. Here, the spectra of 6- and 7-isomer are similar. In both cases, Lb-bands are bathochromically shifted, while La-bands are shifted

* Here, the diagram represents the naphthalene and the quinoline nucleus.

5) S. B. Knight et al., ibid., **76**, 3780 (1954).

** We prepared these compounds by the condensation of appropriate aromatic amines and diethyl β-methoxyethylmalonate[6]. As for the condensation product from *m*-anisidine, two isomers are possible (i and ii). We proved the product as to be 7-methoxy derivative (i), by converting it into evolitrine (iii). See the following paper: T. Sato and M. Ohta, This Bulletin, **31**, 161 (1958).

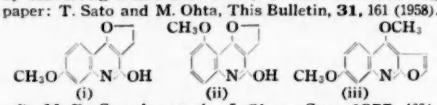

(i) (ii) (iii)

6) M. F. Grundon et al., *J. Chem. Soc.*, **1955**, 4284; T. Sato and M. Ohta, This Bulletin, **30**, 708 (1957).

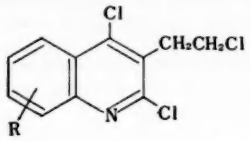

V R=H
VI R=8−OCH_3
VII R=7−OCH_3
VIII R=6−OCH_3

in the opposite direction. As for 8-isomer, the La-band is so much bathochromically shifted as to cover the Lb-band completely.

From these data, we can undoubtedly say that the electronic transition responsible for the Lb-band is of the type of polarization along the axis of molecular length, while that for La-band is of the type perpendicular to this axis, and that even in these rather complicated molecules, the regularity found in the simpler molecules can also be observed.

Nitration of III gave a nitro derivative IX. Reduction of the nitro derivative with stannous chloride gave the amino

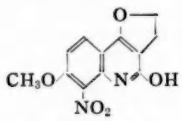

IX

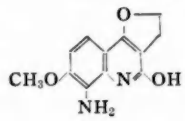

X

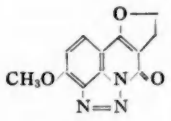

XI

derivative X, from which the triazol derivative XI was derived by the reaction with nitrous acid[7]. From this fact the position of the nitro group in IX could definitely be decided.

Comparing the spectrum of this nitro derivative IX with that of III (Fig. 4), we can see that, in accordance with the above observation, the introduction of the nitro group causes the La-band to displace bathochromically and hyperchromically. Though a little bathochromic shift is also observed with Lb-band, the extent is far smaller than that for La-band. When the spectrum of the amino derivative X is compared with that of III (Fig. 4), it is obvious that the La-band is more influenced than Lb-band.

As we could thus extend this consideration to somewhat complicated molecule, it

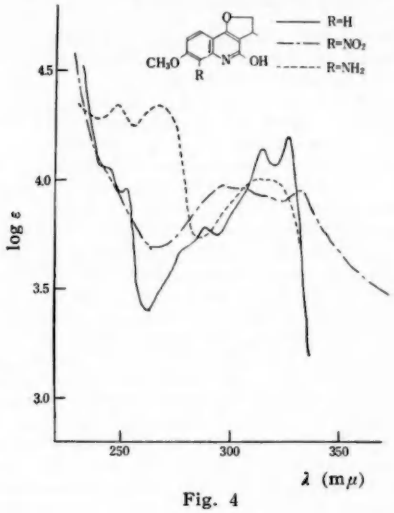

Fig. 4

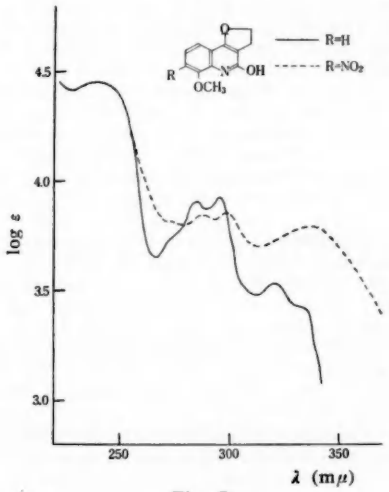

Fig. 5

is now possible to determine which of the two possible products XII and XIII was produced by the nitration of II. The fact that the spectrum of this nitro derivative suffers much bathochromic and hyperchromic shift on the Lb-band when compared with that of II, as shown in Fig. 5, seems to show that it would probably be 7-isomer XII.

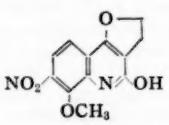

XII

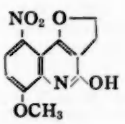

XIII

7) S. E. Krahler and A. Burger, *J. Am. Chem. Soc.*, **64**, 2417 (1942).

Experimental

Absorption Spectra — All spectra were measured in methanol with Beckman Quartz Spectrophotometer, Model DU.

2-Hydroxy-4', 5'-dihydrofuro (3' : 2'—3 : 4) quinoline (I),* 2-hydroxy-8-methoxy-4', 5'-dihydrofuro (3' : 2'—3 : 4) quinoline (II), 2, 4-dichloro-3-(β-chloroethyl) quinoline (V), and 2, 4-dichloro-3-(β-chloroethyl)-8-methoxyquinoline (VI).**—These compounds were prepared according to the methods reported by Grundon and by us[6] All were identified by their melting points and nitrogen analyses.

2-Hydroxy-7-methoxy-4', 5'-dihydrofuro (3' : 2'—3 : 4) quinoline (III) — A solution of *m*-anisidine (12 g.) and diethyl β-methoxyethylmalonate (25 g.) in diphenyl ether (35 cc.) was heated under reflux for 3 hours. After cooling, the product was recrystallized from nitrobenzene. m. p. 250°. A pure sample resulting from the recrystullization from dilute acetic acid. m. p. 252°.

Anal. Found: C, 66.15; H, 5.55; N, 6.69. Calcd. for $C_{12}H_{11}O_3N$: C, 66.35; H, 5.10; N, 6.45%.

Addition of petroleum ether to the diphenyl ether mother liquor gave a solid from which a small amount of unidentified crystals was obtained, in addition to III, by repeated recrystallization from acetic acid. m. p. 334°.

2-Hydroxy-6-methoxy-4', 5'-dihydrofuro (3' : 2'—3 : 4) quinoline (IV)—This was prepared from *p*-anisidine in a manner similar to that used for 7-isomer (III). A pure sample was recrystallized from ethyl "Cellosolve". m. p. 277°.

Anal. Found: N, 6.31. Calcd. for $C_{12}H_{11}O_3N$: N, 6.45%.

2, 4-Dichloro-3-(β-chloroethyl)-7-methoxyquinoline (VII)—A mixture of III (0.5 g.) and phosphorus oxychloride (5 cc.) was heated under reflux for 1.5 hours. Decomposition of the excessive phosphorus oxychloride with ice gave a solid which was recrystallized from dilute methanol. m. p. 121°.

Anal. Found: N, 4.79. Calcd. for $C_{12}H_{10}ONCl_3$: N, 4.82%.

2, 4-Dichloro-3-(β-chloroethyl)-6-methoxyquinoline (VIII) — This was prepared in the same way as described for 7-isomer (VII). Recrystallization from dilute methanol gave a pure sample. m. p. 118°.

Anal. Found: N, 4.95. Calcd. for $C_{12}H_{10}ONCl_3$: N, 4.82%.

2-Hydroxy-7-methoxy-8-nitro-4',5'-dihydrofuro (3' : 2'—3 : 4) quinoline (IX)—To a solution of methoxy-dihydrofuroquinoline derivative III (0.4 g.) in concentrated sulfuric acid (3 cc.) was added powdered potassium nitrate (0.2 g.) in portions with occational cooling. After being kept at 100° for 30 min., the solution was poured into crushed ice. The precipitates were recrystallized from dilute acetic acid. The nitro derivative contained one mole of acetic acid of crystallization. m. p. 256—60° (decomp.).

Anal. Found: C, 51.45; H, 4.47; N, 8.94. Calcd. for $C_{14}H_{14}O_7N_2$: C, 52.17; H, 4.38; N, 8.69%.

The solvent-free sample was obtained by drying over phosphorus pentoxide in vacuo at 100° for 3 hours. m. p. 260° (decomp.).

Anal. Found: C, 54.51; H, 3.76; N, 10.87. Calcd. for $C_{12}H_{10}O_5N_2$: C, 54.96; H, 3.84; N, 10.68%.

2-Hydroxy-7-methoxy-8-amino-4', 5'-dihydrofuro (3' : 2'—3 : 4) quinoline (X)—To a solution of dihydrated stannous chloride (1.2 g.) in concentrated hydrochloric acid (4 cc.) was slowly added powdered nitro derivative IX (0.3g.) with occational cooling. The mixture was kept at 50—60° for 20 min., and then bolied gently for 30 min. The solution was made alkaline with 10% sodium hydroxide and the solid was recrystallized from ethyl "Cellosolve". m. p. 312° (decomp.).

Anal. Found: C, 61.80; H, 5.40; N, 11.85. Calcd. for $C_{12}H_{12}O_3N_2$: C, 62.06; H, 5.21; N, 12.06%.

2-Oxo-1, 2, 4', 5'-tetrahydrofuro (3' : 2'—3 : 4) quinoline-1, 8-diazoimide (XI)—To a solution of the amino derivative X (0.3 g) in 20% sulfuric acid (6 cc.) was added water (4 cc.), and then 7.5% aqueous solution of sodium nitrite (2 cc.) with constant stirring and cooling with ice-water. The mixture was kept at room temperature for 30 min., and the yellow product was recrystallized from "Cellosolve ethyl." m. p. 226—8° (decomp.). This was a monohydrate.

Anal. Found: N, 16.31. Calcd. for $C_{12}H_{11}O_4N_3$: N, 16.08%.

The anhydrate was obtained by drying over phosphorus pentoxide in vacuo at 100° for 2 hours. m. p. 228° (decomp.).

Anal. Found: N, 17.26. Calcd. for $C_{12}H_9O_3N_3$: N, 17.28%.

2-Hydroxy-7-nitro-8-methoxy-4',5'-dihydrofuro (3' : 2'—3 : 4) quinoline (XII) — To a suspension of methoxy-dihydrofuroquinoline derivative II (1 g.) in acetic anhydride (40 cc.) was added a mixture of 60% nitric acid (1 cc.) and glacial acetic acid (4 cc.) under external cooling. The solid went into solution immediately, but soon after, new crystals began to deposit. After 2 hours' standing at room temperature, they were recrystallized from acetic acid. m. p. 260° (decomp.). The sample contained one mole of acetic acid of crystallization.

Anal. Found: C, 52.22; H, 4.51; N, 9.02. Calcd. for $C_{14}H_{14}O_7N_2$: C, 52.17; H, 4.38; N, 8.69%.

The solvent-free sample was obtained by drying over phosphorus pentoxide in vacuo at 100° for 3 hours. m. p. 260° (decomp.).

Anal. Found: C, 54.47; H, 3.92; N, 10.62. Calcd. for $C_{12}H_{10}O_5N_2$: C, 54.96; H, 3.84; N, 10.68%.

The authors are indebted to Mr. A. Kondo for the microanalyses.

Laboratory of Organic Chemistry
Tokyo Institute of Technology
Meguro-ku, Tokyo

*** The furoquinoline derivatives were named as indicated in order to make the numbering accord with that for quinoline derivatives.

Synthesis of Evolitrine, an Alkaloid of Evodia littoralis

By Tadashi SATO and Masaki OHTA

(Received September 3, 1957)

The structure of evolitrine was determined by Cook et al.[1] to be 7-methoxydictamnine (I). The position of the extra methoxyl group was unambigously determined by comparing the degration product II with the product obtained from the

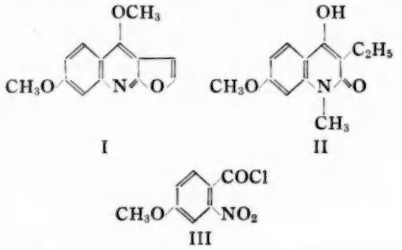

I II III

reaction between 4-methoxy-2-nitrobenzoyl chloride III and diethyl ethoxymagnesiumethylmalonate, followed by the reduction of nitro group, cyclization and *N*-methylation.

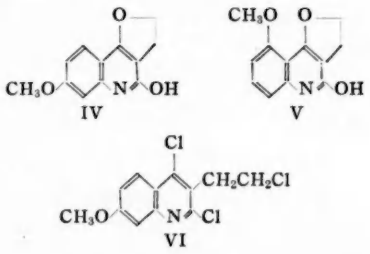

IV V VI

In connection with our spectroscopic study of quinoline derivatives[2], we were obliged to determine which of the two possible products IV or V resulted in fact from the condensation of *m*-anisidine and diethyl β-methoxyethylmalonate. By synthesizing evolitrine starting with this condensation product[3,4] we identified it as IV, thus affirming the structure of evolitrine.

When *m*-anisidine and diethyl β-methoxyethylmalonate were refluxed in diphenyl ether IV was obtained. In search of another possible isomer V, the mother liquor was subjected to repeated purification, but the substance isolated was a small amount of white crystals which had a different and unidentified structure. Treatment of the compound IV with phosphorus oxychloride gave the trichloro derivative VI gave a white solid which was supposed to be a mixture of 2-hydroxy derivative VII and dihydrofuroquinoline derivative VIII in view of the experience gained from our dictamnine synthesis[3]. This mixture afforded the dihydrofuroquinoline derivative VIII on treatment with alkali. When

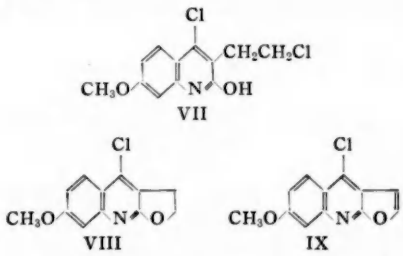

VII VIII IX

the trichloro derivative VI was hydrolysed with acid according to the method of Grundon[4], the intermediate product VII was isolated, which was also cyclized to VIII by alkali. Treatment of VIII with *N*-bromosuccinimide in the presence of a small amount of benzoyl peroxide, and successive treatment with dimethylaniline afforded the chloro-furoquinoline derivative IX. This was converted by sodium methoxide into evolitrine I. The synthetic evolitrine was shown to be identical with the natural product by comparing their melting points, ultraviolet spectra and melting points of their picrates.

Experimental

2-Hydroxy-3-(β-chloroethyl)-4-chloro-7-methoxyquinoline (VII).—A mixture of trichloro derivative VI[2] (0.28 g.), 6N-hydrochloric acid (8 cc.) and dioxane (6.5 cc) was heated under reflux for 3 hours. Additon of water gave a white solid which was recrystallized from dilute methanol. m. p. 193°.

1) R. G. Cook and H. F. Hyne, *Austral. J. Chem.*, **7**, 273 (1954).
2) T. Sato and M. Ohta, This Bulletin, **31**, 157 (1958).
3) T. Sato and M. Ohta, ibid, **30**, 708 (1957).
4) M. F. Grundon et al., *J. Chem. Soc.*, **1957**, 2177.

Anal. Found: N, 5.24, Calcd. for $C_{12}H_{11}O_2NCl_2$: N, 5.15%.

4-Chloro-7-methoxy-2,3-dihydrofuro[2,3-b]quinoline (VIII)—a) To a solution of VII (0.3 g.) of methanol (2 cc.) was added 10% methanolic sodium hydroxide and the solution was kept at 50—60° for 30 min. Addition of water gave a white solid which was recrystallized from dilute methanol m. p. 158°.

Anal. Found: C, 60.63; H, 4.61; N, 5.86. Calcd. for $C_{12}H_{10}O_2NCl$: C, 61.01; H, 4.23; N, 5.94%.

b) A solution of trichloro derivative VI (0.3 g) in glacial acetic acid (3 cc.) was heated under reflux for 1.5 hours. Addition of water gave a white solid which was treated with methanolic sodium hydroxide in the same way as described in a). m. p. and mixed m. p. 158°.

4-Chloro-7-methoxyfuro[2,3-b]quinoline (IX).—A mixture of dihydrofuroquinoline derivative VIII (0.45 g.), N-bromosuccinimide, (0.45 g) a trace of benzoyl peroxide and carbon tetrachloride (15 cc.) was heated under reflux for 2 hours. Succinimide was filtered off and carbon tetrachloride evaporated in vacuo. The resulting residual oil, after dilution with dimethylaniline (4.5 cc.) was heated under reflux for 3 hours. After cooling the mixture was added to 3N-hydrochloric acid (45 cc.). The solid thus formed was collected, and recrystallized from dilute methanol. m. p. 169°. The compound was a semihydrate.

Anal. Found: C, 59.72; H, 3.71; N, 6.04. Calcd. for $C_{24}H_{18}O_5N_2Cl_2$: C, 59.32; H, 3.71; N, 5.77%.

Evolitrine (I).—To the chloro derivative IX (0.1 g) was added methanolic sodium methoxide (5 cc.), containing sodium (0.15 g). The mixture was heated under reflux for 3 hours, and allowed to stand overnight. Sodium chloride was filtered off and the filtrate, after partial evaporation of methanol, was treated with water. Recrystallization from dilute methanol gave pure evolitrine. m. p. 114°.

Anal. Found: C, 67.70; H, 5.22; N, 6.30. Calcd. for $C_{13}H_{11}O_3N$: C, 68.11; H, 4.84; N, 6.11%.

The ultraviolet spectrum in ethanol was also identical with the reported one. The picrate was prepared and recrystallized from methanol. m. p. 192—4°.

Anal. Found: N, 12.50. Calcd. for $C_{19}H_{14}O_{10}N_4$: N, 12.23%.

The authors are indebted to Mr. A. Kondo for the microanalyses.

Laboratory of Organic Chemistry, Tokyo Institute of Technology
Meguro-ku, Tokyo

Studies on the Separation of Alkaline Earth Elements. IV. Coprecipitation of Barium in the Induced Precipitate of Lead Sulfate

By Mutsuaki SHINAGAWA and Toshifumi MURATA

(Received September 16, 1957)

In the preceding paper[1] the precipitation of lead sulfate induced[2] by the barium ion was studied by means of turbidimetry, and it was shown experimentally that there were several relations among the quantities of substances involved. The present paper reports the ratio of coprecipitation of barium measured radiometrically by use of ^{140}Ba as a tracer, and the amount of induced precipitate of lead sulfate measured amperometrically[3]. Freundlich's equation of adsorption isotherm[4] was found to be applicable to the experimental results obtained. It is understood that this induced precipitation furnishes a method of concentration of small amounts of barium in the presence of large amounts of lead.

Experimental

Reagents. — Lead nitrate, guaranteed grade, 0.482 M, aqueous solution.

Barium chloride, 0.005 M/l; Aqueous solution of guaranteed grade salt was mixed with a suitable amount of a hydrochloric acid solution of carrier free $^{140}BaCl_2$.

Ammonium acetate, 10.23 M/l (pH=6.22); prepared from ammonia water and acetic acid, both of which were of guaranteed grade.

Apparatus. — SHIMADZU pen — recording polarograph for amperometry.

SHIMADZU glass electrode pH meter for pH measurement.

1) M. Shinagawa and T. Murata, *J. Science Hiroshima Univ., Series A*, **18**, 429 (1955).
2) F. Feigl. "Spot Tests", Vol. 1. Elsevier Publishing Co., (1954), p. 204.
3) I. M. Kolthoff and J. J. Lingane, "Polarography", Interscience Publishers, Inc., New York, N. Y. (1952), p. 913.
4) H. Freundlich, *Z. physik. Chem.*, **57**, 385 (1907).

KOBE KOGYO End Window G. M. Counter (131 Type. Thickness of the mica window was 3.1 mg./cm^2.) and stainless steel cupped planchets with 2.5 cm. diameter were used for the radioactivity measurements.

Procedure and Results.

1) Determination of the amounts of precipitated barium and lead.—In order to know the quantity of coprecipitated barium with lanthanum fluoride, Gest et al. reported the dilution method[5], while the authors prefered the following method. The specific activity of β-ray of the remaining barium labeled with ^{140}Ba in the supernatant solution was measured and compared with that of the standard solution. Two ml. of either solution was almost evaporated in a cupped planchet under an infrared lamp and less than 0.8 ml. of 0.5 M sulfuric acid was added to make the lead sulfate layer uniform which had a thickness of 18 mg./cm.^{2} This way of preparation facilitated good reproducibility of the counting. Since the solutions labeled with ^{140}Ba usually contain the daughter, ^{140}La, they had been kept more than 20 days after their preparation before the specific activities were measured.

The quantity of precipitated lead ions was also determined indirectly, measuring the lead ions in the supernatant solution by the amperometric titration with potassium chromate solution at -1.0 V of fixed potential.

2) The amount of coprecipitated barium as a function of aging time.—Into a stoppered Erlenmeyer flask 500 ml. of a mixed solution (pH 5.50) containing 0.096 M lead nitrate, 2.07 M ammonium acetate (The molar ratio of ammonium acetate to the lead ion was chosen as in the previous paper[1].), and 2×10^{-4} M barium chloride, was placed and stirred well after the addition of 7.50 ml. or 12.5 ml. of 0.5 M sulfuric acid. The flask was kept in a 20 ± 0.05°C thermostat.

At regular intervals 5 ml. batches of solution were taken out of it and centrifuged. The specific activities of the supernatant solution told the amount of the precipitated barium removed at intervals as shown in Fig. 1. It was found that the percentage of coprecipitation remarkably increased within the first half an hour and remained almost constant thereafter.

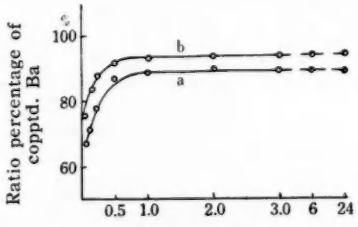

Fig. 1. The amount of coprecipitated barium as a function of aging time.
Solution: $Pb(NO_3)_2$ 0.096 M.
CH_3COONH_4 2.07 M.
Ba^{++} 1×10^{-4} M.
To 500 ml. of the solution 7.50 ml. (Curve (a)) or 12.50 ml. (Curve (b)) of 0.5 M H_2SO_4 was added, aged at 20°C.

3) The precipitations as a function of the amount of sulfuric acid added.—As mentioned in section 2, 40 ml. of the mixed solution was taken into a 100 ml. stoppered Erlenmeyer flask, and 0.50—5.00 ml. of 0.5 M sulfuric acid was added at a rate of 7—8 sec./ml.

It was stirred well and kept being aged at 20°C. After 2 hours it was centrifuged and analysed. Fig. 2 illustrates the results when the coexisting barium concentrations were 0 M, 1×10^{-4} M and 2×10^{-4} M Ba^{++}. Table 1 (A) shows the data of the last case.

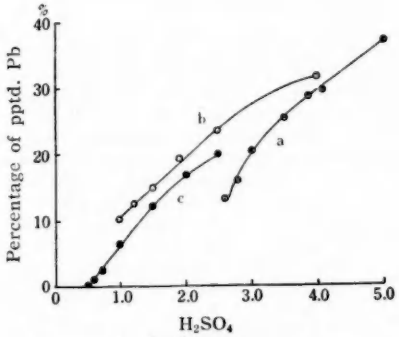

a: Ba^{++} none
b: 〃 1×10^{-4} M
c: 〃 2×10^{-4} M

Fig. 2. Precipitation ratio of lead as a function of the amounts of sulfuric acid added.
Solution: Pb^{++} 800 mg/40 ml., CH_3COONH_4 2.07 M, pH 5.50. 0.5 M H_2SO_4 was added. Aged for 2 hours at 20°C.

TABLE I (A)
AMOUNTS OF SULFURIC ACID AND THE PRECIPITATES

Solution: 800 mg. Pb^{++} and 1098 γ Ba^{++} in 40 ml of 2.07 M CH_3COONH_4. 0.5 M H_2SO_4 was added, aged for 2 hours at 20°C.

H_2SO_4 added ml.	Ba copptd. γ	Ba copptd. %	Pb pptd. mg.	Pb pptd. %	ratio of pptd. (Ba)/(Pb) γ/mg.
0.50	94_3	85.9	3.2	0.4	236
0.60	94_9	86.4	4.8	0.6	198
0.80	103_6	94.4	18.4	2.3	57
1.00	104_2	94.9	40.8	5.1	26
1.50	105_3	95.9	96.0	12.0	11
2.00	106_4	96.8	130.4	16.3	8
2.50	106_9	97.3	156.0	19.5	7

(Mean values of three data.)

5) H. Gest, N. F. Ballov, B. M. Abraham and C. D. Coryell, "Radiochemical Studies; Fission Products", McGraw-Hill Book Co., Inc., New York, Paper **12**, 145 (1951).

TABLE I (B)

Solution: 1600 mg. Pb^{++} and 1098 γ Ba^{++} in 40 ml of 4.14 M CH_3COONH_4, 0.5 M H_2SO_4 was added, aged for 2 hours at 20°C.

H_2SO_4 added ml.	Ba copptd. γ	Ba copptd. %	Pb pptd. mg.	Pb pptd. %	ratio of pptd. (Ba)/(Pb) γ/mg.
1.50	101_3	92.3	52.8	3.3	192
2.00	103_4	94.2	52.8	3.3	195
3.00	104_3	95.0	147.2	9.2	71
4.00	105_3	95.9	241.6	15.1	43
5.00	106_0	96.5	320.0	20.0	33
7.00	108_5	98.8	320.0	20.0	34
10.00	109_6	99.3	588.8	36.8	19

(Mean values of three data.)

As can be seen from Fig. 2, when barium was absent lead ions were not precipitated until 2.60 ml. of sulfuric acid was added, because of the masking effect of acetic acid radical. Since in the presence of barium the precipitate appeared by the addition of less than 2.60 ml. of sulfuric acid, it was possible to regard this as induced precipitation owing to the presence of barium.

In the case of Table 1 (A), 86—96% of barium was coprecipitated with 20% of lead precipitate, while 92—99% of barium with less than 20% of lead in the case of double concentrations of lead ions and ammonium acetate as shown in Table I (B). In this case lead sulfate was not precipitated until 7.50 ml. of sulfuric acid was added, in the absence of barium. Therefore, the more concentrate the lead ion, the greater the readiness with which lead sulfate was induced to precipitate. The amount of coprecipitated barium increased significantly with the increase in lead sulfate precipitate, while the ratio of barium to lead in the precipitate decreased noticeably.

Results

1) The precipitation as a function of the initial concentration of barium. — A mixed solution as prepared in section 2 was used, having several concentrations between 6.86 and 68.6 mg. barium per liter. To each 40 ml. batch of these solutions were added 1.00 and 1.30 ml. of sulfuric acid as the representing amounts of the acid necessary for the induced precipitation taken by the preliminary experiments shown in Fig. 2 curve a and c, and it was then let stand for 30 min. in a thermostat to equilibriate the precipitate as in section 2. Table II (A) and (B) show the data of the experiments.

From Table II where the amount of sulfuric acid is constant, it can be seen that in the presence of more barium ions, more lead sulfate precipitates, while the percentage of coprecipitation of barium is unchanged with the initial concentration of

TABLE II (A)

INITIAL CONCENTRATIONS OF BARIUM AND THE PRECIPITATES

Solution: 800 mg. Pb^{++} in 40 ml. of 2.07 M CH_3COONH_4. 1 ml. of 0.5 M H_2SO_4 was added, aged for 30 min. at 20°C.

Initial Ba γ	copptd. Ba γ	copptd. Ba %	pptd. Pb mg.	pptd. Pb %	ratio of pptd. (Ba)/(Pb) γ/mg.
279	24_4	87.9	28.8	3.6	8.4
549	48_7	88.7	35.2	4.4	13.8
1098	97_3	88.6	42.4	5.3	22.9
1647	145_4	88.3	50.4	6.3	28.8
2196	198_1	90.2	58.4	7.3	33.9
2745	249_0	90.7	72.8	9.1	34.2

(Mean values of three data.)

TABLE II (B)

The same conditions as in (A), but 1.30 ml. of H_2SO_4

Initial Ba γ	copptd. Ba γ	copptd. Ba %	pptd. Pb mg.	pptd. Pb %	ratio of pptd. (Ba)/(Pb) γ/mg.
279	25_3	92.1	87.2	10.9	2.9
549	50_6	92.2	92.8	11.6	5.4
1098	98_6	89.5	100.8	12.6	9.7
1647	146_0	88.7	112.8	14.1	12.9
2196	198_3	90.3	138.4	17.3	14.3
2745	250_3	91.2	146.4	18.3	17.0

(Mean values of three data.)

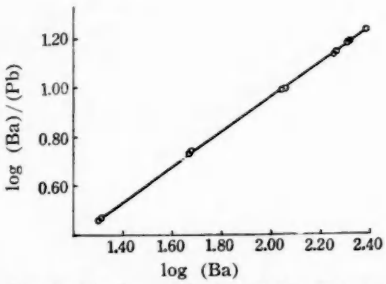

Fig. 3 (A) Logarithmic relation between ppt. ratio and final barium concentration.
Solution: Pb^{++} 800 mg./40 ml., CH_3COONH_4 2.07 M.
1.00 ml. of 0.5 M H_2SO_4 was added, aged for 30 min. at 20°C.

barium in the solution; i.e. 89—90% in the case of (A) and 89—92% in (B).

In Fig. 3 (A) and (B), linear relationship between the logarithmic value of precipitation ratio ((Ba)/(Pb) in γ/mg., in Tables II (A) and (B)) and that of the concentration of barium in the final solution equilibriated with the precipitate (C in γ/40 ml.). Therefore, these relations

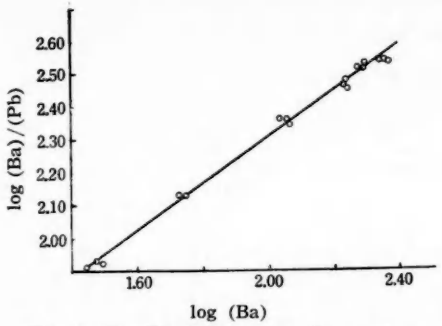

Fig. 3 (B) Conditions were the same as (A), but 1.30 ml. of H_2SO_4 was added.

are expressed by the Freundlich's adsorption isotherm,

$$(Ba)/(Pb) = aC^{1/n}$$

Where a and n are the constants which can be calculated from the intercepts and the inclination of the linear relations; $a=2.63$ and $n=1.38$ in (A) while $a=0.30$ and $n=1.38$ in (B). The value of a is larger in (A) than in (B), indicating that the adsorbability of barium is greater in (A) than in (B); in other words the smaller the amount of sulfuric acid added, the relatively larger the amount of coprecipitated barium. The n values in both cases are identical, indicating that the natures of the adsorption phenomena are of the same quality.

TABLE III

THE PRECIPITATIONS WITHOUT INDUCTION

Solution: 800 mg. Pb^{++} and 549 γ Ba^{++} in 40 ml., 1.5 ml. of 0.5 M H_2SO_4 was added, aged for 30 min. at 20°C.

copptd. Ba		pptd. Pb		ratio of pptd. (Ba)/(Pb)
γ	%	mg.	%	γ/mg.
17_0	$31._7$	$8._0$	1.0	42.5
18_4	$33._5$	$20._0$	2.5	9.2
21_1	$38._5$	$40._0$	5.0	5.3
22_0	$40._0$	$60._0$	7.5	3.6
24_0	$43._8$	$80._0$	10.0	3.0
26_6	$48._4$	$100._0$	12.5	2.7

(Mean values of three data.)

2) Precipitations from the solution without ammonium acetate.—When there was no ammonium acetate, the masking agent for lead ions, the ordinary lead sulfate precipitation was observed. It was not regarded as a precipitation induced by barium sulfate. The experimental results can be seen in Table III.

It was found from Table III that the percentage of the coprecipitated barium without induced lead sulfate was about 32—48%, which was much lower than that with the induced precipitate, i. e. about 85—99%.

Conclusion

On adding 0.5 M sulfuric acid, 0.096 M lead in 2.07 M ammonium acetate solution is precipitated inductively in the presence of $0.5—5\times10^{-4}$ M barium ion.

The amount of the coprecipitating barium follows the Freundlich's adsorption isotherm. The adsorption equilibrium is obtained within 30 min. after the addition of sulfuric acid. The adsorption percentage is greater as the amount of sulfuric acid added decreases in the range of possible amount of producing the lead sulfate.

The amount of coprecipitating barium is not the function of the amount of lead sulfate precipitate; it is almost constant, (85—99%) being much greater than that in the absence of ammonium acetate.

Further investigations with more elaborated experimental conditions are expected to get an excellent method of separation of a small amount of barium from a large amount of lead.

Department of Chemistry
Faculty of Science
Hiroshima University
Hiroshima

Studies on the Separation of Alkaline Earth Elements. V. Coprecipitation of Radium in the Induced Precipitate of Lead Sulfate

By Mutsuaki SHINAGAWA and Toshifumi MURATA

(Received September 16, 1957)

In the former papers[1,2] the authors reported on the lead sulfate precipitation induced by barium, and on its usefulness as a method of separation of a small amount of barium from a large amount of lead. In the present paper an analogous method of accumulation of radium is reported by coprecipitation with inductively precipitated lead sulfate by means of barium. In this case barium plays a role of the inducer for lead sulfate and at the same time that of the carrier for radium.

Experimental

Reagents.—The solutions of lead nitrate, barium chloride and ammonium acetate were the same as those prepared in the preceding paper[2]. Radium chloride solution 100 μC/100 ml. was the officially approved article, N. B. S. (U. S. Department of Commerce).

Apparatus.—RIKEN Lauritsen electrometer was used to measure the radioactivity of radium in the sample in a stainless steel cupped planchet with 2.5 cm. diameter.

SHIMADZU Pen-recording Polarograph was used for the amperometric titration, and SHIMADZU glass electrode pH-meter for the measurement of hydrogen ion concentration.

Procedures.—*1) Experimental conditions.* Into a stoppered Erlenmeyer flask was put 40 ml. of a solution of pH 5.50 containing 0.096 M lead nitrate, 2.07 M ammonium acetate, and 2×10^{-4} M barium chloride as their final concentration. The optimum molar ratio of ammonium sulfate to lead for this induced precipitation is $\simeq$20[1]. After the temperature of the mixture was adjusted to 20$\pm$0.05°C, a suitable amount of 0.5 M sulfuric acid was added at a rate of 7—8 sec. per ml. The precipitate obtained in the solution was stirred, kept standing for 2 hr. at 20°C and centrifuged. The supernatant solution was analysed for radium and lead content.

2) The measurement of radioactivity of radium. To determine how much radium is coprecipitated with lead sulfate, it is easier to analyse radium in the supernatant solution than in the precipitate. According to Tompkins et al.[3], when lead is thoroughly precipitated as lead sulfate, radium will be completely coprecipitated with it, and all the disintegrated products will be included without any appreciable loss. For this reason, the following procedure is preferred; 1 ml. of the supernatant sample solution or the standard solution is taken into a stainless steel cupped planchet, and concentrated under an infrared lamp to half of its original volume. Then to it 0.4 ml. of 0.5 M sulfuric acid is added to obtain the lead sulfate precipitate, which is dried up carefully and kept in a calcium chloride desiccator for eight days till it reaches 3/4 of the secular equilibrium for radium, and the radioactivity was measured by Tompkins' alpha-ray method[3].

This procedure was checked as follows; the standard solution was prepared as the supernatant sample solution mentioned above, except that a known amount of radium was added. The drying condition of lead sulfate in the cupped planchet and the amount of sulfuric acid added had a very subtle effect upon the alpha activity. Amount of sulfuric acid (0.2 to 0.6 ml.) was examined and the use of 0.4 ml. was found to be the best, permitting the determination of 1×10^{-3} μC radium with $\pm$4% average deviation, provided that the drying of the planchet was complete. The calibration curve thus obtained is shown in Fig. 1., and serves as the standard measure of the activity.

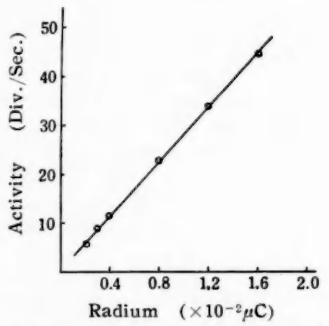

Fig. 1. The calibration curve of radium.

The absorption of alpha rays of radium by lead sulfate was examined and the results were

1) M. Shinagawa and T. Murata, *J. Science Hiroshima Univ.*, **A, 18**, 429 (1955).
2) M. Shinagawa and T. Murata, This Bulletin, **31**, 162 (1958).
3) P. C. Tompkins, W. P. Norris, L. Wish and R. D. Finkle, *MDDC.*, 699 (1946).

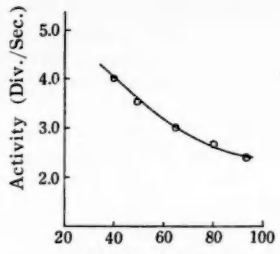

Fig. 2. The absorption of alpha rays by lead sulfate.

obtained as shown in Fig. 2., by which the self-absorption of the sample was calibrated.

3) Measurement of the amount of lead sulfate precipitated. The procedure for amperometric titration was the same as that mentioned in the previous paper[2].

Results

1) The coprecipitation ratio of radium and the induced precipitation ratio of lead as a function of the amount of sulfuric acid added. The solution mixture used had the same composition as in section 1, except 1×10^{-4} M of barium chloride and 40 μC of radium chloride per liter. Forty ml. of this solution was taken and 1.00—3.00 ml. of 0.5 M sulfuric acid was added and aged for 2 hours at 20°C. The analyses of lead and radium were carried out regularly, giving the results as shown in Fig. 3. The amount of lead sulfate precipitate increased as the amount of sulfuric acid added increased, while the amount of coprecipitated radium remained constant on the addition of more than 1.40 ml. of sulfuric acid, where ca. 9% of lead precipitated with ca. 90% of radium. The ratio (Ra)/(Pb) in the precipitate decreased significantly thereafter, just as in the case of coprecipitation of barium[2].

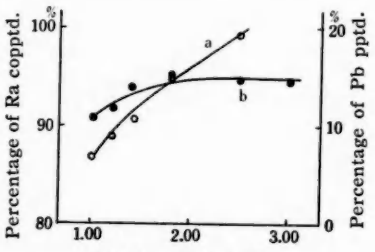

Fig. 3. Results of induced precipitation as a function of the amount of sulfuric acid added.
Curve a: Induced precipitation of lead.
Curve b: Coprecipitation of radium.

2) As a function of the amount of barium present. To each 40 ml. of the mixed solution (see Procedure section 1) which had been mixed with 0.80 μC of radium and a varying amount of barium, 1.20 ml. of 0.5 M sulfuric acid was added. The analyses of radium and lead in these solution gave the results as shown in Table I.

TABLE I

RESULTS OF THE COPRECIPITATION AS A FUNCTION OF THE AMOUNT OF THE BARIUM PRESENT

Solution: 800 mg. Pb^{++} and 0.8 μC $RaCl_2$ in 40 ml. of 2.07 M CH_3COONH_4; 1.20ml. of 0.5 M H_2SO_4 added, aged for 2 hours at 20°C.

Ba added	Ra copptd.		Pb pptd.	
mg.	μC	%	mg.	%
0.549	0.74_9	$93._6$	$66._4$	8.3
1.098	0.76_0	$95._0$	$73._6$	9.2
1.647	0.76_6	$95._8$	$87._2$	10.9
2.196	0.77_2	$96._6$	$98._4$	12.3
2.745	—	—	$113._6$	14.2

It is seen that when a sufficient amount of sulfuric acid, i.e. 1.20 ml. is added in the presence of more barium ions, more lead sulfate precipitates. The percentage of coprecipitation of radium appears to remain constant, although it has an overall trend to increase slightly.

3) As a function of initial concentration of radium. To each 40 ml. of the mixed solution (Procedure section 1), radium was added from 0.2 to 1.6 μC. After the addition of 1.20 ml. of sulfuric acid, the samples were analysed to find the amount of coprecipitated radium. Table II shows the results. In this case, too, the amount of lead sulfate induced was constant (9.2 %), while the amount of coprecipitated

TABLE II

COPRECIPITATION RATIO OF RADIUM AS A FUNCTION OF ITS INITIAL CONCENTRATION

Solution: 800 mg. Pb^{++} and 1.098 mg. Ba^{++} in 40 ml. of 2.07 M CH_3COONH_4. 1.20 ml. of 0.5 M H_2SO_4 was added, aged for 2 hours at 20°C, 9.2% of Pb (73.6 mg.) was precipitated.

Initial Ra	Ra copptd.		pptn. ratio (Ra)/(Pb)
μC	μC	%	$\times10^8$
0.200	0.18_7	$93._6$	2.5
0.400	0.38_2	$95._4$	5.2
0.800	0.76_4	$95._5$	10.4
1.200	1.15_0	$95._9$	15.6
1.600	1.53_0	$96._1$	20.8

radium increased as the initial concentration of radium increased according to Freundlich's adsorption isotherm as in the case of barium in the previous report[2].

4) In the absence of barium. The mixed solution mentioned in Procedure section 1, but without barium was used. To obtain the same amount of lead sulfate much more sulfuric acid was required than when barium was present. The experimental results are shown in Table III.

TABLE III

COPRECIPITATION IN THE ABSENCE OF BARIUM

Solution: 800 mg. Pb^{++} and 0.80 μC Ra^{++} in 40 ml., 2.07 M of CH_3COONH_4, 0.5 M H_2SO_4 was added, aged for 2 hours at 20°C.

H_2SO_4 added	Ra copptd.		Pb pptd.		pptn. ratio (Ra)/(Pb)
ml.	μC	%	mg.	%	$\times 10^3$
2.80	0.77_6	$97._0$	$92._0$	11.5	8.4
3.00	0.77_4	$96._7$	$139._0$	17.4	5.6
3.40	0.77_4	$96._8$	$174._0$	21.7	4.4
3.80	0.77_3	$96._6$	$191._0$	23.9	4.0

It can be understood that even when the amount of lead precipitate increases to a large extent, the coprecipitation ratio for radium remains constant and the precipitation ratio (Ra)/(Pb) decreases accordingly.

5) In the absence of acetate. The solution mixture containing 0.096 M lead nitrate and 20 μC/*l* radium chloride was used. To 40 ml. of this solution, an equivalent amount of sulfuric acid to the measured quantity of lead sulfate precipitate was added. The results of analyses are shown in Fig. 4, curve a. Curve b was derived from the same data shown in Fig. 3, curve b for comparison. In Fig. 4, curve b shows clearly that a small amount of induced precipitate of lead sulfate carries off radium from solution as efficiently as a relatively large amount of it does (curve a). While the ordinary precipitate of lead sulfate catches radium in an almost proportional amount to itself.

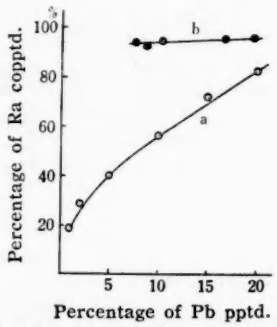

Fig. 4. Comparison of coprecipitation of radium.
Curve a: Ordinary precipitation of lead sulfate.
Curve b: Induced precipitation of lead sulfate in the presence of barium.

Summary

A solution of pH 5.50 composed of 0.096 M lead nitrate, 2.07 M ammonium acetate, $1-5\times10^{-4}$ M barium and 5—50 μC radium per liter, produces an induced precipitate of lead sulfate in proportion to the amount of 0.5 M sulfuric acid added. Under the same conditions, in the absence of barium, a lead sulfate precipitate is obtained in proportion to the amount of sulfuric acid added. But the required amount of sulfuric acid to obtain the same amount of precipitate is larger in this case than that in the case of induction by barium.

In both of the above cases, the ratio of the amount of the radium coprecipitated to the original amount of radium in sample solution is almost constant, i.e. 92—97%, irrespective of the amount of lead sulfate precipitate or of sulfuric acid added. This tendency is the same as in the case of coprecipitation of barium with the induced precipitate of lead sulfate as shown in the previous paper. More than 90% of radium is carried down by a precipitate of lead sulfate of 8—20% of lead. Such an extent was not found in the case of the ordinary precipitation of lead sulfate, i.e. in the absence of the masking agent, ammonium acetate for lead ions.

In conclusion, the induced precipitation of lead sulfate by barium can be made use of as an efficient method of separation or concentration of radium. For a practical usage of this method, more detailed examination according to each sample should be conducted.

Department of Chemistry
Faculty of Science
Hiroshima University
Hiroshima

Hydrogen Bonding Effect on the Electronic Absorption Spectrum of p-Hydroxyazobenzene

By Hiroaki BABA

(Received October 7, 1957)

When the effect of hydrogen bonding on the electronic absorption spectra of organic compounds came to be noticed, attention was drawn to the anomalies of the effects of the solvents on the spectra. It was then pointed out that the hydrogen bonding effect could serve as a new method for the study of the nature of hydrogen bonding itself[1]. Indeed some thermochemical quantities, such as free energy, entropy and enthalpy changes in hydrogen bonds, have been determined for a number of compounds, e.g. phenol[1-5], cresols[6,7], naphthols[7], pyridine *N*-oxide[8] etc. In all these studies the influence of hydrogen bonding on an electronic absorption was made clear by the use of a three-component system: an inert solvent, a solute of a chromophore, and a substance which forms hydrogen bond with the solute molecule. It may be added that this method of three-component system which was originally used in the study of the ultraviolet absorption of phenol[1,2] has recently been utilized by Brealey and Kasha in demonstrating the role of hydrogen bonding in the $n \rightarrow \pi^*$ blue shift phenomenon[9]. Further, it has been applied to the study of the fluorescence of some organic compounds[10].

The present article will suggest that there is another promising application of the studies concerning the hydrogen bonding effect, that is: a new clue to the nature of the absorption bands of a given molecule is to be provided from the spectral changes at the time of formation of a hydrogen bond. For this purpose, however, some additional information is required on the relation between the type of an electronic transition and the change in its corresponding spectrum accompanied by the hydrogen bonding.

With this point in mind, the hydrogen bonding effect on the absorption spectrum of *p*-hydroxyazobenzene has been newly investigated. This substance is provided with features fitted for the present purpose. It has a proton-donating hydroxyl group, and has several absorption bands of different types. Moreover, there is no ambiguity regarding its structure in solution. It is known that *p*-hydroxyazobenzene exists only in the azo-form in any common solvent, and further for this molecule one need not consider the formation of an intramolecular hydrogen bond such as occurs in *o*-hydroxyazobenzene[11].

Azobenzene and its derivatives, including *p*-hydroxyazobenzene, have three absorption bands in the visible and the near ultraviolet regions[12,13]. The band situated in the visible region has been assigned by McConnell[14] to an $n \rightarrow \pi^*$ transition, while the other two bands appearing in the ultraviolet region are considered to be due to $\pi \rightarrow \pi^*$ transitions[13]. In the following, it will be shown that the changes in $n \rightarrow \pi^*$ and $\pi \rightarrow \pi^*$ absorptions caused by the hydrogen bond between *p*-hydroxyazobenzene and ether or pyridine are of entirely different nature.

Experimental

Materials.—*p-Hydroxyazobenzene* (Kanto Chemical Co., Inc., guaranteed) was purified chromatographically through an alumina column by

1) H. Baba and S. Nagakura, *J. Chem. Soc. Japan, Pure Chem. Sect.* (*Nippon Kagaku Zassi*), **72**, 3 (1951).
2) S. Nagakura and H. Baba, *J. Am. Chem. Soc.*, **74**, 5693 (1952).
3) H. Tsubomura, *J. Chem. Soc. Japan, Pure Chem. Sec.* (*Nippon Kagaku Zassi*), **73**, 920 (1952).
4) S. Nagakura, ibid., **74**, 153 (1953); *J. Am. Chem. Soc.*, **76**, 3070 (1954).
5) S. Mizushima, M. Tsuboi, T. Shimanouchi and Y. Tsuda, *Spectrochim. Acta*, **7**, 100 (1955).
6) H. Baba, *Monogr. Res. Inst. Appl. Elec.*, Hokkaido Univ., No. 4, 61 (1954).
7) S. Nagakura, *J. Chem. Soc. Japan, Pure Chem. Sec.* (*Nippon Kagaku Zassi*), **75**, 734 (1954).
8) T. Kubota, *J. Pharm. Soc. Japan*, **74**, 831 (1954); **75**, 1540 (1955).
9) G. J. Brealey and M. Kasha, *J. Am. Chem. Soc.*, **77**, 4462 (1955).
10) N. Mataga, Y. Kaifu and M. Koizumi, *Nature*, **175**, 731 (1955); This Bulletin, **29**, 115 (1956).
11) See, for instance, H. Shingu, *J. Chem. Soc. Japan, Pure Chem. Sec.* (*Nippon Kagaku Zassi*), **60**, 542 (1939).
12) A. Burawoy and J. T. Chamberlain, *J. Chem. Soc.*, **1952**, 3734.
13) P. P. Birnbaum, J. H. Linford and D. W. G. Style, *Trans. Faraday Soc.*, **49**, 735 (1953).
14) H. McConnell, *J. Chem. Phys.*, **20**, 700 (1952).
15) W. R. Brode, *J. Phys. Chem.*, **30**, 56 (1926).

developing with benzene: m. p. 154°C (literature 152°C corrected[15], 155—156°C corrected[16]).

Iso-octane (2, 2, 4-trimethylpentane; Enjay Co., Inc., U. S. A.) was purified using the purification method for hexane[17]: b. p. 99°C, $n_D^{20}=1.3910$.

Ethyl ether (Kanto, guaranteed) was treated with mercury to eliminate peroxides and distilled: b. p. 34.5°C.

Pyridine was added to a solution of oxalic acid in acetone, and from the resulting precipitate of oxalate it was obtained in pure form[18]: b. p. 115—116°C, $n_D^{21}=1.5087$.

Method and Results. — Absorption spectra were obtained with a Beckman Quartz Spectrophotometer Model DU. A set of spectra were measured for the following solutions:

Solution 1, *p*-hydroxyazobenzene in *iso*-octane;
Solution 2, *p*-hydroxyazobenzene in *iso*-octane containing a small quantity of a proton-accepting substance;
Solution 3, *p*-hydroxyazobenzene in *iso*-octane containing a proton-accepting substance, the amount of which is about five times that in solution 2.

Ether and pyridine were used as the proton-accepting substance. The reference liquids adopted in measuring absorbances were *iso*-octane for solution 1, and *iso*-octane-ether or -pyridine mixtures for solutions 2 and 3 in which the concentrations of the latter substance were the same as in solutions 2 and 3, respectively. The concentrations of *p*-hydroxyazobenzene were about 5×10^{-5} mole/*l* in all cases. At such a low concentration one may expect that no association occurs among the *p*-hydroxyazobenzene molecules[19].

Measurements were made at room temperatures: 20°C for ether series, and 15°C for pyridine series. The observed spectra are given as curves 1, 2 and 3 in Figs. 1 and 2.

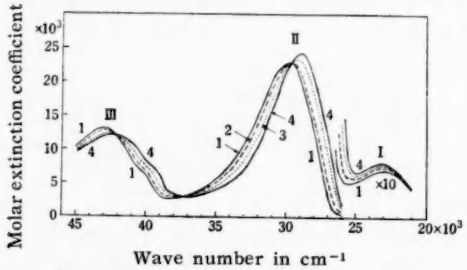

Fig. 1. The absorption spectrum of *p*-hydroxyazobenzene in *iso*-octane solution, and changes therein due to the addition of ether. The concentrations of ether: curve 1, zero; curve 2, 0.0152 mole/*l*; curve 3, 0.0797 mole/*l*. Curve 4 represents the absorption spectrum of the hydrogen bonded *p*-hydroxyazobenzene.

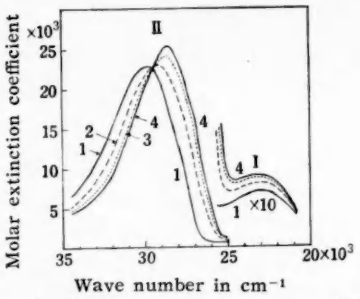

Fig. 2. The absorption spectrum of *p*-hydroxyazobenzene in *iso*-octane solution, and changes therein due to the addition of pyridine. The concentration of pyridine: curve 1, zero; curve 2, 0.00271 mole/*l*; curve 3, 0.0135 mole/*l*. Curve 4 represents the absorption spectrum of the hydrogen bonded *p*-hydroxyazobenzene.

The transitions are referred to as I, II and III in the order of increasing wave number. A remarkable spectral change occurs in the presence of a very small amount of ether or pyridine. Let it be assumed that the change is solely due to the formation of a hydrogen bond between *p*-hydroxyazobenzene and ether or pyridine.

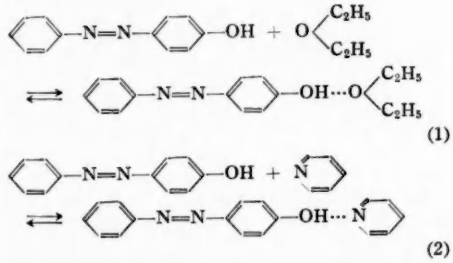

Then the curves 2 and 3 will be interpreted as the superposition of two kinds of absorption; one is due to the free *p*-hydroxyazobenzene, and the other due to the hydrogen bonded *p*-hydroxyazobenzene. This view is substantiated by the existence of several isosbestic points in Figs. 1 and 2.

The equilibrium constant K for equilibriums (1) and (2) can be obtained according to the usual manner[4,6]. Let the total concentrations of the proton-accepting substance in solutions 2 and 3 be C and C', respectively. Then it follows that

$$K=\frac{\varepsilon-\varepsilon_f}{\varepsilon'-\varepsilon}\frac{1}{C}-\frac{\varepsilon'-\varepsilon_f}{\varepsilon'-\varepsilon}\frac{1}{C'}, \qquad (3)$$

16) A. Pongratz, G. Markgraf and E. Mayer-Pitsch, *Ber.*, **71B**, 1287 (1938).
17) T. Kuwada, "Solvents", p. 117, Maruzen, Tokyo (1953).
18) E. L. Whitford, *J. Am. Chem. Soc.*, **47**, 2934 (1925).
19) M. Tsuboi, *Kagaku-no-Ryoiki*, **7**, 611 (1953).

where ε_f is the molar extinction coefficient of free *p*-hydroxyazobenzene (see curve 1), and ε and ε' are apparent coefficients of *p*-hydroxyazobenzene in solutions 2 and 3, respectively (see curves 2 and 3). All these coefficients refer to a given wave number. Using the above K value, the molar extinction coefficient ε_b of the hydrogen-bonded *p*-hydroxyazobenzene is calculated as

$$\varepsilon_b = \varepsilon' + \frac{\varepsilon' - \varepsilon_f}{KC'}. \qquad (4)$$

The values of K obtained from the spectral data are 25 and 450, respectively, for equilibriums (1) and (2). By the relation $\Delta F = -RT \ln K$, these K values lead to the free energy changes of −1.9 kcal./mole and −3.5 kcal./mole, respectively. The calculated molar extinction coefficients of the hydrogen-bonded complexes are indicated as curves 4 in Figs. 1 and 2.

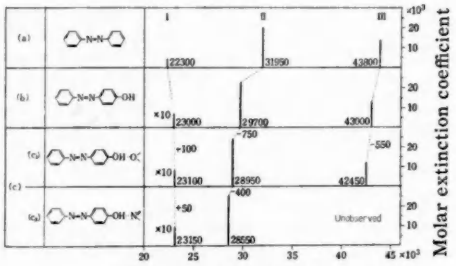

Fig. 3. The location and intensity of the absorption maxima of *p*-hydroxyazobenzene and its related substances.

Fig. 3 shows graphically the location and the intensity of the absorption maxima of both the free and the hydrogen-bonded *p*-hydroxyazobenzene, and also the wave number shifts arising from the hydrogen bond formation. The data for the parent compound, azobenzene[13,20], are given for the sake of comparison.

Discussion

Solvent effects in electronic spectra depend upon a number of factors, among which the dispersion and the polarity of solvents have been regarded as two important factors. The measure of the former is the refractive indices for the visible light and that of the latter is the dipole moments or sometimes the dielectric constants of the solvents. It is generally accepted that when the solvent has no dipole moment, the effect is largely determined by its refractive index, irrespective of whether the solute is polar or non-polar. On the other hand, when both the solvent and the solute are polar the solvent effect is determined by the magnitude of the dipole moment as well as the refractive index of the solvent[21,22].

In the present experiments the solute, *p*-hydroxyazobenzene, is polar and the solvent, *iso*-octane, is non-polar. In the case of solutions 2 or 3 there is an additional polar substance, ether or pyridine. Since the concentration of the last substance amounts to only 1% or less in mole ratio of the main solvent, *iso*-octane, one may expect that both the refractive index and the dielectric constant of the solvent remain almost unchanged with the addition of the polar substance. Therefore it may be reasonable to ascribe the spectral changes, which are observed when passing from *iso*-octane to *iso*-octane-ether or -pyridine mixture, to specific interaction of hydrogen bonding.

The spectral changes due to the hydrogen bonding are not independent of the type of the transition concerned. As is seen from Fig. 3, $n \rightarrow \pi^*$ transition I slightly shifts to the shorter wavelengths in the sequence (a) to (c), while $\pi \rightarrow \pi^*$ transitions II and III shift to the longer wavelengths in the same order. For the interpretation of the above phenomena it will be useful to refer to the fact pointed out by several authors[23] that introduction of an electron-repelling substituent such as OR or NR_2 into a chromophore often results in a red-shift of a $\pi \rightarrow \pi^*$ transition and a blue-shift of an $n \rightarrow \pi^*$ transition.

Let us consider $n \rightarrow \pi^*$ transition I. This transition corresponds to the jump of an electron from the non-bonding orbital of nitrogen atoms of the azo group to the lowest vacant π-orbital. The effect of substitution with an electron-repelling group upon an $n \rightarrow \pi^*$ transition was discussed by the present writer[24,25], and the following conclusions were drawn: (i) The

20) A. Burawoy, *J. Chem. Soc.*, **1937**, 1865.

21) N. S. Bayliss, *J. Chem. Phys.*, **18**, 292 (1950); N. S. Bayliss and E. G. McRae, *J. Phys. Chem.*, **58**, 1002 (1954).

22) Y. Ooshika, *Bull. Kobayashi Inst. Phys. Research*, **2**, 99 (1952); *J. Phys. Soc. Japan*, **9**, 594 (1954).

23) See, for instance, A. E. Gillam, E. S. Stern and E. R. H. Jones, "An Introduction to Electronic Absorption Spectroscopy in Organic Chemistry", Chap. 8, Edward Arnold (1954).

24) H. Baba, *J. Chem. Soc. Japan, Pure Chem. Sec.* (*Nippon Kagaku Zassi*), **72**, 74 (1951).

25) H. Baba, ibid., **72**, 341 (1951).

rate of the electron migration, hence the stabilization energy due to the electron migration, is smaller in the excited state than in the ground state of a substituted molecule. (ii) As a result, the $n\rightarrow\pi^*$ transition energy increases in comparison with that of the parent molecule. (iii) Such an effect will become larger with decreasing ionization potential of the non-bonding electron belonging to the substituent.

From (ii) the increase of the $n\rightarrow\pi^*$ absorption frequency from (a) to (b) may be understood. If the hydrogen bonds expressed in equilibriums (1) and (2) are formed, the ionization potential of the non-bonding electron of the hydroxyl group will decrease. Then from (iii) it follows that the absorption frequency is increased by the formation of the hydrogen bonds (see (b) and (c) of Fig. 3).

According to (i) the electronegativity of the oxygen atom of the hydroxyl group is expected to be lowered as a result of the $n\rightarrow\pi^*$ transition. Therefore the O—H···O$\langle$ or O—H···N$\langle$ hydrogen bonding energy will be smaller in the excited state than in the ground state. This fact will also contribute to the increase of the $n\rightarrow\pi^*$ absorption frequency†.

The situation is entirely different for the $\pi\rightarrow\pi^*$ transitions. In the excited state for a $\pi\rightarrow\pi^*$ transition of a substituted molecule the rate of electron migration is in general larger than in the ground state[24,26]. This illustrates the reduction of the absorption frequency in the order (a) to (c) as contrasted with the case of the $n\rightarrow\pi^*$ transition. This behavior of the $\pi\rightarrow\pi^*$ absorption bands of the *p*-hydroxyazobenzene is quite similar to that of $\pi\rightarrow\pi^*$ bands of other molecules reported in the literature[1-7].

Lastly let consideration be given to the difference between the effects of O—H···O$\langle$ and O—H···N$\langle$ hydrogen bonds. The present experiments have revealed that both the equilibrium constant and the frequency shift for the O—H···N$\langle$ bond are larger than those for the O—H···O$\langle$ bond (see (c_1) and (c_2) of Fig. 3). It is then suggested that the proton-accepting power of the nitrogen atom is stronger than that of the oxygen atom. This is in accord with Tsuboi's conclusion derived from infrared spectroscopy[19].

26) K. F. Herzfeld, *Chem. Revs.*, **41**, 233 (1947).

† As is seen from Figs. 1 and 2, $n\rightarrow\pi^*$ absorption band I is superposed on the tail of $\pi\rightarrow\pi^*$ band II which is of high intensity and is displaced to the red by the hydrogen bonds. This fact may be responsible to some extent for the observed blue-shift of the $n\rightarrow\pi^*$ band.

Summary

The electronic absorption spectra of *p*-hydroxyazobenzene in *iso*-octane and also in the mixtures of *iso*-octane-ether and *iso*-octane-pyridine were measured. The spectral change observed when addition was made of a small amount of ether or pyridine to a solution of *p*-hydroxyazobenzene in pure *iso*-octane was satisfactorily interpreted as due to the formation of a hydrogen bond between the solute molecule and ether or pyridine. The equilibrium constants for the hydrogen bonds and the absorption curves of the hydrogen-bonded complexes were determined from the spectral data.

It is made clear that the effects of hydrogen bonding on the absorption bands are dependent upon the type of the electronic transitions from which the bands originate. The $\pi\rightarrow\pi^*$ bands situated in the ultraviolet region are markedly displaced to the red, while the $n\rightarrow\pi^*$ band in the visible region slightly to the blue. A theoretical explanation for the above phenomena is offered.

The author wishes to express his sincere thanks to Professor K. Higasi for his encouragement and for reading the manuscript. Thanks are also due to Dr. S. Nagakura for his help in carrying out the experiments.

Research Institute of Applied Electricity
Hokkaido University, Sapporo

Studies on the Cobalt(III) Complexes Containing Only One Chelate Ring. I. Syntheses of $[Co(NH_3)_4\,gly]X_2$ *and* $[Co(NH_3)_4\,alan]X_2$[1].

By Yoichi SHIMURA

(Received November 13, 1957)

Limited number of cobalt(III) complexes which contain only one chelate ring are known, in contrast with the numerous series of those containing two chelate rings. The most familiar examples of such "mono-chelate cobalt(III) complexes" hitherto known are monocarbonato-tetrammine and monoxalato-tetrammine complexes. Mono(amino-acido)-tetrammine or monoethylenediamine-tetrammine cobalt(III) complexes were not known heretofore. Recently, Kuebler and Bailar[2] reported that the attempted replacement of the chloride ion or the sulfono group[3], respectively, in $[Co(NH_3)_4Cl_2]^+$ and $[Co(NH_3)_4(SO_3)_2]^-$ by *N*, *N*-diethylglycine was unsuccessful.

In the present paper, the syntheses of monoglycinato-tetrammine and mono-alaninato-tetrammine Co(III) complexes will be reported. Furthermore, the visible and ultraviolet absorption spectra of the (amino-acido)-ammine series of Co(III) complexes will be discussed mainly in relation to the geometrical structures of the complex ions.

Results and Discussion

Method of Syntheses.—For the first place, the reactions between sodium glycinate and $[Co(NH_3)_4(OH_2)_2]^{3+}$ or $[Co(NH_3)_4(OH_2)Cl]^{2+}$ were investigated. Evidences for the formation of some glycinato complexes were obtained, but the complexes were not isolated in pure state. Next, the use of decolorizing charcoal as catalyst[4] was examined. However, in the presence of charcoal glycinate radical gradually expelled the co-ordinated ammonia molecules and consequently the desired tetrammine complexes were not obtained.

Lastly, therefore, the reaction of $[Co(NH_3)_4(OH_2)Cl]SO_4$ with sodium glycinate was examined in the presence of decolorizing charcoal and of aqueous ammonia (see experimental part). This procedure produces a mixture of three or more species of the complex ions which belong to the glycinato-ammine series. From the mixture, $[Co(NH_3)_6]^{3+}$ was removed as the sparingly soluble chloride-sulfate, $[Co(NH_3)_6]Cl\cdot SO_4\cdot 3H_2O$, and the desired complex $[Co(NH_3)_4\,gly]^{2+}$ was separated as sulfate from the mother liquor*. The yield did not exceed 30%. As a by-product, $[Co(NH_3)_2\,gly_2]Cl$ was also obtained in a small yield.

The reaction between sodium alaninate and $[Co(NH_3)_4(OH_2)Cl]SO_4$ proceeds in a similar way. In this case an amount of tris-alaninato cobalt(III) complex also yielded.

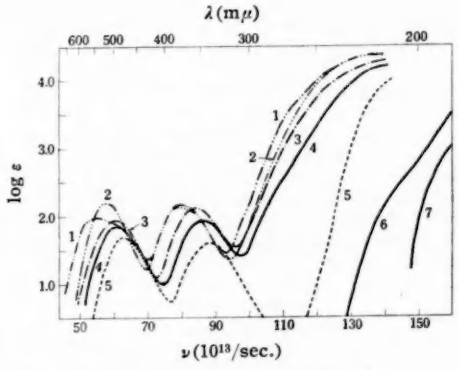

Fig. 1. Absorption curves of $[Co(NH_3)_{6-2x}(gly)_x]$ series.

1. *trans-cis*-$[Co\,gly_3]\cdot 2H_2O$
2. *cis-cis*-$[Co\,gly_3]\cdot H_2O$
3. $[Co(NH_3)_2\,gly_2]Cl$
4. $[Co(NH_3)_4\,gly]SO_4\cdot H_2O$
5. $[Co(NH_3)_6](ClO_4)_3$
6. $NH_2CH_2CO_2Na$[5]
7. NH_3[5]

1) Partly presented at the Symposium on Co-ordination Compounds, Tokyo, October 28, 1956.

2) J. R. Kuebler, Jr. and J. C. Bailar, Jr., *J. Am. Chem. Soc.*, **74**, 3535 (1952).

3) The "sulfono group" is $SO_3^=$ radical bound to the central metal ion by the sulfur atom: See Y. Shimura, This Bulletin, **25**, 46 (1952).

4) J. C. Bailar, Jr. and J. B. Work, *J. Am. Chem. Soc.*, **67**, 176 (1945).

* The following abbreviations are used: am, amino-acid radical in general; gly, $NH_2\cdot CH_2\cdot CO_2^-$; alan, $NH_2\cdot CH(CH_3)\cdot CO_2^-$.

TABLE I

ABSORPTION DATA OF $[Co(NH_3)_{6-2x}(gly)_x]$ AND $[Co(NH_3)_{6-2x}(alan)_x]$ SERIES.

Complex ion	First absorption band				Second absorption band					
	ν_{max} (10^{13}/sec.)	log ε_{max}	l[b] (10^{13}/sec.)	δ[c] (10^{13}/sec.)	ν_{max} (10^{13}/sec.)	log ε_{max}	l[b] (10^{13}/sec.)	δ[c] (10^{13}/sec.)	$\Delta(\nu_{max})$[e]	(log ε_{max})[f]
$[Co(NH_3)_6]^{3+}$	62.9	1.68	10.3	0.5	88.3	1.60	12.5	0.35	25.4	−0.08
$[Co(NH_3)_4gly]^{2+}$	60.8	1.86	11.3	0.55	86.4	1.93	12.3	0.35	25.6	+0.07
$[Co(NH_3)_2gly_2]^{+}$	60.4	1.94	11.3	0.25	84.3	2.11	11.8	0.5	23.9	+0.17
cis-cis-[Co gly_3][d]	57.7	2.20	9.1	0.55	80.2	2.14	12.7	0.6	22.5	−0.06
trans-cis-[Co gly_3]	55.2[a]	1.99	—	—	80.4	2.16	12.1	0.35	—	—
$[Co(NH_3)_4alan]^{2+}$	61.5	1.87	11.0	0.6	86.7	1.90	12.8	0.4	25.2	+0.03
cis-cis-[Co $alan_3$][d]	57.9	2.27	9.0	0.6	80.3	2.21	11.7	0.7	22.4	−0.06
trans-cis-[Co $alan_3$][d]	55.6[a]	2.00	—	—	80.9	2.18	12.3	0.5	—	—

a: This band splits into two or more components (see Figs. 1 and 2).
b: l=half-value width. This corresponds to $\{\delta(+)+\delta(-)\}$ in Jørgensen's notation[6].
c: δ=inclination parameter[7] or Inklination (in German)[8]. This parameter corresponds to $\frac{1}{2}\{\delta(+)-\delta(-)\}$ in Jørgensen's notation[6], and is defined by the equation $\delta=\frac{1}{2}\{\nu_k+\nu_l\}-\nu_{max}$, where ν_k and ν_l are the two frequencies where the formal extinction coefficients are equal to the half of ε_{max}.
d: Measured in 60% perchloric acid.
e: Frequency difference between the maxima of the second and the first absorption band.
f: Difference between log ε_{max}'s of the second and the first band.

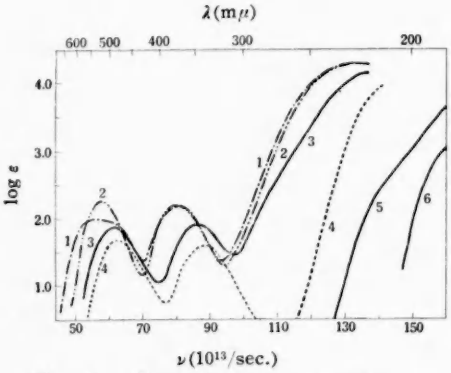

Fig. 2. Absorption curves of $[Co(NH_3)_{6-2x}(alan)_x]$ series.
1. *trans-cis*-[Co $alan_3$]
2. *cis-cis*-[Co $alan_3$]
3. $[Co(NH_3)_4alan]SO_4$
4. $[Co(NH_3)_6](ClO_4)_3$
5. $NH_2CH(CH_3)CO_2Na$[5]
6. NH_3[5]

The aqueous solutions of the $[Co(NH_3)_4am]X_2$-type complexes are rather unstable. These complexes can be recrystallized from warm water, but hot water decomposes the complexes.

Absorption Spectra.—The absorption curves of the cobalt(III) complexes which belong to the glycinato-ammine and the alaninato-ammine series are shown in Figs. 1 and 2. The numerical data of the first and the second absorption bands of these complexes are summarized in Table I.

As is seen in the figures and the table, the successive substitution of ammonia ligands in those complexes by the glycinate or the alaninate ions causes the regular red-shifts of the band maxima and the regular increase in the absorption intensities. The alaninate ion has a slightly higher position in the spectrochemical series[9,10] than the glycinate ion.

The two isomers, α(violet) and β(red), are known for the complexes of $[Co^{III}am_3]$type. The two forms correspond to the geometrical isomers, *cis-cis* and *trans-cis* forms (Fig. 3). As will be seen

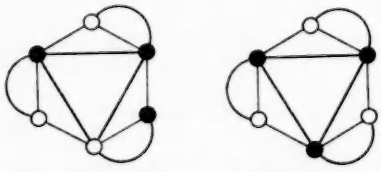

α (*trans-cis*, violet) *β* (*cis-cis*, red)

Fig. 3. Two geometrical isomers of $[Co^{III}am_3]$. (white circle, oxygen atom; black circle, nitrogen atom)

5) H. Ley and B. Arends, *Z. physik. Chem.*, **B 17**, 117 (1932).
6) C. K. Jørgensen, *Acta Chem. Scand.*, **8**, 1495 (1954).
7) Y. Shimura and R. Tsuchida, This Bulletin, **28**, 572 (1955).
8) H. Siebert and M. Linhard, *Z. physik. Chem., N. F.*, **11**, 318 (1957).
9) R. Tsuchida, This Bulletin, **13**, 388, 436 (1938).
10) Y. Shimura and R. Tsuchida, ibid., **29**, 311 (1956).

in Figs. 1 and 2, the main difference between the absorption curves of the two isomers occurred in the first absorption bands. Thus the first band of the β-isomer has a normal pseudo-parabolic form, while that of the α-form distinctly shows an indication of splitting. This splitting may be considered as a proof of the *trans-cis* structure of the α-form, since a similar splitting was reported for the first band of *trans* isomer of $[Co(NH_3)_4(OCOCH_3)_2]ClO_4$ and not for that of the corresponding *cis* isomer[11]. The above conclusion was reported briefly in a previous report[10]. Independently, Basolo et al.[12] came to the same conclusion. The assignment is also supported by the semi-empirical molecular orbital calculations by Nakamoto et al.[13] and by Yamatera[14].

Five geometrical isomers are possible for the complex ion, $[Co(NH_3)_2\,gly_2]^{2+}$ (Fig. 4). In the present study only one species was obtained. Since the first band of the species has no indication of splitting, it has probably a *cis* structure concerning the two oxygen atoms of the two glycinate ligands, i.e., one of (a), (c) or (d) in Fig. 4.

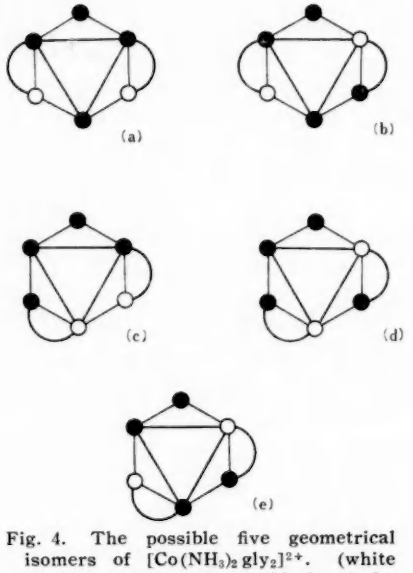

Fig. 4. The possible five geometrical isomers of $[Co(NH_3)_2\,gly_2]^{2+}$. (white circle, oxygen atom; black circle, nitrogen atom)

11) M. Linhard and M. Weigel, *Z. anorg. Chem.*, **264**, 321 (1951).
12) F. Basolo, C. J. Ballhausen and J. Bjerrum, *Acta Chem. Scand.*, **9**, 810 (1955).
13) K. Nakamoto, J. Fujita, M. Kobayashi and R. Tsuchida, *J. Chem. Phys.*, **27**, 439 (1957).
14) H. Yamatera, presented at the Symposium on Coordination Compounds, Osaka, October 30, 1955.

Experimental

Glycinato-tetrammine cobalt(III) sulfate monohydrate, $[Co(NH_3)_4gly]SO_4\cdot H_2O$—Two grams of glycine and one gram of Na_2CO_3 were dissolved in 6 ml. of warm water. To this solution were added 7.4 g. of $[Co(NH_3)_4(OH_2)Cl]SO_4$[15], 0.5 g. of decolorizing charcoal and 0.5 ml. of aqueous ammonia (28 %). The resulting mixture was evaporated on a water bath almost to dryness. The residue was treated with about 60 ml. of warm water and any sparingly soluble materials were filtered off by suction. Upon cooling, some amount of $[Co(NH_3)_6]SO_4\cdot Cl\cdot 3H_2O$* separated from the filtrate in orange-yellow crystals. After removal of the orange-yellow crystals by filtration, a large amount of 95 % ethanol was added to the filtrate. The desired complex separated as the orange precipitate. This was separated by filtration from the red-colored mother liquor. (This mother liquor contains $[Co(NH_3)_2\,gly_2]Cl$.) The crude product was much contaminated by the orange-yellow crystals above mentioned. Therefore it was recrystallized from warm water or by the addition of ethanol to the cold aqueous solution. Three or more recrystallizations were necessary to obtain the pure products. The pure crystals are orange-red plates and effloresced on exposure to the air. The freshly dried crystals were analyzed for water of crystallization.

Anal. Found: H_2O, 5.27 %. Calcd. for $[Co(NH_3)_4\,gly]SO_4\cdot H_2O$: H_2O, 5.72 %.

The analyses for the following components were performed by use of the salts dehydrated at 90–100°C.

Anal. Found: Co, 19.4; C, 8.40; H, 5.50; SO_4^{--}, 32.18 %; Calcd. for $[Co(NH_3)_4(NH_2CH_2CO_2)]SO_4$: Co, 19.83; C, 8.08; H, 5.43; SO_4^{--}, 32.32 %.

Bisglycinato-diammine cobalt(III) chloride, $[Co(NH_3)_2\,gly_2]Cl$—The red colored mother liquor above mentioned was evaporated in vacuo over sulfuric acid at room temperature. The separated red precipitates were dissolved in hot water and filtered. After cooling, 99 % ethanol was added to the filtrate. The pure product was precipitated as red crystals.

Anal. Found: C, 17.45; H, 4.96; Cl, 12.4 %. Calcd. for $[Co(NH_3)_2(C_2H_4O_2N)_2]Cl$: C, 17.37; H, 5.10; Cl, 12.82 %.

Alaninato-tetrammine cobalt(III) sulfate, $[Co(NH_3)_4\,alan]SO_4$—One gram of sodium carbonate and 2.4 g. of *dl*-α-alanine were dissolved in 6 ml. of warm water. To this solution were added 7.4 g. of $[Co(NH_3)_4(OH_2)Cl]SO_4$[15], 0.5 g. of decolorizing charcoal and 0.4 ml. of aqueous ammonia (30 %). The resulting mixture was evaporated on a water bath almost to dryness. The residue was treated with about 100 ml. of

15) S. M. Jørgensen, *J. prakt. Chem.*, **42**, 211 (1890).
* *Anal.* Found: Co, 17.4; H_2O, 15.85%. Calcd. for $[Co(NH_3)_6]SO_4\cdot Cl\cdot 3H_2O$: Co, 17.00; H_2O, 15.53%.

warm water and any sparingly soluble materials** were filtered off by suction. When the filtrate was cooled, some amount of orange-yellow crystals, $[Co(NH_3)_6]SO_4 \cdot Cl \cdot 3H_2O$, separated. After removal of the orange-yellow crystals by filtration, a large amount of 95% ethanol was added to the filtrate. The crude complex was obtained as orange precipitate. This was separated by filtration from the red mother liquor. The product was much contaminated by the orange-yellow crystals above mentioned. Therefore, this was dissolved in warm water and fractionally precipitated by addition of ethanol. The contaminants were concentrated in the first fraction. The second and the following fractions were put together and precipitated twice more by the same manner. The orange red crystals obtained were washed with 95% ethanol and dried in air. The crystals dried in air contained 1—1.5 moles of water of hydration. This was completely dehydrated by heating at about 100°C.

Anal. Found: SO_4^{--}, 31.30%. Calcd. for $[Co(NH_3)_4(C_2H_5O_2N)]SO_4$: SO_4^{--}, 30.87%.

By evaporation of the red mother liquor above mentioned, a small amount of red crystals separates, and this is probably $[Co(NH_3)_2 alan_2]Cl$. Further studies were not intended for this complex, since only a small amount of the sample was available.

trans-cis-[Co gly_3]$\cdot 2H_2O$, *cis-cis*-[Co gly_3]$\cdot H_2O$, *trans-cis*-[Co $alan_3$] and *cis-cis*-[Co $alan_3$] were prepared by the method of Ley and Winkler[16] with reference to the report of Holtzclaw and Sheetz[17]. $[Co(NH_3)_6](ClO_4)_3$ was prepared by the method of Linhard[18].

Absorption Measurement.—The absorption spectra of *cis-cis*-[Co gly_3] and the two isomers of [Co $alan_3$] were measured in 60% perchloric acid. The aqueous solutions were used for the other complexes. The concentrations of the solutions varied from 1.0×10^{-2} to 0.5×10^{-4} gram complex-ion per liter. The absorption measurements were made by a Beckman DU spectrophotometer at room temperature.

Summary

The three new complexes, $[Co^{III}(NH_3)_4 gly]SO_4 \cdot H_2O$, $[Co^{III}(NH_3)_4 alan]SO_4$ and $[Co^{III}(NH_3)_2 gly_2]Cl$, have been synthesized by the reaction of $[Co(NH_3)_4(OH_2)Cl]SO_4$ with the amino-acid radicals in the presence of ammonia and decolorizing charcoal.

The visible and the ultraviolet absorption spectra of the glycinato-ammine and alaninato-ammine series of cobalt(III) complexes have been measured and discussed in relation to the geometrical structures of the complex ions.

The author wishes to thank Professor R. Tsuchida for his kind guidance throughout this work.

Department of Chemistry, Faculty of Science, Osaka University
Kita-ku, Osaka

** This is a mixture of decolorizing charcoal and the two isomers of $[Co^{III}\ alan_3]$.

16) H. Ley and H. Winkler, *Ber.*, **42**, 3894 (1909).

17) H. F. Holtzclaw, Jr. and D. P. Sheetz, *J. Am. Chem. Soc.*, **75**, 3053 (1953).

18) M. Linhard, *Z. Elektrochem.*, **50**, 224 (1944).

Some Remarks on the Spreading of Protein Monolayers (Dynamic Studies on Monolayer. I)

By Maresuke KASHIWAGI

(Received October 16, 1957)

The monolayer of low molecular compounds such as fatty acids has been extensively studied[1]. These molecules dissolve often in benzene and usually they can be spread from the benzene solution, leaving a stable monolayer in the air-water interface after the evaporation of the solvent. In such a case, the spreading process itself does not present any difficulty and much more important are the physico-chemical investigations on the spread monolayer.

Proteins, on the other hand, are quite different from these compounds in respect to surface chemical behavior owing to their unique mloecular structure. Water-soluble protein can not be expected to spread on water substrate. In fact, most proteins fail to spread on pure water.

1) W. D. Harkins, "The Physical Chemistry of Surface Films", Reinhold, New York (1954).

Thus the spreading process becomes important and this spreading is known to be dependent largely on sub strate and other experimental conditions. Many pioneer chemists have emphasized the importance of those experimental conditions since those are rather fundamental for the protein monolayer. Certain proteins may spread immediately on some good substrate, but may take a considerable time to reach equilibrium state on the other substrate. This time effect was attributed mainly to the unfolding of a large complex structure of protein, by Bull and Neurath[2], and also by Jonxis[3].

The author also demonstrated[4] this effect, using one of the largest proteins, myosin. A theoretical equation was derived which was found to fit the experiments quite well. Attempts were made to examine other types of protein (i.e., relatively low molecular weight) in this respect. The spreading of ovalbumin is found to be complete within the first 5 minutes on 20% ammonium sulfate substrate at its isoelectric point and the spreading was not disturbed by different rates of compression. But a partial collapse is observed on 0.1 N hydrochloric acid substrate. Hemoglobin appears to take considerable time to come to equilibrium on account of physical or chemical changes in molecular structure. These results will be discussed on the basis of protein structure in the surface film.

Experimental

Apparatus.—The surface balance used for the present investigation is a vertical plate type of the size $60\times15\times2$ cm. The sensitivity is 0.02 dyn./cm. The whole apparatus is installed in a glass cabinet to avoid accidental contamination during the measurement. The use of such an apparatus is made possible by the courtesy of Professor T. Tachibana of Ochanomizu Women's University. All normal precautions, namely those described by Adam[5] were taken.

Protein.—Ovalbumin is extracted from fresh egg by the usual method[6] and recrystallized three times from saturated sodium sulfate solution. Bovine serum Hemoglobin is purchased from Pentex Corp., Kankakee, Illinois and used without further purification.

To examine the extent of spreading of protein monolayer, surface pressure change is observed with time and the constant value of surface pressure is considered to be that at equilibrium. The measurement is carried out at room temperature, but the temperature remained practically constant during each time of operation.

Experimental procedure.—Protein is spread in the air-water interface from its aqueous solution and the concentration is determined by drying a solution to constant weight. General spreading conditions are as follows: a known amount of protein solution is spread by means of a calibrated micropipet over a very large area (2.5 m^2/mg) and the film is kept there for exactly 5 minutes before the start of compression. The moving barrier is compressed gently to the desired area. The measurement is begun immediately when the barrier is adjusted to the area.

Theoretical Consideration

When a stable monolayer formation is not completed, the film is still in an unstable state. The system therefore will endeavor to reach lower free energy state and such a transitional process may involve change in surface pressure at a constant area, if the area is smaller than that in the gaseous state. Absence of such phenomena would indicate that the monolayer is at equilibrium under that condition. This equilibrium will be achieved quickly only on a good substrate. These structural changes in the film may be grouped, excluding surface interaction phenomena, as follows;

a) *Surface pressure increase with time* ($\Delta F>0$): This increase would mean that a configurational change of molecules in the film is occurring to reach a state of lower free energy. It may include, in a special case, dissociation of molecules.

b) *Surface pressure decrease with time* ($\Delta F<0$): Owing to a strong hydrophilic attraction between protein and water, some molecules in the film are dissolving into the water underneath them. Or else, some proteins are aggregating in the film.

c) *Constant surface pressure* ($\Delta F=0$): This means that all molecules in the film are in a state of the lowest free energy under that experimental condition. The film is thermodynamically in a stable equilibrium.

Results

Table I is a summary of measured values of surface pressure change ΔF as a function of time t at various areas under an identical condition.

2) H. B. Bull and H. Neurath, *Chem. Revs.*, **23**, 391 (1938); *J. Biol. Chem.*, **118**, 163 (1937).
3) J. H. P. Jonxis, *Biochem. J.*, **33**, (1943).
4) K. Kashiwagi and B. Rabinowitch, *J. Phys. Chem.*, **59**, 498 (1955).
5) N. K. Adam, "The Physics and Chemistry of Surfaces", 3rd ed. p. 27-31, Oxford Univ. Press, London (1944).
6) R. A. Kekwick and R. K. Cannon, *Biochem.*, **30**, 227 (1936).

TABLE I

SURFACE PRESSURE CHANGE OF OVALBUMIN AT CONSTANT AREA

Time Allowed For After Spreading, 5 min.
Substrate is 20% Ammonium Sulfate at pH 4.8.

Const. Area m^2/mg.	Temp. °C	Rate of compression cm./min.	ΔF dyn./cm.				
			1 min.	5	15	30	60
0.75	26	15	0	−0.12	−0.12	−0.12	0
0.76	26	100	0	0	0	0	0
0.81	26	12	0	0	0	0	0
0.82	26	90	0	0	0	0	0
0.85	26	80	0	0	0	0.12	0.12
0.90	28	76	0	0	0	0.12	0.12
0.99	30	92	0	0	0	0	−0.12
1.10	26	12	0	0	0	0	0

It is clear that surface pressure is constant over the whole period of experiment and that it is independent of the rate of compression. These facts can be taken as a direct indication that albumin spreading is complete within the first 5 minutes. Concentrated ammonium sulfate solution at isoelectric point is therefore a good substrate. Some proteins are known to spread on strong acid substrate. Whether this is true or not may be tested in the same way.

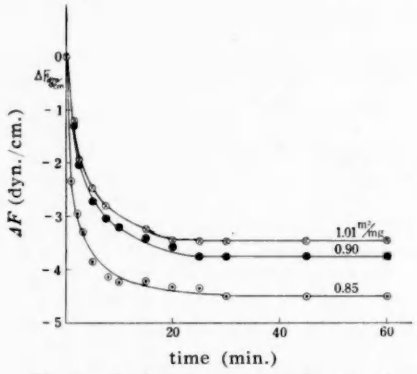

Fig. 1. Surface pressure change of ovalbumin (substrate 0.1 N HCl, 31°C).

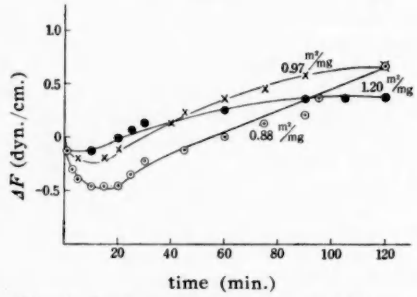

Fig. 2. Surface pressure change of Hemoglobin (substrate 20 % $(NH_4)_2SO_4$, pH 4.2, temp. 31°C).

Fig. 1 shows surface pressure change of ovalbumin on 0.1 N hydrochloric acid at various areas. ΔF decreases with time, in all cases, on 0.1 N hydrochloric acid. It reaches, however, a final pressure after a certain lapse of time. Fig. 2 shows ΔF–t curves of Hemoglobin on 20 % ammonium sulfate at pH 4.2. ΔF decreases with time in the initial stage and, after reaching a definite minimum, increases again. If the main cause for pressure change is attributed to molecular movements in very limited space in the film, those time effects and the values of final pressure will be related to the compressibility, which is expressed as $-I\,dA/A\,dF$.

One convenient way of calculation may be an adoptation of the following approximation.

$$-\frac{I}{A}\frac{dA}{dF} \fallingdotseq -\frac{I}{A}\frac{\Delta A}{\Delta F} \fallingdotseq \frac{I}{\frac{A_1+A_2}{2}}\frac{A_2-A_1}{F_1-F_2}, \quad (1)$$

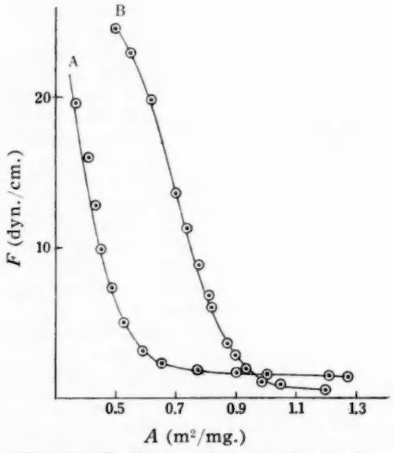

Fig. 3. Surface pressure of protein (time for spreading 20 min.).
A Albumin on 0.1 N HCl, 22°C
B Hemoglobin on 20 % $(NH_4)_2SO_4$, 31°C

where subscripts 1 and 2 refer to specified points close to each other on F–A curve. The F–A curves of albumin on 0.1 N hydrochloric acid and Hemoglobin on 20% ammonium sulfate are shown in Fig. 3.

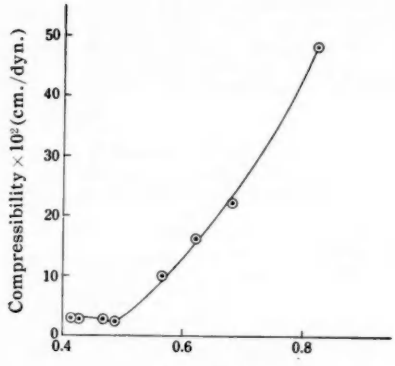

Fig. 4A. Compressibility of Albumin.

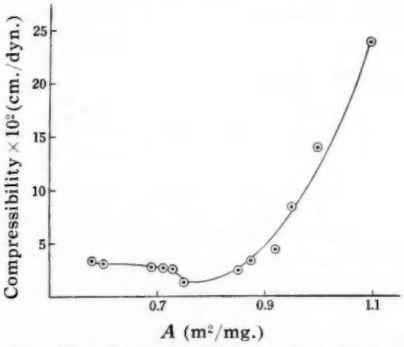

Fig. 4B. Compressibility of Hemoglobin.

Calculated values of compressibility are indicated in Fig. 4. In the region of low compressibility partially unfolded protein will be pushed downward more strongly by the surrounding molecules or will take more time to reach equilibrium. Both surface pressure change and the time needed for complete spreading are thus connected with compressibility.

Discussion

Neurath[7] considered that the unfolding of the protein molecule is a main cause for the time dependence of spreading. In fact, it will readily be thought that polypeptide chains in protein would need considerable time to orient and unfold themselves in the very viscous surface film into positions which yield minimum free energy. The author finds close analogy between behaviors of protein in bulk and in surface film. There seem to be plentiful evidences to prove that protein can take different configurations under different conditions[8,9].

According to Kauzmann et al.[10], the denaturation of protein in bulk may be illustrated as follows (Fig. 5). Stage 1

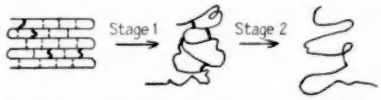

Fig. 5. Possible stages in the denaturation of a protein according to Kauzmann.

represents the initial unfolding reaction caused by rupture of many weak linkages and stage 2 the subsequent loop opening caused by rupture of relatively strong few intramolecular cross links. These ideas lead Kashiwagi and Rabinowitch[3] to the following expression

$$\frac{I}{(F_e+F^0)^2}\ln\frac{(F_e-F_0)(F+F^0)}{(F_e-F)(F_0+F^0)} + \frac{I}{(F_e+F^0)}\left\{\frac{I}{(F_0+F^0)}-\frac{I}{(F+F^0)}\right\} = kt/c, \qquad (2)$$

where F^0, a parameter, F_0, the surface pressure at zero time, F_e, the final equilibrium pressure, and F, the measured surface pressure at time t.

The derivation of this equation involves one assumption that the rate of increase in area occupied by the unfolding molecules at time t is proportional to the pressure under which the film finds itself, that is,

$$dA_0/dt = k(F_e-F) \qquad (3)$$

Although equation (2) fits myosin very well[4], it appears to fail for albumin. The reason for this seems clear, because on 20% ammonium sulfate at pH 4.8 spreading was complete in the first 5 minutes. There should be no increase in surface pressure after 5 minutes. Decrease in surface pressure on 0.1 N hydrochloric acid may indicate that some molecules

7) H. Neurath, *J. Phys. Chem.*, **40**, 361 (1936).

8) J. T. Yang and P. Doty, *J. Am. Chem. Soc.*, **79** 761 (1957).

9) A. Elliott and B. R. Malcolm, *Biochim. et Biophys. Acta*, **21**, 466 (1956).

10) H. K. Frensdorff, M. T. Watson and W. Kauzmann, *J. Am. Chem., Soc.*, **75**, 5157 (1953).

which failed to unfold completely at the time of delivery tend to dissolve slowly into substrate. A once-unfolded molecule in low free-energy state will not dissolve again. These become evident when consideration is given to the difference in molecular structure as shown in Table II.

TABLE II
DIFFERENCE IN MOLECULAR STRUCTURE

	Myosin[11]	Albumin
Mol. Wt.	1,000,000	45,000
Solubility	insoluble	very soluble
Shape	flexible rod-like	globular

Concerning the complicated surface behavior of Hemoglobin, it is difficult to distinguish whether the pressure rise after the initial decrease with time is due to dissociation of molecule and/or chemisorption of oxygen and carbon dioxide from the air.

The author wishes to express deep thanks to Professor T. Tachibana without whom this research would not have been possible. Thanks are also due to Miss E. Hirano and Miss N. Hayashi for their assistance.

Mitsuwa Chemical Laboratory
Marumiya Co. Ltd.
Terajima-machi, Sumida-ku, Tokyo

11) A. Szent-Györgyi, "Chemistry of Muscular Contraction." Academic Press, New York (1951).

*Isotopic Exchange Reaction between Cyclohexane and Deuterium on Evaporated Molybdenum Films**

By Teruo HAYAKAWA and Toshio SUGIURA

(Received October 16, 1957)

Catalytic exchange reactions between cyclic hydrocarbons and deuterium have been the subject of recent investigations. The exchange reaction between cyclohexane and deuterium on evaporated metal films has been studied by Anderson and Kemball[1]. Their results on rhodium and palladium clearly indicated that half of the hydrogen atoms were readily exchanged. For the remaining six hydrogen atoms to be exchanged, they proposed the mechanism in which the adsorbed radical turns over on the surface by second-point adsorption. Although their multiple exchange mechanism is very efficient, the discordance between the experiments and the theoretical calculations based on this mechanism for the initial product distributions was considerably predominant.

The exchange reaction between cyclohexane and deuterium over various nickel catalysts have also been reported by Burwell et al[2,3]. According to their results, no discontinuities which separate the concentrations of $C_6H_6D_6$ and $C_6H_5D_7$ appeared at 160–200°C when evaporated nickel films or reduced nickel oxide were used. In recent years we have also investigated the isotopic exchange reaction between cyclohexane and deuterium on evaporated metal films, since it was of interest to clarify the mechanism of this exchange and the contribution of the deuterium isotope effect.

Experimental

Materials.—Wako Chemicals Pure Grade *cyclohexane* was purified by several fractionations and dissolved gases were removed by pumping under vacuum while chilled. *Deuterated hydrogen* was prepared from complete decomposition of heavy water over pure metallic sodium preliminary outgassed and distilled in vacuo; it was purified by passing through traps cooled in liquid nitrogen under the reduced pressure and then by passing through a sodium-gettered glass tube.

* A part of this paper was read before the 9th Annual Meeting of the Chemical Society of Japan held in Kyoto, April, 1956. Another part of this paper was also presented before the "Symposium on the Catalytic Reactions" held in Tokyo, April, 1957.

1) J. R. Anderson and C. Kemball, *Proc, Roy. Soc.* (London), **A226**, 472 (1954).

2) H. C. Rowlinson, R. L. Burwell, Jr. and R. H. Tuxworth, *J. Phys. Chem.*, **59**, 225 (1955).

3) R. L. Burwell, Jr. and R. H. Tuxworth, ibid., **60**, 1043 (1956).

The mass spectrometric analyses revealed that the deuterium content of this sample was 36.1 atomic %.

Evaporated Molybdenum Films.—Evaporated molybdenum films were prepared by customary procedures including careful degassing at elevated temperatures. The reaction vessel was a cylindrical glass tube (inside diameter 30 mm., length about 20 cm.) and between 5.1 and 10.9 mg. of molybdenum was evaporated onto the inner surface of this tube while the tube was cooled in ice water. After each experiment the weight of evaporated films was determined by the usual volumetric analysis.

Apparatus and Procedure.—The principal diagram of the apparatus is shown in Fig. 1.

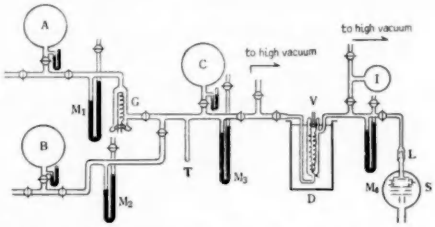

Fig. 1. Principal diagram of the apparatus.

Reservoir A containing purified deuterated hydrogen was connected to a sodium-gettered valve G by which the trace quantity of oxygen or water vapor was removed. The bulb B shows a reservoir of purified cyclohexane vapors, M_1 and M_2 auxiliary mercury manometers. T shows a trap cooled in liquid nitrogen, by which cyclohexane vapors were chilled before mixing. The sample gases were premixed and introduced into the storage bulb C, and the composition of each gas mixture was determined by means of the mercury manometer M_3.

Before commencing each experiment, the reaction vessel V was thoroughly evacuated for several hours and molybdenum was evaporated onto the inner surface of this vessel (the high vacuum was measured by means of the ionization gauge I). Then the reaction vessel was heated and controlled to the required temperature by means of the oil-bath thermostat D; the sample gases were admitted into the reaction vessel and the pressure was measured by means of the mercury manometer M_4. The oil-bath thermostat was operated by the usual electrical relay circuit; the temperature variation recorded by this thermostat was never greater than ± 0.1°C. After a given time, the gases were introduced, through the gas leak L, into the ion source S of a mass spectrometer and the product-compositions were determined. Since the orifice diameter of the gas leak was very small (i. e. smaller than 0.01 mm.), the pressure in the reaction vessel was practically unchanged.

In the present experiments, mass spectrometric analyses were performed on a modified Hitachi RMC mass spectrometer (90° sector type, the radius of curvature of the ion path and the maximum mass resolution were 135 mm. and about 150, respectively). The recording time required for magnetic scanning in the mass range between $m/e=83$ and 96 was about one minute, and other details of this instrument were already given[4]. For cyclohexane, 30 V. electrons were used for ionization, and at this ionizing voltage only a small fragmentation correction was required owing to the production of 6 % of the ion formed by the loss of one hydrogen atom. Corrections for fragmentation were made by assuming that the probability of ionization in the mass spectrometer was independent of isotopic content. Corrections were also made for deuterium and heavy carbon (C^{13}) occurring naturally in cyclohexane.

Results

The experimental conditions are shown in Table I, where the run numbers indicate the chronological order of the experiments. Figs. 2-6 show some typical results on the variation in the percentage of the various cyclohexane molecules with time. In these figures, the notation d_i has been used in place of cyclohexane-d_i ($C_6H_{12-i}D_i$) to facilitate presentation. Typical results on the initial product distributions obtained from measuring the initial slopes of these curves are also listed in Table II.

TABLE I
DETAILS OF ISOTOPIC EXCHANGE RUNS

Run	Temp. (°C)	Partial pressure (mmHg)	
		cyclohexane	deuterated hydrogen
7	111	15.4	15.4
8	75	15.5	15.5
9	97	19.6	19.6
11	56	11.4	11.4
12	102	10.1	10.1
13	86.5	14.8	14.8
14	75	6.8	6.8
15	106	9.0	9.0
16	102	6.9	6.9
17	87	6.7	6.7
18	86.5	6.8	6.8
21	75	20.4	5.1
22	94	3.0	2.0
23	102.5	1.5	1.0
24	97	7.5	7.5
28	97	6.5	6.5
29	97	12.8	6.4
30	97	18.9	6.3
31	97	24.3	6.1

4) T. Hayakawa and T. Sugiura, *Bull. Naniwa Univ., Series A*, **3**, 193 (1955).

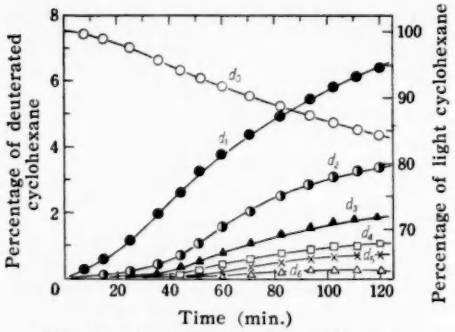

Fig. 2. The exchange of cyclohexane on 6.8 mg. of molybdenum at 75°C (run 14).

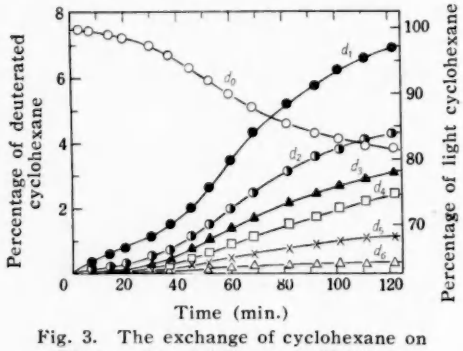

Fig. 3. The exchange of cyclohexane on 6.7 mg. of molybdenum at 86.5°C (run 18).

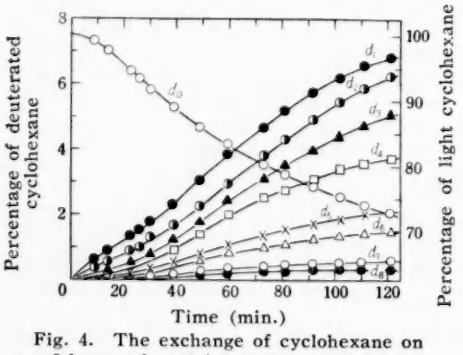

Fig. 4. The exchange of cyclohexane on 8.1 mg. of molybdenum at 102°C (run 16).

As described in the works of Anderson and Kemball[1,5], two different rates were determined from each experiment. The variation in the percentage (n) of light cyclohexane with time followed the equation

5) J. R. Anderson and C. Kemball, *Proc. Roy. Soc.* (London), **A223**, 361 (1954).

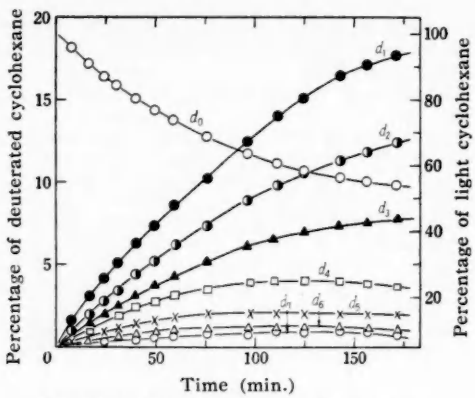

Fig. 5. The exchange of cyclohexane on 9.9 mg. of molybdenum at 97°C (run 29).

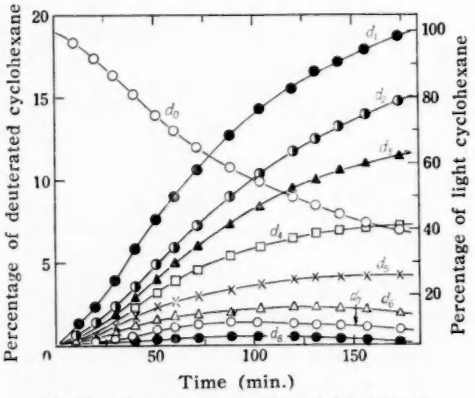

Fig. 6. The exchange of cyclohexane on 5.0 mg. of molybdenum at 97°C (run 31).

TABLE II

PERCENTAGE DISTRIBUTION OF INITIAL PRODUCTS

(Equimolecular mixtures)

Initial rate	Temperature (°C) 75 (run 14)	86.5 (run 18)	97 (run 28)	102 (run 16)
$d(C_6H_{11}D)/dt$	41.0	32.4	30.4	26.2
$d(C_6H_{10}D_2)/dt$	26.4	24.8	24.1	22.2
$d(C_6H_9D_3)/dt$	15.8	20.2	17.4	20.2
$d(C_6H_8D_4)/dt$	10.5	12.1	12.5	15.7
$d(C_6H_7D_5)/dt$	4.2	6.5	7.9	7.0
$d(C_6H_6D_6)/dt$	2.1	4.0	5.3	4.9
$d(C_6H_5D_7)/dt$	—	—	2.4	3.8

$$-\log(n-n_\infty) = \frac{k_H t}{2.303(100-n_\infty)} + \text{constant}, \qquad (1)$$

where n_∞ represents the equilibrium value of n and k_H the initial rate of disappea$_r$-

ance of light cyclohexane in percent. per unit time. For cyclohexane ϕ was defined

$$\phi = \sum_i i \times N_i, \qquad (2)$$

where N_i denotes the percentage of cyclohexane-d_i ($C_6H_{12-i}D_i$, $i=1\sim12$) at the given time. The variation of ϕ with time also followed the equation

$$-\log(\phi_\infty - \phi) = \frac{k_D t}{2.303\phi_\infty} + \text{constant}, \qquad (3)$$

where ϕ_∞ was the equilibrium value of ϕ and k_D the initial rate of entry of deuterium atoms into cyclohexane expressed as the number of deuterium atoms entering 100 cyclohexane molecules in unit time.

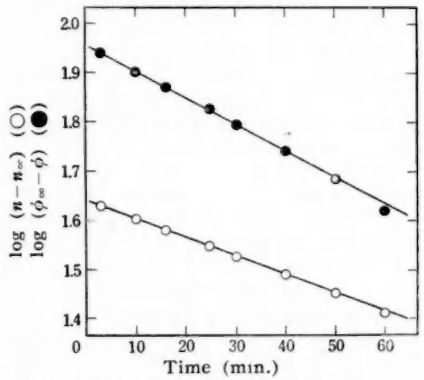

Fig. 7. The exchange of cyclohexane on 5.7 mg. of molybdenum at 97°C plotted according to the rate law expressions (run 28).

TABLE III
INITIAL RATES
(Equimolecular mixtures)

	Temperature (°C)			
	75 (run 14)	86.5 (run 18)	97 (run 28)	102 (run 16)
k_D(%/min.10mg.)	0.705	1.077	1.545	1.922
k_H(%/min.10mg.)	0.309	0.387	0.501	0.556
k_D/k_H	2.28	2.78	3.17	3.46

Fig. 7 shows typical results plotted according to Eqs. (1) and (3). The values of k_H and k_D at various temperatures are summarized in Table III in which the weight of evaporated films was normalized to 10 mg. Arrhenius plots are given in Fig. 8 and the apparent activation energies and the frequency factors in Table IV.

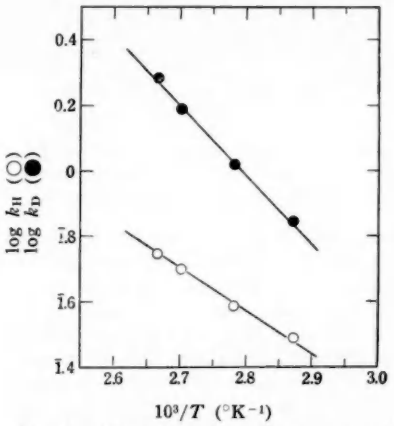

Fig. 8. The effect of temperature on the initial rates of exchange of cyclohexane on molybdenum. k_H and k_D in %/min.10 mg.

TABLE IV
APPARENT ACTIVATION ENERGIES (E) AND FREQUENCY FACTORS (A)

	E(kcal./mol.)	A(mol./min. 10 mg.)	Temp. range(°C)
k_D plot	9.8	7.05×10^{10}	75 to 102
(k_H plot)	(6.2)	(1.10×10^{8})	(75 to 102)

Discussion

Distributions of the Exchange Products.—Considering the fact that the deuterium content of hydrogen in our experiments was only 36.1 atomic %, the production of considerable amounts of highly deuterated products, as seen in Figs. 2–6 and Table II, requires a process of multiple exchange. Anderson and Kemball[1] have reported that isotopic exchange between cyclohexane and deuterium on evaporated films of rhodium (−48 and −28°C) and palladium (18.5°C) leads to distribution patterns in which marked discontinuities separate the concentrations of $C_6H_6D_6$ and $C_6H_5D_7$. On the other hand, Burwell and Tuxworth[3] have reported that at 160–200°C no such discontinuities between $C_6H_6D_6$ and $C_6H_5D_7$ appeared when evaporated nickel films or reduced nickel oxide were used. As seen in Figs. 2–5 and Table II, the present results clearly indicate that at 75–102°C one can observe no discontinuities between $C_6H_6D_6$ and $C_6H_5D_7$ for molybdenum films.

It is well known that both in the liquid and the vapor all cyclohexane molecules are practically present in the chair form,

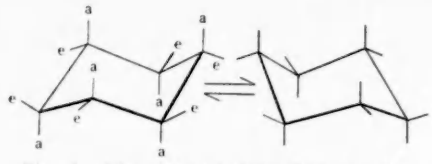

Fig. 9. The chair conformation of cyclohexane. The axial and equatorial bonds are marked (a) and (e) respectively.

as shown in Fig. 9, in which the twelve C–H bonds may be divided into two geometrically different groups of six equatorial (e) and six axial (a)[6]. Furthermore, owing to the flexibility of this chair conformation the two planes (i.e. each plane contains three carbon atoms) may interchange their positions, and all C–H bonds which were axial in the former chair form will be equatorial in the latter, and vice versa[7]. Based on this chair conformation mentioned above, a suggestion has been made by Anderson and Kemball that the reaction easily proceeds by exchanging alternately axial and equatorial hydrogen atoms in one group of three axial and three equatorial and that, for the remaining six hydrogen atoms to be exchanged, the adsorbed radical must turn over on the surface by second-point adsorption. Marked discontinuities between $C_6H_6D_6$ and $C_6H_5D_7$ found by them over evaporated films of rhodium and palladium were attributed to the small probability of this turning over of the adsorbed radicals.

Their explanations, however, contain some uncertainties, since dissociative adsorption of desorbed cyclohexane molecules ($C_6H_{12-i}D_i$, $i<7$) may take place with the same probability of the rupture of a C–H bond on either side of the carbon ring. Moreover, when an adsorbed radical takes an inclined position towards the surface, exchange may proceed between adjacent equatorial hydrogen atoms within different groups and the radical may easily turn over on the surface. Considering the matter from these facts, it seems rather reasonable to consider that there are no definite reasons to support the appearance of a marked discontinuity which separates the concentrations of $C_6H_6D_6$ and $C_6H_5D_7$.

Pressure-Dependence of Reaction Rate.—According to the present experiments, the initial rates of this exchange were found to follow

$$k_D(\text{or } k_H) \propto p(C_6H_{12})^{1.0} \cdot p(\text{d.h.})^{-0.6}, \quad (4)$$

where p(d.h.) denotes the partial pressure of deuterated hydrogen. The uncertainty in the exponents amounts to about 0.1.

The non-activated chemisorption of hydrogen on various metal films has been reported by many investigators[8]; then one can easily deduce the following kinetic relation by assuming that the coverage of the mobile layer of the adsorbed radicals is considerably smaller than that of chemisorbed hydrogen atoms and that the initial rate (k) of this exchange is proportional to the amount of the adsorbed radicals.

$$k \propto \frac{p(C_6H_{12})}{\sqrt{b\,p(\text{d.h.})^{0.5}} + b\,p(\text{d.h.})^{1.0}}, \quad (5)$$

where b indicates the constant which characterizes adsorption and desorption of hydrogen, and p(d.h.) the partial pressure of deuterated hydrogen. Since Eq. (5) indicates that the initial rate is proportional to p(deuterated hydrogen)$^{-1.0\sim-0.5}$, the present results shown in Eq. (4) and those obtained by Anderson and Kemball* approximately coincide with Eq. (5). It may, therefore, be considered probable that the rate-determining step of this exchange is desorption of the adsorbed radicals. On account of the fact that the deuterium content in our experiments was considerably small, the apparent activation energy derived from Arrhenius plot of k_D values is significant. Hence the value of 9.8 kcal./mol. shown in Table IV would imply the activation energy of dissociative adsorption of cyclohexane.

Deuterium Isotope Effect.—In order to examine the influence of the deuterium isotope effect, the compositions in equilibrated mixtures were determined both for the gas phase and for the gases newly desorbed from the surface after rapid evacuation. Typical results are summarized in Table V. Since only a minute quantity of the gases was newly desorbed, the present analytical results on the minor components in newly desorbed gases inevitably contain considerable uncertainties. Considering the problem from this fact, it seems reasonable to consider that, so far as the present experiments

6) O. Hassel, *Quart. Rev.*, **7**, 221 (1953).

7) W. G. Dauben and K. S. Pitzer, "Steric Effects in Organic Chemistry", John Wiley & Sons, Inc., New York (1956), p. 17.

8) M. W. Trapnell, "Chemisorption", Butterworths Scientific Publications, London (1955), p. 60.

* The pressure-dependence for this exchange over evaporated palladium films was found by them to follow $k_H \propto p(C_6H_{12})^{0.8} \cdot p(D_2)^{-1.0}$.

TABLE V

PERCENTAGE COMPOSITIONS OF EQUILIBRATED MIXTURES

Temp. (°C)	Sample	C_6H_{12}	$C_6H_{11}D$	$C_6H_{10}D_2$	$C_6H_9D_3$	$C_6H_8D_4$	$C_6H_7D_5$	$C_6H_6D_6$
94	Gas phase	60.9	28.7	7.5	1.7	0.8	0.4	—
	Newly desorbed gases	61.3	28.8	7.2	1.5	0.9	0.3	—
102	Gas phase	58.1	26.1	9.9	3.6	1.5	0.6	0.2
	Newly desorbed gases	57.4	26.4	9.8	3.8	1.7	0.6	0.3
111	Gas phase	54.7	22.9	12.2	6.1	2.7	0.9	0.5
	Newly desorbed gases	55.1	21.8	12.7	6.5	2.4	1.1	0.4

were concerned, the deuterium isotope effect gives no significant influence upon the overall reaction of this exchange.

Summary

Isotopic exchange reaction between cyclohexane and deuterium over evaporated molybdenum films has been studied mass-spectrometrically at the temperature range 56–111°C. The present results were compared either with Anderson and Kemball's or Burwell and Tuxworth's, and summarized as follows;

1) Since the deuterium content in our experiments was considerably low the production of considerable amounts of highly deuterated products requires a process of multiple exchange.

2) The present results clearly indicate that one can observe no discontinuities which separate the concentrations of $C_6H_6D_6$ and $C_6H_5D_7$.

3) The pressure-dependence was studied for this exchange and the initial rate (k) was found to be expressed as $k \propto p(C_6H_{12})^{1.0} \cdot p(\text{deuterated hydrogen})^{-0.6}$.

4) According to the present kinetic evidence, the rate-determining step of this exchange is probably the desorption of the cyclohexyl radicals.

5) So far as the present experiments were concerned, it seems reasonable to consider that the deuterium isotope effect gives no significant influence upon the present exchange reaction.

The authors wish to express their grateful thanks to Professor N. Sasaki of Kyoto University, Professor T. Titani of Tokyo Metropolitan University and Professor O. Toyama of Osaka Prefectural University for their kind encouragement and discussion. The expense has been defrayed in part from a grant given by the Ministry of Education to which the authors' thanks are due.

Departments of Pure and Applied Chemistry
College of General Education and
Faculty of Engineering
Osaka Prefectural
University, Sakai

*Isotopic Exchange Reaction between Cyclohexane and Deuterium on Evaporated Tungsten Films**

By Teruo HAYAKAWA and Toshio SUGIURA

(Received October 16, 1957)

In the previous communication[1], the authors studied the isotopic exchange reaction between cyclohexane and deuterium over evaporated molybdenum films. It was found that the initial production of highly deuterated products required a process of multiple exchange. No discontinuites which separate the concentrations of $C_6H_6D_6$ and $C_6H_5D_7$ appeared at 56—111°C and the deuterium isotope effect practically gave no significant influence upon the exchange reaction. The pressure-dependence for this exchange and simple kinetic consideration revealed that the rate-determining step may be attributed to desorption of the chemisorbed radicals and hence that the apparent activation energy experimentally found would imply the activation energy of dissociative adsorption of cyclohexane.

It was therefore of interest in the present work to study the same exchange reaction over evaporated tungsten films, since this permits a comparison of the catalytic activities of these metal films.

Experimental

Materials.—The method of preparation and purification of the sample gases was already given in a previous communication[1]. Evaporated tungsten films were prepared by customary procedures including careful degassing at elevated temperatures. Between 7.9 and 16.4 mg. of evaporated film was used in the subsequent experiments.

Apparatus and Procedure.—The apparatus and the procedure were described in the previous communication[1].

Results

The experimental conditions are summarized in Table I, where the run numbers indicate the chronological order of the experiments. Figs. 1, 2 and 3 show some typical results on the variation in the percentages of the various cyclohexane molecules with time. In these figures the notation d_i has been used in place of cyclohexane-d_i

TABLE I
DETAILS OF ISOTOPIC EXCHANGE RUNS

Run	Temp. (°C)	Partial pressures (mmHg) cyclohexane	deuterated hydrogen
2	94	2.0	2.0
5	111	2.0	2.0
6	98.5	2.2	2.2
8	80	2.7	2.7
9	86	1.9	1.9
10	102	2.1	2.1
12	79	1.5	1.5
15	84	2.2	2.2

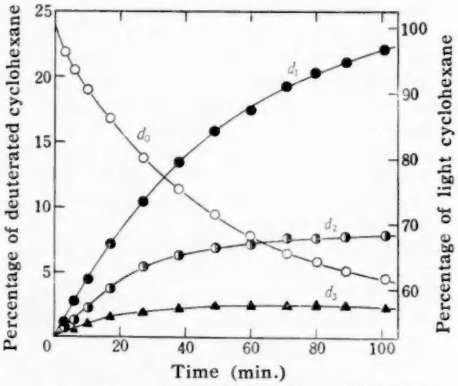

Fig. 1 (a). The exchange of cyclohexane on 12.4 mg. of tungsten at 84°C (run 15, major components).

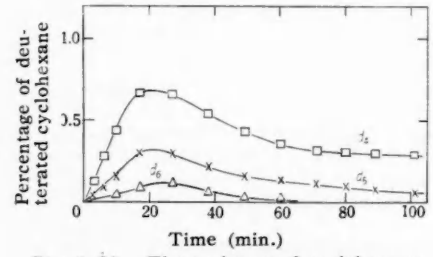

Fig. 1 (b). The exchange of cyclohexane on 12.4 mg. of tungsten at 84°C (run 15, minor components).

* Part of this paper was read before the 10th Annual Meeting of the Chemical Society of Japan held in Tokyo, April, 1957. Another part of this paper was also presented before the Symposium on the Catalytic Reactions held in Tokyo, April, 1957.

1) T. Hayakawa and T. Sugiura, This Bulletin, **31**, 180 (1958).

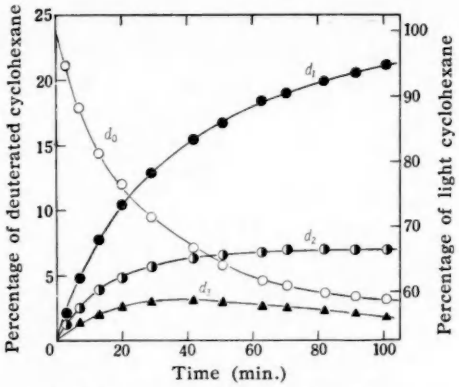

Fig. 2 (a). The exchange of cyclohexane on 16.4 mg. of tungsten at 94°C (run 2, major components).

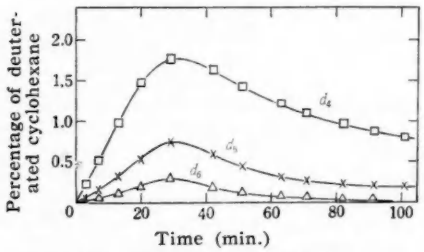

Fig. 2 (b). The exchange of cyclohexane on 16.4 mg. of tungsten at 94°C (run 2, minor components).

TABLE II
PERCENTAGE DISTRIBUTIONS OF INITIAL PRODUCTS

	Temperature (°C)			
Initial rate	84	94	102	111
$d(C_6H_{11}D)/dt$	57.2	51.7	40.6	36.3
$d(C_6H_{10}D_2)/dt$	25.3	27.0	26.0	26.9
$d(C_6H_9D_3)/dt$	9.2	11.9	19.6	18.2
$d(C_6H_8D_4)/dt$	5.8	6.0	7.8	11.8
$d(C_6H_7D_5)/dt$	1.9	2.4	4.5	5.1
$d(C_6H_6D_6)/dt$	0.6	1.0	1.2	1.3
$d(C_6H_5D_7)/dt$	—	—	0.3	0.4

TABLE III
INITIAL RATES
(Equimolecular mixtures)

	Temperature (°C)			
	84	94	102	111
k_D(%/min. 10 mg.)	1.175	1.682	2.281	3.116
k_H(%/min. 10 mg.)	0.742	1.006	1.208	1.611
k_D/k_H	1.58	1.68	1.89	1.93

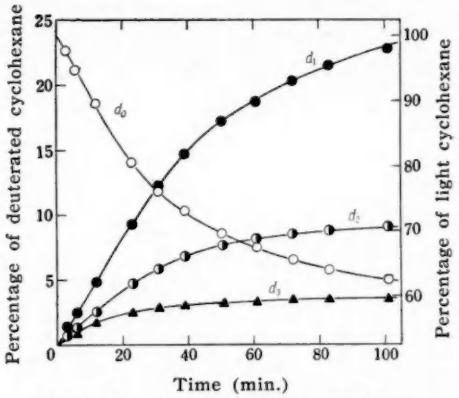

Fig. 3 (a). The exchange of cyclohexane on 9.9 mg. of tungsten at 102°C (run 10, major components).

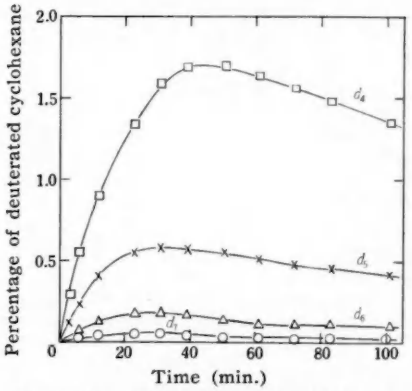

Fig. 3 (b). The exchange of cyclohexane on 9.9 mg. of tungsten at 102°C (run 10, minor components).

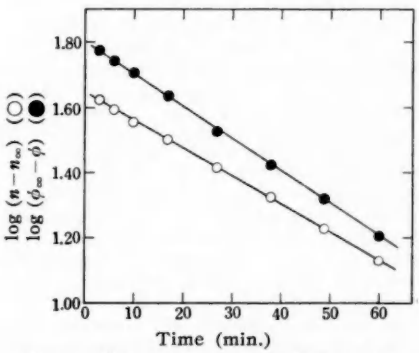

Fig. 4. The exchange of cyclohexane on 12.4 mg. of tungsten at 84°C plotted according to the rate law expressions (run 15).

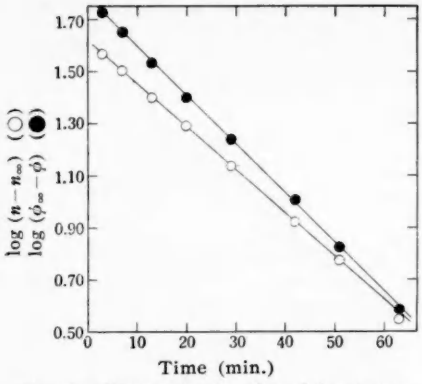

Fig. 5. The exchange of cyclohexane on 16.4 mg. of tungsten at 94°C plotted according to the rate law expressions (run 2).

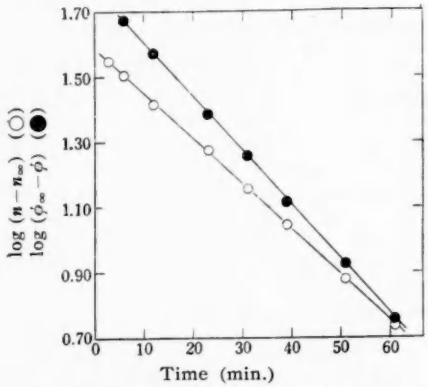

Fig. 6. The exchange of cyclohexane on 9.9 mg. of tungsten at 102°C plotted according to the rate law expressions (run 10).

($C_6H_{12-i}D_i$) to facilitate presentation. Typical results on the initial product distributions obtained from measuring the initial slopes of these curves are summarized in Table II. Two different rates, i.e. the initial rate of disappearance of light cyclohexane (k_H) and the initial rate of entry of deuterium atoms into cyclohexane (k_D), were calculated from the plot of the rate law expressions reported in the preceding paper[1]. Figs. 4, 5 and 6 show typical results plotted according to these expressions. The values of two different rates at various temperatures are summarized in Table III in which the weight of evaporated films was normalized to 10 mg. Arrhenius plots are given in Fig. 7 and the apparent activation energies and frequency factors in Table IV, together with the values obtained by Anderson and Kemball[2].

2) J. R. Anderson and C. Kemball, *Proc. Roy. Soc.* (London), **A226**, 472 (1954).

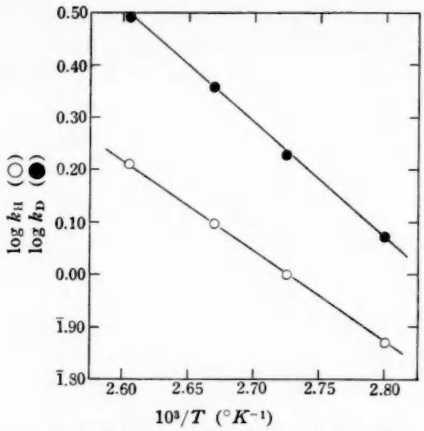

Fig. 7. The effect of temperature on the initial rates of exchange of cyclohexane on tungsten. k_H and k_D in %/min. 10 mg.

TABLE IV
APPARENT ACTIVATION ENERGIES (E) AND FREQUENCY FACTORS (A)

	E (kcal./mol.)	A (mol./min. 10 mg.)	Temp. range (°C)
k_D plot	10.3	7.43×10^{11}	84 to 111
(k_H plot)	(7.9)	(8.80×10^{9})	(84 to 111)
Anderson and Kemball* (k_H plot)	11	4.76×10^{28}	−69 to −48

* The initial deuterium content was 99.7%.

Discussion

Distributions of the Exchange Products.—As seen in Figs. 1~3, considerable amounts of highly deuterated products appeared in the early stage of this reaction. Since the deuterium content of hydrogen in our experiments was only 36.1 atomic %, it is quite reasonable to consider that the process of multiple exchange plays a significant role in the present exchange reaction. These figures clearly indicate that increased temperature results in a marked increase in extensive multiple exchange. Comparing the present product distributions shown in Table II with those already reported in the preceding paper[1], it is obvious that the multiple exchange is more extensive on molybdenum films than on tungsten films.

As seen in Figs. 1~3 and Table II, although decreased temperature results in the decline in concentrations of highly deuterated products, at 84—111°C one can observe no discontinuity which separates the concentrations of $C_6H_6D_6$ and $C_6H_5D_7$.

TABLE V
PERCENTAGE COMPOSITIONS OF EQUILIBRATED MIXTURES

Temp. (°C)	Sample	C_6H_{12}	$C_6H_{11}D$	$C_6H_{10}D_2$	$C_6H_9D_3$	$C_6H_8D_4$	$C_6H_7D_5$
84	Gas phase	60.1	29.6	8.2	1.8	0.3	—
	Newly desorbed gases	60.7	29.4	7.9	1.5	0.5	—
94	Gas phase	56.9	30.9	8.7	2.7	0.8	—
	Newly desorbed gases	57.4	30.6	8.2	2.8	1.0	—
102	Gas phase	58.1	25.8	10.9	3.5	1.3	0.4
	Newly desorbed gases	56.2	26.7	10.9	4.1	1.5	0.6

These results closely resemble those already found for evaporated molybdenum films. Moreover, no such discontinuities between $C_6H_6D_6$ and $C_6H_5D_7$ have been observed either by Anderson and Kemball[2] for evaporated films of platinum (at 0°C) and tungsten (at −69°C) nor by Burwell and Tuxworth[3] for evaporated nickel films (at 160—200°C). From these facts, it seems reasonable for the present authors to consider that marked discontinuities between $C_6H_6D_6$ and $C_6H_5D_7$ observed by Anderson and Kemball[2] for evaporated films of rhodium (at −48 and −28°C) and palladium (at 18.5°C) must not be attributed to the characteristic chair conformation of the cyclohexane molecule.

Apparent Activation Energy.—Since the deuterium content of hydrogen in the present experiments was only 36.1 atomic %, the apparent activation energy derived from k_D plot is of significance. As seen in Table IV, the agreement between the present value and that obtained by Anderson and Kemball is well maintained. Although the pressure-dependence of this exchange over evaporated tungsten films was not further studied, the kinetic consideration discussed in the preceding paper may equally fit the present results. Hence the apparent activation energy experimentally found (10.3 kcal./mol.) would imply the activation energy of chemisorption of cyclohexane.

Deuterium Isotope Effect.—The deuterium isotope effect for the exchange of cyclohexane on evaporated tungsten films was studied by conducting additional experiments. After the usual determination of the gas phase compositions in equilibrated mixtures, the reaction vessel was rapidly evacuated and the gases newly desorbed from the surface were collected and analysed. Typical results are summarized in Table V. As seen in Table V, at 102°C the present exchange reaction might be influenced to some extent by the deuterium isotope effect. However, the present analytical results on the newly desorbed gases shown in Table V inevitably contain some uncertainties, since only a minute quantity of gases was newly desorbed from the surface. From this fact, it seems rather reasonable, so far as the present experiments were concerned, to consider that the deuterium isotope effect gives no significant influence upon the present exchange reaction.

3) R. L. Burwell, Jr., and R. H. Tuxworth, *J. Phys. Chem.*, **60**, 1043 (1956).

Summary

Isotopic exchange reaction between cyclohexane and deuterium over evaporated tungsten films has been studied mass-spectrometrically at the temperature range 79~111°C. The present results are summarized as follows;

1) The production of highly deuterated products in the initial stage of this exchange requires a process of multiple exchange.

2) Evaporated tungsten films showed, however, little tendency for multiple exchange, while evaporated molybdenum films promoted multiple exchange to a large extent.

3) One can observe no discontinuities which separate the concentrations of $C_6H_6D_6$ and $C_6H_5D_7$.

4) It seems reasonable to consider that marked discontinuities between $C_6H_6D_6$ and $C_6H_5D_7$ observed by Anderson and Kemball for evaporated films of rhodium and palladium must not be attributed to the characteristic chair conformation of the cyclohexane molecule.

5) The deuterium isotope effect gives no significant influence upon the overall reaction of this exchange.

The authors wish to express their grateful thanks to Professor N. Sasaki of Kyoto University, Professor T. Titani of Tokyo Metropolitan University and Professor O. Toyama of Osaka Prefectural University

for their kind encouragement and discussion. The expense has been defrayed in part from a grant given by the Ministry of Education to which the authors' thanks are due.

Departments of Pure and Applied Chemistry, College of General Edcation and Faculty of Engineering, Osaka Prefectural University, Sakai

*The Mechanism of the Isotopic Exchange Reaction between Cyclohexane and Deuterium on Evaporated Metal Films**

By Teruo HAYAKAWA and Toshio SUGIURA

(Received October 16, 1957)

In recent years many improved theoretical treatments have been carried out to determine the mechanism of the catalytic hydrogenation and the exchange reaction of various olefinic and paraffinic hydrocarbons[1-6]. Refined theoretical treatments of the catalytic exchange reactions between cyclic hydrocarbons and deuterium on evaporated metal films have also been carried out by Anderson and Kemball[7]. In that work the probabilities of two kinds of multiple exchange were statistically calculated. In the case of cyclohexane, the first was the probability of exchanging alternately axial and equatorial hydrogen atoms in one group (i.e. three axial and three equatorial), and the second was the probability of turning over of the adsorbed radical by second-point adsorption. However, the discordance between the experimental and the calculated values of the initial product distributions was, in general, considerably predominant.

In the former papers[8,9] the authors have investigated the isotopic exchange reaction between cyclohexane and deuterium on evaporated films of molybdenum and tungsten. It was therefore of interest to study the theoretical treatments of this exchange reaction.

Outline of Theoretical Calculation

According to the experimental results and the kinetic consideration already reported in the former papers, it may be considered probable that the isotopic exchange reaction between cyclohexane and deuterium over evaporated films of molybdenum and tungsten proceeds with the following processes.

(1) Dissociative adsorption of deuterated hydrogen takes place on the metal surface. Adsorption and desorption of hydrogen lie in an equilibrium.

(2) Dissociative adsorption of cyclohexane also takes place on the metal surface. Adsorption and desorption of cyclohexane also lie in an equilibrium.

(3) The adsorbed "cyclohexyl" radical may be desorbed to the gas phase as "cyclohexane" (i.e. the single exchange process).

(4) Either by exchanging adjacent hydrogen atoms in one group or by turning over on the surface, the adsorbed "cyclohexyl" radical further migrates over the surface (i.e. the multiple exchange process).

According to Anderson and Kemball, the last process (4) may be termed a "trip". However, as already discussed in the former papers[8,9], there is no definite experimental and geometrical reason to support the appearance of a marked discontinuity which separates the concentrations of $C_6H_6D_6$ and $C_6H_5D_7$. It matters little, therefore, for the present authors to distinguish the multiple exchange among adjacent hydrogen atoms

* Part of this paper was read before the 8th Annual Meeting of the Chemical Society of Japan held in Kyoto, April, 1956. Another part of this paper was presented before the "Symposium on the Catalytic Reactions" held in Tokyo, April, 1957.

1) C. D. Wagner, J. N. Wilson, J. W. Ötvos and D. P. Stevenson, *J. Chem. Phys.*, **20**, 338; 1331 (1952).
2) T. Keii, ibid., **22**, 144 (1954); **23**, 210 (1955); **25**, 364 (1956).
3) C. Kemball, *J. Chem. Soc.*, **1956**, 735.
4) J. R. Anderson and C. Kemball, *Proc. Roy. Soc.* (London), **A223**, 361 (1954).
5) C. Kemball, ibid., **A223**, 377 (1954).
6) K. Miyahara, *J. Res. Inst. Catalysis*, **4**, 143 (1956).
7) J. R. Anderson and C. Kemball, *Proc. Roy. Soc.* (London), **A226**, 472 (1954).
8) T. Hayakawa and T. Sugiura, This Bulletin, **31**, 180 (1958).
9) T. Hayakawa and T. Sugiura, This Bulletin, **31**, 186 (1958).

in one group from that accompanied by the turning over of the adsorbed cyclohexyl radical on the surface.

From the reasons mentioned above, the present authors support the following reaction scheme, in which downward dotted lines, upward broken lines, and sideward full lines represent adsorption, desorption (i.e. the single exchange process) and tripping (i.e. the multiple exchange process) respectively.

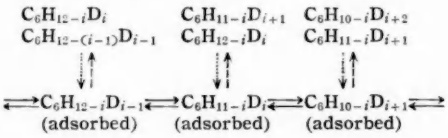

In the present theoretical calculation, the following assumptions were made:

(1) At the initial stage of this exchange, the deuterium content of the adsorbed hydrogen atoms equals to that in the gas phase (i.e. hydrogen lies in an isotopic equilibrium).

(2) The adsorbed hydrogen atoms are randomly distributed on the metal surface.

(3) The deuterium isotope effect is negligible for each process shown in the reaction scheme.

Let V, the overall tripping rate of adsorbed cyclohexyl radicals, V', the overall rate of desorption (or dissociative adsorption) of cyclohexane, C_i, the surface concentration of the cyclohexyl-d_i (i=0~11) radical, C_i', the concentration of cyclohexane-d_i (i=0~12) in the gas phase, Q_i, the concentration ratio of the cyclohexyl-d_i radical to total cyclohexyl radicals on the surface, Q_i', the concentration ratio of cyclohexane-d_i to total cyclohexane molecules in the gas phase, and Ω, the ratio of the fraction covered by deuterium atoms to that by total hydrogen atoms.

The increasing rate of the surface concentration of the cyclohexyl-d_i radical and the gas phase concentration of cyclohexane-d_i are then given by the following Eqs. (1) to (4).

$$dC_i/dt = V'\left(\frac{12-i}{12}Q_i' + \frac{i+1}{12}Q'_{i+1}\right) - V'Q_i + V\left\{\frac{12-i}{11}\Omega Q_{i-1} - \frac{(11-i)\Omega+i(1-\Omega)}{11}Q_i + \frac{i+1}{11}(1-\Omega)Q_{i+1}\right\}, \quad i=1\sim10, \tag{1}$$

$$dC_{11}/dt = V'\left(\frac{1}{12}Q'_{11} + Q'_{12}\right) - V'Q_{11} + V\left\{\frac{1}{11}\Omega Q_{10} - (1-\Omega)Q_{11}\right\}, \tag{2}$$

$$dC_i'/dt = V'\{(1-\Omega)Q_i + \Omega Q_{i-1} - Q_i'\}, \quad i=1\sim11, \tag{3}$$

$$dC'_{12}/dt = V'(\Omega Q_{11} - Q'_{12}). \tag{4}$$

As reported in the work of Anderson and Kemball[7], the extent of multiple exchange may be defined in terms of a parameter P, the ratio of V to V'. At the steady state of this exchange reaction all dC_i/dt (i=1~11) values tend to zero and at the initial stage of this exchange all Q'_i(i=1~12) values may be negligible, so that Eqs. (1)~(4) become respectively

$$P\left\{\frac{(12-i)\Omega}{11}\cdot\frac{Q_{i-1}}{Q_0} - \frac{(11-i)\Omega+i(1-\Omega)}{11}\cdot\frac{Q_i}{Q_0} + \frac{(i+1)(1-\Omega)}{11}\cdot\frac{Q_{i+1}}{Q_0}\right\} - \frac{Q_i}{Q_0} = 0, \quad i=1\sim10, \tag{5}$$

$$P\left\{\frac{\Omega}{11}\cdot\frac{Q_{10}}{Q_0} - (1-\Omega)\frac{Q_{11}}{Q_0}\right\} - \frac{Q_{11}}{Q_0} = 0, \tag{6}$$

$$dC_i'/dt = V'Q_0\left\{(1-\Omega)\frac{Q_i}{Q_0} + \Omega\frac{Q_{i-1}}{Q_0}\right\}, \quad i=1\sim11, \tag{7}$$

$$dC'_{12}/dt = V'Q_0\cdot\Omega\frac{Q_{11}}{Q_0}. \tag{8}$$

Since assumption (1) indicates that at the initial stage of this exchange Ω stays in a constant value*, one can obtain each Q_i/Q_0(i=1~11) value for each given value of P by solving Eqs. (5)~(6). Then, by inserting each Q_i/Q_0 value thus obtained in Eqs. (7)~(8), one can calculate the relative values of dC_i'/dt(i=1~12) at the initial stage of this exchange.

Results

The present results on the theoretical distributions of the initial products as functions of $\log P$ are shown in Fig. 1. The theoretical values of the percentage distributions of the initial products at various temperatures over evaporated films of molybdenum and tungsten are

* As already reported in the former papers[8,9], the experimental value of Ω was 0.361. In the present theoretical calculation, however, the value of Ω was taken as 1/3 to facilitate calculations.

TABLE I

PERCENTAGE DISTRIBUTIONS OF INITIAL PRODUCTS ON EVAPORATED MOLYBDENUM FILMS

Temp. (°C)	P		$d(C_6H_{12-i}D_i)/dt$ $i=1$	2	3	4	5	6	7	8
75	6	calcd.	40.2	27.8	17.1	9.0	4.1	1.4	0.4	—
		obsd.	41.0	26.4	15.8	10.5	4.2	2.1	—	—
86.5	9	calcd.	32.3	26.6	19.3	12.2	6.3	2.5	0.8	—
		obsd.	32.4	24.8	20.2	12.1	6.5	4.0	—	—
97	10.5	calcd.	30.1	25.8	20.1	12.1	7.2	3.4	1.2	0.1
		obsd.	30.4	24.1	17.4	12.5	7.9	5.3	2.4	—
102	13	calcd.	26.5	24.6	20.8	14.6	8.3	3.6	1.3	0.3
		obsd.	26.2	22.2	20.2	15.7	7.0	4.9	3.8	—

TABLE II

PERCENTAGE DISTRIBUTIONS OF INITIAL PRODCUTS ON EVAPORATED TUNGSTEN FILMS

Temp. (°C)	P		$d(C_6H_{12-i}D_i)/dt$ $i=1$	2	3	4	5	6	7
84	2.8	calcd.	56.3	26.5	11.2	4.2	1.4	0.4	—
		obsd.	57.2	25.3	9.2	5.8	1.9	0.6	—
94	3.8	calcd.	50.2	27.6	13.6	5.8	2.1	0.7	—
		obsd.	51.7	27.0	11.9	6.0	2.4	1.0	—
102	5.8	calcd.	40.6	28.2	17.0	8.7	3.8	1.4	0.3
		obsd.	40.6	26.0	19.6	7.8	4.5	1.2	0.3
111	7.4	calcd.	36.3	27.5	18.4	10.6	4.9	1.8	0.5
		obsd.	36.3	26.9	18.2	11.8	5.1	1.3	0.4

TABLE III

ACTIVATION ENERGY DIFFERENCES AND FREQUENCY FACTOR RATIOS

Catalyst	E(tripping) − E(desorption) (kcal./mol.)	A(tripping) / A(desorption)	Temp. range (°C)
Molybdenum films	6.8	1.15×10^5	75 to 102
Tungsten films	9.7	2.43×10^6	84 to 111

TABLE IV

ACTIVATION ENERGIES

Catalyst	E(desorption) (kcal./mol.)	E(tripping) (kcal./mol.)	Temp. range (°C)
Molybdenum films	$9.8+(-\Delta H)$	$16.6+(-\Delta H)$	75 to 102
Tungsten films	$10.3+(-\Delta H)$	$20.0+(-\Delta H)$	84 to 111

summarized in Tables I and II, together with the observed values by the present authors[8,9]. Arrhenius plots of P values are given in Fig. 2. The differences between the activation energy of tripping and that of desorption (or chemisorption) for these evaporated films are listed in Table III, together with the ratios of the frequency factor of tripping to that of desorption (or chemisorption).

Discussion

Initial Product Distributions.—In spite of the fact that the value of Ω used in the present theoretical calculations was slightly different from that experimentally found, the agreements between the theoretical and the experimental values of the initial product distributions for these metal films shown in Tables I and II are well maintained. This is attributed to the fact that the theoretical distributions shown in Fig. 1 were practically unchanged by a slight difference in the value of Ω. Refined statistical calculations of the initial product distributions for the same exchange reaction have been carried out by Anderson and Kemball[7]. However, the discrepancies between the theoretical and the experimental values were considerably predominant except for the results on palladium films at 44°C. The incompleteness of their theoretical treatments may be mainly attributed to the fact that the steady state conditions were not taken into consideration.

Mechanism of the Present Exchange

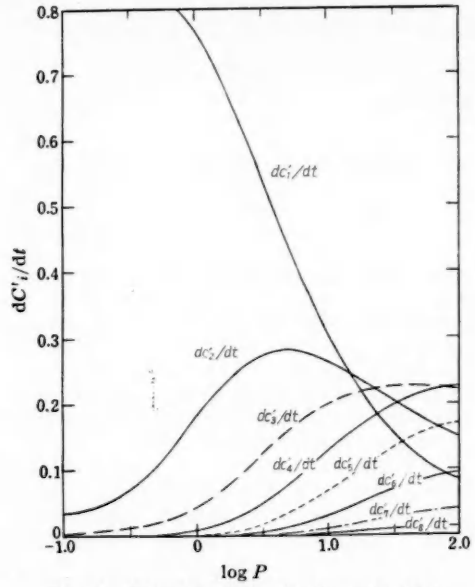

Fig. 1. Theoretical distributions of initial products as functions of log P. dC'_i/dt is fraction of initial rate of increase of cyclohexane-d_i.

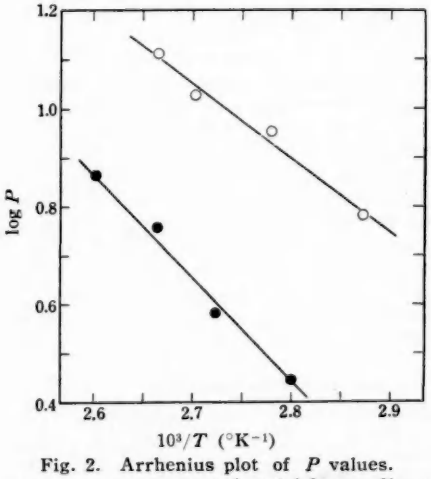

Fig. 2. Arrhenius plot of P values.
—○—○—, on evaporated molybdenum films;
—●—●—, on evaporated tungsten films.

Reaction. — As already discussed in a preceding paper[8], the rate-determining step of this exchange reaction may be the desorption of the cyclohexyl radicals. This coincides well with the fact that, as seen in Tables I and II, the theoretical values of P at various temperatures are considerably greater than unity. Since, as described in a preceding paper[8], the apparent activation energy experimentally found for this exchange would imply the activation energy of chemisorption of cyclohexane, one can obtain the activation energy for each process by combining the present theoretical calculations with the experimental results already reported in the fomer papers[8,9]. The present results on these activation energies are summarized in Table IV, where $(-\Delta H)$ denotes the heat of chemisorption of cyclohexane.

Summary

The theoretical treatments of the isotopic exchange reaction between cyclohexane and deuterium over evaporated metal films have been studied. The present results of the theoretical calculations were compared with the experimental results already obtained by the present authors for evaporated films of molybdenum and tungsten. The present results are summarized as follows:

1) The agreements between the theoretical and the experimental values of the initial product distributions for these metal films are well maintained.

2) The initial rate of tripping of the adsorbed radicals on evaporated films of molybdenum or tungsten at each temperature is considerably greater than that of desorption (or chemisorption) of cyclohexane. This coincides well with the experimental fact that the rate-determining step of this exchange reaction may be attributed to desorption of the adsorbed radicals.

3) The differences between the activation energy of tripping of the adsorbed radicals and that of desorption for evaporated films of molybdenum and tungsten amount to 6.8 and 9.7 kcal./mol. respectively.

The authors wish to express their sincere thanks to Professor N. Sasaki of Kyoto University, Professor T. Titani of Tokyo Metropolitan University and Professor O. Toyama of Osaka Prefectural University for their encouragement and discussion. The expense has been defrayed in part from a grant given by the Ministry of Education to which the authors' thanks are due.

Departments of Pure and Applied Chemistry
College of General Education and Faculty of Engineering, Osaka Prefectural University, Sakai

Alkylalkoxypolysiloxanes. VII.[1] *Lower Members of tert-Butoxy End-blocked Dimethylpolysiloxanes with One to Four Silicon Atoms*

By Rokuro ŌKAWARA and Shōhei IMAEDA

(Received November 14, 1957)

Ethoxy end-blocked dimethylpolysiloxanes[2] have been prepared by the partial hydrolysis of dimethyldiethoxysilane. Also, the lower members of methoxy[3] and isopropoxy[4] end-blocked dimethylpolysiloxanes have been prepared by the sodium bicarbonate treatment of partially methanolyzed and *iso*-propanolyzed dimethyldichlorosilane respectively. In this paper, we wish to report on the preparation and properties of *tert*-butoxy end-blocked dimethylpolysiloxanes as indicated by formula T_n.

$$T_n: \quad (CH_3)_3CO\left[-\overset{CH_3}{\underset{CH_3}{Si}}O-\right]_n C(CH_3)_3 \quad (n=1-4)$$

The higher members of the series T_n may be synthesized by the partial hydrolysis of dimethyldi-*tert*-butoxysilane. In this paper, two other routes of preparation will be reported. It has been known that *tert*-butanol does not react with chlorosilanes without an acid acceptor to form *tert*-butoxysilanes. Accordingly, an equivalent amount of pyridine to chlorosilane was used as an acid acceptor in these experiments. In the first route, dimethyldichlorosilane was added to the mixture of aqueous *tert*-butanol, pyridine and benzene. After refluxing, the pyridine hydrochloride was dissolved with an excessive amount of water and the separated organic layer was fractionated. In this route, the water in the reaction medium reacted with dimethyldichlorosilane more rapidly and there was obtained a relatively large amount of dimethylcyclopolysiloxanes (D_n) in the product. D_n distilled out between the plateaus of linear polymers, T_{n-3} and T_{n-2}, and the lower members of these polymers were not difficult to separate, but the separation was supposed to become difficult with the increasing polymer size. In a hope of obtaining the linear polymers with the formation of as small an amount of cyclopolymers as possible, the following second route was carried out.

In the second route, dimethyldichlorosilane was added to the mixture of pyridine, benzene and various insufficient amounts of *tert*-butanol and refluxed to complete the alcoholysis. By adding excess of water to the product, dissolving of the pyridine hydrochloride and hydrolysis of the remaining Si—Cl were carried out at the same time. Fractionation gave a small amount of crystalline solid with the fraction of T_2. This crystalline solid was confirmed to be tetramethyldisiloxane-1,3-diol. It is interesting to note that an unstable diol is obtained through the distillation. The higher diols were also supposed to be present at the fore part of the plateaus of T_n ($n=3,4$ and 5), considering from the higher refractive index at this part, but they could not be isolated. The amount of this crystalline diol was decreased by redistillation or by refluxing the partially alcoholyzed product with a slight excess of water to convert the remaining Si—Cl into Si—O. Properties of T_n are shown in Table I.

Experimental

Starting Materials.— Dimethyldichlorosilane supplied by Shin-etsu Chem. Ind. Co. and *tert*-butanol of Shell Chemicals were used without further purification.

Reaction of Dimethyldichlorosilane with Aqueous *tert*-Butanol.—A mixture of pyridine (0.4 mole), benzene (50 g.), *tert*-butanol ($x^*=2$ to 1) and water ($0.2\times(2-x)/2$ mole) was placed in a 300 cc. three-necked flask equipped with an efficient stirrer, a dropping funnel and a reflux condenser. Dimethyldichlorosilane (0.2 mole) was added drop by drop with vigorous

1) Part VI of this series, R. Ōkawara, G. Minami and Z. Oku, This Bulletin, **31**, 22 (1958).
2) H. J. Fletcher and M. J. Hunter, *J. Am. Chem. Soc.*, **71**, 2918 (1949).
3) T. Tanaka and R. Ōkawara, This Bulletin, **28**, 364 (1955).
4) R. Ōkawara, T. Ando and K. Ayama, *Technol. Repts. Osaka Univ.*, **8**, 171 (1958).

* x indicates molar ratios: *tert*-butanol/ dimethyldichlorosilane

TABLE I

tert-BUTOXY END-BLOCKED DIMETHYLPOLYSILOXANES:

$$(CH_3)_3CO\left[\begin{array}{c}CH_3\\|\\-SiO-\\|\\CH_3\end{array}\right]_n C(CH_3)_3$$

Polymer Size $n=$	Boiling Point °C/mm Hg	Density d_4^{20}	Refractive Index n_D^{20}	Molar Refraction Found (Calcd.)*	Molecular Weight Found** (Calcd.)	%Si Found (Calcd.)
1	50.5/15	0.8295	1.3970	59.34 (59.58)	202 (204.39)	13.72 (13.74)
2	85/15	0.8666	1.4001	77.94 (78.22)	276 (278.55)	20.20 (20.17)
3	115/15	0.8936	1.4010	95.90 (96.86)	353 (352.71)	23.98 (23.89)
4	95/1	0.9178	1.4025	113.37 (115.50)	430 (426.87)	26.10 (26.32)

* Calculated from bond refractivities by E. L. Warrick, *J. Am. Chem. Soc.*, **68**, 2455 (1946).
** Cryoscopic measurements in benzene.

stirring to the mixture which was cooled with an ice-bath. After the addition the mixture was refluxed for one hour with stirring. An excessive amount of water was added to the mixture which was cooled with a water-bath to dissolve the precipitated pyridine hydrochloride. The separated benzene layer was thoroughly washed with 50 cc. water over five times to separate the dissolved chloride completely. The organic layer was dehydrated with sodium sulfate and simply distilled to drive off benzene, *tert*-butanol and pyridine. The composition of the oily product (Yield: ca. 45—60%) was determined by fractionation through a Stedman column of about 30 theoretical plates. The crystalline hexamethylcyclotrisiloxane (D_3) distilled out at first, the amount of which increased with decreasing x, and then the fraction of monomer (T_1) distilled out, the amount of which decreased from 90 to 55% of the product as x became 2 to 1. All the fractions higher than T_1 and residues thus obtained were united and distilled through the same column. Succeeding to the plateau of T_1, there was found a small plateau of octamethylcyclotetrasiloxane (D_4) at the boiling point of 82°—83°C/35 mm. n_D^{20} 1.3961 (Reported[5]: b. p. 175°C, n_D^{21} 1.3968)

Hydrolysis of Partially *tert*-Butanolyzed Dimethyldichlorosilane.—An insufficient amount of *tert*-butanol ($x=1.6$, 1.2 and 0.8) without water was caused to react with dimethyldichlorosilane (0.2 mole) under the same conditions as described above. By adding water, hydrolysis and dissolving of pyridine hydrochloride were carried out at the same time. Crystals of D_3 were not found in the product of experiments when x is 1.6 or 1.2, but they were found when x is 0.8. When x is 1.2, a portion having a slightly higher refractive index was found at the fore part of the plateau of T_2, and when x is 0.8, a small amount of a crystalline solid was found in that part and the portion which dissolved the crystals showed a higher refractive index than T_2.

To obtain a sufficient amount to characterize this crystalline solid, the alcoholysis was carried out with the same conditions by the use of a larger amount of the starting materials, i. e. 1 mole of dimethyldichlorosilane and 1.2 moles of *tert*-butanol ($x=1.2$). To the mixture, water (9 g.) was added and refluxed for ten minutes with stirring. Fractionation of the product (Yield: 45%) gave a large amount of solid with T_2. The recrystallized solid from benzene-ether mixture having m. p. 63°~65°C and specific gravity 1.118 at 16°C, which was determined by flotation method in the mixture of carbon tetrachloride and benzene, was identified to be tetramethyldisiloxane-1,3-diol (Reported[6]: m. p. 67°~68°C).

Anal. Found: C, 29.41; H, 8.66%. Calcd. for $C_4H_{14}O_3Si_2$: C, 28.91; H, 8.49%.

Further fractionation gave T_3, but no plateaus higher than this could be obtained. Accordingly, starting with 1 mole of dimethyldichlorosilane and 1 mole of *tert*-butanol, refluxing was carried out after addition of water (11 g.) for thirty minutes to condense diol. Fractionation of the product (Yield: 50%) gave plateaus of T_1 and then D_4. The refractive indices of T_1 and D_4 are nearly the same but the boiling points are so different that T_1 may be separated from D_4 by distillation. Also, a small plateau succeeding to the fraction of T_2 would be assigned to that of D_5. Above T_2, the portion having the higher refractive index was found at the fore part of the plateau, which was supposed to be caused by a contamination of dimethylpolysiloxane-α,ω-diol. As to T_4 (in Table I) and T_5 (b. p. 113°C/1 mm., d_4^{20} 0.9311, n_D^{21} 1.4055. *Anal.* Found: Si, 28.31%. Calcd. for T_5: Si, 28.03%), though small in amount, they were separated but the amount was not enough to be taken as pure compounds,

5) W. I. Patnode and D. F. Wilcock, *J. Am. Chem. Soc.*, **68**, 358 (1946).

6) G. R. Lucas and R. W. Martin, ibid., **74**, 5225 (1952).

in view of the question from the increment of refractive index and analysis of silicon.

Analysis of Silicon.—Samples were weighed in gelatin capsule[7] and decomposed by concentrated sulfuric acid.

Summary

1) *tert*-Butoxy end-blocked dimethylpolysiloxanes were prepared from dimethyldichlorosilane, *ter*.-butanol and water by the use of pyridine as an acid acceptor.

2) The lower members of those polysiloxanes having one to four silicon atoms were characterized.

Department of Applied Chemistry
Faculty of Engineering
Osaka University
Higashinoda, Miyakojima-ku, Osaka

7) T. Tanaka and R. Ōkawara, This Bulletin, **28**, 354 (1955).

Tricalcium Phosphate and its Variation

By Jumpei ANDO

(Received September 24, 1957)

Tricalcium phosphate is important as the principal component of phosphate fertilizers. Literature on this substance is voluminous but often contradictory. For example, the inversion point from β to α modification was reported by many investigators as 1100°C[1], 1150°C[2], 1180°C[3], 1350°C[4] or 1400°C[5] and also the solubility of both modifications was reported variously. It seems that the contradiction was caused by the effects of a small amount of impurities which vary the properties of the phosphate considerably, and also by admixture of hydroxy apatite or pyrophosphate.

In the present work, the properties of tricalcium phosphate and the effect of other ingredients upon the structure and solubility of the phosphate were investigated in order to clarify the nature of fused and calcined phosphate fertilizers consisting mainly of tricalcium phosphate.

Experimental and Results

(I) Precipitated Tricalcium Phosphate—Tricalcium phosphate and hydroxy apatite were prepared in aqueous solution with sodium or ammonium phosphate and calcium nitrate or chloride under various conditions as indicated in Table I.

Some of the samples (SS-1, SA-2, etc.) were prepared by slow addition of the reagents with continuous agitation in order to obtain crystalline products, pH of the solution being adjusted by adding diluted ammonia from a capillary tube all

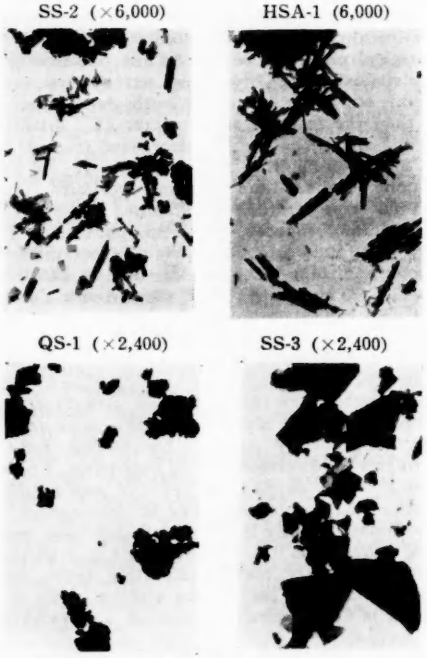

Photographs by Electron Microscope

1) Britske, E. V. and V. K. Veselovskii, *Izvest. Akad. Nauk. S.S.S.R, Otdel. Tekh. Nauk*, No. 4, 479-88 (1937).
2) A. O. McIntosh and W. L. Jablonski, *Anal. Chem.*, **28**, 1424-27 (1956).
3) M. A. Bredig, H. H. Franck and H. Z. Fülder, *Elektro. Chem.*, **38**, 158-64 (1932).
4) W. F. Bale, J. F. Bonner, H. C. Hodge, H. Adler, A. R. Wreath and R. Bell, *Ind. Eng. Chem., Anal. Ed.*, **19**, 491-5 (1945).
5) F. Körder and G. Trömel, *Arch. Eisenhüttenw.*, **7**, 7-20 (1933).

TABLE I
CONDITIONS OF PREPARATION AND MOLE. RATIOS OF THE PRODUCTS

Sample	Reagent	Temp. (°C)	pH	Time of Adding	CaO/P_2O_5 Added	Mole. Ratios Products
SS-1	$Na_2HPO_4+CaCl_2$	65	7.2—8.0	3.5 hr.	3.00	3.08
SS-2	〃	60	6.8—7.6	〃	〃	2.95
SS-3	〃	50	6.2—6.8	〃	〃	2.69
SS-4	〃	65	〃	〃	〃	2.84
HSS	$CaCl_2+Na_2HPO_4$	70	7.6—8.2	〃	3.33	3.22
SA-2	$(NH_4)_2HPO_4+Ca(NO_3)_2$	65	7.0—7.6	2.5 hr.	3.00	3.04
SA-3	〃	60	〃	〃	〃	2.98
SA-4	〃	〃	6.8—7.4	〃	〃	2.95
SA-6	〃	45	7.4—7.8	〃	〃	2.91
SA-7	〃	25	〃	〃	〃	2.90
HSA-1	$Ca(NO_3)_2+(NH_4)_2HPO_4$	70	8.0—8.6	〃	3.33	3.33
HSA-2	〃	65	8.0—8.4	〃	〃	3.25
QS-1	$Ca(NO_3)_2+(NH_4)_2HPO_4$	20	10	5 sec.	3.00	3.11
QA-2	〃	25	8.2	〃	〃	2.87
QA-3	〃	〃	9.0	〃	〃	2.97
PQA-1	〃	〃	8.9	〃	〃	2.95
PQA-2	〃	〃	9.2	〃	〃	2.96

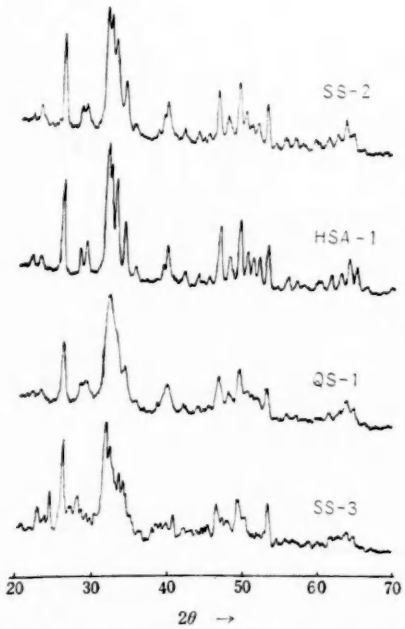

Fig. 1. X-ray diffraction patterns of the samples by Geiger-counter spectrometer. (Cu K_α, Ni Filter)

the while. Others (QS-1, QA-2 etc.) were prepared by quick addition of the reagents in order to obtain colloidal products. In this case, ammonia was added previously to the phosphate solution to adjust pH of the solution after the reaction. The amount of products, after being filtered, washed with water and then dried at 90°C, was 10—15 g., and the amount of the total solution was 1.5—2 liters for each preparation. These products were tested by electron microscope, X-ray diffraction and chemical analysis as shown in the Photographs, Fig. 1, and Table I.

Structure of both samples, SS-2 and QS-1, CaO/P_2O_5 ratio of which are 2.97 and 3.11 respectively, is the same as that of hydroxy apatite HSA-1 with the ratio 3.33, though the state of crystallization differs. Sample SS-3 with the ratio 2.69 consists of hydroxy apatite and dicalcium phosphate; the latter forms larger, thin crystals as shown in the photograph. These results confirm the modern view that tricalcium phosphate hydrate with a definite structure may not be formed but hydroxy apatite with excessive phosphoric acid may be formed.

(II) Variation by Heating—This precipitated apatite contains about 5% zeolitic water which is gradually evaporated by heating under 700°C. Then the hydroxy apatite with excessive phosphoric acid varies to form β-tricalcium phosphate between 700—800°C (Figs. 2 and 3) and solubility of the phosphate increases (Figs. 4 and 5). However, if the CaO/P_2O_5 ratio of the phosphate is slightly more than 3.0, a considerable amount of hydroxy apatite remains above 800°C, which gradually loses water of crystallization (OH) above 1100°C but scarcely ever decomposes even at 1450°C in air. Above 1500°C it is almost decomposed to form α-tricalcium phosphate

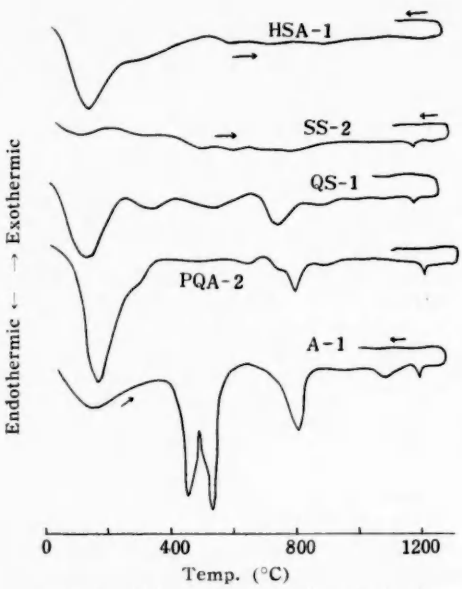

Fig. 2. Differential thermal analysis of phosphates.

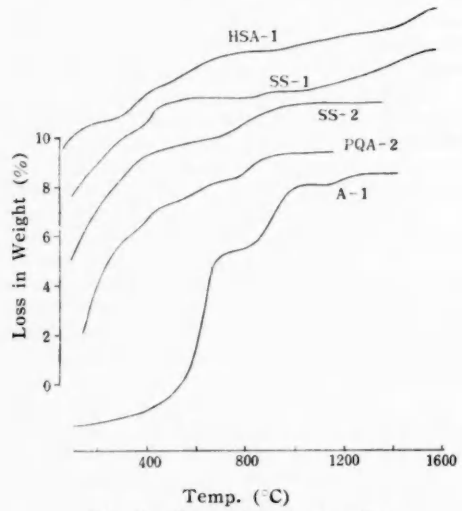

Fig. 3. Weight loss by heating.

and tetracalcium phosphate which are both soluble in citric acid. Calcined samples with CaO/P_2O_5 ratio less than 3.0 is mixed with pyrophosphate.

Sample A-1, prepared by adding phosphoric acid to refined lime by the ratio of 3 mol. CaO to 1 mol. P_2O_5, consists mainly of γ-pyrophosphate at 700°C, the ratio varies above 800°C on reaction with lime to form β-tricalcium phosphate (Figs. 2, 3, and 4). Then β-tricalcium phosphate thus formed inverts to α modification at 1180°C by endothermic reaction (Fig. 2). This inversion point coincides exactly with that described by Bredig[3]. α modification thus formed inverts to β modification slowly, by more than several hours heating at 1100°C. This $\alpha \rightarrow \beta$ inversion is somewhat promoted by the presence of a slight excess of P_2O_5.

On the other hand, β-tricalcium phosphate prepared with samples of Table I inverts to α modification not exactly at 1180°C but between 1160 and 1200°C, and moreover, inverts from α to β modification easily by slow cooling. It seems that these were caused by a small amount of impurity such as Na_2O or MgO derived from the reagents.

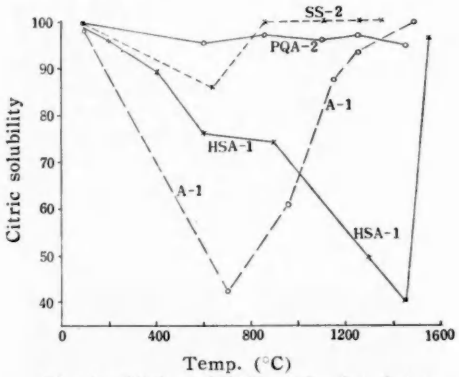

Fig. 4. Citric solubility of phosphates tested by the Japanese official method (150 ml. method).

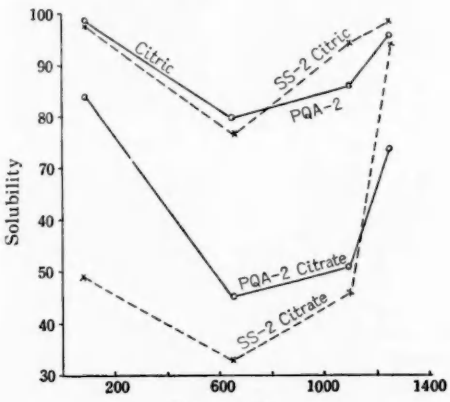

Fig. 5. Citric solubility by the 100 ml. method and citrate solubility by the American official method.

TABLE II

TYPE OF MODIFICATIONS OF TRICALCIUM PHOSPHATE COOLED QUICKLY IN AIR FROM VARIOUS TEMPERATURES (°C)

(C=CaO, P=P_2O_5, A=Al_2O_3, F=Fe_2O_3, M=MgO, B=BaO, N=Na_2O, S=SiO_2)

Samples	Chemical Composition (Mol. Ratios)	Type of Modifications			
		1100	1250	1350	1450
a	3C·P	β	α	α	α
b	3C·P·0.1A	β	β	β	$\alpha+\beta$
c	3C·P·0.1F	β	β	$\alpha+\beta$	α
d	2.9C·0.1M·P	β	β	β	β
e	2.7C·0.3M·P	β	β	β	β
f	2.9C·0.1B·P	$\alpha+\beta$	α	α	α
g	2.9C·0.1N·P	β	$\beta+\alpha$	$\beta+\alpha$	$\beta+\alpha$
h	2.8C·0.2N·P·0.1A	—	β	$\alpha+\beta$	—
i	2.7C·0.2N·0.1M·P	β	β	β	—
j	2.8C·0.2B·P·0.1A	—	$\alpha+\beta$	α	—
k	2.7C·0.2B·0.1M·P	β	$\beta+\alpha$	$\alpha+\beta$	—
l	a+0.35(2C·S)	—	—	α	α
m	b+0.35(2C·S)	—	—	α	—
n	d+0.35(2C.S)	—	—	$\alpha+\beta$	—

(III) Solubility of Phosphates—Solubility was tested by the Japanese official method (150 ml. method), [150 ml. of 2% citric acid for 1 g. of sample ground to pass 100 meshes/inch sieve; shaking for 1 hour (Fig. 4)], by an other method (100 ml. method) which is being practised in other countries, [100 ml. of 2% citric acid for 1 g. of sample; shaking for half an hour], and also by the American official method with neutral ammonium citrate (Fig. 5).

It was found that hydroxy apatite could be dissolved in 2% citric acid to an extent of 1.1 g./100 ml. ultimately at room temperature, and tricalcium phosphate could be dissolved furthermore, so that citric solubility of these compounds was a matter of velocity of dissolution which relates to the grain size, the structure and the state of crystallization of the phosphates.

Precipitated hydroxy apatite HSA-1 is almost soluble in citric acid by the 100 ml. method because of its fineness, though citrate solubility is about 50%. Other samples with less lime are more soluble than the sample HSA-1.

Solubility of these phosphates decreases gradually by heating below 700°C. By this heating zeolitic water contained in the apatite lattice is lost and the distance between the lattice planes becomes slightly smaller.

Contrary to many other reports, it was found that β-tricalcium phosphate was fairly soluble in citric acid. Citric solubility of the phosphate with moderate grain size (mostly 120~40 μ) is 90~95% by the 150 ml. method and 80~90% by the 100 ml. method, and citrate solubility is about 40~50%. The solubility decreases when the phosphate contains a small amount of impurity as described below.

α-Tricalcium phosphate is completely soluble by the 150 ml. method and 95~100% soluble by the 100 ml. method. Though usually a small amount of insoluble residue remains in testing the citric solubility of the phosphate calcined at 1200~1500°C, the residue is not tricalcium phosphate but hydroxy apatite or pyrophosphate or β-tricalcium phosphate stabilized by a small amount of impurities.

Citrate solubility of α-tricalcium phosphate is much higher than that of β-tricalcium phosphate, but it does not reach 90% when the grains of the sample are not fine enough to pass 170 meshes/inch sieve (−88 μ).

(IV) Crystalline Solutions with other Ingredients—Phosphate rocks usually contain small amounts of silica, alumina, iron oxide, and sometimes magnesia. Moreover, in the manufacture of phosphate fertilizers, other materials are added to the phosphate rocks. So, it is thought that tricalcium phosphate in fertilizers is a crystalline solution with other ingredients. In order to clarify the effect of these ingredients upon the structure and the solubility of tricalcium phosphate, many samples with various compositions (Table 2) were prepared with calcium oxalate, phosphoric acid, hydroxides of alumina, iron and magnesium, sodium and barium carbonate and colloidal silica, all

of which were refined in the laboratory. These were first mixed like a paste, dried with frequent mixing, heated at 1000°C, ground to pass 100 meshes/inch sieve, and again heated in a platinum crucible for half an hour at various temperatures as indicated in Table II. Then the products, after being cooled quickly in air, were tested by X-ray diffraction and chemical analysis. Citric and citrate solubility were tested after the products were ground to pass 100 meshes/inch sieve again. Solubility of sample (a) in Table II calcined at 1100°C (β-tricalcium phosphate) was 93.2% by the 150 ml. method, 84.2% by the 100 ml. method, and 45.1% by the citrate method.

It was found that β-tricalcium phosphate was stabilized by the addition of small amounts of alumina, ferric oxide or magnesia. β-Tricalcium phosphate with alumina hardly ever inverts to α modification at 1250°C, moreover it is less soluble in citric acid and especially in citrate. At a higher temperature, α-modification is formed to some extent and the solubility becomes higher (Table II and Fig. 6).

The effect of ferric oxide to stabilize β modification diminishes at 1450°C. The effect of magnesia which substitutes for lime is most remarkable. Containing 0.1 mol. MgO, the distance between crystal planes of the β modification becomes apparently smaller, solubility decreases, and does not invert to α modification even at 1450°C.

On the contrary, it was found that barium, the larger cation, stabilizes α modification. Tricalcium phosphate with 0.1 mol. BaO (sample f) inverts from β to α modification at 1100°C. This temperature is 80°C lower than the inversion temperature of pure tricalcium phosphate.

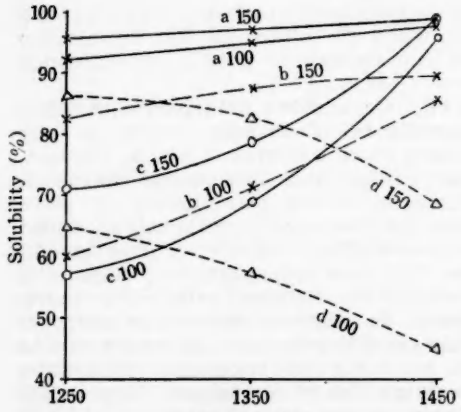

Fig. 6. Citric solubility of samples in Table II tested by 150 ml. and 100 ml. method.

Sodium oxide affects variously according to the ratio of substitution for lime. The inversion of tricalcium phosphate from α to β is so much quickened by replacing a small amount of Na_2O for CaO that α modification almost inverts to β modification even when quenched from a high temperature (Sample g). When more than 0.2 mol. of Na_2O to 1 mol. P_2O_5 is introduced into phosphate α-rhenanite type crystalline solution is formed.

By addition of small amounts of alumina, ferric oxide, magnesia, or silica, inversion of tricalcium phosphate from α to β is somewhat quickened.

Addition of 0.2 mol. Na_2O or BaO or 0.35 mol. $2CaO \cdot SiO_2$ to the tricalcium phosphate with alumina favors the formation of α modification (Samples h, j and m). Citric solubility of samples h, j and m calcined at 1350°C and air-quenched was 99.1%, 92.7%, and 98.5% respectively, by 150 ml. method showing considerable increase compared with the solubility of the sample b. The effect of magnesia to stabilize β modification is so intense that solubility of the phosphate with magnesia is hardly ever raised by adding these materials (Samples i, k and n).

Discussion

As is illustrated by the above results, magnesia reacts most remarkably to stabilize β modification of tricalcium phosphate and to depress the solubility. This explains why satisfactory results could not be obtained in the manufacture of calcined phosphate with a Swedish phosphate rock (with about 5% MgO)[6], and also why addition of serpentine to raw materials of calcined phosphate was unfavorable[7].

Alumina and iron oxide usually contained in phosphate rocks also react to prevent the formation of α-tricalcium phosphate. In calcined phosphate produced by calcining phosphate rock with silica in steam, the effect of alumina and iron oxide is not manifested very much, because excessive lime and silica react with

6) J. A. Hedvall, H. O. Gernandt and Y. Akesson, *Transactions of Chalmers Univ. of Tech.* Göteborg, Sweden, Nr. 100 (1950).

7) S. Nagai and J. Ando, *J. Chem. Soc. Japan, Ind. Chem. Sec.* (*Kogyo Kagaku Zassi*), **57**, 707 (1954).

these oxides to depress the effect. However, in calcined phosphate, produced by calcining phosphate rock with a small amount of phosphoric acid to promote defluorination, alumina and iron oxide affect remarkably to stabilize β modification, because excess of lime is combined with phosphoric acid to form tricalcium phosphate[8]. The phosphate obtained by such a method consists of β-tricalcium phosphate even when cooled quickly from 1350°C. The addition of a small amount of barium to the phosphate causes partial formation of α modification at 1300°C, but solubility of the phosphate is not easily raised because evaporation of fluorine in the phosphate is interrupted to some extent. Addition of 0.1 mol. Na_2O to 1 mol. P_2O_5 of the phosphate is unfavorable but more than 0.2 mol. of Na_2O favors the formation of soluble phosphate[8].

It is often said that tricalcium phosphate hydrate is formed in reverting superphosphate by adding ammonia or serpentine or by using other basic materials. However, as is illustrated by the above results, hydroxy apatite or fluor apatite must be formed instead of tricalcium phosphate. Under such conditions as in the reversion of superphosphate, the state of apatite thus formed is colloidal or crystalline. Such hydroxy apatite is almost entirely soluble in 2% citric acid and even fluor apatite can be dissolved in 2% citric acid to the extent of 0.5 g./100 cc.

8) J. Ando, ibid., **60**, 542 (1957).

Summary

Properties of tricalcium phosphate and effects of many other ingredients upon the structure and solubility of the phosphate were investigated. By the reaction of calcium salts with phosphates in aqueous solution, tricalcium phosphate hydrate with a definite structure is not formed but hydroxy apatite with an excess of phosphoric acid is formed, which varies to β-tricalcium phosphate by heating between 700—800°C. Contrary to many other reports, it was found that β-tricalcium phosphate was fairly soluble in citric acid. The solubility is reduced remarkably by a small amount of admixtures, especially of magnesia. Magnesia stabilizes the β modification and prevents $\beta \rightarrow \alpha$ inversion of the phosphate. The effect of alumina and ferric oxide is similar but not so intense as magnesia. On the contrary, barium oxide stabilizes the α modification. Sodium oxide affects variously according to the ratio of substitution for lime. Constitution and solubility of phosphate fertilizers were discussed in relation to these results.

Department of Industrial Chemistry
Faculty of Engineering
Chuo University
Bunkyo-ku, Tokyo

Phase Diagrams of $Ca_3(PO_4)_2$-$Mg_3(PO_4)_2$ and $Ca_3(PO_4)_2$-$CaNaPO_4$ Systems

By Jumpei ANDO

(Received September 24, 1957)

$Ca_3(PO_4)_2$-$Mg_3(PO_4)_2$ system is important for a fundamental study of fused phosphate fertilizers such as calcium magnesium phosphate (serpentine fused) or defluorinated tricalcium phosphate with magnesia. However little information is found in literature on phases of this system except in the case of tricalcium phosphate.

On the other hand, $Ca_3(PO_4)_2$—$CaNaPO_4$ system is important for the study on calcined phosphate fertilizer, especially on low-alkali phosphate as was produced in England under the name of silicophosphate or as has been produced in Japan for these several years. Among the phases of this system, $CaNaPO_4$ is well known as rhenanite which is a principal constituent of Rhenania phosphate in Germany, and the structure of a phosphate with a composition $Ca_4Na(PO_4)_3$ was stated by Klement[1].

1) R. Klement and F. Steckenreiter, *Z. anorg. allg. Chem.*, **245**, 236-253 (1940).

In the present work, phase systems were investigated systematically by means of differential thermal analysis, X-ray diffraction, microscopy and chemical analysis.

Experimental and Results

(I) $Ca_3(PO_4)_2$-$Mg_3(PO_4)_2$ System Samples were prepared by calcining or fusing the mixture of refined calcium oxalate, magnesium hydroxide and phosphoric acid, and were tested by thermal analysis in a small platinum vessel during fusion and cooling at a rate of 5°C/min.

Fig. 1 illustrates the results of thermal analysis. Within the range from 3 $CaO \cdot P_2O_5$ to 1.5 $CaO \cdot 1.5\,MgO \cdot P_2O_5$ tricalcium phosphate first crystallizes from the melt. In this range the liquidus temperature was not detected clearly by thermal analysis and was determined by quenching the melt from various temperatures and examining it with microscope and X-rays.

It was found that the phase diagram of this system was of peritectic type and that a new compound $Ca_3Mg_3(PO_4)_4$ was formed below 1175°C (Fig. 1, 2 and 4).

Samples with more than 1.5 mol. MgO to 1 mol. P_2O_5 consist of trimagnesium phosphate and $Ca_3Mg_3(PO_4)_4$. Even in samples with more than 1.5 mol. CaO to 1 mol. P_2O_5, formation of trimagnesium phosphate was detected by thermal analysis. This shows that the reaction of tricalcium phosphate and the melt to form $Ca_3Mg_3(PO_4)_4$ is not accomplished under such a cooling condition.

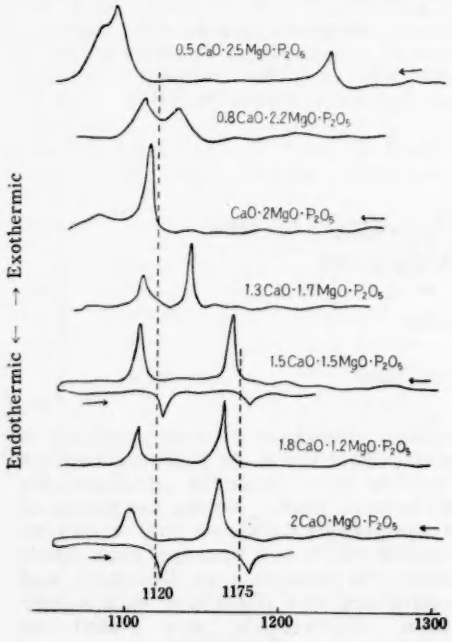

Fig. 1. Differential thermal analysis of samples.

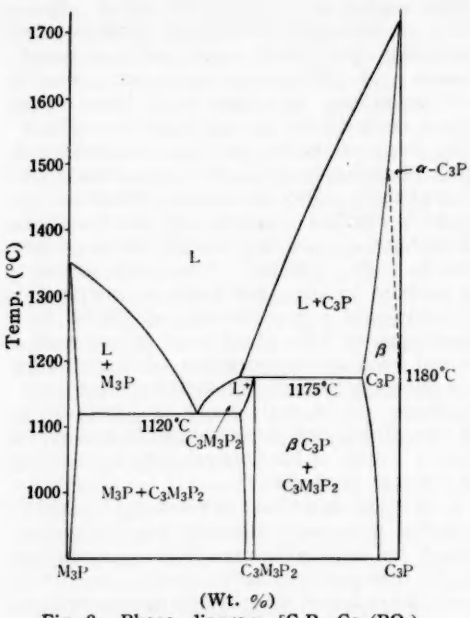

Fig. 2. Phase diagram [$C_3P = Ca_3(PO_4)_2$, $M_3P = Mg_3(PO_4)_2$, $C_3M_3P_2 = Ca_3Mg_3(PO)_4)_4$].

Fig. 3 illustrates the solubility of samples treated in various ways. Samples with the mark A were prepared by calcining at 1100°C. Samples with the mark B

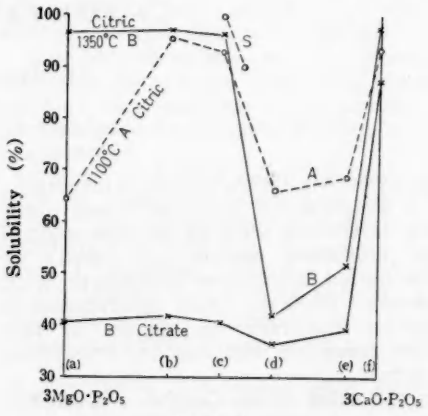

Fig. 3. Solubility of samples.

were heated in a platinum crucible at 1350°C and then cooled quickly in air. 'Citric' means the solubility tested by the Japanese official method, (150 ml. of 2% citric acid to 1 g. of sample pulverized to pass 100 meshes per inch sieve; shaking for an hour). 'Citrate' means the solubility tested by the American official method with neutral ammonium citrate solution.

Samples with less than 1 mol. MgO to 1 mol P_2O_5 consist mainly of tricalcium phosphate. By substitution of magnesia for lime β modification of tricalcium phosphate is stabilized. The distance between the crystal planes becomes smaller and the solubility of the phosphate is reduced remarkably.

The fused product with the composition of $1.5CaO \cdot 1.5MgO \cdot P_2O_5$ consists mostly of the compound $Ca_3Mg_3(PO_4)_4$; however as mentioned above, small amounts of unchanged β-tricalcium phosphate and trimagnesium phosphate are mixed. The melt of this sample was quenched, powdered and then sintered at 1140°C for 5 hours; thus pure $Ca_3Mg_3(PO_4)_4$ was obtained. Samples prepared by such a procedure are indicated in Fig. 3 by the mark S.

The compound $Ca_3Mg_3(PO_4)_4$ is completely soluble in citric acid by the Japanese official method. Citric solubility of the compound, tested by the method with 100 ml. of 2% citric acid for 1 g. of sample (shaking for half an hour), was 91%. However the compound is less soluble in citrate by the American official method. Also the sample with more magnesia is soluble in citric acid but less soluble in citrate.

X-ray diffraction pattern of $Ca_3Mg_3(PO_4)_4$ resembles that of α-tricalcium phosphate (Fig. 4 and Table I). Possibly these two compounds are isomorphous but can hardly form a crystalline solution with each other because of the difference of axial ratio.

Formation of trimagnesium phosphate was not accomplished by calcining the sample with the composition of $3MgO \cdot P_2O_5$ at 1100°C but a considerable amount of insoluble magnesium pyrophosphate was mixed. By fusing the sample at 1350°C pure trimagnesium phosphate was obtained. Also trimagnesium phosphate is soluble in citric acid but less soluble in citrate.

Fused trimagnesium phosphate with an excess of P_2O_5 is mixed with magnesium pyrophosphate, and the fused product with excessive magnesia is mixed with crystals of MgO.

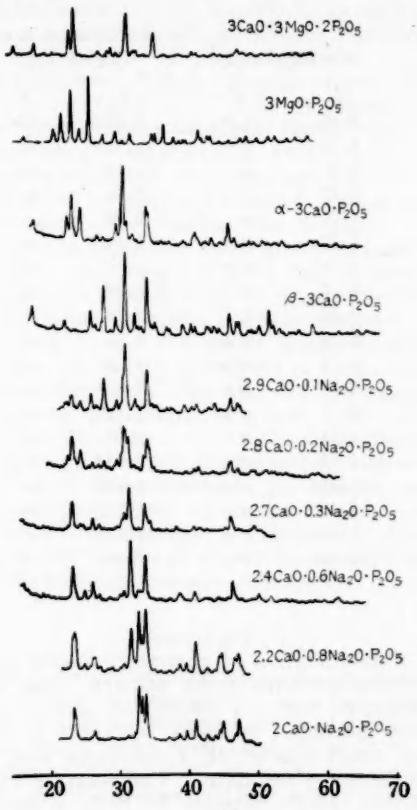

Fig. 4. X-ray diffraction patterns by Geiger-counter spectrometer. (Cu, Kα, Ni Filter)

(II) $Ca_3(PO_4)_2$-$CaNaPO_4$ Systems Samples of this system were prepared by calcining the mixture of refined calcium oxalate, sodium carbonate and phosphoric acid for half an hour at 1300°C. X-ray diffraction patterns of samples, cooled quickly in air after calcination, are shown in Fig. 4 and Table I.

$CaNaPO_4$ has β-rhenanite structure, low-temperature modification of rhenanite $CaNaPO_4$. Inversion of this compound from α (high temperature) to β modification occurs so quickly that α modification can not be obtained at room temperature even if the phosphate is cooled quickly from a high temperature as was described by Bredig[2]. Reversible $\alpha \rightleftarrows \beta$ inversion was observed at 660°C by thermal analysis. X-ray diffraction patterns of the sample $2.4CaO \cdot 0.6Na_2O \cdot P_2O_5$ coincides with that

2) M. A. Bredig, *J. Phys. Chem.*, **46**, 478 (1942).

TABLE I
RESULTS OF X-RAY ANALYSIS OF SAMPLES

$Ca_3Mg_3(PO_4)_4$		$Mg_3(PO_4)_2$		α-$Ca_3(PO_4)_2$		2.4 CaO·0.6 Na_2O·P_2O_5	
d	*I*	*d*	*I*	*d*	*I*	*d*	*I*
8.42	w w	5.61	w w	7.31	w w		
6.11	w w	4.35	w	5.18	w w	4.79	w w
5.01	w	4.12	m	4.02	m		
3.87	m	3.85	s	3.90	m s	3.90	m s
3.75	s	3.66	w	3.69	m	3.60	w
3.25	w w	3.45	s			3.44	m w
3.11	w w	3.20	w			3.31	w w
3.05	w	3.00	w	2.91	s	2.93	w
2.82	s	2.79	w	2.87	w	2.85	s
2.75	w w	2.54	w	2.63	m s	2.67	s
2.71	w w	2.50	w	2.60	m s		
2.51	m s	2.42	m	2.25	w w	2.32	w
2.17	w w	2.13	m w	2.17	m w	2.20	m w
2.14	w w	2.07	w	2.405	w	2.03	w w
2.02	w w	2.045	w	1.943	m	1.94	m
1.877	w	1.831	w	1.907	w	1.80	w
1.807	w w	1.725	w	1.821	w w		
1.629	w w	1.692	w	1.800	w w		
1.605	w w	1.563	w	1.759	w w	1.743	w
				1.670	w	1.490	w

of α modification of rhenanite tested by a high-temperature X-ray camera. Also the sample 2.6 CaO·0.4 Na_2O·P_2O_5 shows the same pattern. Samples with 0.3 or 0.2 mol. Na_2O consist of α-rhenanite and α-tricalcium phosphate. The sample with 0.8 mol. Na_2O consists of both α and β modification of rhenanite.

Thermal analysis of samples with 0.5~0.8 mol. Na_2O shows endothermic reaction on heating and exothermic reaction on cooling between 615~620°C, corresponding to the $\alpha \rightleftarrows \beta$ inversion of rhenanite. This illustrates the fact that by partial substitution of lime for Na_2O of rhenanite, high-temperature modification of rhenanite is stabilized and can easily be obtained at room temperature. The α-rhenanite type crystalline solution is most stable when nearly half of Na_2O is replaced by CaO. Inversion of these crystalline solutions is not reversible. By repeated cooling and heating of the sample, the inversion temperature detected by thermal analysis gradually approaches that of $CaNaPO_4$, the crystalline solution being decomposed to β-rhenanit and β-tricalcium phosphate. Samples with 0.2 or 0.3 mol. Na_2O do not show any distinct peak of reaction between 600~700°C. These samples are easily decomposed to β-tricalcium phosphate and β-rhenanite by slow cooling.

Thermal analysis of the sample with 0.1 mol. Na_2O gives distinct peaks of endothermic reaction on heating and exothermic reaction on cooling between 1130~1180°C. $\alpha \rightarrow \beta$ inversion of tricalcium phosphate is so much quickened by substituting a small amount of Na_2O for CaO that the phosphate almost inverts to β modification even if cooled quickly from high temperature.

Solubility of these samples is illustrated in Fig. 5. The sample with 0.1 mol. Na_2O is less soluble because this consists mainly of β-tricalcium phosphate. α-Rhenanite type crystalline solution is highly soluble in both citric acid and neutral ammonium citrate. The solubility is reduced when the crystalline solution is cooled slowly and decomposed to β-tricalcium phosphate and β-rhenanite.

The α-rhenanite type crystalline solution is furthermore stabilized by the addition of calcium orthosilicate. A sample with a composition of 2.9 CaO·0.1 Na_2O·P_2O_5+0.35 (2 CaO·SiO_2), calcined at 1350°C and cooled quickly, consists of a mixture of α-rhenanite, α-tricalcium phosphate and β-tricalcium phospate. A sample with a composition of 2.8 CaO·0.2 Na_2O·P_2O_5+0.35 (2CaO · SiO_2) treated in the same way consists of α-rhenanite type crystalline solution and a small amount of α-tricalcium phosphate.

However, the sample 2.8 CaO·0.2 Na_2O·

P_2O_5+0.7 (CaO·SiO) treated in the same way consists mainly of α-tricalcium phosphate, illustrating that Na_2O is combined

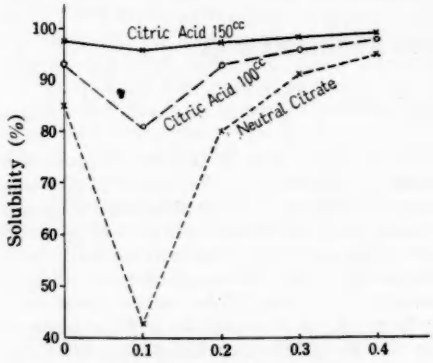

Fig. 5. Solubility of samples cooled quickly from 1300°C.

with excess of silica and does not react with calcium phosphate, so that in the manufacture of low-alkali calcined phosphate, addition of excessive silica must be avoided.

Discussion

Magnesia in fused phosphate fertilizers affects seriously the constitution and the solubility of the phosphate. In order to render the phosphate soluble, magnesia content in the phosphate which usually contains 20—30% of silica must be kept less than 5% so that the formation of α-tricalcium phosphate is not prevented; otherwise it must be kept around more than 12% so that the melting point of the phosphate is lowered and the phosphate can easily be rendered to a glass state by quenching with water[3].

In a usual fused phosphate fertilizer, the compound $Ca_3Mg_3(PO_4)_4$ is not easily formed because magnesia combines with silica to form Mg_2SiO_4, $MgSiO_3$ and $CaMg(SiO_3)_2$[4].

3) J. Ando, *J. Chem. Soc. Japan, Ind. Chem. Sect. (Kogyo Kagaku Zassi)* **59**, 1112 (1956).
4) J. Ando, ibid, **60**, 1101 (1957).

The compound $Ca_3Mg_3(PO_4)_4$ as well as the serpentine fused phosphate fertilizer is less soluble in neutral citrate or in Petermann's citrate, though these are highly soluble in citric acid. It seems that the low solubility of these phosphates in these citrate solutions is attributable to the low solubility of magnesium phosphate in neutral or alkaline solution with much ammonia. For testing the solubility of phosphate fertilizer with much magnesia neither the neutral nor the alkaline ammonium citrate method is suitable, but citric acid or acidic citrate method is preferable. On the other hand, calcium sodium phosphate is soluble in both citric acid and citrate. On the calcination of low-alkali phosphate fertilizer with 0.2—0.6 mol. Na_2O to 1 mol. P_2O_5, Na_2O reacts with phosphate rock to promote decomposition and defluorination of apatite, to depress the effect of alumina and iron oxide which stabilize β-tricalcium phosphate and to form a soluble crystalline solution of α-rhenanite structure.

Summary

The small amount of magnesia contained in tricalcium phosphate replacing lime stabilizes β modification of the phosphate. However, a new compound $Ca_3Mg_3(PO_4)_4$ is formed below 1175°C when more than 0.6 mol. of MgO to 1 mol. of P_2O_5 is introduced into the phosphate. This compound is soluble in citric acid but less soluble in neutral ammonium citrate similarly as is serpentine-fused phosphate fertilizer.

In $Ca_3(PO_4)_2$-$CaNaPO_4$ system, a crystalline solution with α-rhenanite structure is easily formed within the range of 2.6 CaO·0.4 Na_2O·P_2O_5—2.4 CaO·0.6 Na_2O·P_2O_5, and is furthermore stabilized by the admixture of calcium orthosilicate. This crystalline solution is highly soluble in both citric acid and citrate, composing a principal part of low-alkali calcined phosphate fertilizers.

Department of Industrial Chemistry
Faculty of Engineering
Chuo University
Bunkyo-ku, Tokyo

The Scattering of Beams of Alkali Atoms in Various Gases. I. Sodium and Argon

By Kumasaburo KODERA and Teijiro TAMURA

(Received November 7, 1957)

The collision between gaseous molecules is the fundamental process in various phenomena which occur in the gas phase. By means of the molecular beam, it is possible to observe directly the process, which enables us to evaluate the effective collision radii and to get information about the mutual interaction between the molecules.

When the atoms in a molecular beam are scattered by an atom which is at rest in the co-ordinate system, the scattering cross-section Q is expressed by

$$Q=2\pi\int_0^\pi I(\theta)\sin\theta d\theta \qquad (1)$$

where $I(\theta)$ is the scattering intensity per unit solid angle of the beam atoms scattered through the angle θ from the direction of the incident beam. From the classical kinetic theory, it is easy to show, for a hard sphere model, that $I(\theta)$ is independent of θ and expressed as

$$I(\theta)=\frac{1}{4}\sigma^2, \qquad (2)$$

where σ is the sum of the radii of colliding molecules; hence Q is equal to $\pi\sigma^2$. On the other hand, from the quantum mechanical calculation for the hard sphere model, $I(\theta)$ is approximately given by the curve A in Fig. 1[1]. The curve shows that $I(\theta)$ becomes larger than the classical value when θ is smaller than $\theta_0=\pi/k\sigma$.

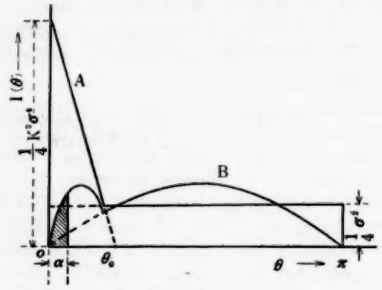

Fig. 1.

In this case, the collision cross-section given by equation (1) is equal to the area between the curve B and the abscissa multiplied by 2π, and therefore, is larger than the classical value. Q varies with $k\sigma$ in such a way that it becomes $2\pi\sigma^2$ when $k\sigma$ is very large, and approaches $4\pi\sigma^2$ when $k\sigma$ is zero. k is equal to $2\pi/\lambda$, where λ is the de Broglie wave length $\lambda=h/\mu v_r$, $\mu=m_Am_G/(m_A+m_G)$ is the reduced mass, and v_r is the relative velocity of the colliding molecules.

Since in actual experiments, both the molecular beam and its detector have definite widths, e. g., α in Fig. 1, the atoms scattered inside this region, i. e., the shaded region, are counted as unscattered, hence giving smaller Q. To minimize this error the resolving power of the apparatus should be increased by making α much smaller than θ_0.

The existence of van der Waals' force should be considered between the actual molecules. In this case, the classical kinetic theory predicts also the marked increase of $I(\theta)$ in the region of small θ, and gives infinite cross-section Q. On the other hand, quantum mechanical treatment with molecules having intermolecular potential of the type

$$V(r)=-Cr^{-s} \qquad (3)$$

gives a finite $I(\theta)$ at θ equal to zero, provided that s is larger than 3, thus giving a finite Q. Therefore, it is necessary to make the widths of the beam and its detector small compared with θ_0. If it were not the case, i. e., if the resolving power of the apparatus were small, the measured cross-section and hence the collision radius would be too small. This can be ascertained from the values presented by several authors. For instance, Mais[2] with the apparatus which excludes the atoms scattered more than 4.5′, obtained the collision radius of 6.91 Å for potassium and helium, Rosin and Rabi[3] with the angle of exclusion 1.7′, gave the values

1) H. S. M. Massey and C. B. O. Mohr, *Proc. Roy. Soc.*, **A141**, 454 (1933).

2) W. H. Mais, *Phys. Rev.*, **45**, 773 (1933).

3) S. Rosin and I. I. Rabi, ibid., **48**, 373 (1935).

7.25 Å for the same pair and 7.18 Å for cesium and helium. Estermann, Foner and Stern[4] obtained the value 12.5 Å for cesium and helium by reducing the angle to 5′. Further, Jawstusch, Schuster and Jaeckel[5], using potassium beams, have shown that the collision radii increase markedly with the resolving power of the apparatus. Since in these instances angles of exclusion α were very small compared with θ_0, it was inferred that an appreciable interaction exists between colliding atoms, and the increase in $I(\theta)$ is greater than for hard spheres. Therefore, in order to measure the effective collision radii, it is essential to make the resolving power of the apparatus as great as possible, and the comparision of the values for various molecules should be done with the apparatus of the same dimensions.

In the works cited above, the collision radii of alkali atoms with, mainly, rare gases were measured to verify the quantum mechanical collision theory. One of the present authors[6] carried out the experiments with potassium beam and various gases including chlorine. In the experiments described below, the apparatus was improved and, in addition to simpler molecules, more complex ones were measured, giving information of chemical interest. In this report, the details of the apparatus and the result with sodium and argon will be mentioned.

Apparatus

The methods to measure the scattering of a molecular beam by gases are roughly classified into the following two. In the first method, the scattering gas is confined in a small region in the path of the beam, while in the second, the gas fills the whole region behind the collimating slit. The former method was employed by Rosin and Rabi, Estermann, Foner and Stern; the crossing beam method of Jawtusch, Schuster and Jaeckel can also be classified into this type. In this method, the angle of scattering of beam atoms and their angular distribution can definitely be determined; since the beam path in the scattering region is short, it is possible to make use of a high pressure, which makes the measurement easier and more accurate. On the other hand, the accuracy in the measurement of the length of the scattering region decreases and the effect of escaping gas molecules from the region increases.

Mais and one of the present authors employed the second method. Although the apparatus can be simplified by this method, the beam detector placed in the scattering gas detects atoms scattered in large angles from points directly in front of it, making the overall resolving power decrease. The determination of the pressure of scattering gas, in this case, is rather difficult because the pressure must be kept low to avoid multiple collisions. These points being considered, in the experiments described below, the first method was employed to raise the resolving power, but a rather large region of scattering gas was taken to facilitate precise determination of its length. The pressure of the scattering gas, which should be low in this case, was measured by a sensitive Pirani gauge calibrated carefully by a McLeod gauge.

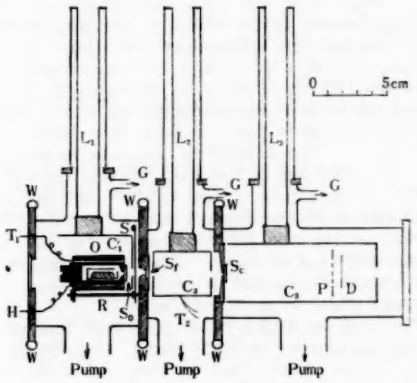

Fig. 2. Apparatus.
O, oven; S_o, oven slit; S_f, fore slit; S_c, collimating slit, S, shutter; D, detector; P, ion collector; T_1 T_2, thermocouples; H, heater; L_1 L_2 L_3, traps; C_1 C_2 C_3, cooling plates; G, to Pirani gauge; W, cooling water; R, supporting rod.

The vertical section of the apparatus is shown in Fig. 2. It consists of three chambers, i. e., the oven chamber I, the scattering gas chamber II and the detector chamber III. The source of the beam was the small oven O made of a single piece of nickel-chromium steel. It had six holes inside the side wall, in five of which were inserted tungsten heater filaments coated with alumina; the last hole contained a copper-constantan thermocouple. The junction was placed near the front wall of the oven to measure the temperature near the oven slit. The oven was joined by three thin iron rods R to the wall separating I and II. S shows a magnetically operated shutter to screen the beam. The beam path was surrounded by plates C_1, C_2 and C_3 which were cooled by liquid air or carbon dioxide snow contained in traps, L_1, L_2 and L_3, respectively. The temperature of C_2 was

4) J. Estermann, S. N. Foner and O. Stern, ibid., **71**, 250 (1949).
5) W. Jawstusch, G. Schuster and R. Jaeckel, *Z. Physik*, **141**, 146 (1955).
6) K. Kodera, *J. Chem. Soc. Japan, Pure Chem. Sect.*, (*Nippon Kagaku Zassi*), **65**, 645 (1944); **66**, 52 (1945); **67**, 80 (1946); N. Sasaki and K. Kodera, *Mem. Col. Science, Univ. Kyoto*, **A, 25**, 83 (1949).

measured by a copper-constantan thermocouple T_2 fastened to it.

The beam was formed by an oven slit S_o, a fore slit S_f and a collimating slit S_c. The widths of the slits were 0.019 mm., 0.5 mm. and 0.015 mm., for the oven slit, fore slit and collimating slit, respectively; all of them were 3 mm. high and the fore slit had a thickness of 1.5 mm. to form a canal. The length of the beam was 1.55 cm. in the chamber I, 5.06 cm. in II of which 4.10 cm. was inside C_2, and 7.91 cm. in III. The beam atoms (sodium) were detected by a Langmuir Taylor surface ionization gauge[7], D, made of a tungsten filament of a diameter 0.016 mm. The filament could be moved across the beam from outside by a screw device. Sodium ions emitted from the filament were collected on a negatively charged plate P and measured by a Lindemann electrometer connected to it. The detector filament subtended an angle 2.0×10^{-4} radian = 41″ at the collimating slit. This angle was low compared with θ_0, which was estimated to be about 2° for sodium and argon under the experimental conditions.

The chambers I, II and III were separately evacuated by three Hickman oil diffusion pumps, which in turn were connected to a one stage mercury diffusion pump and then to a mechanical fore pump. The scattering gas was introduced into the chamber II from a reservoir through a glass capillary tube. The inlet of the gas was provided on the evacuation tube of the chamber II and during the introduction of the gas the pump was kept working. After the pressure in the chamber reached a stationary value, the measurements were carried out.

The sodium which was used was melted in vacuo to remove oxide coating, distilled three times and poured into a glass tube in high vacuum. Just before the experiment, it was cut into a suitable length and put into a stainless steel sheath and introduced into the oven; then, the apparatus was evacuated as fast as possible. Argon (99.9 %) was purchased on the market.

Experimental Procedure

As described above, it is necessary to measure the beam intensity in vacuo I_0 and the weakened intensity in the scattering gas I, along with the pressure and temperature. The experimental procedure was as follows:

The apparatus was evacuated until the McLeod gauge registered "sticking" for both the scattering and the detector chamber. The trap L_1 was cooled by a mixture of carbon dioxide snow and ethanol, L_2 and L_3 by liquid oxygen. The oven was heated to about 250°C by a constant current supplied through a current stabilizer. The detector was then traversed across the beam and its intensity distribution was measured to find the position of maximum intensity. All the measurements described below were carried out with the detector fixed at that position. The intensity in vacuo I_0 was measured, then the scattering gas, argon, was introduced into the scattering chamber. After the pressure of the gas reached the stationary value, the weakened intensity I and the pressure were measured. The vacuum intensity I_0 was measured again and this value was averaged with the former I_0 and taken as the beam intensity at the instant of measurement of I. These processes were repeated for different pressures of the scattering gas.

Since the pressure range was below about 10^{-4}mmHg, its precise measurement was rather difficult. The McLeod gauge could not be used as it showed a rather large margin of error in this pressure range. For this purpose, a Pirani gauge improved by Yoshida[8] was employed. Since the deflections of the gauge were linear with respect to the pressures below 2×10^{-2}mmHg, it was calibrated by the McLeod gauge at relatively high pressures where high precisions were expected. The sensitivity was tested every time after the measurement to confirm its constancy. It was found that in certain cases a slight change in sensitivity did occur at long intervals but not during the measurements.

The probability that a beam atom will pass 1 cm. through the scattering gas without collision is given by the equation,

$$P=\exp(-l/\lambda) \tag{3}$$

where λ is the mean free path of the atom. If the scattering gas were confined within the chamber II, and the temperature of the gas were homogeneous, then l would be equal to 5.06 cm. In practice, however, some of the scattering gas would flow out of the chamber through the slits S_f and S_c into the chambers I and III, respectively. Moreover, the temperature of the gas in II was low inside C_2 and high outside it. From the pressure and the widths of the slits, the flows could be assumed as molecular effusions. The collision of the beam atoms with the effusing molecules might be ignored, as the density of the effusing molecules just outside the slit is half that inside and decreases rapidly with the distance. But these effusing molecules, although they were evacuated continuously, produced certain stationary pressures in the chambers so that the scattering of the beam atoms could not be ignored. Taking into consideration these effects, equation (3) can be written as follows;

$$P=\exp\left\{-\left(\frac{l_1}{\lambda_1}+\frac{l}{\lambda}+\frac{l_2}{\lambda_2}+\frac{l_3}{\lambda_3}\right)\right\} \tag{4}$$

where λ and l are mean free path and beam length inside C_2, respectively, and λ_2 and l_2 those outside C_2 in the chamber II. Suffixes 1 and 3 show the corresponding values in the chamber I and III, respectively. When the distribution of the pressure and temperature for each chamber is assumed to be independent of the pressure introduced into II, the equation (4) can be rewritten by using an effective path length l_e, as follows:

7) J. B. Taylor, *Z. Physik*, **57**, 242 (1929).

8) S. Yoshida, *J. Chem. Soc. Japan, Pure Chem. Sect.*, (*Nippon Kagaku Zassi*), **63**, 383, 391, 520, 527 (1942).

$$P=\exp -l_e/\lambda \tag{5}$$

where l_e can be evaluated from the knowledge of the pressure and temperature distribution in each chamber. If the beam atoms experienced no multiple collision, P should be equal to I/I_0, where I_0 and I are the beam intensities in vacuo and with scattering gas, respectively. Then,

$$I/I_0=\exp -l_e/\lambda \tag{6}$$

Therefore,

$$\lambda=l_e/\ln(I_0/I) \tag{7}$$

From the λ obtained by Eq. (7) the collision radius can be calculated by the equation of Taits' mean free path[9], i. e.,

$$\left.\begin{aligned}\lambda&=\frac{2}{\pi^{1/2}\nu_G\sigma^2}\left(\frac{T_GM_A}{T_AM_G}\right)^2\\&\int_0^\infty\frac{x^5e^{-(T_GM_A/T_AM_G)x^2}dx}{\psi(x)}\\\psi(x)&=xe^{-x^2}+(2x^2+1)\int_0^\infty e^{-y^2}dy\end{aligned}\right\}\tag{8}$$

where ν_G is the number of scattering molecules per cc., T_A, T_G, M_A and M_G are the temperatures and molecular weights of beam atoms and scattering molecules. x is equal to v/α_G, in which v is the velocity of beam atoms and $\alpha_G=\sqrt{2RT_G/M_G}$, Numerical values of $\psi(x)$ have already been calculated by Rosin and Rabi.

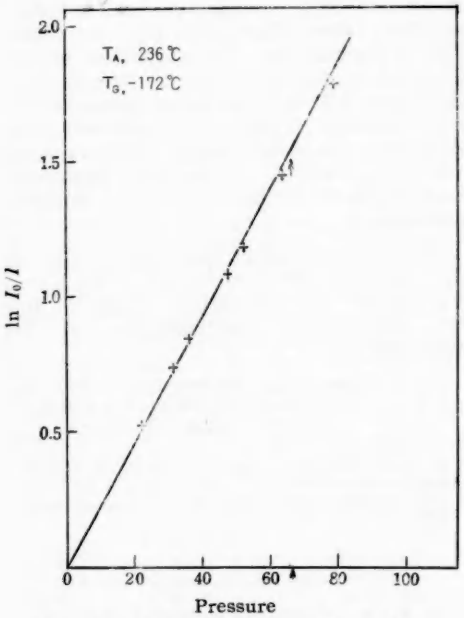

Fig. 3. Weakening of sodium beam scattered by argon.

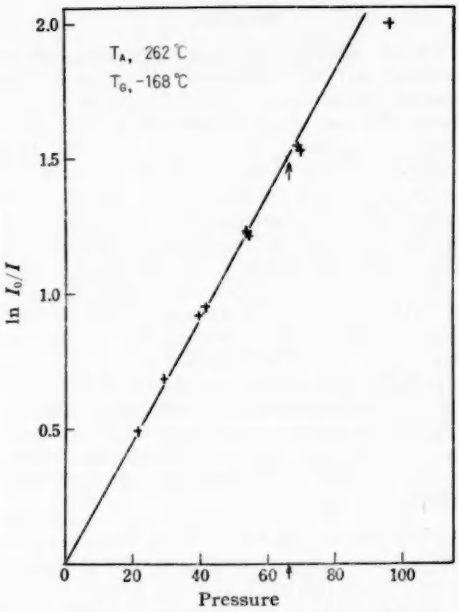

Fig. 4. Weakening of sodium beam scattered by argon.

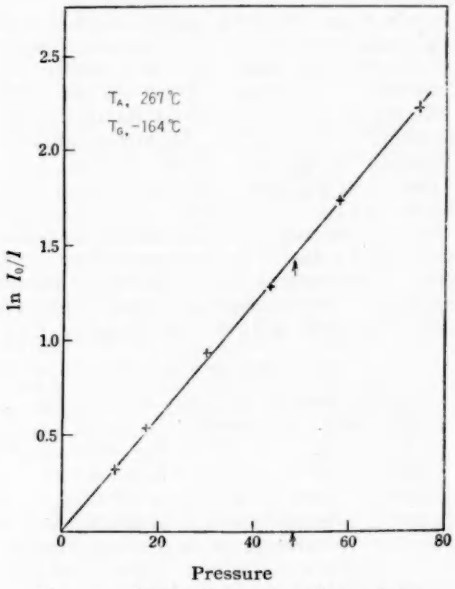

Fig. 5. Weakening of sodium beam scattered by argon.

It should be remarked here that the Pirani gauge was kept at 0°C but the temperature of the chamber whose pressure had to be known differed from 0°C, so that the effect of the thermal transpiration must be taken into account to evaluate the true pressure.

9) J. H. Jeans, "Dynamical Theory of Gases", Combridge, 4th ed. (1916) p. 255; N. F. Ramsey, "Molecular Beams", Oxford, (1955), p. 24.

Results

Three series of measurements were carried out on different days and the results are shown in Figs. 3, 4 and 5. In these figures the values of $\ln I_0/I$ are plotted against the pressure of the scattering gas. The pressure are shown by the readings of the Pirani gauge, and arrows in the figures show the pressure in the unit of 10^{-4}mmHg in the gauge. The plots coincide with straight lines below 10^{-4}mmHg, which show that Eq. (6) is satisfied in this pressure region. For higher pressures, trends are seen to deviate downwards from the straight lines; this fact may be explained by the multiple collisions experienced by the beam atoms.

The measured pressure distribution of the scattering gas in each chamber, collected with the thermal transpiration effect was as follows:

$$p : p_1 : p_3 = 1 : 0.34 : 0.013$$

where p, p_1 and p_3 represent the pressure in the chamber II, I and III, respectively. From these values, together with the temperature distribution in the scattering chamber and the beam length in each chamber, the effective beam length l_e was evaluated as 5.06 cm., i. e., the same value as the beam length in the scattering chamber. It means that the scattering in chambers I and III was compensated by its decrease in the low density region in chamber II outside C_2, where the temperature of the gas was higher than that inside of C_2.

Results calculated from Figs. 3 to 5 are listed in Table I. λ is the mean free path of the beam atoms when the Pirani gauge registered 10^{-4}mmHg. σ is the collision radius between sodium and argon.

TABLE I

COLLISION RADIUS BETWEEN SODIUM AND ARGON

T_A	T_G	λ	σ
236°C	−172°C	3.36 cm.	$12.4^7\times10^{-8}$ cm.
262	−168	3.36	$12.3^8\times10^{-8}$
267	−164	3.47	$12.3^6\times10^{-8}$
	average		12.4×10^{-8} cm.

Discussion

As mentioned above, the quantum mechanical theory for the collision of hard spheres without interaction predicts that $I(\theta)$ increases in the region of small θ; hence, when $k\sigma$ is large, cross-section Q assumes the value twice as great as the classical theory value, consequently σ becomes $\sqrt{2}$ times the classical value. When $k\sigma$ approaches zero, i.e., the relative velocity of colliding particles approaches zero, Q increases four times and σ twice the classical value. In the present experiment σ should be about $\sqrt{2}$ times that of classical theory. When the classical theory radius of argon is assumed to be 1.8×10^{-8}cm. as evaluated from the viscosity of the gas[10], and the radius of sodium in the gas phase to be 3.0×10^{-8}cm.*, the collision radius will be evaluated to be 4.8×10^{-8} cm. The measured value 12.4×10^{-8}cm. is 2.6 times as great as this value, thus much greater than the value given by multiplying 4.8×10^{-8}cm. by $\sqrt{2}$. This discrepancy can be ascribed to the presence of an appreciable van der Waals' force between the colliding particles.

The value 11.3×10^{-8}cm. presented by Rosin and Rabi for sodium and argon is slightly lower than the present value. The difference may be attributed to the smaller resolving power in the former case, i. e., 1.7′ in the former whereas 41″ in the latter. That is, the shaded area in Fig. 1 seems to be appreciable in these small regions of θ. This is also explained by the attractive force between coolliding particles.

The authors take this opportunity to thank Professor N. Sasaki of Kyoto University for permitting them to use the Lindemann electrometer in his laboratory.

Department of Chemistry, Faculty of Industrial Arts, Kyoto Technical University, Sakyo-ku, Kyoto

10) E. H. Kennard, "Kinetic Theory of Gases", McGraw-Hill, (1938), p. 149.

* This value is assumed by the similar consideration as Mais. See also Ref. 6.

Diamagnetism of Azeotropic Binary Liquid Mixtures

By K. VENKATESWARLU and S. SRIRAMAN

(Received October 29, 1957)

A large amount of work has been reported on the diamagnetism of organic liquid mixtures. Ranganathan[1] investigated the mixtures benzene-carbon tetrachloride, acetone-chloroform, acetone-water, and ethanol-water and found small deviations from additivity, the deviations being least in mixtures of two non-polar liquids. Molecular deformation by dipole-dipole interaction and compound formation was invoked to explain the deviation. Rao and his collaborators[2-6] studied a large number of mixtures of liquids having large electric moments and having molecules of different shapes and concluded that in the cases studied there were no variations from additive law. Kido[7] reported that in all the mixtures investigated by him there were no departures from the additive law. Broersma[8] from his study of a few organic liquid mixtures concluded that the departures from the additive law are not appreciable. The work of Farquharson[9] and Angus and Hill[10] suggests a method of explaining small deviations from additivity observed by some authors, on the basis of hydrogen bond formation.

Though a large amount of work has been done on the subject, the reports published so far regarding the behavior of such mixtures from the point of view of the additive law have not been unanimous. Probably more accurate data on a larger number of liquids may help to arrive at some definite conclusions. It was with this object the present investigations were undertaken. All the mixtures chosen for study are azeotropic mixtures. None of the previous workers have chosen binary mixtures from this point of view though a few mixtures studied might come under this category. The results obtained regarding the magnetic measurements in the case of the mixtures studied are reported in this paper.

1) Ranganathan, *Indian J. Physics*, **6**, 421 (1931).
2) Rao and Sivaramakrishnan, ibid., **6**, 509 (1932).
3) Rao, ibid., **8**, 483 (1934).
4) Rao and Varadachari, *Proc. Indian Acad. Sci.*, **1A**, 77 (1934).
5) Rao and Narayanaswamy, ibid., **9A**, 35 (1939).
6) Rao and Sriraman, *J. Annamalai Univ.*, **7**, 187 (1938).
7) Kido, *Sci. Rep. Tohoku Imp. Univ.*, **21**, 385 (1932).
8) Broersma, *J. Chem. Phys.*, **17**, 873 (1949).
9) Farquharson, *Trans. Faraday Soc.*, **32**, 219 (1935).
10) Angus and Hill, ibid., **36**, 923 (1940).

Experimental

Thorough purification of the liquids studied and the adoption of a magnetic method which could give reliable and consistant results were the chief guiding features of this investigation. The procedure adopted for the purification of the liquids was generally based upon Weissberger, 'Organic Solvents', Interscience, New York, 1956.

The determination of the specific susceptibility was made by a perfected form of Gouy method. The pole faces of the large PYE electromagnet used were 3 cm. in diameter and the air gap had a width of 1.2 cm.

Measurements were made with two ground glass stoppered tubes of slightly different cross-sections and at different field strengths ranging from 12 to 15 kilogauss. The experimental tube which was about 30 cm. long and 0.8 cm. in diameter was suspended from one arm of a sensitive balance and was arranged to be vertical with the liquid meniscus symmetrically situated between the pole faces. The field at the lower end of the liquid column was negligible. By a preliminary experiment the position of exact compensation for the glass tube was determined. Pure benzene was taken as the standard.

Assuming the influence of the vapor of the liquid to be negligible, the susceptibility values have been corrected for the residual air in the space above the liquid in the manner described by Rao and Narayanaswamy[5]. The refractive indices of the mixtures were measured with an Abbe refractometer made by Hilger's firm. The densities of the mixtures were found with a special type of stoppered specific gravity bottle.

Results

The mixtures were prepared by weight and due care was taken to minimise any possible change in concentration by evaporation. In Table I are given the values of the density, refractive index and specific susceptibility of the pure liquids and of the mixtures studied at various concentrations. The observed values of the density, refractive index, and magnetic susceptibility of the pure liquids are in good agreement with the previously

TABLE I

ρ, μ AND χ FOR THE PURE LIQUIDS AND MIXTURES

Component A	Component B	wt. % of A	$\rho_4^{35°}$	μ	χ_1 Observed	χ_2 Calcd.	$\chi_2-\chi_1$
Ethanol	Benzene	100.0	0.782	1.3545	0.727		
		80.0	0.800	1.3810	0.721	0.722	+0.001
		60.0	0.813	1.4053	0.718	0.717	−0.001
		40.0	0.830	1.4330	0.712	0.712	0.000
		32.4	0.835	1.4431	0.711	0.710	−0.001
		20.0	0.845	1.4621	0.706	0.707	+0.001
		0.0	0.870	1.4925	0.702		
	Carbon tetrachloride	80.0	0.872	1.3610	0.667	0.669	+0.002
		60.0	0.980	1.3792	0.610	0.611	+0.001
		40.0	1.121	1.3923	0.553	0.552	−0.001
		20.0	1.311	1.4205	0.495	0.494	−0.001
		15.8	1.353	1.4263	0.481	0.482	+0.001
		0.0	1.577	1.4540	0.436		
	Ethyl acetate	80.0	0.800	1.3590	0.702	0.705	+0.003
		60.0	0.812	1.3609	0.677	0.683	+0.006
		40.0	0.838	1.3629	0.656	0.660	+0.004
		30.8	0.851	1.3638	0.648	0.650	+0.002
		20.0	0.863	1.3650	0.636	0.638	+0.002
		0.0	0.889	1.3777	0.616		
	n-propyl bromide	80.0	0.864	1.3668	0.687	0.688	+0.001
		60.0	0.940	1.3751	0.647	0.649	+0.002
		40.0	1.037	1.3889	0.610	0.611	+0.001
		20.5	1.147	1.4012	0.574	0.573	−0.001
		0.0	1.310	1.4257	0.533		
	Chloroform	80.0	0.880	1.3670	0.679	0.681	+0.002
		60.0	0.974	1.3788	0.634	0.635	+0.001
		40.0	1.095	1.3927	0.587	0.589	+0.002
		20.0	1.269	1.4142	0.544	0.543	−0.001
		7.0	1.393	1.4302	0.511	0.513	+0.002
		0.0	1.473	1.4393	0.497		
Methanol	Chloroform	100.0	0.791	1.3285	0.686		
		80.0	0.870	1.3386	0·648	0.648	0.000
		60.0	0.995	1.3505	0.609	0.610	+0.001
		40.0	1.097	1.3695	0.574	0.573	−0.001
		20.0	1.256	1.4042	0.533	0.535	+0.002
		12.6	1.325	1.4165	0.520	0.521	+0.001
		0.0	1.473	1.4393	0.497		
	Carbon tetrachloride	80.0	0.879	1.3340	0.637	0.636	−0.001
		60.0	0.982	1.3460	0.587	0.586	−0.001
		40.0	1.127	1.3790	0.534	0.536	+0.002
		20.6	1.304	1.4110	0.485	0.486	+0.001
		0.0	1.577	1.4540	0.436		
	Benzene	80.0	0.805	1.3475	0.688	0.689	+0.001
		60.0	0.820	1.3663	0.693	0.692	−0.001
		39.6	0.837	1.4215	0.695	0.696	+0.001
		20.0	0.854	1.4601	0.698	0.699	+0.001
		0.0	0.870	1.4945	0.702		

Component A	Component B	wt. % of A	$\rho_{4^\circ}^{32^\circ}$	μ	χ_1 Observed	χ_2 Calcd.	$\chi_2-\chi_1$
Methanol	Acetone	80.0	0.789	1.3337	0.666	0.665	−0.001
		60.0	0.787	1.3394	0.643	0.644	+0.001
		40.0	0.785	1.3454	0.626	0.624	−0.002
		20.0	0.783	1.3509	0.602	0.603	+0.001
		12.1	0.783	1.3524	0.593	0.595	+0.002
		0.0	0.782	1.3534	0.582		
n-propanol	Acetal	100.0	0.797	1.3815	0.750		
		80.0	0.800	1.3811	0.739	0.738	−0.001
		60.0	0.807	1.3806	0.725	0.725	0.000
		37.0	0.813	1.3793	0.712	0.711	−0.001
		20.0	0.816	1.3781	0.702	0.700	−0.002
		0.0	0.819	1.3761	0.688		
	Toluene	80.0	0.812	1.4019	0.746	0.745	−0.001
		60.0	0.823	1.4218	0.739	0.740	+0.001
		52.5	0.827	1.4298	0.737	0.738	+0.001
		40.0	0.834	1.4440	0.734	0.735	+0.001
		20.0	0.847	1.4662	0.731	0.730	−0.001
		0.0	0.856	1.4908	0.725		
Acetic acid	Toluene	100.0	1.041	1.3648	0.525		
		80.0	0.990	1.3937	0.567	0.565	−0.002
		60.0	0.950	1.4171	0.603	0.605	+0.002
		40.0	0.914	1.4417	0.644	0.645	+0.001
		34.0	0.905	1.4491	0.656	0.657	+0.001
		20.0	0.885	1.4666	0.686	0.685	−0.001
		0.0	0.856	1.4908	0.725		
	Chlorobenzene	80.0	1.048	1.3951	0.542	0.544	+0.002
		58.5	1.054	1.4253	0.563	0.564	+0.001
		40.0	1.067	1.4530	0.583	0.581	−0.002
		20.0	1.081	1.4849	0.600	0.600	0.000
		0.0	1.099	1.5198	0.618		
	Ethylene bromide	80.0	1.157	1.3843	0.502	0.504	+0.002
		60.0	1.302	1.4038	0.484	0.484	0.000
		55.0	1.340	1.4092	0.478	0.479	+0.001
		40.0	1.495	1.4312	0.465	0.463	−0.002
		20.0	1.761	1.4700	0.442	0.443	+0.001
		0.0	2.157	1.5332	0.422		
Formic acid	Diethyl ketone	100.0	1.206	1.3686	0.435		
		80.0	1.092	1.3722	0.482	0.482	0.000
		60.0	1.003	1.3770	0.531	0.530	−0.001
		33.0	0.904	1.3830	0.596	0.595	−0.001
		20.0	0.865	1.3855	0.624	0.625	+0.001
		0.0	0.811	1.3887	0.672		
	Methyl *n*-propyl ketone	80.0	1.091	1.3720	0.484	0.482	−0.002
		60.0	1.003	1.3761	0.528	0.529	+0.001
		40.0	0.922	1.3808	0.578	0.577	−0.001
		32.0	0.892	1.3821	0.594	0.595	+0.001
		20.0	0.859	1.3842	0.623	0.624	+0.001
		0.0	0.800	1.3871	0.671		
Acetone	Chloroform	100.0	0.782	1.3534	0.582		
		80.0	0.864	1.3639	0.564	0.565	+0.001
		60.0	0.964	1.3764	0.547	0.548	+0.001
		40.0	1.089	1.3922	0.532	0.531	−0.001
		20.4	1.247	1.4124	0.514	0.514	0.000
		0.0	1.473	1.4393	0.497		

recorded values. In the case of mixtures the values of χ calculated on the basis of additive law are also given for comparison. The values of the azeotropic concentrations are underlined.

Discussion

All the mixtures with an alcohol as one of the components, except ethanol-ethyl acetate show practically little or no deviation from the additive law, with regard to magnetic susceptibilities. However, in all the cases departures from additive law were observed in their densities and refractive indices. The Raman spectra of ethanol benzene mixture have been studied by Cennamo and Vitale[11] and Sundara Rao[12]. The former authors found evidence of the existence of association in the mixture and the results of the latter indicated no such association. Ethanol-ethyl acetate and methanol-acetone mixtures are cases of two polar liquids for the mixtures. The magnetic data for ethanol-ethyl acetate mixture show slight departures from additive law. The observed χ values are lower than the additive values, the maximum deviation being nearly 1% at a concentration of 60% of alcohol. Ethyl acetate is an electron donor with a strong anionoid center C=O. When this is mixed with ethanol, the two types of molecules may associate through a hydrogen bond, lowering the anionoid power of C=O. The variation of χ from additive values might be due to the formation of hydrogen bonds between ethanol and ester molecules as represented below.

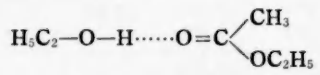

Murthy and Seshadri[13] found from Raman spectra of this mixture a diffuseness in the C=O frequency towards the shorter wavelength and they have taken this as evidence for the formation of hydrogen bonds as shown above.

The Raman spectra of methanol-acetone have been studied by Koteswaram[14], Joerges and Nikuradse[15] and Murthy and Seshadri[16]. From a study of the infrared spectra of this mixture Gordy[17] reported a shift of the C=O frequency of acetone. Koteswaram[14] observed a perceptible shift of C=O line at 1712 cm.$^{-1}$ towards shorter frequency. In 1:1 mixture, the C=O line was found to have a structure with two peaks. Also he reported a shift of C—C line towards higher frequency. These he attributed to the formation of association complexes. Joerges and Nikuradse[15] have also suggested the possibility of the formation of complexes by hydrogen bonding.

Acetone has a strong anionoid C=O center and hence it is normal to expect the formation of such complexes in this mixture. Any large change in the C=O bond strength will normally manifest itself in a susceptibility change. But the magnetic data do not show any such change from additive law. Murthy and Seshadri[16] studied the Raman spectra of this mixture but did not find any shift in the C=O line of acetone at 1710, thus indicating no evidence for the formation of hydrogen bonds. They distinguished between an ordinary hydrogen bond and a true hydrogen bond by postulating that a true hydrogen bond is one where both the cationoid and the anionoid center (OH and CO group) are affected. In the weaker type the OH group only will be affected. Quite possibly this mixture belongs to the case where the weaker type of hydrogen bond is formed and hence no deviation from additive law is observed.

The case of *n*-propanol acetal mixture is similar to methanol acetone mixture. Acetal has two anionoid centers. Because of this, one can expect the formation of associated complexes through a hydrogen bond. But the negative charge on the oxygen atom is very weak and the hydrogen bond that might be formed will consequently be weak. That this might be the case is evidenced by the magnetic data which show that the mixture obeys additive law.

The magnetic data of all the five mixtures having for one of their components a fatty acid, either acetic or formic, show fairly good agreement with additive values. Both acetic and formic acid are known to exist as associated molecules.

From a study of Raman spectra of some liquid mixtures Koteswaram[14] has observed that certain general changes might be expected when a fatty acid is mixed with a polar solvent. According to him the

11) Cennamo and Vitale, *Nuovo Cemento*, **13**, 465, (1936).
12) Sundara Rao, *J. Indian Chem. Soc.*, **22**, 260 (1945).
13) Murthy and Seshadri, *Proc. Indian Acad. Sci.*, **14A**, 593 (1941).
14) Koteswaram, *Indian J. Physics*, **14**, 341 (1940).
15) Joerges and Nikuradse, *Naturforsch*, **5A**, 25 (1950).
16) Murthy and Seshadri, *Proc. Indian Acad. Sci.*, **15A**, 154 (1942).
17) Gordy, *Phy. Rev.*, **50**, 1151 (1936).

changes expected are (i) breaking up of associated molecules into simpler ones and (ii) the formation of complexes between the solvent molecule and the monomeric molecule. Hence in such a mixture the possibilities are three fold.

1) The associated molecules are not affected by the presence of the solvent. If this is the case the magnetic susceptibility will be additive. 2) Depolymerisation may take place. This by itself will to some extent affect the susceptibility. 3) These simpler molecules may associate with the solvent molecules forming 'addition compounds'. This again may result in a change in the value in the reverse direction.

As all these five mixtures obey additive law, it might be inferred that the solvents used with these acids act merely as diluents without affecting the association in the acid molecules. If the association in the acid molecules is broken and the monomers form complexes with the solvent molecules, the two competing processes may compensate each other. But exact compensation is a remote possibility. Hence it may be taken that association between the acid molecules is not affected when the two acids are dissolved in the solvent used.

The acetone-chloroform mixture is of special interest. Its magnetic susceptibility, Raman spectrum and infrared spectrum have been studied by several workers. But the conclusions arrived at from these studies are not in agreement with one another. In view of the divergent views expressed regarding this mixture, the magnetic study has been repeated several times for each concentration. The data obtained show that the maximum departure from additive law is only about 0.2%. Even this small variation is not progressive. Hence the results may be taken to indicate that this mixture obeys additive law in conformity with the observations of Rao and his collaborators[2-4] and contrary to those made by Trifonov[18], Trew and Spencer[19], Buchner[20], Ranganathan[1] and Sibaiya and Venkataramiah[21].

Gordy[22] from a study of infrared spectra of this mixture has reported a shift of C=O absorption towards longer frequency in chloroform solution. A new absorption frequency at $4\mu(\Delta\nu=2500)$ was found and is attributed to a hydrogen bond between oxygen in C=O and hydrogen in C—H in chloroform as represented below.

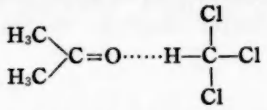

This he claimed[23] to be the first discovery of the direct spectrum of the hydrogen bond, all other evidences being indirectly based upon the changes in frequency.

Koteswaram[14] studied the Raman spectra of this mixture and found that even prolonged exposures did not give any trace of a line or band at $\Delta\nu=2500$. Even assuming that the band excited by the hydrogen bond is only infrared active, there must be a pronounced effect on the C=O frequency in acetone. No such effect was observed.

Murty and Seshadri[16] found no shift or diffuseness in the C=O line either. In the case of methanol-acetone and chloroform-acetone mixtures they found that the C=O frequency is not affected. If hydrogen bond existed, it should only be a weak one which could not affect the C=O group. If this group is affected, then it would produce a change from additivity. But these mixtures obey additive low. Hence in these mixtures either no hydrogen bonds are formed or the hydrogen bonds formed are so weak that the C=O group is not affected.

Though azeotropic mixtures have been specially chosen for this investigation, it has been found that the magnetic data in general seem to be unaffected even at the azeotropic concentrations. Hence any peculiarity that might be characteristic of the mixtures at the azeotropic concentrations could not be detected by the magnetic investigations.

From the present study and from previous literatures available, it may be concluded that, in general, binary organic liquid mixtures obey very closely additive law unless the bonds linked to the carbon atoms are affected.

Summary

An exhaustive study of the diamagnetic susceptibilities of the two types of azeotropic binary mixtures has been made

18) Trifonov, *Ins. Anal, Physico-Chem. Leningrad*, **3**, 434 (1925).
19) Trew and Spencer, *Proc. Roy. Soc.*, **131A**, 209 (1931).
20) Buchner, *Z. Physik*, **72**, 344 (1931).
21) Sibaiya and Venkatramiah, *Indian J. Physics*, **7**, 393 (1932).
22) Gordy, *J. Am. Chem. Soc.*, **60**, 605 (1938).
23) Gordy, *Nature*, **142**, 831 (1938).

with a view to find out any correlation between the magnetic data and the azeotropic behavior of the mixtures. The results obtained in the case of seventeen mixtures show that in almost all the cases additive law is obeyed even at the azeotropic concentrations. The small deviation from additivity observed in the case of ethanol-ethyl acetate mixture is explained on the basis of the formation of hydrogen bonds. The magnetic data are not affected by the azeotropic nature of the mixtures.

Department of Physics, Annamalai University, Annamalainagar South India

Activation Analysis of Manganese in Ferromanganese Alloy Using Radium-Beryllium Neutron Source

By Yuzuru KUSAKA

(Received April 26, 1957)

The method of analysis using slow neutron activation was early suggested by Hevesy and Levi[1], who used a 200 to 300 mc radium-emanation beryllium source in their determination of certain rare-earth elements possessing high neutron activation cross sections. More recently Boyd etc.[2] have reviewed the principles of radioactivation analysis, and a large number of papers have been published on their applications to various problems.

In 1953 Meinke and Anderson[3] explored the possibility of using low level neutron sources, 25 mg. radium–beryllium source, for activation analysis of rhodium, silver and indium.

The thermal neutron activation with a low-level neutron source has one major advantage over activation with higher sources; only those isotopes with a very high activation cross section and a short half-life are detected after a short irradiation. The profusion of neutron-induced activity obtained when a mixture of elements is irradiated in a nuclear reactor is eliminated. Thus it is possible to perform activation analysis without subsequent chemical separation; therefore analysis for favorable elements can be completed rapidly. Morever the amount of activity formed in the irradiation is so small and decays out so rapidly that the sample used for the irradiations is unchanged at the end of the analysis.

Recently, the writer reported the fundamental studies on activation analysis of manganese[4]. This paper describes some results of activation analysis of manganese in ferromanganese alloy using a low-level neutron source, 50 mg. radium-beryllium with a thermal neutron flux of about 10^2 —10^3 neutrons/cm^2/sec.

Nuclear Data for the Elements under Consideration

The radioactive isotopes and other nuclear data for the elements considered in this work are listed in Table I[5].

From Table I, one can expect that, an irradiation of eighteen hours will practically lead to the saturation activity of ^{56}Mn, whereas the activities of ^{55}Fe and ^{59}Fe will be negligible owing to their long half-lives, small cross sections and low abundance.

Experimental

The activation source consisted of a mixture of 84.2 mg. of radium bromide (49.3 mg. as radium element) with beryllium, which was sealed in a platinum tube, length 40.0 mm., diameter 5.0 mm., wall-thickness 0.5 mm., and certificated by the State Radiological Institute of the Czchoslovak Republic in 1938. The source was surrounded by paraffin to moderate the fast neutrons to thermal velocities. At the distance of 3.0 cm. around of the source, eight samples were arranged in the paraffin block of a 26.5×24.0×24.0 cm. cube; and the weight of each sample was 6.000 g. of granular powders (being sifted through a 100 mesh screen), which were put in the polyethylene tubes (inner diameter : 0.8 cm.,

1) G. V. Hevesy and H. Levi, *Kgl. Danske Videnskab. Math-Fys. Medd.*, **14**, 5 (1936); **15**, 11 (1938).
2) G. E. Boyd, *Anal. Chem.*, **21**, 335 (1949); J. V. Jakovlev, International Conference on Peaceful Uses of Atomic Energy, Geneva, Paper 632 (1955); A. A. Smales, ibid., Paper 770 (1955); M. P. Lévêque, ibid., paper 342 (1955); N. Saito, *Japan Analyst* (*Bunseki Kagaku*), **4**, 254 (1955).
3) W. W. Meinke and R. E. Anderson, *Anal. Chem.*, **25**, 778 (1953).
4) Y. Kusaka., Radioisotopes, **6**, 1 (1957), (In Japanese).

height: 5.4 cm.) with cork stoppers. The standard samples were prepared by mixing metallic iron and manganese powders in an appropriate ratio.

The irradiated time was about eighteen hours. After irradiation, the specimens and the standards were spread into the copper counting cup (diameter: 2.9 cm., height: 0.6 cm.) and their induced radioactivities were directly measured for 5 minutes by means of an end window type G. M. tube (thickness of mica window: 1.96 mg./cm^2) in the same geometrical position. These measured values of radio-activity were corrected to the value at the end of the irradiation. A comparision of the activity of the unknown and the standard makes possible an estimate of the amount of manganese in the unknown sample.

Results and Discussion

Induced Radioactivity.—An example of the decay curve of the induced radioactivity of the ferromanganese sample (Mn content: 80.1%) is shown in Fig. 1. The measured value of half-life was 2.6 hours, being in good agreement with that of ^{56}Mn. The same results were obtained in every sample. From these results, it was recongnized that in those experiments all induced radioactivities were due to ^{56}Mn only.

Self-shadowing Effect for Neutrons.—The radioactivity strength produced by this method were approximately proportional to the manganese content in the samples. Concerning the specific activity of the samples of a higher manganese content, a significant decreasing effect was recognized, to a greater extent for 6 g. of the sample than for 1 g. of the sample, as shown in Fig. 2.

This phenomenon will be based upon the self-shadowing effect for the neutrons used for activation of manganese. The

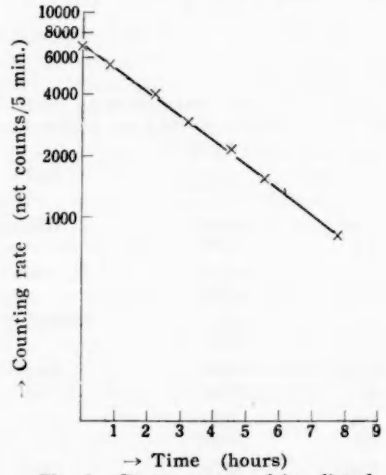

Fig. 1. Decay curve of irradiated ferromanganese.

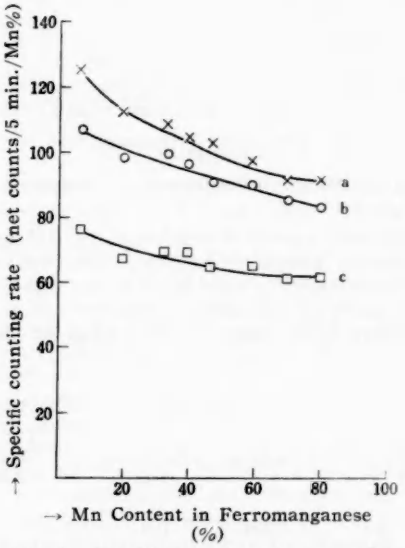

Fig. 2. Specific counting rate formed as a function of Mn content of ferromanganese.
(a)……sample weights 6 g.
(b)……sample weights 3 g.
(c)……sample weights 1 g.

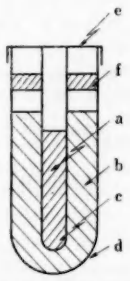

Fig. 3. Irradiation sample for self-shadowing experiments.
(a): manganese powder (2 g.)
(b): ferromanganese powder (15 g.)
(c): glass tube (inner diameter: 0.5 cm., thickness: 0.1 cm, height: 5.0 cm.)
(d): polyethylene tube (inner diameter: 1.7 cm., thickness: 0.1 cm., height: 5.4 cm.)
(e): polyethylene cup
(f): cork stopper

5) D. J. Hughes and J. A. Harvey, "Neutron Cross Sections", BNL 325 (1955).

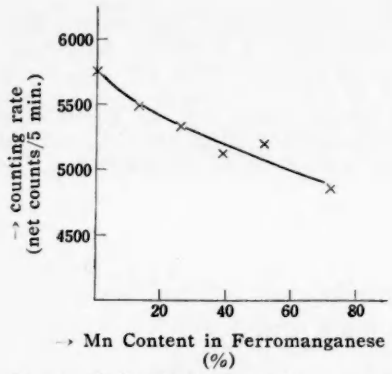

Fig. 4. Radioactivity formed in manganese powders.

manganese atoms in the samples did not encounter identical neutron flux during the irradiation, —that is, the flux for the inner part of the sample may be entirely different from that for the skin of the specimen. The next experiment was designed to investigate the flux depression caused by increasing manganese content. Two grams of manganese powder and 15 g. of ferromanganese powder of various manganese contents were separately put in a polyethylene tube as shown in Fig. 3 and irradiated in the paraffin block, at a distance of 3.0 cm. from the source. After irrradiation under the same condition, the radioactivity induced in 2 g. manganese powder was measured. In Fig. 4 the radioactivity strength was plotted against the content of manganese in ferromanganese.

Fig. 4 shows that under the experimental conditions the flux at the center of the 80% ferromanganese is about 0.85 of the flux without manganese and with iron.

Radioactivation Analysis of Manganese in Ferromanganese.—Manganese content of ferromanganese alloy is in 70—80% as manganese metal. In this region of

TABLE I

NUCLEAR CHARACTERISTICS OF THE ELEMENTS DETERMINED

Element	Isotope	Abundance (%)	Thermal Neutron Cross Section σ abs. (barn)	σ act. (barn)	Radioactive Nuclide Formed	Half -life	Radiations (Energy, Mev)
Mn	^{55}Mn	100	13.2 ±0.4	13.4±0.3	^{56}Mn	2.58 hr.	β^-(2.81), γ
Fe			2.53±0.06				
	^{54}Fe	5.84	2.2 ±0.2	2.2±0.5	^{55}Fe	3.0 yr.	k
	^{56}Fe	91.68	2.6 ±0.2				
	^{57}Fe	2.17	2.4 ±0.2				
	^{58}Fe	0.31	2.5 ±2.0	0.9±0.2	^{59}Fe	45.1 d	β^-(0.46), γ

TABLE II

ONE EXAMPLE OF EXPERIMENTAL RESULTS

Sample	Mn Content (%)	Measurment Time* (minutes)	Counting rate (net counts/5 min.) Obtained	St. Dev. (%)	Activity at the end of irradiation	Mean
ferromanganese	unknown	43— 48	5013	1.4	6157	6137
		67— 72	4484	1.5	6117	
ferromanganese	unknown	19— 24	5624	1.3	6193	6136
		92— 97	3982	1.6	6079	
standard	78.7	7— 12	6301	1.3	6577	6240
		105—110	3648	1.8	5903	
standard	78.7	31— 36	5497	1.3	6384	6331
		80— 85	4338	1.5	6278	
standard	73.8	37— 42	5046	1.4	6036	5983
		73— 78	4228	1.5	5930	
standard	73.8	25— 30	5171	1.4	5850	5874
		86— 91	3970	1.6	5899	
standard	68.9	13— 18	5383	1.4	5770	5576
		98—103	3434	1.7	5382	
standard	68.9	49— 54	4395	1.5	5535	5519
		61— 66	4144	1.5	5503	

* The time after the end of irradiation.

TABLE III

EXPERIMENTAL RESULTS OF MANGANESE ANALYSIS IN FERROMANGANESE

Exp. No.	Manganese Content (%) Radioactivation Method						Mean	Chemical Method
1.	78.4	78.1	76.1	77·9	77.8		77.7	77.4
2.	76.6 77.1	76.6 77.8	74.6 77.3	74.2 76.7	79.5 74.0	76.6	76.5	78.7
3.	74.0	74.6	78.0	76.3			75.7	78.2
4.	75.0	75.3	77.3	71.1	73.2	72.3	74.0	77.1

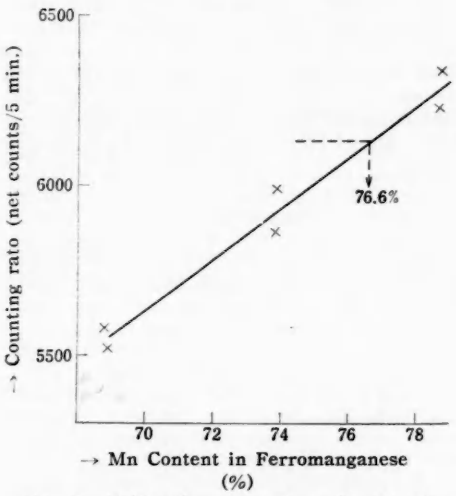

Fig. 5. Calibration curve in radioactivation analysis of Mn in ferromanganese.

manganese content, within experimental error it is possible to assume that the specific counting rate has a definite value. In these experiments, the manganese contents of the standard samples were 68.9%, 73.8% and 78.7%. A pair of samples, one a standard sample and the other, an unknown sample, were irradiated at the same time. One example of experimental results is shown in Table II.

From Table II, the manganese content of an unknown sample was graphically determined as shown in Fig. 5.

The experimental results of manganese analysis in various ferromanganese alloys by this method and comparison with the chemical analysis by the bismuthate method[6] are summarized in Table III.

Summary

A method was developed to determine macro-amounts of manganese in ferromanganese by radioactivation, using 50 mg. radium–beryllium as thermal neutron source. By activation of a sample (6 g.) for 18 hours and directly counting the activity with an end-window G. M. counter, the induced radioactivity was found to be entirely due to the 154.8 min. ^{56}Mn radioisotope. The amount of radioactivity was approximately proportional to the manganese content, but with samples of higher manganese content the self-shadowing phenomenon was recognized. By this method, it was possible to determine the manganese content in ferromanganese with a mean error of 2.5% without chemical procedures.

The writer wishes to express his hearty thanks to President Bunsaku Arakatsu and other members of the Chemical and Physical Laboratory of Konan University and to Professor Masayoshi Ishibashi of Kyoto University for their kind guidance and valuable advice through this study, and to Itsuo Araki of Kobe Seiko Co. for furnishing samples. A part of the expense for this study was defrayed from the Scientific Research Grant from the Ministry of Education, to which the author's thanks are due.

Department of Chemistry, Faculty of Science, Konan University
Higashinada-ku, Kobe

6) Treadwell-Hall, "Analytical Chemistry", Vol. II, p. 551 (ninth edition).

*The Electrolytic Separation Factor of Hydrogen Isotopes on Metal Electrodes**

By Yōichi TAKAHASHI, Shumpei OKA and Mitsuru OIKAWA

(Received October 10, 1957)

The electrolytic separation factor of hydrogen isotopes (α) usually represents the ratio between the evolution velocities of light hydrogen and heavy hydrogen under the same condition, viz;

$$\alpha = d\frac{(H/D)\text{ gas}}{(H/D)\text{ liq.}}$$

So we can get a competent side view for the study of the hydrogen evolution reaction from the measurement of α.

Some investigations were done previously on the problems of how α depends upon the sort of electrode materials, current density and other conditions. According to Horiuti and Okamoto[1], and Walton and Wolfenden[2], α does not vary much with the change of current density, but depends mainly upon the cathode materials. They pointed out that α of many metals were either about 3 or about 6, and that these two groups of α correspond respectively to two different hydrogen electrode mechanisms. Assuming that these two mechanisms exist, Horiuti, Okamoto and Hirota[3] calculated the values of α, and showed the correspondence between the measured value and the theoretical one.

On the other hand, however, these data are lacking in reproducibility. This poor reproducibility may be caused, firstly, by the difficulty in the micro-isotope analysis of hydrogen. Moreover, it is considered that the electrode process of hydrogen evolution reaction is very sensitive to changes of conditions, such as the state of electrode surface or of electrolyte.

Therefore, in order to discuss the mechanisms of hydrogen electrode reaction from the value of α, more extensive works are needed on the point of getting reproducible data. Rome and Hiskey[4] have investigated the separation factor on mercury cathode making use of a mass spectrometer for isotope analysis. Concurrently with Rome and Hiskey, the authors have investigated the separation factor on the various electrodes making use of mass spectrometer, and found some interesting facts about the electrolytic separation factor.

Experimental

Apparatus.—The apparatus used is illustrated in Fig. 1. The capacity of the cell was about 70 cc.

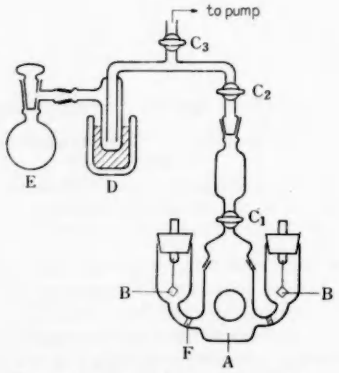

Fig. 1. Schematic diagram of the cell used.
A: Cell
B: Anode
C1, C2, C3: Stop cocks
D: Cold trap
E: Sample bulb
F: Sintered glass disc

As shown in Fig. 1, the cell was divided into three sections separated from each other by a pair of sintered glass discs. Attention was paid to avoid the contamination of electrolyte and electrode surfaces with tap grease.

The cathode part was inserted into the cathode compartment using a glass joint, for which no grease was used. As shown in Fig. 2, the cathode holder was specially devised so that

* Part of this paper was read at the discussion meeting of the Electrochemical Society of Japan on November 5, 1956.

1) Horiuti and Okamoto, *Sci. Pap. Inst. Phys. Chem. Res. Tokyo*, **28**, 231 (1936).

2) Walton and Wolfenden, *Trans. Faraday Soc.*, **34**, 436 (1938).

3) Horiuti, Okamoto and Hirota, *Sci. Pap. Inst. Phys. Chem. Res. Tokyo*, **29**, 223 (1936).

4) Rome and Hiskey, *J. Am. Chem. Soc.*, **76**, 5207 (1954).

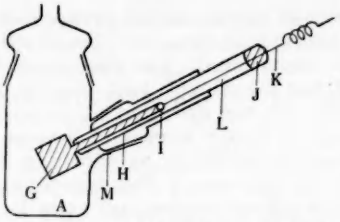

Fig. 2. The cathode and its setting device.

A: Cell	J: Paraffin
G: Cathode metal	K: Lead wire
H: Glass tube	L: Closed air
I: Solder	M: Glass joint

metal parts except cathode might not come into contact with electrolyte.

When mercury was used as the cathode it was put in a little glass vessel which was laid on the bottom of the cell; and a platinum-wire sealed in the glass tube, as in the cases of other cathode materials, was inserted into the mercury without coming into contact with the electrolyte. The surface area of the cathode was in all cases 2 cm^2.

Electrode and Solution—The separation factor was measured on such cathodes as platinum, gold, silver, nickel, iron, lead, copper, tin and mercury.

The mercury used was purified by electrolysis after distillation. The electrode plates were carefully polished, just before use, with emery paper and washed with distilled water. These electrodes were used repeatedly, being given the same treatment before each experiment. In the cases of iron, nickel, silver and tin, two specimens were used for each metal, but no difference was found between these specimens. The platinum electrode was cleaned, in some cases, by dipping it in concentrated hydrochloric acid at 100°C for an hour, and it was washed with distilled water.

The anodes, two small plates of platinum, had the total surface area of 2 cm^2.

The electrolyte of 0.2 N sulfuric acid solution was prepared from the re-distilled water containing as much deuterium as 0.2 atomic per cent. and guaranteed concentrated sulfuric acid. The solution was then purified by pre-electrolysis for about 15 hours at 0.5 mA/cm^2, and for an hour at 40 mA/cm^2.

Just before the experiment, tank-hydrogen was bubbled into the solution for an hour to saturate the solution with hydrogen and to remove dissolved air.

Procedure.—After setting the electrode to the cell, the hydrogen-saturated solution was poured into the anode compartment. Then it was sucked into the cathode compartment by evacuating this compartment through the cock 1 in Fig. 1.

The cathodic current density was 10 mA/cm^2. It was impossible to prevent entirely the oxygen, evolved by anode reaction, from coming through the glass discs into the cathode compartment, but according to Bockris[5], under such a high current density as in the present experiment, the depolarization effect of oxygen is so small as to be ignored.

The hydrogen gas evolved during the first 15 minutes, being contaminated with the pre-saturated tank-hydrogen, was purged by evacuation. Then, the hydrogen gas evolved during the next 30 minutes was introduced into the evacuated sample bulb, after drying the gas by passing it through a cold trap cooled with a mixture of solid-carbon dioxide and ethanol.

In order to measure the time variation of the value of α, sampling was performed every 30 or 15 minutes as mentioned above. The electrolytic current was never cut off during the run of an experiment. The hydrogen gas gathered in the sample bulb was then analysed on the mass spectrometer, the type of CEC 21—103 A.

For isotope analysis of the solution, the exchange equilibrium method[6] was used. The tank-hydrogen, led to the isotopical equilibrium with the solution at 25°C (equilibrium constant 3.87) by making use of Adams' catalyst for five hours, was analysed similarly on the mass spectrometer.

Results

The data of the electrolytic separation factor are shown in Table I. The values of the separation factor were derived from the following equation;

$$\alpha = 3.87 \frac{(D/H)_{\text{evol.}}}{(D/H)_{\text{equil.}}}$$

where the subscripts evol. and equil. designate the hydrogen evolved and the hydrogen equilibrated with the solution, respectively, and the factor 3.87 is the equilibrium constant of the following reaction

TABLE I

THE ELECTROLYTIC SEPARATION FACTOR OF HYDROGEN ISOTOPES ON SEVERAL METALS

0.2 N H_2SO_4 solution containing 0.2 atomic per cent. deuterium.

current density at 10 mA/cm^2

metal	α						average
Fe	6.7	6.9	6.6				6.7
Cu	7.0	6.9	7.1	5.2	5.4	6.4	6.3
Ni	5.7	5.5	6.7	5.4	4.9		5.6
Ag	4.6	4.2	4.6				4.5
Pt	4.4	4.8	4.4	4.3	4.4		4.5
Au	4.1	4.3	5.2	4.1			4.4
Pb	3.7	3.6					3.7
Hg	3.7	3.7	3.8				3.7
Sn	2.6	2.2					2.4

5) Bockris, *Chem. Rev.*, 43, 547 (1948).
6) Kirshenbaum, "Physical Properties and Analysis of Heavy Water", (McGraw-Hill, 1951) p. 205.

$$(H_2O)_{liq.} + (HD)_{gas} \rightleftarrows (HDO)_{liq.} + (H_2)_{gas}$$

at 25°C.

The values listed above refer to the sample gas evolved during 30 minutes after purging initial gas evolved during first 15 minutes of electrolysis.

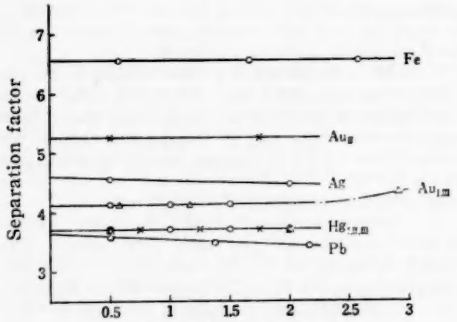

Fig. 3. Time variation of separation factors on several metal cathodes (I). ○, ×, △ designates 1st, 2nd and 3rd run, respectively, on the same metals.

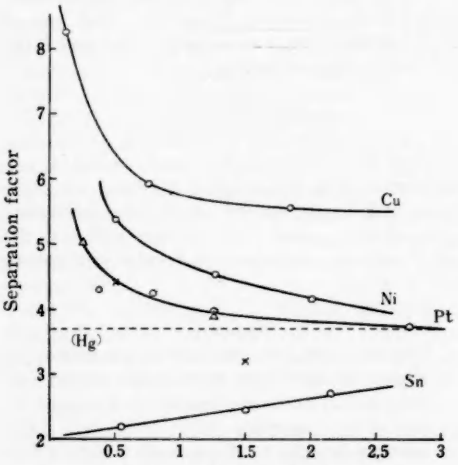

Fig. 4. Time variation of separation factors on several metal cathodes (II). ○, ×, △ designates 1st, 2nd and 3rd run, respectively, on platinum cathode. (Except platinum, typical curves are shown to avoid confusion.)

The time variation of α is shown in Fig. 3 and Fig. 4. In the cases of mercury, iron and gold, values of α were nearly constant in the lapse of time (Fig. 3). As to mercury, values of α obtained in three runs of the experiment coincided within the limit of experimental error, not only in an individual run, but also in all runs of the experiment. On the other hand, for platinum, nickel and copper α decreased with the duration of electrolysis. These decreasing curves of α were lacking in reproducibility, as shown in Fig. 4. but the three runs of the experiments on platinum showed undoubtedly the decrease of α with time. On the contrary, α on tin increased with time (Fig. 4).

Discussion

Time variation of separation factor.— Rome and Hiskey[7] found out that, on mercury cathode, the separation factor decreased markedly when the solution was contaminated with tap grease. Thus, if the cause of the time variation of separation factor in our experiment were imputed to the impurities in the solution, such as dissolved oxygen, tap grease etc., α on mercury, iron and gold must also vary with time. But the fact that not only on mercury but also on iron and gold, the separation factor did not vary with time indicates that the time variation of the separation factor on platinum, nickel etc. was not caused by the effect of impurities.

Apart from this, it may be considered that, since platinum, nickel and copper are all effective catalysts for hydrogen-exchange reaction[8], the secondary exchange reaction of evolved hydrogen gas with the solution may occur at the electrode surface, and as the result of this effect α approaches 3.87, the equilibrium value, with the lapse of time. But in this experiment, evolved hydrogen gas was taken into the sample bulb successively at the same intervals; hence, if decrease of α owes to the secondary exchange reaction, the catalytic activity of electrode surface must increase with time. This increase in catalytic activity with time is also unlikely.

For these reasons, and moreover from the fact that on platinum or nickel the hydrogen over-potential continues to increase for a much longer time than on the other metals[9-11] it may be presumed

7) Rome and Hiskey, *J. Am. Chem. Soc.*, **76**, 5209 (1954).
8) Hirota and Horiuti, *Sci. Pap. Inst. Phys. Chem. Res. Tokyo*, **30**, 151 (1936).
9) Hickling and Salt, *Trans. Faraday Soc.*, **36**, 1226 (1940).
10) Bockris and Azzam, ibid., **48**, 153 (1952).
11) Cousens, Ives and Swaroopa, *J. Chem. Soc.*, **1955**. 3482.

that the time variation of the separation factor is chiefly caused by the hydrogen electrode process itself.

Separation factor and mechanisms of hydrogen evolution reaction.— Horiuti and Okamoto[1] found out that the separation factors of several metals fell into two groups, viz. ca. 3 and 6, and discussed the fact that these experimental results set forth the mechanisms of the hydrogen evolution reaction, namely the catalytic mechanism for which α was about 6 and the electrochemical mechanism for which α was about 3 at room temperature. Walton and Wolfenden supported this theory, mainly because they found out that the temperature coefficient of α of these two groups showed clearly different tendencies.

However, the measured values of α in our experiment are rather distributed in the range from 2 to 7 at room temperature. For example, α on platinum, silver and gold shows an intermediate value, namely about 4.5. This tendency of distribution can be seen also in the Walton and Wolfenden's results. In their experiments, the separation factors at very low current density (0.03 mA/cm^2) at 15–20°C are as follows[12]:

Ni : 7.8_5, Ag : 6.8, Pt : 5.0,
Hg : 3.5_5, Sn : 3.5_5.

The fact that the values of α are distributed between 2 and 7 as mentioned above may be explained as follows. The path of hydrogen evolution reaction may not be only one, but probably two or more. If on a cathode metal the evolution of hydrogen took only one reaction path, or at least very predominantly one, separation factors of many metals could be classified according to the mechanisms of hydrogen evolution. This situation was adopted by Horiuti et al. But it is surely possible that on some metals the intermediate state may exist on which the evolution of hydrogen takes several paths in parallel. Supposing this, it is likely that the separation factor has an intermediate value. In addition to this, the value of α will be very sensitive to the condition of the electrode and the solution.

This sensitivity also can be seen, in the case of platinum especially. In our experimental condition α on platinum decreased with the lapse of time, and in addition to this, some preliminary experiments showed that the value of α on the platinum electrode, without any re-treatment after using it once for a run, was ca. 3.6 (the three runs of experiments showed the same results), and that after anodic pre-polarization α had the value higher than before as already reported by Eucken and Bratzler[13].

Moreover, it must be pointed out that, although, in general, good agreement is seen between the values of α obtained by Walton and Wolfenden and those obtained by Horiuti and Okamoto, in the case of platinum a remarkable discrepancy is found between the two.

These facts may indicate, at least on platinum electrode, that under some conditions the evolution of hydrogen has the possibility of taking several reaction paths in parallel, and that the state of the hydrogen evolution changes with the change of condition of the electrode surface—for example, changes due to pre-treatment of electrode, or to hydrogen saturation of electrode surface with the duration of electrolysis.

Conclusion

According to our experimental data, the values of electrolytic separation factor of hydrogen isotopes on various metals were distributed in the range from 2 to 7. On platinum, nickel and copper, a remarkable time variation of the separation factor was observed. These results do not coincide with the theory of Horiuti and Okamoto, in which two different mechanisms of hydrogen evolution reaction were assumed. The intermediate values of α and the noticeable sensitivity of α on several metals suggest us that it seems rather likely that the hydrogen evolution reaction may take several parallel paths. The time dependence of α may indicate the change of reaction process which follows the change of surface conditions of electrode, probably caused by the electrode process itself.

Considering the above discussion, the measurement of the electrolytic separation factor of hydrogen isotopes will be very useful for the study of hydrogen evolution reaction, though it involves still a complicated aspect. The theory of electrode process at hydrogen evolution is at present yet incomplete, especially in regard to

12) Walton and Wolfenden, *Trans. Faraday Soc.*, **34**, 444 (1938).

13) Eucken and Bratzler, *Z. phys. Chem.*, **A174**, 273 (1935).

the relation between the reaction and the state of electrode.

From this standpoint, the authors are now studying in more detail the nature of the electrolytic separation factor, especially the relation between the change of over-potential with conditions of electrode and that of the separation factor.

The authors wish to express their sincere gratitude to Assistant Professor S. Araki, Tokyo University, for affording us the convenience of using a mass spectrometer.

Labolatory of Applied Electrochemistry and Photochemistry, Faculty of Engineering, University, of Tokyo, Hongo, Tokyo

Ultraviolet Absorption Spectra of Three Isomeric Pyridinemethanols and Their N-Oxides

By Norisuke HATA

(Received June 27, 1957)

In recent years, the ultraviolet absorption spectra of pyridine derivatives were investigated by various workers[1-3], and several studies were also made for pyridine *N*-oxides[4-6]. However, the ultraviolet absorption spectra of hydroxymethyl, aldehyde, and carboxyl derivatives of pyridine were not studied in detail, although these compounds are important in the fields of organic and biological chemistry.

In the present investigation, the author measured the ultraviolet absorption spectra of three isomeric pyridinemethanols and their *N*-oxides in various solvents, and discussed the solvent effects on their spectra and also the effects of introduction of a hydroxymethyl group on the absorption spectra of pyridine and pyridine *N*-oxide.

Experimental

The synthesis of 2-, 3- and 4-pyridinemethanols were carried out by methods given in the literature and these compounds were purified several times by recrystallization or vacuum distillation.

2-Pyridinemethanol[7]: b. p. 100°~3°C/5 mmHg.
3-Pyridinemethanol[8]: b. p. 144°~5°C/20 mmHg.
4-Pyridinemethanol[7]: m. p. 176°~7°C (from butanol).

The syntheses of 2-, 3- and 4-pyridinemethanol *N*-oxides were done by treating the corresponding pyridinemethanol with aqueous hydrogen peroxide in glacial acetic acid and they were purified by recrystallization from ethyl acetate several times[9].

2-Pyridinemethanol *N*-oxide: m. p. 141°C. 3-Pyridinemethanol *N*-oxide: m. p. 93°~4°C. 4-Pyridinemethanol *N*-oxide: m. p. 125°C.

Solvents used in the spectral measurements were purified[10] *n*-hexane, carbon tetrachloride, ethanol and water.

The ultraviolet absorption spectra were measured with a SHIMADZU Quartz Spectrophotometer Type QB-50, using a fused quartz cell of 1 cm. thickness.

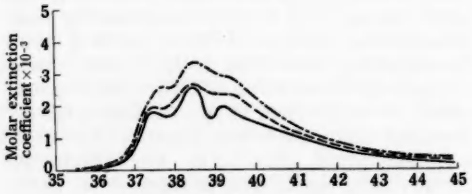

Fig. 1. Absorption curves of 2-pyridinemethanol.
——— *n*-Hexane.
– – – – Ethanol.
– – – – – Water.

1) H. Sponer and H. Stückeln, *J. Chem. Phys.*, **14**, 101 (1946); J. H. Rush and H. Sponer, ibid., **20**, 1847 (1952); W. K. Miller et al., *J. Am. Chem. Soc.*, **72**, 1629 (1950).
2) R. J. L. Andon et al., *Trans. Faraday Soc.*, **50**, 918 (1954); N. Ikekawa et al., *Pharm. Bull.*, **2**, 209 (1954).
3) H. P. Stephenson, *J. Chem. Phys.*, **22**, 1077 (1954).
4) H. Hirayama and T. Kubota, *Annual Reports of Shionogi Research Laboratory*, **2**, 47 (1952); T. Kubota, *J. Pharm. Soc. Japan (Yakugaku Zassi)*, **73**, 140 (1953); **74**, 831 (1954); H. H. Jaffe, *J. Am. Chem. Soc.*, **77**, 4451 (1955).
5) N. Ikekawa and Y. Sato, *Pharm. Bull.*, **2**, 400 (1954).
6) M. Ito and N. Hata, This Bulletin, **28**, 260 (1955); N. Hata, ibid., **29**, 82 (1956).
7) V. Boekelheide and W. Linn, *J. Am. Chem. Soc.*, **76**, 1286 (1954).
8) R. G. Jones and E. C. Kornfeld, ibid., **73**, 107 (1951).
9) The synthesis was performed by Mr. S. Furukawa of our laboratory, to whom the author's thanks are due. For the details, see S. Furukawa, *J. Pharm. Soc. Japan (Yakugaku Zassi)*, in press.
10) A. Weissberger and E. S. Proskauer, "Organic Solvents", 2nd, Ed. (1955).

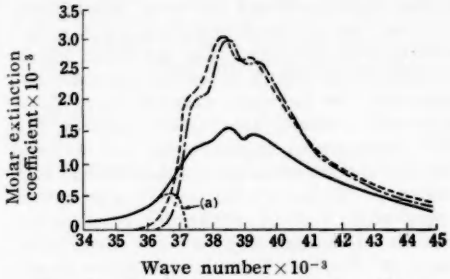

Fig. 2. Absorption curves of 3-pyridinemethanol.
——— *n*-Hexane.
– – – Ethanol.
– · – · Water.
(a)··· n-π^* Absorption curve separated by peak analysis. (c. f., refs. 3 and 6).

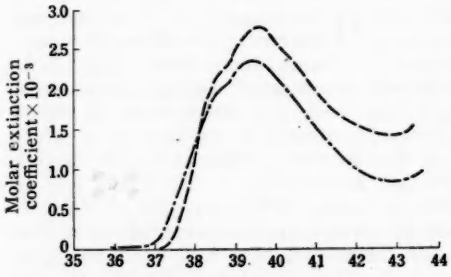

Fig. 3. Absorption curves of 4-pyridinemethanol.
– – – Ethanol.
– · – · Water.

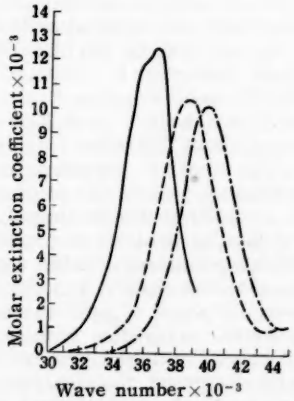

Fig. 4. Absorption curves of 2-pyridinemethanol *N*-oxide.
——— Carbon tetrachloride.
– – – Ethanol.
– · – · Water.

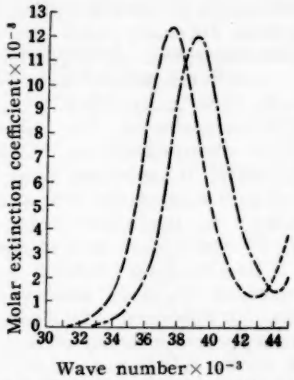

Fig. 5. Absorption curves of 3-pyridinemethanol *N*-oxide.
– – – Ethanol.
– · – · Water.

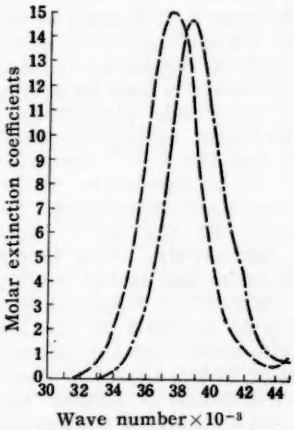

Fig. 6. Absorption curves of 4-pyridinemethanol *N*-oxide.
– – – Ethanol.
– · – · Water.

Results and Discussion

Figs. 1 to 6 show the absorption curves of three isomeric pyridinemethanols and their *N*-oxides in various solvents. The observed values of maximum wavelength, wave number, molar extinction coefficient, and oscillator sterength[11] are listed in Table I.

(1) Effect of Solvent *a) Pyridinemethanols.* — These compounds show the absorption bands (ε=2000~5000) with some vibrational structure in the region between 35000 cm.$^{-1}$ and 44000 cm.$^{-1}$ like correspond-

11) The calculations of the oscillator strengths were made according to the method described in Stephenson, *J. Chem. Phys.*, **22**, 1077 (1954).

ing three isomeric picolines. On account of the wavelength of the absorption region, the absorption intensity, and the solvent effect, this absorption is regarded to be due to a $\pi-\pi^*$ transition corresponding to an A_1-B_1 type in pyridine.

In 2-pyridinemethanol, the absorption maximum at about 38450 cm.$^{-1}$ does not essentially shift in solvents such as *n*-hexane, ethanol and water, but the intensity increases in the above order of solvents. $n-\pi^*$ Absorption due to the excitation of a non-bonding electron localized on the nitrogen atom as observed in 2-picoline was not observed in this compound.

The absorption spectrum of 3-pyridinemethanol shows a solvent effect similar to that of 2-pyridinemethanol, but when *n*-hexane is used as solvent, a shoulder absorption is observed near 36400 cm.$^{-1}$. This is regarded to be due to an $n-\pi^*$ transition like that observed in 3-picoline. This assignment is supported by the facts that when ethanol or water, acting as a proton donor to the nitrogen atom of a pyridine nucleus, is used as solvent, this absorption completely disappears and the ratio of oscillator strength between this absorption and the $\pi-\pi^*$ absorption near 39100 cm.$^{-1}$ is in the order of 10^{-2}. In ethanolic or aqueous solution, however, the intensity of the $\pi-\pi^*$ absorption increases remarkably. This fact may be considered to be due to the overlap with the $n-\pi^*$ absorption displaced to shorter wavelength as a result of the hydrogen bond formation between the nitrogen atom of ethanol or water, since the non-bonding electron of nitrogen is largely stabilized in energy as a result of such a hydrogen bond formation.

The solvent effect for 4-pyridinemethanol absorption differs somewhat from other pyridine derivatives and is similar to that of pyridine. That is, $\pi-\pi^*$ absorption of 4-pyridinemethanol shifts to red and the intensity dereases by changing the solvent from ethanol to water.

In the spectra of 2-, 3- and 4-pyridinemethanols mentioned above, the $n-\pi^*$ absorption is observed only for 3-pyridine methanol in *n*-hexane. The explanation for this fact is qualitatively given as follows. If a hydrogen atom of the methyl group were replaced by a hydroxyl group, the inductive effect of methyl group would decrease to some extent. Therefore, the binding energy of a non-bonding electron localized on the nitrogen atom in 2-pyridinemethanol would increase compared with that of 2-picoline. Such an increase in binding energy causes the $n-\pi^*$ absorption shift to the spectral region of the $\pi-\pi^*$ transition or further. On the other hand, the inductive effect of of hydroxymethyl group for the nitrogen atom of 3-pyridinemethanol is negligible. Consequently, the $n-\pi^*$ absorption is observed in *n*-hexane solution as a shoulder absorption like pyridine. However, the $n-\pi^*$ absorption is not observed in ethanolic or aqueous solution, because the $n-\pi^*$ absorption which is displaced to shorter wavelength by the hydrogen bonding between the solute and the solvent falls in the spectral region of $\pi-\pi^*$ transition.

In 4-pyridinemethanol, it is presumed that the $n-\pi^*$ absorption occurs in the region at about 34500cm.$^{-1}$, because this compound is insoluble in non-polar solvents.

b) *Pyridinemethanol N-oxides.*—The solvent effects for the strong absorption bands of pyridinemethanol *N*-oxides appearing at 31000 cm.$^{-1}$ to 43000 cm.$^{-1}$ are noticeably different from those of pyridinemethanols mentioned above. As is seen from Figs. 4~6, the absorption of these compounds shows a greater blue shift when the solvent is changed from carbon tetrachloride to ethanol and water, just as does the absorption of pyridine *N*-oxide[4,6]. This phenomenon is considered to be due to the formation of a hydrogen bond between N—O group and R—OH of the solvent acting as a proton donor, a phenomenon similar to that found in pyridine *N*-oxide.

(2) Effect of Hydroxymethyl Group.—Since several pyridinemethanols and their *N*-oxides are insoluble in non-polar solvents, the effect of hydroxymethyl substitution on pyridine or pyridine *N*-oxide absorption is discussed in relation to the spectra in ethanolic solution.

As seen from Table I and Fig. 7, the absorption at about 38900 cm.$^{-1}$ of pyridine shifts to the shorter wavelength in 4-pyridinemethanol and to the longer wavelength in 2- or 3-pyridinemethanol. This tendency is similar to those in picoline[2] or monohalogeno-pyridines[3]. Such a shift of absorption maxima caused by substituting a group for hydrogen of pyridine nucleus is in agreement with the results of the molecular orbital calculations by Tsubomura[12] who discussed the electron migration effect from the substituent to the conjugated system of pyridine ring. The

12) H. Tsubomura, *J. Chem. Soc. Japan, Pure Chem. Sec.*, (*Nippon Kagaku Zassi*), **78**, 293 (1957).

Table I

WAVE LENGTH, WAVE NUMBER, MOLAR EXTINCTION COEFFICIENT, AND OSCILLATOR STRENGTH OF THREE ISOMERIC PYRIDINEMETHANOLS AND THEIR *N*-OXIDES

Compound	Solvent	Wave length (mμ)	Wave number (cm.$^{-1}$)	Molar extinction coefficient	Oscillator strength
2-Pyridinemethanol	*n*-Hexane	267	37430	1850	0.032
		260	38450	2600	
		255.5	39100	1950	
	Ethanol	266.5	37500	1850	0.046
		260	38450	2700	
	Water	265	37700	2600	0.056
		259.5	38500	3400	
3-Pyridinemethanol	*n*-Hexane	260	38400	1650	0.0043
		255.5	39100	1500	
		275s†	36350	400	0.00036
	Ethanol	261	38350	3000	0.0056
		256	39100	2700	
	Water	259.5	38500	2980	
		254	39300	2700	0.0050
4-Pyridinemethanol	Ethanol	253	39570	2760	0.040
	Water	253.5	39450	2340	0.035
2-Pyridinemethanol *N*-oxide	CCl_4	276	36240	12600	0.210
	Ethanol	259	38580	10500	0.204
	Water	252	39600	10300	0.201
3-Pyridinemethanol *N*-oxide	Ethanol	264	37800	12400	0.239
	Water	254	39300	12000	0.234
4-Pyridinemethanol *N*-oxide	Ethanol	266	37600	15000	0.285
	Water	257	38800	14800	0.279

† denotes the shoulder absorption ($n-\pi^*$)

smaller shift of absorption maximum to the shorter wavelength in 2-, 3- and 4-pyridinemethanols compared with the corresponding picolines may be considered to be due to the decrease in hyperconjugative power of the methyl group. The decrease in shift is caused by the replacement of a hydrogen atom in the methyl introdution group with a hydroxyl group.

In pyridinemethanol *N*-oxides, the absorption at 38000 cm.$^{-1}$ shifts to the longer wavelength by the substitution of hydroxymethyl group at 3- or 4-position and to the shorter wavelength by substitution at 2-position. A similar tendency of shift is found in picoline *N*-oxides[5]. Previously, Ikekawa and Sato[5] have reported that the absorption maximum of pyridine *N*-oxide shifted to blue by the introduction of 2-methyl group. For the cause of this shift they attributed the formation of a weak intramolecular hydrogen bond between the oxygen atom of N—O group and the hydrogen atom of 2-methyl group as shown in (A), which hindered the

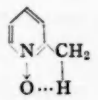

(A)

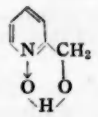

(B)

resonance of pyridine *N*-oxide. In the present work the blue shift caused by the introduction of 2-hydroxymethyl group was also observed. If the formation of a weak intramolecular hydrogen bond is assumed to 2-pyridinemethanol *N*-oxide as one of the main factors for such a blue shift phenomenon, the electron migration from the oxygen atom of N—O group to the pyridine ring may be prevented by the increase in its electronegativity caused by the formation of the intramolecular hydrogen bond as shown in (B). Therefore, the maximum wavelength of 2-pyridinemethanol *N*-oxide may be close to that of pyridine. As is seen from Fig. 7 and Table I, the ethanol solution of 2-pyridinemethanol *N*-oxide has a similar

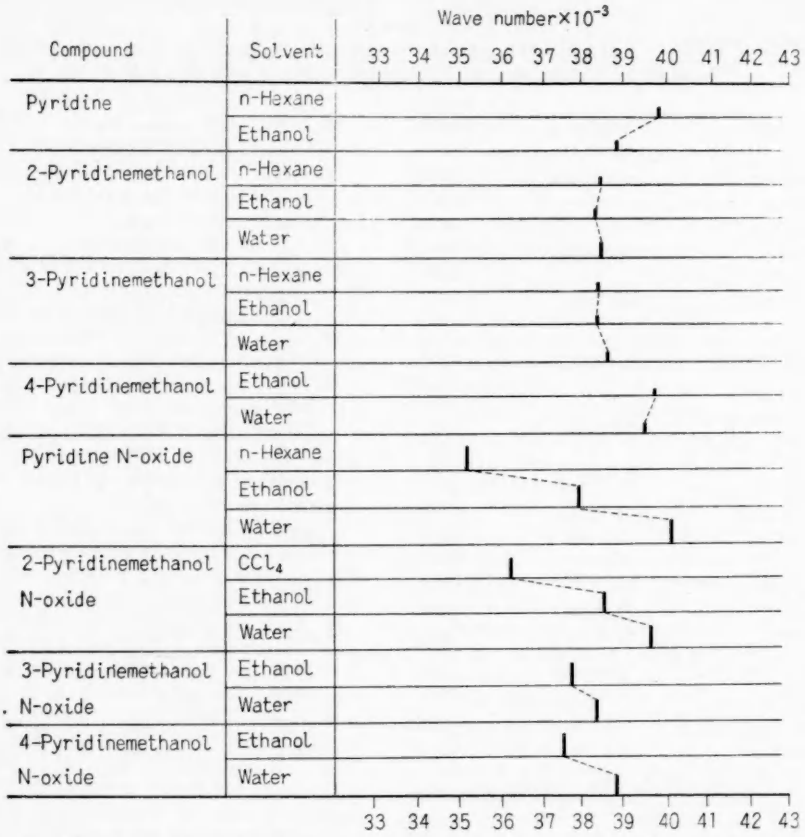

Fig. 7. Schematic expression of absorption spectra of three isomeric pyridinemethanols and their *N*-oxides.

value of the maximum wavelength with pyridine, while in 3- or 4-pyridinemethanol *N*-oxide its maximum wavelength differs remarkably from that of pyridine. These facts also support the intramolecular hydrogen bond formation in 2-pyridinemethanol.

Summary

The ultraviolet absorption spectra of three isomeric pyridinemethanols and their *N*-oxides were measured in various solvents. $n-\pi^*$ Absorption was observed as the shoulder absorption only in *n*-hexane solution of 3-pyridinemethanol, for which a qualitative discussion was made.

It was also found that the substituiton of a hydroxymethyl group in 4-position of pyridine or 2-position of pyridine *N*-oxide caused the blue shift. To explain this fact the presence of a weak intramolecular hydrogen bond in 2-pyridinemethanol *N*-oxide was assumed.

In conclusion, the author wishes to express his hearty thanks to Professor S. Imanishi of Kyushu University for his kind guidance and encouragement. Thanks are also due to Dr. E. Suenaga of Nagasaki University for his helpful advice.

Faculty of Pharmacy, Nagasaki University, Nagasaki

Polymerization of Olefins with Trialkylboron Catalysts. I. Polymerization of Vinylchloride and Acrylonitrile

By Nobuyuki ASHIKARI

(Received September 20, 1957)

Since the discovery of Ziegler's catalyst, organometallic compounds have been studied by many investigators. Recently, Kolesnikov[1] studied the polymerization of acrylonitrile with a mixed catalyst of tributylboron and borontrifluoride. However, there are few studies on the polymerization with trialkylboron catalyst only.

The author studied the polymerization of olefins with trialkylborons, and found that they are excellent catalysts to some olefins such as acrylonitrile, vinylchloride, vinylacetate and styrene.

Reaction mechanism of trialkylalminium catalyst to ethylene has been considered as[2],

$$\mathrm{RAl}+n(\mathrm{CH_2}=\mathrm{CH_2}) \rightarrow \mathrm{R}(\mathrm{CH_2}-\mathrm{CH_2})_n-\mathrm{al}$$

where, $\mathrm{al}=1/3\mathrm{Al}$

Similarly, in the case of trialkylboron catalyst, an anionic reaction can be considered in some cases. But in other cases, a radical reaction also can be considered.

Experimental and Results

1. On some trialkylborons. — There are several methods of preparation of trialkylboron, and the author adopted the common method, i.e., the reaction of Grignard reagent and borontrifluoride-etherate in ether.

The catalysts prepared in this experiment are triethyl-, tri-*iso*-propyl-, and tri-*iso*-butylboron. Triethylboron was prepared by dropping borontrifluoride-etherate into cooled ether solution of ethylmagnesiumbromide. After the reaction was over, the ether solution was distilled.

Thus, from the Grignard reagent prepared with 24 g. (1 mol.) of magnesium and 40 g. (0.28 mol.) of borontrifluoride-etherate, 22 g. of triethylboron was obtained. The yield to magnesium used was 67%.

Similarly, tri-*iso*-propyl- and tri-*iso*-butylboron were prepared from borontrifluoride-etherate and the corresponding alkylmagnesiumbromide.

Tri-*iso*-butylboron (b. p. 188°C) is very stable even in water, so that it can be used in the emulsion system. Tri-*iso*-propylboron (b. p. 150°C) fumes but does not flame in the air. Triethylboron is very flamable in the air so that it was diluted with hexane or toluene when it was used.

2. Polymerization of vinylchloride.— Vinylchloride has large polarity, and it can be polymerized very easily. The reaction proceeded slowly at −60°C, and rapidly at room temperature. Usually, the product was colorless except in cases when the reaction was carried out in tetrahydrofuran or cyclohexanon.

2.1 Bulk polymerization of vinylchloride.—Since the rate of reaction in the beginning of the polymerization was very great it was easy to obtain up to about 50 per cent. conversion. However, it was fairly difficult to obtain more than 50 per cent. conversion, because the rate of polymerization dropped.

The monomer whose amount is shown in Table I, with 0.1225 g. of triethylboron was sealed in a glass tube under a nitrogen stream. The reaction was carried out at 50°C for five hours. The solution became to solidify within three hours after the reaction occurred. After five hours the sealed tube was opened and the polymer was poured into ethanol, filtered, dried under reduced pressure at 50°C, and weighed. The results are shown in Table I.

TABLE I

BULK POLYMERIZATION OF VINYLCHLORIDE

exp. No.	monomer (g.)	polymer (g.)	Yield (%)
VCB-1	10	2.8795	28.80
VCB-2	15	4.7273	31.52
VCB-3	20	6.9894	34.95
VCB-4	25	8.6975	34.79
VCB-5	30	10.8695	36.23
VCB-6	35	16.8486	48.14

2.2 Solution polymerization.—To look over the rate of polymerization of vinylchloride in alcohol solvent, the author did the following experiment.

Vinylchloride (10 g., 0.16 mol.) was polymerized with 0.148 g. (0.00075 mol.) of tri-*iso*-butylboron catalyst in 30 cc. of ethanol. The reaction was carried out in a sealed tube at 35°C. Each sealed

1) G. S. Kolesnikov and L. S. Fedorova, *Izv. An. USSR*, No. 2, 236 (1957).

2) K. Ziegler and E. Holzkamp, *Angew. Chem.*, **67**, 543 (1955).

tube was opened after a certain time, and the polymer was separated by filtration. Then, the polymer was dried and weighed. The results are shown in Fig. 1.

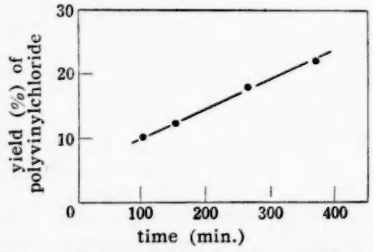

Fig. 1. Relation between the yield and the reaction time.

Vinylchloride also polymerized in tetrahydrofuran or cyclohexanon. In these solvents the product was colored. On account of the reaction system being homogenious, in tetrahydrofuran, the reaction proceeded smoothly.

The monomer (25 g.) was polymerized with 0.1225 g. of triethylboron in 25 g. of tetrahydrofuran at 50°C, for eight hours, and 12.444 g. of the polymer was obtained. The yield was 49.78%.

2.3 Emulsion polymerization.—In emulsion polymerization of vinylchloride the reaction proceeded rapidly. Of course, the rate of polymerization is varied by the concentration of catalyst. Fig. 2 represents the relation between the yield and the concentration of catalyst.

In this experiment, the monomer (20 g.) was polymerized with a certain weight of tri-*iso*-butylboron catalyst in 20 g. of aqueous solution containing 1 g. of emulsifier at 40°C in a sealed tube. After four hours, each sealed tube was opened and the solution was treated with five per cent. aqueous sodium chloride solution. Then the polymer was separated, filtered, washed throughly with water, dried and weighed.

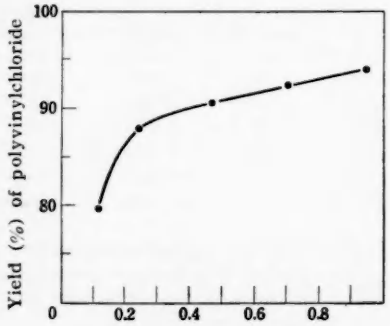

Fig. 2. Relation between the yield and the concentration of catalyst.

2.4 Influence of addition of titaniumtetrachloride.—As is well known, in the polymerization of ethylen, the mixed catalyst of trialkylaluminum and titaniumtetrachloride is used.

Similarly, an experiment using the mixted catalyst of trialkylboron and titaniumtetrachloride for the polymerization of vinylchloride was done, i.e., the monomer (20 g.) and the mixed catalyst consisting of 0.07 g. of tri-*iso*-butylboron and 0.05 g. of titaniumtetrachloride were sealed and maintained at 30°C. After one month, only 7.4 g. of polymer was obtained. Therefore, it is considered that the addition of titaniumtetrachloride to trialkylboron drops the rate of polymerization.

2.5 Measurement of molecular weight of polyvinylchloride.—Each sample got in the experiments of Table I was dissolved in cyclohexanon and the viscosity was measured at 30°C with Ubbelohde viscometer. The specific viscosity by concentration (η_{sp}/C) is represented in Fig. 3.

From Fig. 3, the intrinsic viscosity is 0.275–0.620. Therefore, the weight-average molecular weight calculated from Nakajima's equation[3] $M=313\times10^2\left(\log^{-1}\frac{[\eta]}{2}-1\right)$

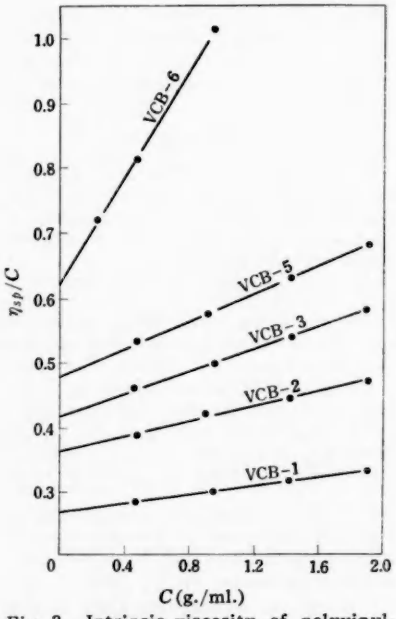

Fig. 3. Intrinsic viscosity of polyvinylchloride.

3) A. Nakajima, *Chemistry of High Polymers, Japan, Kōbunshi Kagagu*, **7**, 309 (1950).

is 11675-32615. The molecular weight of the polymer prepared in emulsion system, is 40500 (exp. No. VCH-4).

The condition of polymerization of exp. No. VCH-4 is as follows: monomer, 20 g.; aqueous solution containing five per cent. sodium lauryl sulfate, 20 g.; tri-*iso*-butylboron, 0.148 g.; temperature, 40°C; reaction time, four hours.

3 Polymerization of acrylonitrile.—Acrylonitrile was very easily polymerized by trialkylboron catalyst. Generally, a white polymer was obtained except for such case as those in which the reaction was very vigorous or polymerization proceeds in dimethylformamide.

3.1 Relation between the yield and the reaction time.—Each sealed tube which contained 12 g. of monomer, 20 cc. of *n*-hexane, and 0.693 g. of triethylboron, was set at 50°C. After certain intervals of time, the polymer was taken out from the sealed tube, treated with ethanol, dried, and weighed. The yield is shown in Table II.

TABLE II
RELATION BETWEEN THE YIELD AND THE REACTION TIME

exp. No.	time (hr.)	polymer (g.)	yield (%)
A-1	1	1.6757	13.8
A-2	3	5.7621	48.0
A-3	5	10.2811	85.0
A-4	7	10.6320	88.6

Proceeding of polymerization in ethanol with tri-*iso*-butylboron catalyst was slower than that of polymerization in hexane, and usually a white product was obtained. For example, when the polymerization of 20 g. of monomer was carried out with 0.396 g. (0.0015 mol.) of tri-*iso*-butylboron, in 25 cc. of ethanol, at 50°C for seven hours, 13.674 g. of polymer was obtained. The yield is 70%.

3.2 Influence of concentration of catalyst on the yield of polymer.—The result of polymerization that was carried out at 50°C, for five hours, with triethylboron catalyst is shown in Table III. In this case, the amount of catalyst is constant (0.0693 g.), and that of monomer is varied.

TABLE III
RELATION BETWEEN THE YIELD AND THE CONCENTRATION OF CATALYST

exp. No.	monomer (g.)	catalyst*	polymer (g.)	yield (%)
B-1	8.06	0.4602	7.66	94
B-2	12.09	0.3068	11.49	95
B-3	16.16	0.2301	15.12	94
B-4	20.15	0.1841	19.14	90
B-5	24.18	0.1534	20.55	85

* catalyst/monomer, mol. %

3.3 Relation between the intrinsic viscosity and the concentration of catalyst.—The same sample in Table III was dissolved in dimethylformamide and the viscosity measured at 25°C. The intrinsic viscosity was calculated from specific viscosity by the following equation;

$$[\eta] = [(1-4k'\eta_{sp})^{1/2}-1]/2k'C \qquad (1)$$

where, $k'=0.33$[4].

The relation between $[\eta]$ and the concentration of catalyst is represented in Fig. 4.

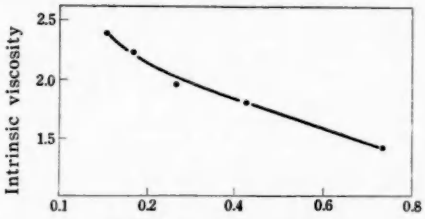

Fig. 4. Relation between the intrinsic viscosity and concentration of catalyst (triethylboron).

3.4 The molecular weight of polyacrylonitrile.—The value of intrinsic viscosity calculated from equation (1) is slightly greater than that extrapolated in Fig. 5. The molecular weight calculated from Stockmayer's equation[5], $[\eta]=2.43\times10^{-4}M^{0.75}$, is 100,000—200,000.

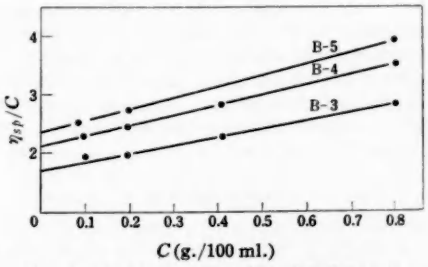

Fig. 5. Intrinsic viscosity of polyacrylonitrile.

Summary

It was found that trialkylboron is an excellent catalyst for the polymerization to some olefins which have comparatively large polarities. Vinylchloride and acrylonitrile were polymerized with this catalyst at a comparatively low temperature, and

4) R. Clealand and W. Stockmayer, *J. Polymer Sci.*, **17**, 473 (1955).
5) B. Cleland and W. Stockmayer, ibid., **17**, 476 (1955).

white polymers were usually obtained.

Vinylchloride was polymerized in bulk-, solution- and emulsion-system, and the rate of polymerization or the relation between the yield and the concentration of catalyst was investigated. Generally, the molecular weight of the polyvinylchloride was small (less than 50,000).

The polymerization of acrylonitrile was studied chiefly in a solution system. Usually, the molecular weight of polyacrylonitrile was fairly large.

Electrical Communication Laboratory
Nippon Telegraph and Telephone
Public Corporation, Musashino
Tokyo

The Ignition of Methane-Oxygen Mixture by Shock Wave

By Momotaro SUZUKI, Hajime MIYAMA and Shiro FUJIMOTO

(Received June 28, 1957)

The ignition of detonable gaseous mixtures by shock wave has been investigated by several authors. In many of those investigations the shock tube was used for the measurement of the ignition temperature of gaseous mixtures. Most of the authors[1-3] claimed the ignition temperature generated by shock waves is essentially lower than that obtained by any other means. Recently, however, Steinberg et al.[4] reported that they could not find any appreciable difference in temperatures between the various methods. Shepherd[2] has made similar investigations on the methane-oxygen mixture under ordinary pressure, for the purpose of measuring the ignition temperature. The present investigations dealing with a variety of pressures and gaseous compositions determined the minimum ignition pressure under these various experimental conditions.

Experimental

The brief scheme of the measuring system is given in Fig. 1. As shown in Fig. 2, the shock tube made of mild steel of 2.5 cm. internal diameter and 214.7 cm. length is divided into two sections, the reservoir chamber of 51.3 cm. length and the ignition test chamber of 163.4 cm. length, respectively. Furthermore, the test chamber can be divided into two; the first portion or buffer chamber, which is adjacent to the reservoir, has a length of 57.2 cm. and can be separated with a

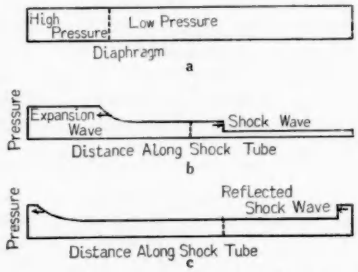

Fig. 1. Shematic of shock tube (a) and pressure distributions in shock tube (b and c).

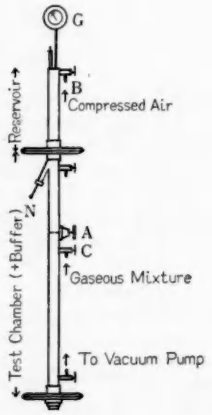

Fig. 2. Diagram of shock tube.

A; Sluice valve
B, C; Needle valve
N; Needle
G; Pressure gauge

1) J. A. Fay, "Fourth Symposium on Combustion", p. 501, Baltimore, The Williams and Wilkins Co. (1953).
2) W. C. F. Shepherd, "Third Symposium on Combustion" p. 302, ibid. (1949).
3) D. J. Berets, E. F. Greene and G. B. Kistiakowsky, *J. Am. Chem. Soc.*, **72**, 1080 (1950).
4) M. Steinberg and W. E. Kaskan, "Fifth Symposium on Combustion", p. 664 (1955).

sluice valve A from the second or remaining part of the test chamber on necessary occasions. The second portion then serves as the actual test chamber. The reservoir and the test chamber are separated by suitable sheets of cellophane films of 0.040 and 0.027 mm. thickness. The number of sheets of cellophane films is so chosen that it barely withstands the pressure difference between the two chambers without rupturing before the start of the experiment.

To carry on the measurement, compressed air is first sent into the reservoir chamber and this air pressure acts as firing pressure for the gaseous mixture. The test chamber is filled with a detonable gaseous mixture of desired composition of methane and oxygen. After valve B is closed, the diaphragm is punctured by the needle N through a side tube attached obliquely to the shock tube.

When the buffer chamber is used, it is filled with air of the same pressure as that of the detonable gaseous mixture in the test chamber after the two chambers are separated by closing the sluice valve A. The reservoir chamber is filled with compressed air in the same way as described above. After the sluice valve A is opened, the diaphragm is broken with the help of a hand-operated needle N.

As shown in Fig. 1, the air in the reservoir spurts out and generates a shock wave. The gaseous mixture will be ignited by the direct shock wave or by the wave reflected from the bottom of the tube and superposed on the direct shock wave. At the ignition, the sound of detonation is clearly audible. On opening the tube after the experiment, the cellophane diaphragm is found to be discolored, and white smoke drifts out from the interior of the shock tube. As the bottom of the tube, the plane end plate is mainly used but, on necessary occasions, the conical bottom of the vertical angle 90° as shown in Fig. 3 is used, so as to cause the reflected shock wave to converge at a certain distance from the bottom on the center axis of the tube and thus produce a high temperature and high pressure region locally.

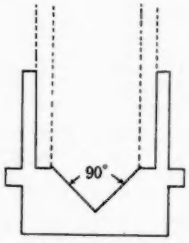

Fig. 3. Conical end of shock tube.

As to the experimental materials, commercial oxygen and methane in cylinders were used. For the experiment, both gases, through a sodium hydroxide tube to eliminate the carbon dioxide, are mixed to the desired composition and the mixture was kept in a tank over 24 hours. The methane in the cylinder consists usually of 87.8% methane, 9.7% nitogen, 0.3% carbon dioxide and 0.2% oxygen.

The buffer chamber serves to eliminate the effect of puncturing the diaphragm. As both sluice valve A and the needle N are operated by hand, the opening of the valve and puncture of the diaphragm can not possively be carried out at the same moment. Especially the fact that the opening of the valve has taken time, seems to cause the diffusion of the gases of the buffer and test chambers. Also the experimental result with the buffer chamber often shows poor reproducibility. At the puncture of the separating films the fragments of these will be scattered all about in the ignition mixture and these may cause some error in the experiment. To avoid the effect, some authors used a trap device such as metal coil or gauze to catch the fragments. In the experiment of Shepherd[2], he found some effect of fragments of copper film on the pressure value under which ignition occurs but in case of using cellophane films he could not find any of these effect. Accordingly, we eliminated the trap, as we used cellophane films only.

Results and Discussion

We have carried out a series of experiments of ignition by shock waves with various pressures in the reservoir against a certain gaseous mixture with definite composition and definite pressure. With a pressure in the reservoir lower than a certain limiting value, the ignition does not take place. The lowest pressure value necessary for the ignition is called minimum ignition pressure P_1 for the gaseous mixture of definite composition and definite pressure P_0. In Fig. 4, the ratio P_1/P_0 is plotted against various compositions of methane and oxygen. The values of P_1/P_0 correspond to the temperature of ignition for the mixtures of pressure P_0.

Owing to the mechanical strength of the shock tube used, the maximum pressure of the reservoir was limited to 30 kg./cm^2. Up to this value it was not possible to find any pressure values above which ignition does not occur. Such upper limiting pressure values for the ignition of gaseous mixtures of various compositions were reported by Shepherd[2]. In his case a higher pressure in the reservoir could be attained than is possible for us. As will be seen from Fig. 4, the minimum values of P_1/P_0 tends to decrease with the increase of P_0, and at the same time the minimum point drifts to the methane rich side. The limit concentration for the explosion of this gaseous mixture lies between 3 to 42% methane,

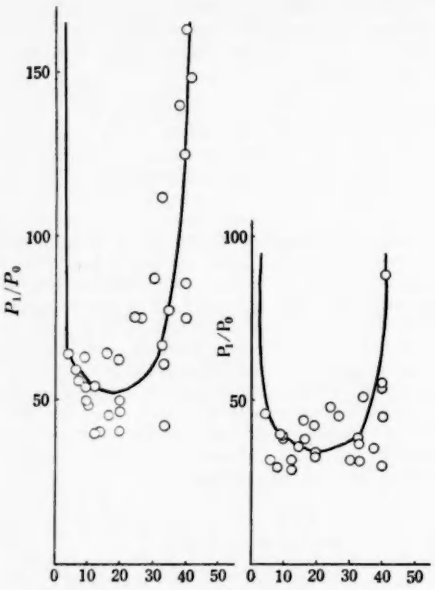

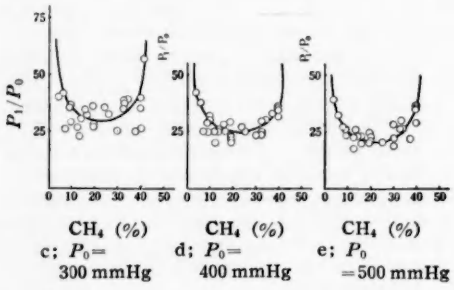

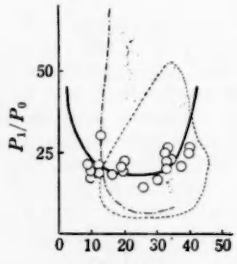

------ Shepherd's data with trap at 760 mmHg

---- Shepherds's data without trap at 760 mmHg

Fig. 4. Variation of P_1/P_0 with concentration of CH_4.

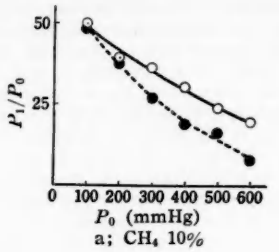

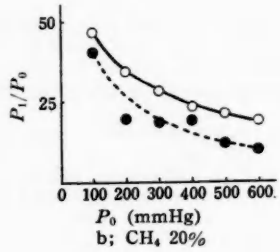

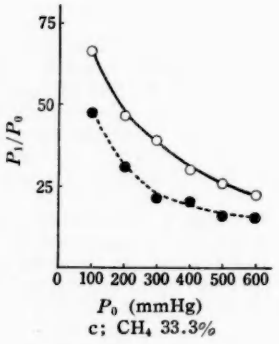

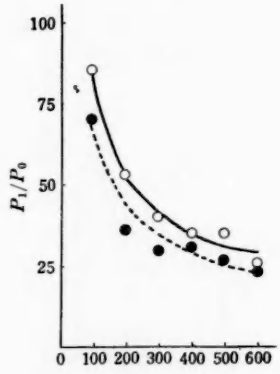

Fig. 5. Variation of P_1/P_0 with pressure of gaseous mixture.

○; with plane end

●; with conical end

and is entirely independent of the gaseous pressure. The minimum ignition point observed is at the gaseous mixture of about 20—25% methane.

As seen from Fig. 5, P_1/P_0 values decrease in accordance with the increasing value of P_0, which means that the higher the pressure of gaseous mixture, the easier to detonate the gas under the same conditions. The curves in thick lines in Fig. 5 denote the values using the plane bottom, and the dotted lines the conical bottom of the shock tube, respectively. The values obtained using the buffer chamber were found not to be sufficiently reproducible, probably for the reasons described above. We have selected some reliable values of both cases, with and without buffer which are tabulated in Table I. Though it seems that the ignition with buffer is easier than without buffer, the differences are by no means remarkable.

TABLE I

COMPARISON OF P_1/P_0 BETWEEN WITH AND WITHOUT BUFFER

P_0 (mmHg)	P_1/P_0 with buffer	P_1/P_0 without buffer
200	46.1	52.4
300	32.8	34.4
400	25.8	27.6

The ignition limits in Fig. 4f manifest some difference from those obtained by Shepherd. The discrepancies may be attributed to the fact that, in our experiment, a shock tube with closed end was used and in his case open tube was employed. Accordingly, in his experiment the gaseous mixture in the ignition chamber may have been diluted by the air diffused through open end. In spite of these differences, the concordance of the results from both investigations manifest themselves to be satisfactory.

In our experimental conditions the ignition temperatures could not be determined directly. But they may be estimated indirectly and theoretically with help of the equation[5]

$$[yP_0/P_1]^{(\gamma_1-1)/2\gamma_1} = 1-C_0(\gamma_1-1)(y-1)/C_1[2\gamma_0\{(\gamma_0-1)+(\gamma_0+1)y\}]^{1/2} \quad (1)$$

where P is the pressure of the shock wave; C_1 and C_0 are each the sound velocity in the reservoir and the test chamber respectively; γ_1 and γ_0 are the ratio of specific heat at constant volume and at constant pressure of both gases in two chambers cited above; and $y=P/P_0$. The gases are all assumed to be perfect gases. In taking $\gamma_0=\gamma_1=1.4$, $C_1=C_0$ and $T_1=T_0$ where T_0 is the temperature of the gas in reservoir and T_1 that of the test chamber, we have

$$P_1/P_0=y[1-\{(y-1)/(7+42y)^{1/2}\}]^{-7} \quad (2)$$

The values of y or the values of P can be determined by substituting the experimental values in the equation (2). Furthermore the temperature T of the direct shock wave and T_r of the reflected one can be expressed as follows[5];

$$T/T_0=(P/P_0)(1+\mu^2 P/P_0)/(P/P_0+\mu^2) \quad (3)$$

$$T_r/T_0=\{(2\mu^2+1)P/P_0-\mu^2\}\{2\mu^2P/P_0-(\mu^2-1)\}/\{(P/P_0+\mu^2)(\mu^2+1)\} \quad (4)$$

where $\mu^2=(\gamma_0-1)/(\gamma_0+1)$.

Using the expressions (2), (3) and (4) the values of T and T_r can be estimated approximately. In spite of those simplifications used above, the values obtained may serve as an orientation of the ignition temperature. In Fig. 6 we have shown the temperature values of T and T_r with plane end shock tube together with the

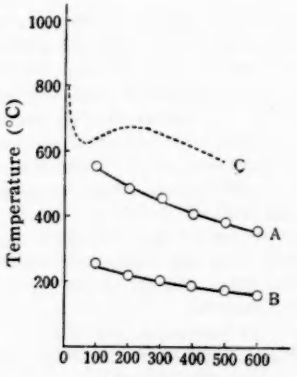

Fig. 6. Variation of ignition temperature with pressure of gaseous mixture CH_4+2O_2.
A; Reflected shock ignition
B; Direct shock ignition
C; Thermal ignition

5) W. Bleakney, *Rev. Mod. Phys.*, **21**, 584 (1949); I. I. Glass, W. Martin and G. N. Patterson, *UTIA Report* No. 2 (1953); R. N. Hollyer, Jr., "Engineering Research Institute Report", Univ. of Michigan, July (1953).

6) N. Semenoff, "Chemical Kinetics and Chain Reaction", p. 308, Oxford at the Clarendon Press. (1955).

results of thermal ignition[6]. In the respective cases, the higher the pressure of the detonable gaseous mixture, the easier the ignition. The peninsula-shaped region which is seen in thermal ignition is lacking in both direct and reflected shock wave detonation. Ignition in the shock tube with conical bottom is more easily produced by the reflected shock wave, than it is with the plane bottom. In general the temperatures of shock wave ignition are essentially lower than those of thermal ignition.

All these estimations however are indirect. They should be determined in a more direct way, and we are now preparing to take up such further investigations.

Summary

Using the shock tube, the authors measured the minimum ignition pressure P_1 of the reservoir for the methane-oxygen mixture of various pressure P_0 and various compositions, and obtained the following results.

1) The higher the value of P_0, the easier the ignition.

2) The concentration range of methane in the gaseous mixture for shock ignition is 3—42%, and the minimum value of P_1/P_0 or the ignition temperature, was found at a gaseous mixture of about 20—25% methane.

3) The ignition easier is by the use of the shock tube with conical end rather than with the plane end.

4) Shock ignition temperatures estimated indirectly were found to be remarkably lower than the thermal ignition temperature.

Department of Chemistry
Defense Academy
Yokosuka, Kanagawa

---

*On the Mechanism of the Coalescence of Drops at an Oil-Water Interface**

By Takehiko WATANABE and Makoto KUSUI

(Received May 16, 1957)

In regard to the stability of emulsions[1], the following three phenomena should be considered; (1) concentration of the dispersed droplets towards the top or the bottom of the emulsion, on account of a difference in density between the liquids, which is known as "creaming" or "settling", (2) flocculation or clumping of the dispersed droplets to form larger aggregates, without the droplets actually losing their identity, (3) coalescence of droplets to form larger ones and eventually bulk liquid.

Of these phenomena, only the third represents instability in the sense of the reverse process of dispersion. Therefore, the third phenomenon may be the most important clue in order to discuss the stability of emulsions. From this point of view, coalescence of drops at an oil-water interface has been studied. A more reasonable mechanism of the coalescence of drops at the oil-water interface than ever previously accepted is proposed.

Experimental

Materials.—The following surfactants were used as the emulsifier.

Anionic surfactant—Sodium dodecyl sulfate (SDS), (purity, 98.9%), was offered by the Kaō Sekken Co.

Cationic surfactant—Cetyl-oxymethyl-trimethyl-ammonium chloride (CEA), purity, ≃100%, was kindly offered by Professor Nirō Murata of our University.

Non-ionic surfactant—Emulgen 120 (polyoxyethylene-lauryl ether), HLB, 15.5; Emulgen 220 (polyoxyethylene-cetyl ether), HLB, 14.0; Emulgen 408 (polyoxyethylene-oleyl ether), HLB, 9.0; Emasol 320 (sorbitan di-stearate), HLB, 2.7; Emasol 410 (sorbitan mono-oleate), HLB, 5.9, were offered by the Kaō Sekken Co.

Cholesterol was a product from Wakō Pure Chemicals Ltd.

* Presented in part at the Symposium on Colloid Chemistry of the Chemical Society of Japan, held at Nagoya, in November 6, 1955 and at the 9th Annual Meeting of the Chemical Society of Japan, Kyoto, April 3, 1956.

1) C. G. Sumner, "Clayton's the Theory of Emulsions and their Technical Treatment", J. & A. Churchill Ltd., London (1954), p. 198.

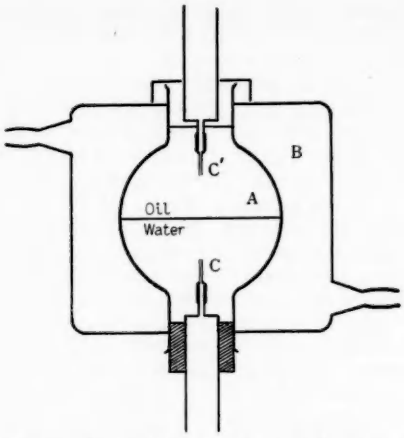

Fig. 1. Apparatus for determining the life-time of drops.

Apparatus and Procedure.—To measure the stability or persistency of water or oil drops at the oil-water interface, an apparatus shown in Fig. 1, similar to that of Cockbain and McRoberts[2] was used. It consists of a spherical part A (its diameter, 5 cm.) in which the oil-water interface is made, a thermostatted water jacket B, and tips, C and C' to form oil or water drops respectively. Both C and C' consist of three parts, a syringe (capacity, 2 cc.), a syringe needle with flattened tip, and a micrometer which was modified to push the syringe piston and at the same time to measure the distance travelled by the piston. A drop which was detached from the top of C or C', will ascend or descend in the vessel A and come into contact with a plane oil-water interface and then will coalesce after a certain time. The time of coalescence, life-time of drop, was measured with a stop watch and was taken as the interval in which one drop appears to be in contact with the interface and coalesces. In some cases, the drop did not completely coalesce in a single stage with the bulk liquid phase; partial coalescence occurred leaving a smaller drop, which also partially coalesced after some longer time than in the case of the parent drop, leaving still a smaller drop. In such cases, the time required for the first stage was taken as the life-time of the drop. Each drop was separately formed and its life-time was measured. Drops used for one experiment were 30 to 40.

Results

The life-time of drops at the interface.—The experiment has been made with benzene-water system, in which the surfactant was dissolved in either liquid as an emulsifier. In the given system, the life-times of individual drops were not constant. When N the number of drops whose life-time$\geqq$time t, were plotted in logarithmic scale against t, it was observed that most plots were found to be linear, as shown AB in Fig. 2, in agreement with the results obtained by Cockbain et al.[2].

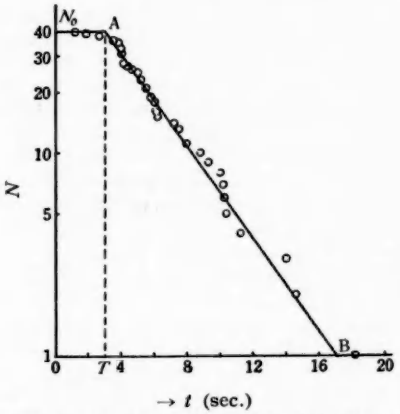

Fig. 2. Typical relationship between N (in logarithmic scale) and t; water phase—pure water, oil phase—2.0 g. cholesterol/100 cc. benzene, drop—pure water drop, temperature—25°C.

Then, the value T was estimated as the time of the intersection (A) of the AB with the straight line drawn parallel to the t axis through N_0, which is the total number of drops experimented. The experimental values are given in Table I. T_o and T_w are the values of T, for oil and water drops respectively.

Behavior of drop at the interface.—Two series of experiments on the behavior of water drop at the oil-water interface were made. First, in order to observe the behavior of the water drop in detail, the drop was colored with various dyes or colored inorganic salts. The experiments were made in the combinations of a drop and an oil-water interface with equal or different interfacial tension to the drop. The behavior of the colored drop is schematically shown in Fig. 3. When a drop comes into contact with an oil-water interface, the interface is deformed and consequently a concave surface is formed around the drop [(I) of Fig. 3]. After a while, coalescence of the drop occurs. If the interfacial tension around the drop (σ_d) is lower than that of the oil-water interface (σ_s), the process of coalescence will proceed as follows.

2) E. G. Cockbain and T. S. McRoberts, *J. Colloid Sci.*, **8**, 440 (1953).

TABLE I

T_W AND T_O OBTAINED WITH BENZENE-WATER SYSTEMS USING VARIOUS SURFACTANTS AS THE EMULSIFIER

Surfactant (dissolved phase)	Concn. of surfactant (g./100 cc.)	Water drop		Oil drop		Temp. (°C)
		Drop volume (cc.)	T_W (sec.)	Drop volume (cc.)	T_O (sec.)	
None	—	0.03	2	0.02	3	20
SDS	1.0	0.003	3	0.004	3×10^2	15
(water)	1.0	0.003	4	0.004	1×10^2	25
	0.1	0.009	1	0.01	2×10	15
	0.1	0.008	1	0.01	2×10	25
	0.01	0.02	1	0.03	5	15
	0.01	0.03	1	0.03	5	25
Emulgen 120	0.02	0.02	3	0.03	2×10	15
(water)	0.02	0.02	1	0.03	1×10	25
Emulgen 220	0.02	0.02	1	0.02	2	15
(water)	0.02	0.02	1	0.02	2	25
Emulgen 408	0.02	0.03	0.5	0.03	3	15
(benzene)	0.02	0.03	0.4	0.03	3	25
Emasol 320	0.02	0.03	0.6	0.03	2	15
(benzene)	0.02	0.04	1	0.04	4	25
Emasol 410	0.02	0.02	2×10	0.02	8	15
(benzene)	0.02	0.02	3	0.02	2	25
Cholesterol	2.0	0.02	3	0.03	2	15
(benzene)	2.0	0.02	3	0.03	1	25
	0.5	0.03	2	0.04	3	15
	0.5	0.03	1	0.04	3	25

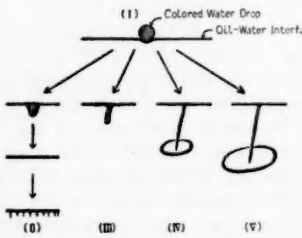

Fig. 3. Schematic presentation of the behavior of water drop at the interface.

Although the interface which is in contact with the drop, is deformed momentarily, the colored liquid can not penetrate into the bulk water phase through the interface. The momentarily deformed portion of the interface is restored to the original flat state and at the same time the colored liquid spreads along the interface, as if it soaked into the interface, and a layer of colored liquid is formed. After the formation of the colored layer, the colored liquid diffuses into the bulk water phase as illustrated in (II) of Fig. 3. If σ_d is approximately equal to σ_s or higher than it, the most part of the colored liquid penetrates into the bulk water phase through the interface, and the rest spreads along the interface as shown in (III) or (IV) of Fig. 3. The rate of penetration of the colored liquid increases with rise of the value, σ_d. The behavior of a colored liquid, having the greater rate of penetration at the moment of coalescence is shown in (IV) and (V) of Fig. 3. The formation of a ring of the colored liquid is observed around the straight penetrating stream of the same colored liquid. The last case (V) illustrated in Fig. 3 is the extreme one of the (IV), where $\sigma_d \gg \sigma_s$, and the spreading of the colored liquid along the oil-water interface is hardly ever observed.

From the above observations, it may be concluded that the main process of the coalescence of a drop at an oil-water interface, is the formation of a defect in the emulsifier layer around the drop at the portion in contact with the interface, and it is followed by the flowing out of the liquid of the drop through the defective portion. If the flowing liquid can make a hole in an oil-water interface owing to the pressure of flowing, the liquid will

penetrate into the bulk liquid phase of the same kind. If not, the liquid will spread along the oil-water interface. Here it is supposed that the main factor which may determine the life-time of a drop at an oil-water interface would be the characteristics of the layer of emulsifier around the drop.

The second series of experiments have been carried out in order to investigate the mechanism of the coalescence of a drop from another standpoint. Pure benzene and distilled water or bentonite suspension were used as the oil and the aqueous phase respectively. A drop (volume $\fallingdotseq$0.002 cc.) of 10^{-4} mol./l. solution of CEA was made to flow out from C′ in Fig. 1. When distilled water was used as the aqueous phase, the gradual increase in the life-time of the drop was observed as dropping proceeded, but this regular increase was only until nearly the tenth drop. On the contrary, when bentonite suspension was used as the aqueous phase, the same phenomenon could not be observed.

In these experiments, σ_d is lower than σ_s. Therefore, according to the results obtained with the colored drop mentioned above, it may be concluded that the liquid of the drop spreads along an oil-water interface and thereafter diffuses into the bulk aqueous phase as shown in (II) of Fig. 3. It may be assumed that, compared with the time required for a series of experiments, the diffusion rate of the liquid which forms the drop into the bulk aqueous phase may be slow, so that the marked decrease in the interfacial tension of an oil-water interface may be induced with the successive coalescence of the drop at the interface at least in the initial period of the experiment. The conclusion may be further developed that the lower the interfacial tension of an oil-water interface, the longer the life-time of the drop being in contact with that interface, provided that the interfacial tension around the drop remains constant. The reason why the life-time does not increase as dropping proceeds with bentonite suspension, may be as follows. The cationic surfactant, CEA dissolved in the drop solution may be fixed on the bentonite particles owing to the cationic exchange reaction or adsorption, so that the decrease in the interfacial tension of an oil-water interface may be reduced considerably compared with the above case without bentonite.

Discussion

On the experimental method.—Both Cockbain et al.[2] and Gillespie and Rideal[3] found with benzene-water system that the stability of the drops was markedly increased by putting a cover on A (Fig. 1). The latter authors found that the drops become more stable when the whole apparatus is further surrounded by an air bath whose temperature is approximately the same as that of the water jacket B. These effects were attributed to the elimination of convection currents at the interface. In the present experiments, similar phenomena were also observed when measurements were made under a tightly-fitting cover. However, in the present investigation, where the value of T is simply taken to discuss the observed data and also the singular significant figure is taken to represent the magnitude of the value T, the influence of the above operation on the experimental results can be neglected.

Cockbain et al. observed that the stability of the drops had not been markedly affected by volume in the range 0.0005~0.01 cc., whereas below 0.0005 cc. the stability had increased rapidly with decreasing volume. On the other hand, Gillespie et al. reported that in the absence of surfactant the stability of the drops had increased with increasing volume in the range 0.014~0.38 cc. (drop radius; 0.15~0.45 cm.). In the present experiments, the value of T was not markedly affected by the change of the drop volume as shown in Table I. where singular significant figure was taken to represent the magnitude of the value of T.

In order to obtain a clean oil-water interface in the vessel A, the method by Cockbain et al. was employed. But our experiences showed that it is not necessary to be extremely careful for the cleanliness of the interface to obtain well reproducible values of T. In the present experiments the reproducibility was satisfactory with T in any case.

On the process of the coalescence of a drop.—Cockbain et al. have suggested that the life-times of the drops are determined by two distinct processes, viz., drainage of the continuous phase from the space between the drop and the plane oil-water interface, followed by rupture of the adsorbed film of surfactant. They

3) T. Gillespie and E. K. Rideal, *Trans. Faraday Soc.*, 52, 173 (1956).

concluded that the main factor determining stability is the resistance to wetting of segments of the adsorbed film by the discontinuous phase. But it was not substantiated whether both the films, viz. the film around the drop and that of the plane oil-water interface, must be wetted by the discontinuous phase simultaneously or only one of them.

According to Gillespie et al., the coalescence of a drop at an oil-water interface is very unlikely until the film formed between the drop and the interface has been drained to a certain thickness for which it takes a certain time. The coalescence of a drop will occur owing to the rupture of the film which will be brought about by thermal and possibly mechanical disturbances.

In contrast to the processes proposed by Gillespie et al., the present experiments showed that the main process of the coalescence of a drop at an oil-water interface is the formation of a defect in the emulsifier layer around the drop at the portion in contact with the interface. It is consequently concluded that though the initial process, the drainage of the continuous phase from between the drop and the interface, will occur in the same manner as proposed by them, the final process which includes the main process as mentioned above, will proceed in the following manner.

When a defect has been formed in the emulsifier layer around the drop at the portion in contact with the plane oil-water interface, the local disturbance will be induced at that portion and this will be promoted by thermal or mechanical disturbances such as convection currents etc. Consequently the liquid of the drop will flow out through the defective portion owing to the internal pressure due to the interfacial tension around the drop itself. At the same time, since the interfacial tension of the defective portion becomes higher than that of the other portion of the same drop which is surrounded by the emulsifier layer, the transference of the emulsifier to the defect from the other portion of the drop interface will take place to repair the defect with the new emulsifier layer. In this case, so far as the repairing of the defect with new emulsifier layer has been completed before the arrival of the flowing liquid at the oil-water interface, the coalescence of the drop will not occur. If not, the reformation of emulsifier layer around the drop becomes impossible and the liquid of the drop will flow out through the defective portion progressively and the interface will be exposed to the pressure of the flowing liquid. At this stage if the flowing liquid can make a hole in an oil-water interface owing to the pressure of flow, the liquid will penetrate into the bulk liquid phase of the same kind. If not, the liquid will come into direct contact with the bulk liquid phase of the same kind. As seen from our experimental data using a drop of colored solution, the latter phenomenon can be observed only in the case where σ_d is less than σ_s. Therefore, when the liquid of the drop comes into direct contact with the bulk liquid, it may be considered that the interfacial tension between the former and the latter liquid would be nearly null. In the present case, the interfacial tension between the liquid of the drop and the original continuous phase liquid (σ_d) is lower than that of the oil-water interface (σ_s), so that the liquid of the drop spreads along the oil-water interface and produces the new oil-water interface between the spreading liquid and the original continuous phase liquid, resulting in the disappearance of the original interface.

However, also in the present experiments, it can be still expected that the probability of coalescence will be small until the continuous phase between a drop and an interface has been drained to a certain thickness. Therefore, the values of T may also depend on a factor which is influenced by the rate of drainage of the continuous phase.

On the treatment of the experimental data.—Cockbain et al. have found that after a time t_D (drainage time), $\ln N = -kt + \text{constant}$ holds. The quantity t_D corresponds to T in the present experiments. The constant k (rate constant for the film rupture) will be obtained from the slope of AB in Fig. 2. These authors have discussed the stability of drop using both the values t_D and k. Gillespie et al. have further discussed the probable effect of electric double layer forces, electroviscosity and other factors on the values t_D and k. In the present report, however, an attempt was made to discuss the stability or persistency of drops only referring to the values of T, from the following reasons.

(1) The well-reproducible values of T can be readily obtained, as shown in the above discussion, while the values

of k are readily influenced even by the slight differences in the experimental conditions. Therefore, in order to obtain the significant values of k, the experimental conditions must be more strictly controlled and moreover, according to Gillespie et al., the measurements of the life-time must be made with from 100 to 200 drops.

(2) T denotes, as will be stated later, the time during which most drops can exist without coalescence, while k is a rate constant for the coalescence after time T. Consequently, the stability or persistency of drops may be primarily defined by the value of T and the contribution of k to the same problem is by far less important.

On the life-time of drops.—From the results mentioned above, it is concluded that the values of T are determined by two factors, viz., drainage of the continuous phase from between the drop and the plane oil-water interface, and formation of a defect in the emulsifier layer around the drop.

Now let us consider the latter factor, irrespective of the former one. In the present experiments it was assessed from 30 to 40 drops to obtain the value of T. The number of drops which coalesced within the time T was from 1 to 5 drops. Hence, it may be said that the value of T is the life-time at which the probability of coalescence is about 0.1.

Subsequently, the factors which affect the coalescence of drops will be considered. When a drop comes into contact with an oil-water interface, the interface will be deformed and consequently a concave surface will be formed around the drop as illustrated in (I) of Fig. 3. In this case, it is assumed that the drop remains on the interface at equilibrium position without deformation and the radius of curvature of the concave surface (a) is equal to the radius of the drop (r) itself. The area of the concave surface at the interface which comes into contact with the drop is A. For small drops it may be supposed that this contact portion is a plane surface, since the contact portion itself must be quite small. Then, the following relation is given, since a equals to r

$$\frac{4}{3}\pi d g r^3 \fallingdotseq \frac{2\sigma_s}{a}\cdot A = \frac{2\sigma_s}{r}\cdot A \qquad (1)$$

where d is the difference in the density between the drop and the surrounding medium and g the gravity constant. We see that the contact area A is proportional to r^4.

Next, the probability of the formation of a defect in the emulsifier layer around the drop will be considered. It may be assumed that this probability is constant anywhere around the surface of the drop, since no deformation of the drop is considered. So that the probability of forming the defect at the portion of the drop in contact with the interface will be proportional to A/B, where B is the total surface area of the drop and proportional to r^2. Therefore, the probability of forming a defect at the contact portion of the drop and the interface should be proportional to r^2. However, it may be suggested that the above condition is strictly satisfied only when the diameter of the drop is smaller than 1 mm., which can be deduced from the data obtained by Cockbain et al. or by the present investigation on the effect of the drop volume and also by the calculated values of A using relation (1) with the substitution of appropriate values for σ_s and r.

The experimental results reported in page 239 that if σ_d is smaller than σ_s and at the same time σ_d and the drop volume are constant, the lower the interfacial tension of an oil-water interface, the longer the life-time of the drop being in contact with the interface may be explained as follows.

From the relation (1), it may be expected that the higher the σ_s, the smaller the A; consequently the life-time of a drop would increase. The experimental result is, however, contrary to the above expectation. This inconsistency may be caused by the assumption, viz. $a=r$, and this assumption will not be satisfied under the present experimental conditions. Here it should be expected that a changes with the change of σ_s and consequently a is not equal to r. Therefore, if the value of σ_s is higher, the value of a also becomes greater and consequently variation of the value A with the variation of σ_s will be smaller than that given by the relation (1).

If the area A is constant, the deformation of the drop corresponding to the change of a must be expected. Consequently the strain will be induced on the emulsifier layer of the drop at the contact portion. Under these conditions, the higher the σ_s, the larger the difference between a and r and the larger the strain induced on the emulsifier layer. On the other hand, it is expected that a defect on the emulsifier layer will be more

readily formed at the portion on which the strain is induced. As a conclusion, it is expected that when the drop volume and σ_d are constant and σ_d is less than σ_s, the lower the value of σ_s, the longer the life-time of the drop in accordance with the present experimental results.

The above discussion has been presented without the consideration on the drainage process of the continuous phase from between the drop and the plane oil-water interface. However, the time necessary for this drainage process is also included in the values of T, so that it must also be taken into consideration, when the meaning of the value T is strictly discussed. On the other hand, it is hard to say that the values t_D obtained by Cockbain et al. and also probably by Gillespie et al. are determined only by the drainage process. Therefore, the extent of the contribution of the drainage process to the value T, may be estimated from the minimum value of the life-time assessed with a number of drops. Since the life-time of each drop is short in the system without surfactant, the time necessary for the net drainage will be obtained from the data assessed from 100 to 200 drops in each experiment such as in the case carried out by Gillespie et al.

According to Gillespie et al. the time required for drainage process t_D decreases with the decrease in the drop volume. On the other hand, from the results obtained by Cockbain et al. and also by the present authors, it was shown that if the diameter of the drop is about 1 mm. or less, the stability or the life-time increases rapidly with the decrease of the volume. From these results, it is concluded that the time required for drainage with such droplets as in ordinary emulsions whose diameters are in the range of a few μ, will be practically negligible, compared with their whole life-times.

Cockbain et al. have reported that the stability of the drops was not markedly affected by volume in a fairly wide range, whereas below a certain volume the stability increased rapidly with decreasing volume. From the above results, it is concluded that in the range of the volume at which the stability of the drops is nearly constant, the factor increasing the life-time will be compensated by that decreasing it. Therefore, it may be said that one can estimate the life-time of a drop less than 1 mm. in diameter by using the value of T in the present investigation or t_D obtained by Cockbain et al., regarding it as the one which does not include any contribution from the factor of the drainage process. Now, if it can be assumed that the life-time of the drops is determined only by the value of A/B, it may be suggested that when the experiments are made with the drops of 1 μ in diameter under the same condition as the present investigations, the values of T will be about 10^6 times greater than those listed on Table I.

From the discussions mentioned above, the main process of the coalescence of a drop at an oil-water interface may be said to be the formation of a defect in the emulsifier layer around the drop at the portion in contact with the interface. Consequently, the more readily the emulsifier (surfactant) escapes from the oil-water interface around the drop, the more readily the defect on the emulsifier layer will be formed and also the shorter the life-time of the drop will be.

To consider the stability or persistency of the droplets in the ordinary emulsions (droplet diameter=a few μ) referring to that of the drops as discussed above, it must be first examined whether the escaping tendency of the emulsifier from the oil-water interface of the former small droplets is the same as that of the latter. This can be studied by the following Kelvin-Gibbs relation[4,5], where the electric double-layer effect can be neglected;

$$\ln\frac{S_r}{S}=\frac{2\sigma M}{dR\Theta r} \qquad (2)$$

where

S_r=escaping tendency of emulsifier molecule from interface of radius r (r is negative for concave interface).
S=escaping tendency from plane interface.
σ=interfacial tension.
M=molecular weight of emulsifier (surfactant).
d=density of emulsifier molecule at the interface.
R=gas constant.
Θ=absolute temperature.

After the examination with relation (2), having substituted the appropriate values into (2), it was found that the variation of S_r/S with r becomes appreciable only when r is less than $10^{-4}\sim10^{-5}$ cm. So that, it

4) R. M. Wiley, *J. Colloid Sci.*, **9**, 427 (1954).
5) E. A. Guggenheim, "Thermodynamics, an Advanced Treatment for Chemists and Physicists", Interscience Publishers Inc., New York, (1950), p. 41.

is concluded that the escaping tendency of emulsifier from the interface of the large drops investigated in the present experiments, is practically the same as that of the small droplets with the diameter of a few μ. Referring to effects of the electric double layer on the solubility[6], the effects of the electric double layer on the escaping tendency of the emulsifier from the oil-water interface may be neglected under the present experimental conditions.

According to the relation (2), the escaping tendency of the emulsifier from the interface to the water or oil phase is independent of the state of the interface, whether it is convex or concave. Therefore it can not be determined by the relation (2) which more stable or persistent, the oil drop or the water drop is. However, if it is assumed that the escaping of the emulsifier molecule into the continuous phase is likely to be hindered by the close juxtaposition of the interfaces, the probability to form a defect will be determined by the escaping tendency of the emulsifier into the aqueous phase or the oil phase, in the case of water drops or oil drops respectively. The difference of the life-time between the aqueous and oil drops, as can be seen in Table I, may clearly be explained with the above assumption.

The type of the emulsion produced with the combination of oil, water and emulsifier will be determined by several factors, including volume ratio of oil to water, characteristics of the emulsifier used and mechanical conditions such as stirring, shaking etc. Therefore, it can not be foretold from the difference of the values T_O and T_W, whether the O/W type emulsions will be produced or W/O type. However, in the system in which the difference in viscosity between oil and water is small such as benzene and water, it may be said that O/W type emulsion is more stable or persistent if T_O is greater than T_W and, W/O type, if T_O is less than T_W, as the emulsions produced using a given emulsifier.

It is not easy to estimate the stability of emulsions according to the values of T. However, it may be said qualitatively that the system having the value of T at least a few times greater than ten seconds must be used in order to obtain the emulsions in which the breaking of emulsions is not observed after a month or more.

6) A. E. Alexander and P. Johnson, "Colloid Science", Oxford University Press, London (1949) p. 37.

Summary

The stability or persistency of drops at an oil-water interface in the presence of emulsifier has been studied. The behavior of drops at an oil-water interface has been observed using colored drops to interpret the process of the coalescence.

A mechanism, which explains the coalescence of drops at an oil-water interface more reasonably, was proposed as follows: the main process of the coalescence of drops at an oil-water interface is the formation of a defect in the emulsifier layer around the drops at the portion in contact with the plane interface.

The stability or persistency of emulsions may be estimated qualitatively by the values of T obtained in the present investigations.

The authors would like to express their gratitude to Professor Sôzaburo Ono for his kind guidance and discussion throughout this work. The cost of the present research has been partly defrayed from the Scientific Research Grant from the Ministry of Education.

Laboratory of Biophysical Chemistry
College of Agriculture, University of
Osaka Prefecture, Sakai

SHORT COMMUNICATIONS

Synthesis of L-Pyroglutamyl-L-glutaminyl-L-glutamine

By Tetsuo SHIBA, Shigeo IMAI and Takeo KANEKO

(Received January 6, 1958)

The synthesis of eisenine[1] isolated from a brown marine alga *Eisenia bicyclis* Setchell had been recently performed by us[2]. Eisenine is a tripeptide having the structure L-pyroglutamyl-L-glutaminyl-L-alanine. In 1949 a tripeptide fastigiatine* was isolated by J. S. Fruton and his collaborators[3] from American brown alga *Pelvetia fastigiata*. In the present investigation L-pyroglutamyl-L-glutaminyl-L-glutamine proposed by J. S. Fruton for the structure of fastigiatine was synthesized according to the following scheme similar to the synthetic route of eisenine.

A mixed anhydride from γ-methyl-carbobenzyloxy-L-glutamate (I) and ethyl chloroformate was coupled with L-glutamine to yield carbobenzyloxy-L-(γ-methyl ester)-glutamyl-L-glutamine (II) (37%), $C_{19}H_{25}O_8N_3 \cdot 2H_2O$, m. p. 184.5—185°C**. Compound (II) was converted by methanolic ammonia into amide ammonium salt (III) (77%), m. p. 195—196°C (dec.), which was heated at 100°C over phosphorous pentoxide in vacuo to give carbobenzyloxy-L-glutaminyl-L-glutamine (IV), m. p. 177—178°C. Carbobenzyloxy diamide (IV) was

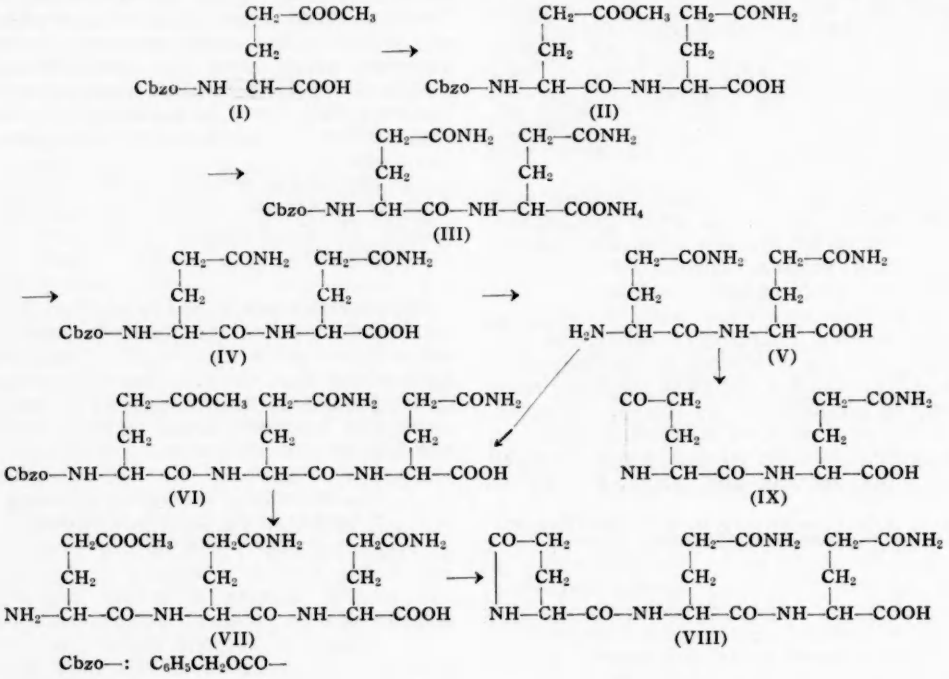

1) T. Ohira, *J. Agr. Chem. Soc. Japan* (*Nogei Kakaku Zassi*) **15**, 370 (1939).
2) T. Kaneko, T. Shiba, S. Watarai, S. Imai, T. Shimada and K. Ueno, *Chem. & Ind.* (London), **1957**, 986.
3) C. A. Dekker, D. Stone and J. S. Fruton, *J. Biol. Chem.*, **181**, 719 (1949).
4) A. Meister, "Biochemistry of the Amino Acids", Academic Press Inc., Publishers, N. Y. (1957), p. 56.

* For this tripeptide, J. S. Fruton has expressed in the term of "peptide from *Pelvetia fastigiata*". While the name "pelvetine" was used by us early, A. Meister[4] employed the nomenclature "fastigiatine". Now, we use fastigiatine instead of pelvetine to avoid the confusion of these nomenclatures.

** All melting points were uncorrected.

hydrogenated using palladium charcoal to L-glutaminyl-L-glutamine (V) (78%), $C_{10}H_{18}O_5N_4\ 1\frac{1}{2}H_2O$, m. p. 208—209°C (dec.). $[\alpha]_D^{29}$ +24.54° (*c*, 1.74, in H_2O). Furthermore diamide (V) and γ-methylcarbobenzyloxy-L-glutamate (I) were combined through the mixed anhydride method as described above, to yield carbobenzyloxy tripeptide derivative (VI) (53%), m. p. 175—180°C (dec.), which was hydrogenated to compound (VII) (61.3%), m. p. 221°C (dec.). Compound (VII) was cyclized in absolute methanol saturated with ammonia, followed by treatment with Dowex 50 to obtain L-pyroglutamyl-L-glutaminyl-L-glutamine (VIII)*** (80%), m. p. 203—204°C (dec.), $[\alpha]_D^{28}$ −36.24° (*c*, 2.02, in H_2O), pK_a' 3.5.

Anal. Found: C, 46.75; H, 5.81; N, 18.47; equiv. 427. Calcd. for $C_{15}H_{23}O_7N_5$: C, 46.75; H, 6.02; N, 18.17%; equiv. 385.

While this substance failed to give a color with ninhydrin, it gave a strong biuret reaction. From the results obtained above, however, it is not necessarily concluded that this synthetic product was identical with natural fastigiatine, since the latter has m. p. 190—195°C and $[\alpha]_D$ −43.7～−46.5° (in H_2O).

The cyclization of a γ-amide to a pyroglutamyl derivative can also be successfully produced by boiling the aqueous solution of the former. For example, L-glutaminyl-L-glutamine (IV) was converted by this procedure into L-pyroglutamyl-L-glutamine (IX) (73%), m. p. 178—180°C (dec.), $[\alpha]_D^{15}$ −22.14° (*c*, 1.65 in H_2O).

Department of Chemistry, Faculty of Science, Osaka University
Kita-ku, Osaka

*** After this synthesis had been accomplished, a private communication from Professor J. Rudinger to Professor S. Akabori indicated that Professor Rudinger and his collaborators have also succeeded in the synthesis of the same peptide independently of ours.

On the Volatility of Polonium Compounds

By Hisao MABUCHI

(Received January 14, 1958)

As reported before[1], polonium dithizonate sublimes at about 120°C under atmospheric pressure. In order to confirm whether or not such a low-temperature sublimation is characteristic of dithizonate, the volatility of other polonium compounds was studied. The compounds investigated were those which are extractable with organic solvents. They are divided into two groups according to their chemical species.

Group I: The compounds resulting from the interaction of polonium with organic reagents. The organic reagents used for this study are as follows: 8-hydroxyquinoline, sodium diethyl-dithiocarbamate, thenoyltrifluoroacetone, thiourea, *sym*-diphenylthiourea, thiosemicarbazide, 1-phenylthiosemicarbazide, diphenylcarbazone, diphenylcarbazide, diphenylthiocarbazone and di-β-naphthylthiocarbazone.

Group II: The polonium compounds which are extracted in the absence of organic reagents;

(a) polonium compound which is extracted with *iso*-propyl ether from an aqueous solution of 0.5 M potassium iodide and 3 N hydrochloric acid[2].

(b) polonium compound which is extracted with methyl *iso*-butyl ketone from an aqueous solution of 0.5 M potassium iodide and 1.5 N hydrochloric acid[2].

The samples were mounted in stainless steel dishes and the heating was carried out on a hot plate. The measurement of polonium activity was made with a Lauritsen electroscope.

The results of the experiment are summarized below;

1) All polonium compounds of Group I sublime below 160°C/1 atm., while no sublimation is observed even at 200°C/1 atm. for the compounds of Group II.

(2) The volatility of the polonium compounds with organic reagents of a similar type tends to decrease in the following order.

thiourea > *sym*-diphenylthiourea.

diphenylcarbazone, diphenylcarbazide > diphenylthiocarbazone > di-β-naphthylthiocarbazone.

(3) The volatility is remarkable for the compounds with diphenylcarbazone, diphenylcarbazide and diphenylthiocarbazone. Above all, the compounds with the first two reagents sublime below 100°C/1 atm.

From the results mentioned above, it follows that the low-temperature sublima-

1) K. Kimura and H. Mabuchi, This Bulletin, **28**, 535, (1955).

2) K. Kimura, N. Saito, Y. Koda and K. Tanaka, paper presented before the 9th Annual Meeting of the Chemical Society of Japan (1956).

tion is not characteristic of polonium dithizonate, but common to many organo-compounds of polonium.

As an application of this property of polonium organo-compounds to radiochemical analysis, the carrier-free separation of radium-F (polonium) from radium-D (lead) and radium-E (bismuth) was carried out by distillation of polonium compounds with diphenylcarbazide. The most effective procedure for distillation is as follows.

Fifty milliliters of nitric acid solution of radium-D, -E, -F mixture is taken in an all-glass distilling apparatus. The acidity of the solution should be adjusted between 0.1 and 0.5 N in nitric acid. To this solution is added 30 mg. of diphenylcarbazide. Then the distillation is carried out until one half of the initial volume of the solution is distilled. Radiochemically pure radium-F is found in the distillate. Moreover, this aqueous distillate is almost free from the excess of the organic reagent. The presence of strong oxidizing agents and the chloride ion in the initial solution decreases the efficiency of separation.

The detail of these studies will be reported in a separate paper.

The author would like to express his sincere thanks to Professors N. Saito and Y. Yokoyama of this laboratory and to Dr. K. Kimura of Japan Atomic Energy Research Institute for their valuable advice and helpful discussion.

Department of Chemistry, Faculty of Science, The University of Tokyo
Hongo, Tokyo

Rate Equation for the Chemisorption of Nitrogen on Ammonia Synthesis Catalysts

By Takao KWAN

(Received December 26, 1957)

The present author put forward a power rate law[1] expressed by

$$-\frac{dp}{dt}=kp\theta^{-\alpha} \qquad (1)$$

to describe adequately the rate of the chemisorption of nitrogen on a promoted iron catalyst. Zwietering and Roukens[2] also investigated the same system and applied their data to the Elovich type equation of the form

$$-\frac{dp}{dt}=kpe^{-\beta\theta} \qquad (2)$$

Recently Scholten and Zwietering[3] expressed their view that the experimental data due to Kwan are well subscribed in the Eq. (2) rather than (1). Whether or not experiments conform to these equations can be demonstrated viz., power rate law should give a linear relation in the logarithmic plot of $-1/p\cdot dp/dt$ against θ while the Elovich equation a linear semi-log plot. The purpose of the present note is to show a semi-log plot on the data already published by this author and discuss the consequences.

Rate data at 300 and 400C given in Table II of the previous paper[4] are far below equilibrium and permit ignoring the desorption of nitrogen. They are reproduced in Fig. 1 in a semi-log scale. Apparently experimental plots are curved convexly against θ-axis. Such curvilinear plots in a semilog scale were reproducible with respect to any $p-t$ run measured in a constant volume on the re-reduced catalyst, hence throwing doubt on the validity of the Elovich equation.

Experimental data obtained repeatedly on a re-reduced catalyst were found however to shift more or less in relation each other with each run, probably due to different surface states. Thus, if one plot several runs in a semi-log scale, than an approximate linear relation may appear within the experimental accuracy. A straight line of this kind has been demonstrated by Scholten and Zwietering[3].

If, on the other hand, one plot the experimental data for any single run in a logarithmic scale, a good linear relation holds with a break near $\theta=0.08$. Such a plot has been preferred by this author and presented together with those of other runs in the previous paper[4]. Unfortunately the measurements were only within a small range of coverage. Further works are needed to confirm the linearity of the latter kind at a higher coverage.

Assuming that the linear portion extends far beyond $\theta=0.08$, activation energies for

1) T. Kwan, *J. Res. Inst. Catalysis*, **3**, 16 (1953); This Bulletin, **27**, 70 (1954).

2) P. Zwietering and J. J. Roukens, *Trans. Faraday Soc.*, **49**, 543 (1954).

3) J. J. F. Sholten and P. Zwietering, ibid., **53**, 1363 (1957).

4) T. Kwan, *J. Res. Inst. Catalysis*, **3**, 109 (1955).

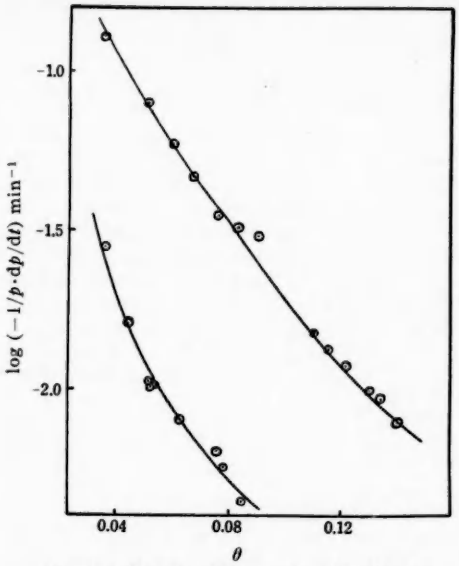

Fig. 1. Chemisorption rate of nitrogen as a function of coverage θ constructed from a single $p-t$ run obtained by Kwan[4]. T: 300° and 400°C.

the chemisorption of nitrogen were given by[4]

$$E=11\log\theta+23 \text{ kcal./mole}$$

Apart from the numerical value, this functional form for E seems compatible with the result of Zwietering and Roukens that the experimental E is not linear but concave against θ-axis at higher coverage of their measurements. Such a curved portion, when plotted against $\log\theta$, gives a linear portion in accordance with the above function—a family of power rate law.

Such an argument has been a frequent problem in adsorption—for instance the shape of adsorption isotherm and the corresponding heat curve. The author expressed his view elsewhere[5] that the Langmuir type isotherm is useful at lower coverage only, whereas the Freundlich equation provides an excellent validity at higher coverage. As a consequence, the isothermal heat curve appears to be somewhat reverse-s-shaped or linear against $\log\theta$ at higher coverage, e.g., hydrogen on a reduced nickel powder[6]. Schuit et al. observed adsorpiton isotherms for hydrogen on nickel-on-silica and derived a linear heat decrease with θ. On closer inspection, the heat-coverage relation is, according to them[7], slightly sigmoidal in character. It is the opinion of this author that different viewpoints expressed by Zwietering et al. and the author mentioned above may lie in a situation such was revealed in the adsorption of hydrogen on a nickel sample.

Research Institute for Catalysis and Chemistry Department, Hokkaido University, Sapporo

5) T. Kwan, *Advances in Catalysis*, **6**, 67 (1954).
6) S. Ohkoshi and T. Kwan, *J. Res. Inst. Catalysis*, **4**, 199 (1957).
7) G. C. A. Schuit et al., "Chemisorption" edited by Garner, 39 (1957) Butterworths Scientific Pub. London.

X-ray Determination of the Molecular Weight of Luteoskyrin

By Hiroshi Okuto*, Yoshio Sasada and Kiichi Sakurai

(Received January 6, 1958)

A chemical study on luteoskyrin, one of the toxic components produced by penicillium islandicum, has been carried out by T. Yamamoto, Y. Yamamoto, Kanatomo, Tanimichi and Kikui[1]. According to their results, this substance exists in two different crystal forms; one is needle-like and the other cube-shaped. The former is obtained by recrystallization from an ethanolic solution, and the latter from a mixed solvent of aceton, petroleum benzine and water (2:1:1). Both forms of crystals have the same composition, $C_{2.45}H_{2.05}O_1$.

Since ordinary methods failed to give a reliable value for the molecular weight, we applied the single crystal X-ray diffraction method to its determination. The samples used in this study were supplied by the above-mentioned authors.

The unit-cell dimensions of each form were determined from oscillation and Sauter-Schiebold photographs about the c axis taken with Cu K_α radiation. The length of the c axis was measured from layer-line spacings. The other two axial lengths were first estimated roughly from Sauter-Schiebold photographs and accurately determined using the spectra on a set of oscillation photographs which were

* Present address: Research Laboratories, Takeda Pharmaceutical Industries, Ltd.

1) Y. Yamamoto, T. Yamamoto, S. Kanatomo, K. Tanimichi and H. Kikui, *J. Pharm. Soc. Japan*, (*Yakugaku Zassi*) **76**, 670, (1956).

completely indexed by the graphical method.

The densities were measured by the floatation and the pyknometer methods** at 20°C. In the former method, aqueous solution of zinc chloride was used as floatation liquid. The results are tabulated in Table I.

TABLE I
CRYSTAL DATA

Crystal form	needle-like	cube-shaped
Crystal system & lattice type	orthorhombic primitive lattice	monoclinic primitive lattice
Lattice constants		
a	14.8_4 Å	15.1_7 Å
b	15.0_3	12.6_4
c	12.5_0	21.5_0
α	90°	90°
β	90°	135°***
γ	90°	90°
Volume of cell	2.79×10^3 Å^3	2.91×10^3 Å^3
Density	1.48 g.cm^{-3}.	1.47 g.cm.$^{-3}$

From the volume of the unit cell V and the density ρ, the molecular weight M can be calculated according to the formula

$$M=\rho VN/Z,$$

where N is the Avogadro number and Z the number of molecules in the unit cell, which is necessary to calculate M. From symmetry consideration, Z should be 2^n. However, the value of Z greater than eight can be excluded on account of the fact that the molecular weight of this substance has been supposed to be of the order of several hundreds[2], and this is also supported by its high melting point (273°C decomp.). It is highly improbable that Z equals to unity. The value of Z is four or two, the former being more probable.

When Z is assumed to be four, the molecular weight is found to be 621 ± 30 for needle-like crystals and 644 ± 20 for cube-shaped.

The difference, if it is significant, between these two values may be due to the fact that one or both forms crystallize with solvent molecules, but this can not be concluded from this experiment alone.

Faculty of Science, Osaka University
Kita-ku, Osaka

** In order to lower interfacial tension, a small amount of surface-active substance was added.

*** This value was estimated using layer-line reflections on the oscillation photographs.

2) T. Yamamoto, Private communication.